

The formulation of a microsphere based fixed dose combination for oral antiretroviral delivery



By Omobolanle Ayoyinka OMOTESO

A thesis submitted in fulfilment of the requirements for the degree of
DOCTOR OF PHILOSOPHY

School of Pharmacy, Faculty of Natural Sciences,
University of the Western Cape, South Africa.

Supervisor: Prof Marique Elizabeth Aucamp

Co-Supervisor: Dr Marnus Milne

August, 2023

Declaration (plagiarism declaration)

I, Omobolanle Ayoyinka OMOTESO, hereby declare that this thesis titled "**The formulation of a microsphere-based fixed dose combination for oral antiretroviral delivery**" constitutes my entire work. Therefore, it has never been submitted for any degree or examination at a university.

Signed: 

Date: 07/08/2023



Dedication

The thesis is dedicated to God the Father, Son (Jesus Christ), and Holy Spirit. Christ is my firm foundation. The rock on which I stand. What God cannot do, doesn't exist.



Acknowledgements

I want to thank my supervisors, Prof. Marique Elizabeth Aucamp and Dr Marnus Milne, for the once-in-a-lifetime opportunity, supervision, guidance, and mentorship. I will be eternally grateful to you.

I thank the School of Pharmacy, Department of Pharmaceutical Sciences, Faculty of Natural Sciences, University of the Western Cape, South Africa, for providing a welcoming environment to conduct my research. I am grateful for the financial assistance provided by the Future Leaders African Independence Research Fellowship (FLAIR).

I would like to appreciate my colleagues, friends, and South African family: Musafili, Nnamdi, Yusuf, Candidah, Jean, Sandrine, Geoffrey, Dr Kolajo, Samson, Mrs Adewumi, Olagbegi family, Bode-Aluko family, Professor Micheal Odeniyi, Abegunde family, Dr Dipo, Fatoba family, Dr Ajayi, Dr Ayo, and Adeola Egunlusi; thank you for motivating, praying, and showing me love far from home.

My first family, Mrs Oyeyinka Obembe (Mum), Boluwatife Obembe (Brother), and Mayokun Obembe (Brother), deserves a special thank you for being my rock, source of inspiration, and head of financial support.

To my second family; Dr Sunday Omoteso (Father-in-law), Mrs Omoteso (Mother-in-law), and Mr Oluwaseun Omoteso (Husband), thank you for the four years sacrifice.

My children, Tanitoluwa Joshua Omoteso and Taseoluwa Jeremiah Omoteso, whom I consider God's greatest gifts to me in life, deserve a particular word of gratitude for enduring without me for four years. I breathe love for both of you.

ABSTRACT

Introduction: The cost of providing antiretroviral therapy (ART) remains a significant economic burden on African countries due to poverty and a lack of resources. To reduce the economic burden of HIV infection, a formulation scientist must use the limited resources available in Africa to develop drug dosage forms of antiretrovirals (ARVs) that are cost-effective, adaptable, and accessible, as well as result in successful therapeutic outcomes of HIV/AIDS treatment, raise the average life expectancies of HIV-positive adults, and increase the availability of the limited resources for other purposes. According to the literature, lamivudine (3TC) is still used in first-line HIV treatment regimens, and several 3TC-based fixed-dose combinations (FDCs) are on the market. These FDCs are typically relatively large and require patients to take medication daily. As a result, patients will accept a flexible dosage form that can be ingested once and provides adequate therapeutic efficacy for more than 24 hours, thereby increasing treatment adherence, decreasing drug resistance, and improving therapeutic efficacy. Formulation scientists must create dosage forms that provide better patient treatment and patient experience, focusing on patient-centred medicine development. Hence, this study focused on 3TC and tenofovir disoproxil fumarate (TDF), which are still among the cornerstones of many HIV treatment regimens.

Aim: The goal of this study was to investigate the development of 3TC- and TDF-loaded polymeric microparticles (P-MPs) with varying drug release profiles using natural polymers (Chitosan (CH), gelatin (GEL), xanthan gum (XG), and sodium alginate (SA)) and low-cost preparation methods (ionic gelation and spray drying) to achieve a cost-effective solution for patient-oriented HIV treatment.

Methods: The physicochemical properties of the drugs, excipients, and drug-excipient compatibility were determined before incorporated into a drug delivery system using different analytical techniques like hot stage microscopy (HSM), differential scanning calorimetry (DSC), thermogravimetric analysis (TGA), Fourier-Transform infrared spectroscopy (FTIR), powder X-ray diffraction (PXRD), and high-performance liquid chromatography (HPLC). The 3TC- and TDF-loaded P-MPs were made using ionic gelation and an optimised spray drying process with various natural polymers and experimental parameters. This study was informative because the resulting drug-loaded microspheres could be further formulated into tablets, capsules, or powders. DSC, TGA, FTIR, PXRD and scanning electron microscopy (SEM) were used to determine the

physiochemical properties of the drug-loaded polymeric microspheres. The production yield, content uniformity, moisture content, drug loading, and encapsulation efficiency (%EE) of the formulated 3TC- and TDF-loaded P-MPs were determined. The *in vitro* dissolution testing was performed at pH 1.2 to simulate the gastric condition in the stomach, and the rate of drug release from the polymeric matrix system was quantified using a newly developed and validated HPLC method.

Results: The physicochemical results revealed that both 3TC and TDF raw materials were crystalline, and that 3TC existed as Form II and TDF as Form I. The drug-excipient(s) compatibility studies revealed no interaction between 3TC- or TDF-polymer(s) in physical combinations or seven days isothermal stress testing.

The results of the different formulated drug-loaded P-MPs by ionic gelation method varying polymers, such as production yield, content uniformity, drug loading and encapsulation efficiency (%EE), and *in vitro* dissolution testing in pH 1.2 medium, revealed that the SA-GEL-calcium chloride polyelectrolytes complexation matrix system provided sustained release of a highly hydrophilic drug with drug release sustained at +/- 85% for a period of 6 hours with a decline in dissolved 3TC observed only after 5 hours. Due to the rigid polymeric structure formed with SA, microspheres prepared from high concentrations of GEL (10% w/v) in both GEL-SA- and GEL-SA (plus 1% w/v CH)-calcium chloride polyelectrolyte complexation can significantly retain 3TC in their matrix. Notably, the 3TC-loaded 1% w/v CH and 5% w/v SA-calcium chloride microspheres demonstrated a significantly slower onset of drug release compared to other prepared formulations, with $94.73 \pm 1.51\%$ of 3TC released in 40 minutes but maintaining a concentration of 95.70% over a 6-hour *in vitro* dissolution period.

This study demonstrated the successful preparation of 3TC-loaded spray dried PMPs. The DSC, TGA, FTIR, and PXRD measurements revealed that the physical state of 3TC in the GEL/ CH-GEL matrix system changed from crystalline to amorphous during the spray drying process, that 3TC was well encapsulated or incorporated into the wall-forming materials, and that there was strong intramolecular hydrogen bonding or interaction between 3TC molecules and the polymer(s) chains. During *in vitro* dissolution testing in pH 1.2 medium, the spray dried formulation of 3TC:GEL (5:10% w/v) demonstrated the best modified drug release with high production yield (64.50%), drug loading ($53.10\% \pm 0.213.05$), low moisture content (3.05%), and excellent %EE

(102.74 ± 1.67). Furthermore, spray-dried microspheres prepared from 3TC: CH-GEL (5:2:3% w/v) dissolved in a 1% w/v citric acid solution demonstrated reduced initial burst release followed by a steady and controlled release profile for 3TC for 7 hours at pH 1.2, with the highest concentration of 3TC being 97.63 ± 1.59%.

TDF-loaded spray-dried microspheres were successfully prepared from the natural polymer GEL. However, it is unnecessary to formulate a modified drug delivery system for TDF alone due to its known long plasma and intracellular half-lives. Nevertheless, the behaviour of TDF when subjected to the same microsphere processing techniques when incorporated in a supposed 3TC-microsphere-based FDC formulation or other ARV-modified release combinations must be investigated. The HSM, FTIR, and PXRD results of the TDF-loaded spray-dried microspheres showed a change in the solid-state form of the API, an average degree of TDF encapsulation in the gelatin matrix, and a weak drug-polymer interaction. The dissolution profile of 3TC:GEL (3:12 % w/v) in the pH 1.2 medium revealed a faster dissolution rate of TDF from the polymeric matrix of 109 ± 1.87% in 10 minutes, due to improved wetting caused by intimate contact between the drug molecules and a higher GEL concentration.

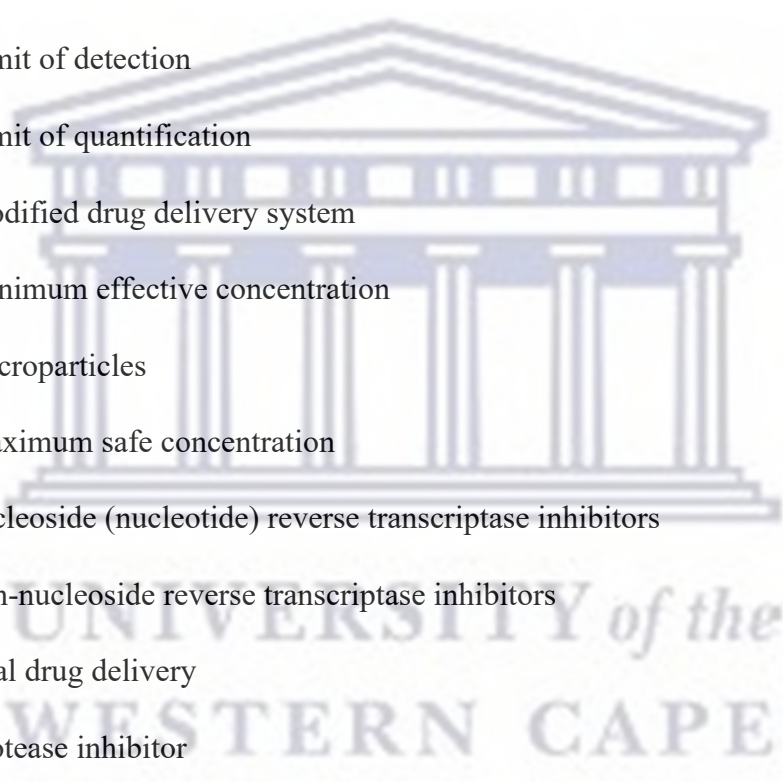
Conclusion: CH-GEL/ GEL-based drug-loaded microspheres can either enhance or retard the dissolution rate of the drug of the same biopharmaceutical classification system (BCS) class contained in its matrix, depending on the physical state of the drug in the polymeric matrix, drug-polymer interaction, polymer properties and polymer concentration.

Keywords: HIV/AIDS, cost-effective dosage forms, modified drug delivery systems, microspheres, ionic gelation, spray drying, natural polymers

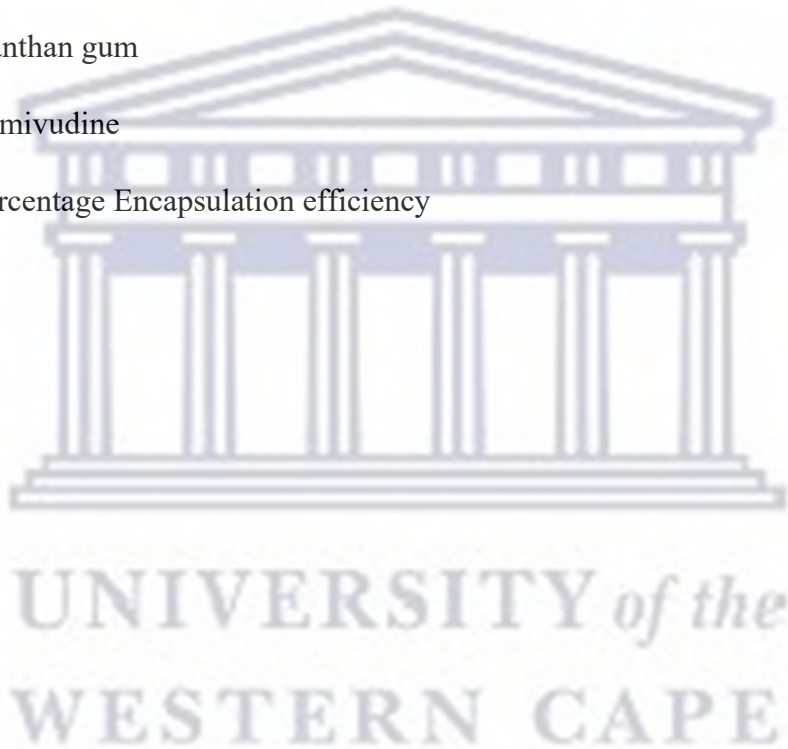
List of Abbreviations

AIDS	Acquired Immunodeficiency Syndrome
APIs	Active pharmaceutical ingredients
ART	antiretroviral therapy
ARVs	Antiretroviral drugs
BCS	Biopharmaceutical Classification System
BSA	Bovine serum albumin
CaCl ₂	Calcium chloride
CCR5	Chemokine co-receptor
CD ₄ ⁺	Clusters of differentiation 4
CH	Chitosan
CYP450	Cytochrome P450
DDSs	Drug delivery system
DSC	Differential scanning calorimetry
DTG	Dolutegravir
EC	Ethyl cellulose
EFV	Efavirenz
FDC	Fixed-dose combination
FTC	Emtricitabine
FT-IR	Fourier transform infrared
GEL	Gelatin
GIT	Gastrointestinal tract
gp120	Glycoprotein

HIP	HIV-infected people
HIV	Human Immunodeficiency Virus
HPLC	High-performance liquid chromatography
HSM	Hot stage microscopy
IEP	Isoelectric point
ICH	International Conference on Harmonization
LOD	Limit of detection
LOQ	Limit of quantification
MDDS	Modified drug delivery system
MEC	Minimum effective concentration
MPs	Microparticles
MSC	Maximum safe concentration
NRTIs	nucleoside (nucleotide) reverse transcriptase inhibitors
NNRTIs	non-nucleoside reverse transcriptase inhibitors
ODD	Oral drug delivery
PI	Protease inhibitor
PHBV	Poly(3-hydroxybutyrate-co-3-hydroxy valerate)
PLGA	Poly(lactide-co-glycolide)
PM	Physical mixture
P-MPs	Polymeric microparticles
PXRD	Powder X-ray diffraction
SA	Sodium alginate
SD	Spray dried



TDF	Tenofovir disoproxil fumarate
T_g	Glass transition temperature
TGA	Thermogravimetric analysis
TPP	Tripolyphosphate
WHO	World Health Organization
W/O	Water in oil
XG	Xanthan gum
3TC	Lamivudine
% EE	Percentage Encapsulation efficiency



Publications and Conferences

Academic output

Part of this research was published internationally

Research paper: The validation of a simple, robust, stability-indicating RP-HPLC method for the simultaneous detection of lamivudine, tenofovir disoproxil fumarate, and dolutegravir sodium in bulk material and pharmaceutical formulations.

Omobolanle Ayoyinka Omoteso¹ Marnus Milne² and Marique Aucamp¹

¹School of Pharmacy, University of the Western Cape, Bellville, Cape Town, 7530, South Africa

²School of Pharmacy, Sefako Makgatho Health Sciences University, Ga-Rankuwa, Pretoria 0208, South Africa

Omobolanle Ayoyinka Omoteso, Marnus Milne, Marique Aucamp. (2022). The validation of a simple, robust, stability-indicating RP-HPLC method for the simultaneous detection of lamivudine, tenofovir disoproxil fumarate, and dolutegravir sodium in bulk material and pharmaceutical formulations. Hindawi International Journal of Analytical Chemistry Volume 2022, Article ID 3510277, 11 pages <https://doi.org/10.1155/2022/3510277>. (Appendix I)

Conferences attended

The effect of spray-dried gelatin on the encapsulation, physicochemical and the release properties of selected antiretroviral-loaded polymeric microparticles, (2023). Omobolanle Ayoyinka Omoteso, Marique Aucamp At the 8th Annual Research Symposium of School of Pharmacy, University of the Western Cape, South Africa.

Table of Contents

Declaration

Dedication

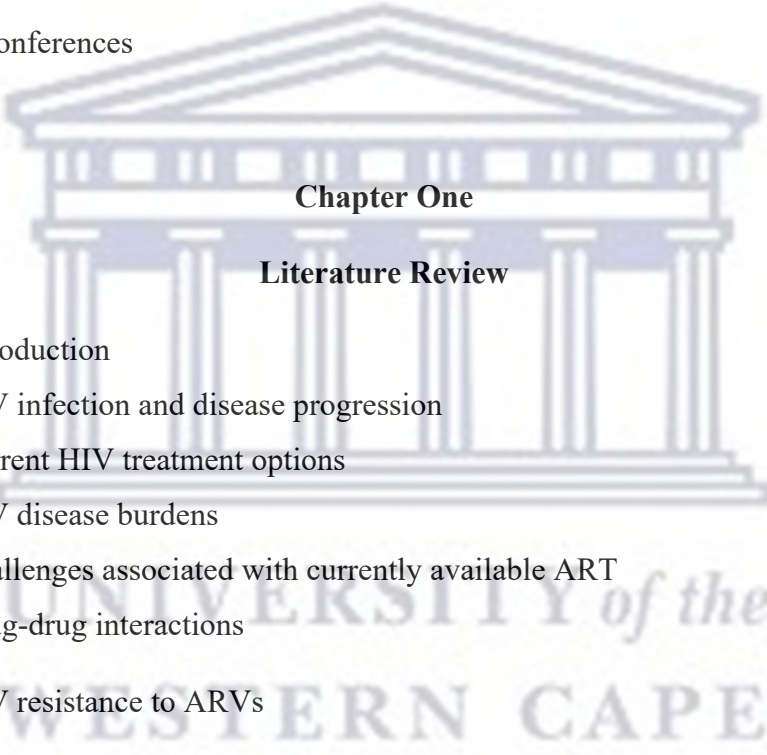
Acknowledgements

Abstracts

List of abbreviations

Publications and conferences

Table of contents



Chapter One

Literature Review

1.1	Introduction	1
1.2	HIV infection and disease progression	2
1.3	Current HIV treatment options	3
1.4	HIV disease burdens	4
1.5	Challenges associated with currently available ART	6
1.5.1	Drug-drug interactions	6
1.5.2	HIV resistance to ARVs	6
1.5.3	Adherence to ART	7
1.5.4	Bioavailability of orally administered ARVs	7
1.6	Proposed solutions for HIV burdens through drug dosage form development	9
1.7	Fixed-dose combinations (FDCs)	9
1.7.1	Benefits of FDC therapies	10
1.7.2	Drawbacks of FDC therapies	11

1.7.3	Types of fixed-dose combinations (FDCs)	12
1.7.3.1	Monolithic systems	12
1.7.3.2	Multi-layered system	13
1.7.3.3	Multi-particulate systems	13
1.8	Microparticles (MPs) as multi-particulate drug delivery systems	14
1.8.1	The design and formulation of polymeric microparticles (P-MPs) for oral drug delivery	17
1.8.1.1	Physical size of P-MPs	17
1.8.1.2	Physico-chemical properties of API to be incorporated into P-MPs	17
1.8.1.3	Typical polymers used for the preparation of P-MPs	18
1.8.1.4	Polymeric microparticle (P-MP) synthesis methods in relation to processability	19
1.8.1.4(a)	Solvent extraction/evaporation involving a single emulsion process	19
1.8.1.4(b)	Solvent extraction/evaporation involving double (multiple) emulsion process	20
1.8.1.4(c)	Spray drying method	20
1.8.1.5(d)	Coacervation (phase separation) method	21
1.8.1.5(e)	Hot melting method	22
1.8.1.5(f)	Ionic gelation	22
1.8.1.5(g)	Electrospraying method	23
1.8.2	Application of P-MPs in ARV delivery	23
1.9	Hypothesis on possible solutions	24
1.10	Motivation for this study	25

1.11	Study aim	25
1.12	Objectives	25
1.13	References	27

Figures and Tables

Figure 1.1:	Human immunodeficiency virus (HIV) (Sampson & Workman, 2016).	3
Figure 1.2:	Monolithic fixed-dose combination system (Fernández-García <i>et al.</i> , 2020).	12
Figure 1.3:	Multi-layer fixed-dose combination system (Fernández-García <i>et al.</i> , 2020).	13
Figure 1.4:	Multi-particulate fixed-dose combination system (Fernández-García <i>et al.</i> , 2020).	14
Figure 1.5:	The two types of microparticles (microcapsule and microsphere) (Lengyel <i>et al.</i> , 2019).	15
Figure 1.6:	Typical methods used in the preparation of drug-loaded P-MPs (Das <i>et al.</i> , 2019; Fontes <i>et al.</i> , 2012; Li <i>et al.</i> , 2008; Shi <i>et al.</i> , 2020; Lin & Yu, 2000; Malik <i>et al.</i> , 2016; Timilsena <i>et al.</i> , 2017).	19
Table 1.1:	A summary of the advantages P-MPs may offer in terms of FDC formulation and to patients (Bale <i>et al.</i> , 2016; Campos <i>et al.</i> , 2013; Deshmukh & Mohite, 2017; Farooq <i>et al.</i> , 2015; Lengyel <i>et al.</i> , 2019; Meghna <i>et al.</i> , 2017; Princely <i>et al.</i> , 2016; Vasir <i>et al.</i> , 2003).	16

Chapter Two

The physicochemical characteristics of lamivudine and tenofovir disoproxil fumarate and an overview of natural polymers explored as part of polymeric microsphere formulation

2.1	Introduction	44
2.2	Lamivudine (3TC)	44
2.2.1	Physicochemical and pharmacokinetic properties of 3TC	45
2.3	Tenofovir disoproxil fumarate (TDF)	46
2.3.1	Physicochemical and pharmacokinetic properties of TDF	47
2.4	Natural Polymers used in pharmaceutical preformulation and formulation	48
2.4.1	Chitosan (CH)	49
2.4.2	Gelatin (GEL)	50
2.4.3	Xanthan gum (XG)	51
2.4.4	Sodium alginate (SA)	53
2.5	Conclusion	59
2.6	References	60

Figures and Tables

Figure 2.1:	The chemical structure of 3TC (Harris <i>et al.</i> , 1998).	45
Figure 2.2:	The chemical structure of TDF (Pubchem, 2022a).	47
Figure 2.3:	The chemical structure of chitosan (Pubchem, 2022c).	50
Figure 2.4:	The chemical structure of Gelatin (Devi <i>et al.</i> , 2017).	51
Figure 2.4:	The chemical structure of Xanthan gum (Jansson <i>et al.</i> , 1975).	52

Figure 2.6: The chemical structure of Sodium alginate (Foroughi *et al.*, 2018). 53

Table 2.1: A summary of the physicochemical and functional properties playing significant roles in P-MP synthesis and possible drug release mechanisms for CH, GEL, XG and SA (Aguero *et al.*, 2017; Khan & Ram, 2014; Lengyel *et al.*, 2019; Mishra & Rautray, 2020). 54

Chapter Three

Materials and Methodology

3.1	Introduction	70
3.2	Materials	70
3.3	Methodology	70
3.3.1	Physicochemical characterisation of pure APIs, excipients and prepared microspheres	70
3.3.1(a)	Hot stage microscopy (HSM)	70
3.3.1(b)	Differential Scanning Calorimetry (DSC)	71
3.3.1(c)	Thermogravimetric analysis (TGA)	72
3.3.1(d)	Fourier-Transform infrared spectroscopy (FTIR)	72
3.3.1(e)	Powder X-ray diffraction (PXRD)	73
3.3.1(f)	High-performance liquid chromatography (HPLC)	73
3.3.2	Preparation of microspheres	74
3.3.2(a)	Formulation of drug-loaded microspheres <i>via</i> ionic gelation	74
3.3.2(b)	Formulation of drug-loaded microspheres by spray-drying	76
3.3.2.1	Physicochemical characterisation of drug-loaded microspheres	76
3.3.2.1(a)	Percentage yield	76

3.3.2.1(b)	Content uniformity, drug loading and encapsulation efficiency (% EE)	77
3.3.2.1(c)	Characterisation of drug-loaded microspheres	77
3.3.2.1(d)	Swelling behavior	77
3.3.2.1(e)	<i>In vitro</i> dissolution testing	78
3.3.3	Drug-excipient compatibility studies	78
3.3.3(a)	Preparation of compatibility testing samples	80
3.3.3(b)	Examination of organoleptic properties	80
3.3.3(c)	Isothermal Stress Testing (IST)	81
3.4	Conclusion	81
3.5	References	82

Figures and Tables

Figure 3.1:	Summary of the types of drug-drug or drug-excipient incompatibilities (Di Perri <i>et al.</i> , 2005; Jeličić <i>et al.</i> , 2020; Jeličić <i>et al.</i> , 2021).	79
Figure 3.2:	Decision tree for drug-drug and drug-excipient compatibility study (Chadha & Bhandari, 2014; Chaves <i>et al.</i> , 2013).	80

Chapter Four

The formulation of lamivudine- and tenofovir disoproxil fumarate-loaded microparticles

4.1	Introduction	86
4.2	Physicochemical characterisation of 3TC and TDF, and drug-excipient compatibility studies	86
4.2.1	Thermal analyses of 3TC and TDF	86
4.2.2	Fourier-Transform infrared spectroscopy of 3TC and TDF	89

	raw material	
4.2.3	Powder X-ray diffraction of 3TC and TDF raw material	90
4.3	Investigation of ionic gelation as a potential formulation method for 3TC-loaded microspheres	92
4.3.1	A screening study into formulation of 3TC-loaded microspheres	93
4.3.2	Investigation of 3TC-loaded microsphere formulation using higher SA and crosslinker concentrations	96
4.3.3	Conclusion on ionic gelation as a microsphere formulation strategy	101
4.4	Preparation of 3TC-loaded polymeric microparticles <i>via</i> spray drying	102
4.4.1	Optimisation of 3TC:polymer spray drying process	102
4.4.2	Determination of <i>in vitro</i> drug release from spray dried 3TC-loaded microspheres	105
4.4.3	Determination of the swelling behaviour of 3TC-loaded spray dried microspheres	107
4.4.4	The physicochemical properties of F2SD in comparison with 3TC, GEL and F2SD(PM)	108
4.4.5	Combination of GEL and CH as polymers for the formulation of 3TC-loaded microspheres by spray drying	118
4.4.6	<i>In vitro</i> dissolution testing and physicochemical characterization of F1cSD	119
4.4.7	Conclusion on the formulation of 3TC-loaded microspheres by incorporating CH into the polymeric network	125
4.5	Formulation of TDF-loaded microspheres <i>via</i> spray drying	126

4.5.1	Drug release determination from spray-dried TDF loaded microspheres	128
4.6	Conclusion	136
4.7	References	141

Figures and Tables

Figure 4.1:	DSC thermogram obtained with 3TC with inset (a) depicting the morphology of 3TC raw material at ambient temperature and (b) micrograph captured of molten 3TC at $\cong 184.0$ °C.	87
Figure 4.2:	DSC thermogram obtained with TDF raw material with inset (a) depicting the onset of the first melting event of TDF raw material at $\cong 114.0$ °C and (b) micrograph captured of the onset of the second melting endotherm of TDF raw material at $\cong 118.0$ °C.	88
Figure 4.3:	An overlay of the TGA traces obtained with 3TC and TDF raw material.	89
Figure 4.4:	The FTIR spectra obtained for (a) 3TC raw material and (b) TDF raw material.	90
Figure 4.5:	The PXRD diffractograms obtained for 3TC and TDF raw material.	91
Figure 4.6:	<i>In vitro</i> release profiles of 3TC from drug-loaded microspheres prepared <i>via</i> ionic gelation using various natural polymers.	99
Figure 4.7:	3TC release from F1b - F6b microsphere formulation only depicting the 3TC concentrations quantified during the first 20 minutes of <i>in vitro</i> dissolution testing.	100
Figure 4.8:	A picture indicating remaining residue on the spray dryer glassware post spray drying of a 1:1 3TC:GEL feed solution	103

with 3TC and GEL solubilised in distilled water.

- Figure 4.9:** An overlay of the in vitro dissolution results obtained with 3TC raw material, F1SD(PM), F1SD, F2SD(PM), F2SD, F3SD(PM) and F3SD in pH 1.2 dissolution medium at 37 ± 0.5 °C. 106
- Figure 4.10:** The swelling behavior of 3TC-loaded gelatin microspheres formulations at pH-1.2 and pH-6.8 at ambient temperature over a period of 24 hours. 108
- Figure 4.11:** DSC thermograms of (a) pure 3TC, (b) GEL, (c) F2SD(PM) and (d) F2SD. 109
- Figure 4.12:** The overlay of TGA thermograms obtained for 3TC raw material, GEL, F2SD(PM) compared to F2SD during heating at a rate of 10°C/min from 30 to 600 °C. 111
- Figure 4.13:** FTIR spectrum pure of 3TC, GEL, F2SD(PM) compared to F2SD obtained at ambient temperature within a scanning range of 650 - 4000 cm^{-1} . 113
- Figure 4.14:** The PRXD patterns obtained for 3TC, GEL, F2SD(PM) compared to F2SD at room temperature within a scanning limit of 4 - 40° 2 θ . 117
- Figure 4.15:** Overlay of the dissolution profiles obtained for 3TC raw material in comparison with F1cSD and F1cSD(PM). 120
- Figure 4.16:** DSC thermograms obtained for (a) F1cSD(PM) and (b) F1cSD. 121
- Figure 4.17:** FTIR spectrum pure of 3TC, F1cSD(PM) compared to F1cSD obtained at ambient temperature within a scanning range 122

of 650 - 4000 cm^{-1} .

- Figure 4.18:** Overlay of PXRD diffractograms obtained with (a) 3TC raw material, (b) F1cSD(PM) and F1cSD. 124
- Figure 4.19:** Overlay of the dissolution profiles obtained for TDF raw material in comparison with F5SD, F5SD(PM), F6SD, F6SD(PM), F7SD and F7SD(PM) in pH 1.2 dissolution medium at 37 ± 0.5 °C. 129
- Figure 4.20:** DSC traces obtained for (a) TDF raw material, (b) GEL, (c) F7SD(PM) and (d) F7SD. 130
- Figure 4.21:** FTIR spectrum pure of TDF, GEL, F7SD(PM) compared to F7SD obtained at ambient temperature within a scanning range of 650 - 4000 cm^{-1} . 132
- Figure 4.22:** The PRXD patterns obtained for TDF, GEL, F7SD(PM) compared to F7SD at room temperature within a scanning limit of 4 - 40° 2 θ . 135
- Table 4.1:** Outline of different polymers investigated in combination with SA and calcium chloride as crosslinkers in the first phase of the study on 3TC microencapsulation 94
- Table 4.2:** Outline of different polymers investigated in combination with SA and calcium chloride as crosslinkers in the first phase of the study on 3TC microencapsulation 98
- Table 4.3:** The 3TC and polymer concentration, percentage yield (%), moisture content, drug loading (%) and encapsulation efficiency 105

(%EE) obtained with the three 3TC:polymer feed solutions as obtained from optimisation efforts

Table 4.4:	The summary table for pure 3TC, GEL, F2SD and F2SD(PM) outlining the onset of degradation temperatures and percentage mass losses acquired between 30 to 600 °C at 10°C/min. and polymer chains (Yin <i>et al.</i> , 2009).	111
Table 4.5:	Table of 3TC and GEL chemical structures describing the wavenumbers depicted in FTIR analysis with corresponding functional groups when compared to F2SD(PM) and F2SD` absorption spectra.	115
Table 4.6:	Outline of CH-GEL combinations dissolved in a 1% w/v CA-solution spray dried for the formulation of 3TC-loaded Microspheres	118
Table 4.7:	Outline of TDF:GEL ratios which were dissolved in 10 %v/v ethanolic solution and subsequently spray dried	127
Table 4.8:	Table of TDF and GEL chemical structures describing the wavenumbers depicted in FTIR analysis with corresponding functional groups when compared to F7SD(PM) and F7SD` absorption spectra.	133

Chapter Five

Concluding remarks

5.1	General conclusions	153
5.2	References	158

Appendix I

161

Appendix II

172



UNIVERSITY *of the*
WESTERN CAPE

Chapter One

Literature Review

1.1 Introduction

Acquired Immunodeficiency Syndrome (AIDS) caused by infection with the Human Immunodeficiency Virus (HIV) is a debilitating disease that affects over 39 million people worldwide (WHO, 2023). The treatment goals for antiretroviral therapy are as follows: complete and long-term suppression of viral replication, improvement of Clusters of differentiation 4 (CD₄⁺) cell counts to support immune function, improvement in the quality of life of HIV-infected people (HIP), and reduction of HIV-associated infection and mortality (Rathbun *et al.*, 2006).

In terms of treatment, the oral route of drug administration is the most feasible and universally acceptable route for all patients of all ages. HIV positive patients are burdened with the use of antiretroviral drugs (ARVs) every day of their lives, leading to stigmatisation, poor patient adherence, and the development of drug resistance. Also, because of the poor pharmacokinetic properties of conventional ARVs due to first-pass metabolism, erratic absorption and degradation in the gastrointestinal tract (GIT), oral administration of these drugs will naturally result in fluctuation of drug concentration in the systemic circulation. However, this frequently results in the inability to maintain a desired therapeutic level of the drug(s) for an extended period of time (Eagling *et al.*, 2002; Ramana *et al.*, 2014). Inevitably, increased dosing frequency for the patient, potentially increasing non-adherence to antiretroviral therapy (ART), leads to virologic and immunologic therapeutic failure (Gunaseelan *et al.*, 2010; Ramana *et al.*, 2014; Vyas *et al.*, 2006).

As a result, the development of fixed-dose combination (FDC) dosage forms of ARVs through utilisation of a modified drug delivery system (MDDS) is required to overcome the aforementioned burdens and limitations and to improve patient treatment efficacy (Ramana *et al.*, 2014). As disease treatment strategies become more patient-centred, the evolution of DDSs are critical in altering the pharmacodynamics, biopharmaceutical, and pharmacokinetic behaviour of conventional dosage forms (Padalkar *et al.*, 2011). MDDSs are typically designed to effectively transport active pharmaceutical ingredients (APIs) in the body while also controlling a specifically designed release mechanism for one or more of the incorporated drugs (Vilos & Velasquez, 2012).

Pharmaceutical formulators rely on various drug carriers, either combined or as single systems, to achieve specifically designed drug targeting and tailored drug release mechanisms. Typical examples of MDDSs include nanoparticles, osmotic pumps, dendrimers, micelles, microspheres, liposomes, and hydrogels. These DDSs are primarily investigated to achieve efficient targeted and/or extended drug delivery, increase the bioavailability of drugs with low aqueous solubility or permeability across epithelial cells, and prevent drug degradation in the gastro-intestinal tract (GIT).

1.2 HIV infection and disease progression

HIV is spread from infected to uninfected persons through mucosal contact (semen, anal and vaginal secretion), maternal-infant contact (during pregnancy, delivery, and breastfeeding), blood transfusion, and percutaneous inoculation (reusing or sharing needles or sharp objects infected with HIV blood) (Coovadia, 2004; Klimas *et al.*, 2008; Lucas, 2001). Acute HIV illness manifests itself as rashes and a flu-like syndrome a few weeks after HIV infection. This early stage of HIV disease is marked by a steady decline in immune system effectiveness (Klimas *et al.*, 2008). HIV attacks the immune system by inserting its viral genes into host cells for reproduction. The virus binds to the host cell's T-helper lymphocytes (CD_4^+) and macrophages *via* the envelope glycoprotein (gp120) protein (**Figure 1.1**) (Littman, 1998). The entry of HIV into these target cells occurs in stages, with the first being the adsorption of HIV to the host cell's surface. This step brings the virus into close proximity to the host cell, putting it in the best position to interact with the host cell's surface receptors and co-receptors. This is possible because the negatively charged gp120 protein attracts positively charged heparan sulphate molecules on the host cell surface (De Clercq, 2002; Kumari & Singh, 2012). The second step is for HIV to bind to a CD_4^+ receptor and a chemokine co-receptor (CCR5 or CXCR4) *via* the gp120 protein, resulting in the formation of a viral envelope (De Clercq, 2002; Kumari & Singh, 2012). The third step is the fusion of the viral envelope with gp41, followed by virus entry into the host or target cells. CD_4^+ T-cells, follicular dendritic cells, CD_4^+ monocytes or macrophages, intestinal immunocytes, microglial cells, epidermal Langerhans' cells, and dendritic cells are all examples of host cells (Gunaseelan *et al.*, 2010; Kazmierski *et al.*, 2006; Kumari & Singh, 2012; Sierra *et al.*, 2005; Warr & Šljivić, 1974).

CD4⁺ cells are important in the immune response (Fahey *et al.*, 1990; Klimas *et al.*, 2008). A healthy person exhibits a CD4⁺ cell count between 800 and 1200 cells/mm³ of blood (Klimas *et al.*, 2008). Half of the immune system cells are damaged when the CD4⁺ cell count falls below 500 cells/mm³ (Klimas *et al.*, 2008; Mirchandani & Chien, 1993). If the CD4⁺ cell count falls below 200 cells/mm³ of blood, patients become vulnerable to life-threatening opportunistic infections such as tuberculosis, *pneumocystis carinii* pneumonia (PCP), and cancer, leading to AIDS (Mirchandani & Chien, 1993).

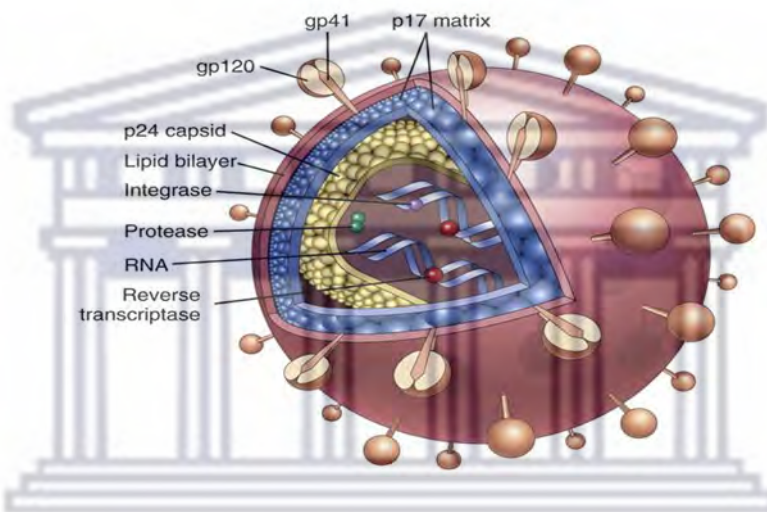


Figure 1.1: Human immunodeficiency virus (HIV) (Sampson & Workman, 2016).

1.3 Current HIV treatment options

The 2021 World Health Organization (WHO) Consolidated Guidelines recommended a first-line regimen consisting of two nucleoside (and nucleotide) reverse transcriptase inhibitors (NRTIs), particularly tenofovir disoproxil fumarate (TDF) combined with lamivudine (3TC) and a third drug from the non-nucleoside reverse transcriptase inhibitors (NNRTIs), such as efavirenz (EFV) or an integrase inhibitor. More successful treatment outcomes are achieved following such a treatment regimen. To reduce treatment costs and increase patient tolerability, the WHO recommended an alternative first-line treatment regimen that replaced the key first-line drug, EFV, with an integrase inhibitor, dolutegravir (DTG), particularly in low-income countries (Bhatti *et al.*, 2016; Dellar & Karim, 2015; Lee *et al.*, 2014; WHO, 2021).

When the first-line NNRTI (EFV-based treatment) fails, two NRTIs plus a boosted protease inhibitor (PI) are recommended as second-line antiretroviral therapy (ART). When first and

second-line ART fails, the WHO recommends using integrase inhibitors in combination with second-generation NNRTIs and protease inhibitors (Bhatti *et al.*, 2016; Lee *et al.*, 2014; WHO, 2021).

According to the July 2018 WHO HIV Treatment Interim Guidance, DTG with a nucleoside reverse-transcriptase inhibitor backbone is the ideal second-line regimen for HIV patients for whom non-DTG-based regimens are ineffective. Furthermore, a DTG-based regimen consisting of TDF, 3TC, and DTG is recommended as an ideal first-line regimen for adults and adolescents starting ART with HIV (WHO, 2018a). The DTG-based regimen was recommended due to the association of the EFV-based regimen with short and long-term adverse events such as pre-treatment drug resistance and acquired drug resistance in a large number of HIV-positive patients (WHO, 2017). This is superior to EFV-based treatments in several ways: (a) DTG-based regimens are more potent by suppressing viral load faster, (b) increasing CD4⁺ count recovery speed, and (c) reducing the risk of therapy discontinuation compared to EFV-based regimens (Fettiplace *et al.*, 2017; WHO, 2018a; WHO, 2018b).

1.4 HIV disease burdens

When compared to other infectious diseases that affect humans, HIV is the leading cause of death (Klimas *et al.*, 2008). According to the most recent WHO statistics, over 40 million people have succumbed since the beginning of this epidemic. Globally, more than 39 million people were infected with HIV in 2022, and currently there is still no cure for this debilitating disease (WHO, 2022). HIV infection is associated with a number of burdens and this study was motivated by the burdens associated with HIV infection.

Globally, HIV infection remains an economic burden on all continents, particularly Africa (Waziri *et al.*, 2016). As a result of HIV disease progression, the vast majority of HIV patients develop AIDS (Waziri *et al.*, 2016). The increasing AIDS-associated death rate as well as AIDS patients requiring extensive medical care, the significant loss of skilled population and thereby the labour force gives rise to HIV/AIDS having a negative impact on economic growth (Dauda, 2018; Odugbesan & Rjoub, 2019; Waziri *et al.*, 2016). Because of poverty and a lack of resources, funding, and infrastructure to improve nutrition and health care systems, as well as a lack of available and affordable medicine, HIV/AIDS is highly prevalent in developing countries. Furthermore, significant funds are continuously diverted to disease management through the

development of prevention strategies, treatments and health information systems for tracking people infected with HIV (Rosen & Fox, 2011). The number of patients receiving antiretroviral (ARV) treatment has grown over time, with Africa having the highest number of patients on antiretroviral therapy (ART) (Miantezila Basilua *et al.*, 2021). According to Abah's research, the cost of providing ART places a significant economic burden on African countries (Abah, 2020).

It is a well-known fact that HIV infection causes severe immunosuppression and therefore in comparison with healthy individuals HIV-infected patients are more susceptible to chronic diseases such as cancer, liver cirrhosis, cardiovascular diseases, diabetes, to name but just a few (CDC, 2017; Kwong, 2021; Rathbun *et al.*, 2006; Van Epps & Kalayjian, 2017; Yang *et al.*, 2019). Considering this, it is clear that HIV/AIDS places a significant burden on the health care sector of developing countries.

Other than the effect this disease has on economic growth and the health care systems of affected countries, the associated stigma is a significant contributor to the HIV/AIDS epidemic, especially in low-income communities (Campbell *et al.*, 2011). Currently, HIV infection cannot be cured; instead, it must be managed and treated. For some patients the action of taking ARVs throughout their lives goes hand-in-hand with stigma and discrimination, which is very traumatic and leads to non-adherence to the antiretroviral regimen (Sayles *et al.*, 2009). Shame and isolation from family members and the community are examples of HIV-related stigma. Because these individuals are afraid of being stigmatised, such individuals avoid getting tested in time before disease progression, which results in continuous HIV transmission from infected people to others. Furthermore, due to the associated stigma many patients refuse to collect their chronic medicine from pharmacies, clinics or hospitals thus not receiving the required treatment (Mbonu *et al.*, 2009; Rankin *et al.*, 2005; Rintamaki *et al.*, 2006). Therefore, finding better solutions to provide effective ART to infected patients will significantly reduce the global impact of HIV disease. ARV dosage forms that could improve the current poor adherence to ART could improve patients' livelihoods. These include strategies such as formulating dosage forms that requires less frequent dosing, combining several ARVs into single dosage forms to reduce the number of dosage forms and even to improve ARV bioavailability in an effort to reduce the negative effects associated with higher doses.

1.5 Challenges associated with currently available ART

1.5.1 Drug-drug interactions

Drug interactions are typically the result of taking multiple medications concurrently. These interactions can result in therapeutic failure or drug toxicity. Some ARVs are susceptible to drug interactions because they are metabolised in the liver by cytochrome P450 (CYP450) isoenzymes. Integrase inhibitors, NRTIs, and fusion inhibitors show negligible drug interactions because they are not subjected to CYP450 hepatic metabolism, whereas chemokine receptor inhibitors, PIs, and NNRTIs are extremely susceptible to drug interactions due to their high CYP450 isoenzyme metabolism. Furthermore, the pharmacokinetic properties of PIs and NNRTIs can reduce the efficacy of concurrent drugs that are typically metabolised *via* the CYP450 system (Clarke, 2008; Rathbun *et al.*, 2006).

When certain classes of ARVs are co-administered with anti-tuberculosis drugs, numerous treatment complications may arise. Rifamycins also undergo hepatic metabolism *via* CYP450 and therefore the use of PIs and NNRTIs with rifamycins can reduce the pharmacokinetic properties of the anti-tuberculosis drug. It is further well-known that these classes of ARVs can alter the plasma concentration of any drug that is metabolised by CYP450 enzymes. Changes in antitubercular pharmacokinetic parameters can result in toxicity, loss of or reduced efficacy, or the emergence of intolerance. When HIV and tuberculosis drugs are co-administered, drug-drug interactions can result in therapeutic failure, toxicity, and intolerance (Di Perri *et al.*, 2005; Rathbun *et al.*, 2006).

1.5.2 HIV resistance to ARVs

Changes in the HIV virus' genetic code causes changes in the proteins used for replication, such as reverse transcriptase, protease, and integrase enzymes (Liao *et al.*, 2013). When HIV-infected patients do not receive prompt treatment or adhere to their ART diligently, the virus mutates and develops resistance to treatment (drug-resistant mutations), making viral suppression and CD4⁺ cell count improvement difficult. HIV drug resistance can occur before or after ART treatment. Some naive patients may have acquired a mutated HIV strain during transmission, this is known as transmitted/primary HIV drug resistance. The other type of HIV drug resistance occurs when

infected patients do not adhere to their treatment regimens; this is referred to as acquired/secondary HIV drug resistance (Marin *et al.*, 2022; Nadia & Elvira, 2022).

Despite the fact that HIV is being treated with multiple drugs at the same time, drug resistance still occurs. It was expected that if HIV developed resistance to one of the multiple drugs co-administered, the other drugs would suppress the viruses' resistance, ensuring the treatment's efficacy. A study by Feder *et al.* (2021) used various models to demonstrate the patterns of multi-drug resistance in HIV. The results revealed that the use of multiple drugs, is successful in converting HIV from a fatal condition to a chronic condition, that HIV mutation to drugs is unavoidable because the concentration of these agents cannot be maintained at the optimum therapeutic level at all times (Feder *et al.*, 2021; Gupta & Jain, 2010; Hogg *et al.*, 1999; McCluskey *et al.*, 2019).

1.5.3 Adherence to ART

Poor adherence to therapy in HIV treatment has the potential to affect outcomes on multiple levels. Treatment adherence is commonly regarded as an important factor in achieving optimal results across a wide range of disease states. Poor ART adherence is associated with less effective viral suppression, putting the patient's immediate health at risk as well as the possibility of developing long-term treatment resistance to that specific agent or class of agents within a specific combination therapy regimen. As a result, both treatment costs and therapy options may be impacted. The complexity of therapeutic regimens (such as the number of dosage forms and frequency of dosing), social stigma, adverse effects of treatment, mental illness, low health literacy, a poor patient-physician relationship, drug abuse, and limited access to ART are all factors that contribute to poor adherence to ART (Bhatti *et al.*, 2016; Schaecher, 2013; Tadesse *et al.*, 2014). Pill burden is a significant issue in HIV treatment since taking multiple medications on a daily basis is time-consuming and often results in non-adherence. HIV-related comorbidities such as tuberculosis add to the pill burden. Aside from the multiple drugs used to manage HIV, the pill burden increases when antitubercular drugs are co-administered with ARVs (Rehman *et al.*, 2022).

1.5.4 Bioavailability of orally administered ARVs

The oral route is the most commonly used for drug administration, but it presents several challenges. When compared to other routes of administration, the main advantages of oral drug

delivery (ODD) are simplicity, suitability, convenience, safety, dosage form design flexibility, improved patient compliance, and cost-effectiveness. Gastrointestinal transit takes several hours, therefore, drug formulations can be altered to accommodate this feature. However, the shortcomings of this route of drug administration should be considered when developing dosage forms for oral administration. These limitations include erratic absorption and degradation of some drugs by enzymes and secretions of the GIT (Aulton & Taylor, 2013; Devi & Pai, 2006; Sosnik & Augustine, 2016). Furthermore, before reaching its target of action *via* systemic circulation, a drug must pass through specific biological phenomena, such as dissolution in gastrointestinal fluids, gut membrane permeability, and first-pass metabolism (Amidon *et al.*, 1995; Devi & Pai, 2006).

The majority of currently marketed ARVs are formulated as solid dosage forms such as tablets and capsules or liquid dosage forms such as solutions and suspension for oral administration, all of which are referred to as conventional dosage forms of ARVs. While oral dosage forms are convenient, delivery of ARVs as a conventional dosage form *via* this route suffers from the shortcomings mentioned above. The duration of action is constrained for all conventional oral dosage forms that are currently used since medication absorption is dependent on how long it remains in the gastrointestinal tract (GIT) after administration (Devi & Pai, 2006). Conventional ARV dosage forms, also known as immediate-release dosage forms, deliver or release the drug(s) as quickly as possible (Andonova, 2017). The concentration of ARVs available in the systemic circulation is determined by the 'therapeutic window,' which is defined as the drug concentration ranging above the minimum effective concentration (MEC) and below the maximum safe concentration (MSC), allowing therapeutic efficacy (Padalkar *et al.*, 2011). Immediate drug release will naturally cause a fluctuation in drug concentration between the MEC and MSC, which is highly dependent on the drug's pharmacokinetic and pharmacodynamic properties. However, this frequently results in the inability to maintain a desired therapeutic level of the drug(s) for an extended period of time. Inevitably, this will result in increased dosing frequency for the patient, potentially increasing the likelihood of patient non-compliance with the prescribed dosing intervals (Devi & Pai, 2006; Padalkar *et al.*, 2011).

Other drawbacks of conventional oral dosage forms of ARVs include decreased efficacy due to low bioavailability, which is caused by poor aqueous solubility. It is essential to maintain the

systemic drug concentration consistently above the target antiretroviral concentration throughout the course of treatment and to improve localisation and intracellular delivery of the drug in order to be successful in an effective therapy for AIDS. However, due to the low biological half-lives of many ARVs the conventional, immediate release dosage forms are fundamentally incapable of maintaining a consistent plasma level within the desired therapeutic range for an extended period of time. To compensate for these shortcomings, the ARV dose is increased, which may result in adverse patient reactions. Therefore, insufficient ARV concentrations at specific sites leads to difficulty in the eradication of this virus and may result in viral drug resistance (Devi & Pai, 2006; Panda *et al.*, 2014; Sosnik & Augustine, 2016).

1.6 Proposed solutions for HIV burdens through drug dosage form development

To begin, in order to reduce the economic burden of HIV infection, it is critical for a formulation scientist to effectively use the limited resources available in Africa to develop drug dosage forms of ARVs that are cost-effective and easily accessible. Secondly, to reduce or prevent HIV-associated diseases or comorbidities, the design and development of ARV dosage forms that are easier to swallow which could lead to successful ART to effectively reduce HIV disease progression. Thirdly, the development of ARV dosage forms that could result in fewer daily doses and inconspicuous dosing could potentially reduce the social burden associated with this disease.

The use of fixed-dose combinations (FDCs) ART to simplify dosing has been shown to improve HIV adherence (Schaecher, 2013). However, at this point in time all marketed ART FDCs offer immediate drug release, thereby not addressing the burdens related to patient adherence and stigmatisation. Considering this, an unaddressed need for FDC formulations that could provide controlled and sustained drug release exists. Such an MDDS should be able to provide consistent drug plasma levels of the ARVs within the desired therapeutic range for an extended period of time. Most importantly however, for the African context, such an MDDS should be cost-effective to manufacture. As a result, it is therefore important to thoroughly discuss FDCs as MDDS.

1.7 Fixed-dose combinations (FDCs)

The most important aspect of any disease treatment is achieving patient adherence to drug therapy. Researchers conducted several surveys to determine whether patients prefer single, combination, or FDC therapy. According to Melikian *et al.* (2002), switching patients from multiple tablets or

capsules to therapy utilising FDCs improved patient adherence significantly. FDCs are single dosage forms that contain two or more active pharmaceutical ingredients (APIs) with distinct pharmacological actions that are available in specific fixed doses (Desai *et al.*, 2013; Mitra & Wu, 2012). FDCs play important roles in the treatment of various diseases because they can be used to target both single and multiple diseases (Mitra & Wu, 2012; Podolsky & Greene, 2011). FDCs are now present in almost all therapies. The top diseases for which FDCs are used or developed are malaria, congestive heart failure, HIV, hypertension, tuberculosis, and diabetes. Furthermore, FDCs have been developed into formulations that can be administered *via* various routes such as oral, inhalation, and parenteral (Desai *et al.*, 2013; Melikian *et al.*, 2002; Mitra & Wu, 2012; Podolsky & Greene, 2011). Oral administration remains by far the most common route of administration for FDCs, followed by inhalation (Desai *et al.*, 2013).

1.7.1 Benefits of FDC therapies

One of the advantages of FDC therapies is a reduction in pill burden, which directly or indirectly leads to a reduction in HIV stigma and an increase in patient adherence (Sebaaly & Kelley, 2017). Taking multiple medications at the same time several times a day can lead to missed doses or treatment discontinuation. The most important factor for effective HIV treatment is consistent adherence to ART (Anderson & Bartlett, 2005; Bell, 2013). FDCs such as Combivir™ (zidovudine + lamivudine), Kaletra® (lopinavir + ritonavir), Truvada® (tenofovir + emtricitabine), and Epzicom® (abacavir + lamivudine) reduced pill burden by half (Podolsky & Greene, 2011). When compared to using individual drugs twice daily, the use of lamivudine/abacavir FDC combination one pill once daily improves both adherence and patient satisfaction (Anderson & Bartlett, 2005). In a study on patient satisfaction on ART, approximately half of the survey participants indicated dissatisfaction with using multiple therapy frequently. It was discovered that the patients were embarrassed to use their medications in public, that they sometimes forget to use their medications, and that it was very inconvenient to stop work or activities to use their drugs (Miller *et al.*, 2002).

FDC products are usually more cost effective to manufacture and it has been reported that the total wholesale price for two or more medications is usually higher than for a corresponding FDC regimen (Bell, 2013). Even the logistics of distributing and packaging FDCs are simplified, which may directly reduce formulation costs (Desai *et al.*, 2013; Sadia *et al.*, 2018). The development

of FDC regimens for a specific disease, such as HIV, has created a huge opportunity for easier life cycle management of these products in the market, as opposed to the cumbersome chain management for several monotherapies required to be co-administered for HIV treatment at the same time (Mitra & Wu, 2012).

FDC ART has better therapeutic outcomes than the maximum dose of a single medication or a combination of medications (Bell, 2013). Because of the additive effect of each API, reports show that FDCs for ART significantly improves clinical outcomes, due to dose reduction and a decrease in side effects (Mitra & Wu, 2012; Moriarty *et al.*, 2019). According to Scott Sutton *et al.* (2016), adherence to a single tablet regimen (a FDC consisting of two or more ARVs of different classes) resulted in exceptional viral suppression, leading to greater therapeutic outcomes. FDCs can also change the *in vivo* pharmacokinetic and pharmacodynamic parameters of the incorporated drugs through changes in the API release profiles (Moriarty *et al.*, 2019; Schlosser, 2019). An FDC of abacavir/lamivudine resulted in plasma HIV RNA suppression comparable to that obtained during administration of individual dosage forms. This formulation is also associated with lower lipotrophy and less metabolic distress and therefore improves patient tolerability (Anderson & Bartlett, 2005; Cohen *et al.*, 2008).

1.7.2 Drawbacks of FDC therapies

Even though there are several benefits associated with FDCs, it is critical to be aware of the disadvantages and take them into account when using regimens developed as FDC formulations. Firstly, many physicians are unfamiliar with the drug components in FDC, which may cause confusion. Unfortunately, when a patient is taking multiple medications, unsuitable therapy may occur, in which two different drugs from the same class are administered (Bangalore *et al.*, 2007). Secondly, because FDC formulations contain multiple drugs administered as a single dosing unit, determining the source of adverse drug reactions could prove to be difficult (Caplan *et al.*, 2018; Desai *et al.*, 2013). Thirdly, FDCs formulated as tablets or capsules for oral administration may result in fairly large dosage forms, thereby negatively affecting patient adherence (Caplan *et al.*, 2018; Desai *et al.*, 2013). The EFV-based regimen, for example, consists of TDF (300mg), 3TC (300mg) and EFV (600mg); however, this FDC consisting of 1200 mg API is a large tablet that could be difficult to swallow by many patients (WHO, 2016). Finally, FDCs can prevent dosing variation. The treatment of any disease should be patient-centred and therefore give rise to clinical

cases where FDC regimens are ineffective for some patients (Desai *et al.*, 2013; Xu *et al.*, 2012). Patients with renal or hepatic impairment, for example, will experience toxicity if they use a general FDC formulation; therefore, dosing adjustments are recommended when using individual drugs (Caplan *et al.*, 2018).

1.7.3 Types of fixed-dose combinations (FDCs)

FDCs are classified into three types based on the manner in which the API(s) are to be released from such a system. The different types include: (a) monolithic systems, (b) multi-layered systems and (c) multi-particulate systems, which will be discussed in more detail in the following sections.

1.7.3.1 Monolithic systems

These are single-layer formulations (**Figure 1.2**) and are the most commonly used FDC systems due to the simplicity associated with the manufacturing.

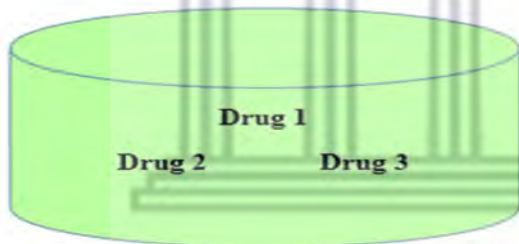


Figure 1.2: Monolithic fixed-dose combination system (Fernández-García *et al.*, 2020).

The dissolution profiles of each of the APIs used in the formulation are critical to the successful production of such a system. The APIs must have similar dissolution rates. The development of a monolithic FDC system of Biopharmaceutical Classification System (BCS) class II in combination with a BCS class III drug, for example, will not be appropriate. While APIs from these classes may show therapeutic compatibility, the differences in their solubility and subsequent permeability are critical and must be considered before formulation. BCS class III drugs can reduce BCS class II drug solubility, resulting in extremely variable bioavailability (Desai *et al.*, 2013). It should also be considered that drug-drug compatibility between APIs and significant differences in drug dose ratios can lead to segregation in monolithic FDC systems (Desai *et al.*, 2013; Fernández-García *et al.*, 2020).

1.7.3.2 Multi-layered system

This system is an improved version of the well-known traditional single-layer tablet system (**Figure 1.3**). Multi-layered FDC systems are typically used for the development of drugs with incompatibility issues and varying dissolution profiles. Drugs with different or separate release mechanisms can be combined in multi-layered tablets, which can be bi-layered or tri-layered. This system can produce predictable drug-release profiles for a variety of drugs (Desai *et al.*, 2013; Fernández-García *et al.*, 2020). To achieve a sustained release dissolution profile, a multi-layered tablet with an immediate release layer and a controlled release layer can be designed (Mandal & Pal, 2008; Shiyani *et al.*, 2008).

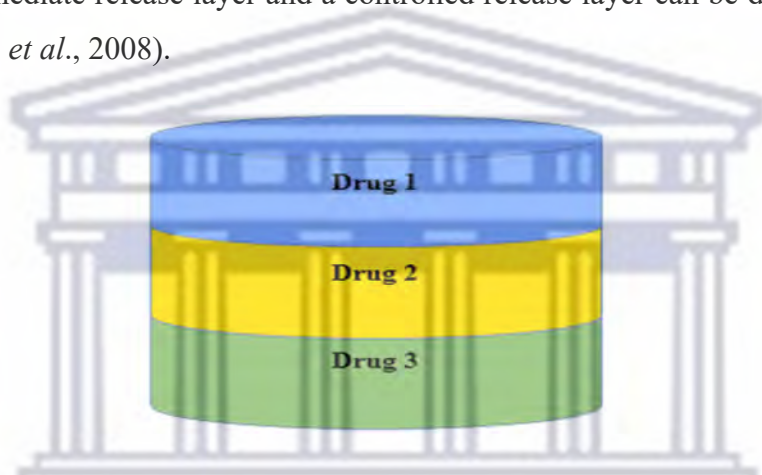


Figure 1.3: Multi-layer fixed-dose combination system (Fernández-García *et al.*, 2020).

Multi-layered tablets could potentially be challenging to manufacture due to various manufacturing processes which may be required. For example, one layer may require wet granulation while another may require dry granulation or direct compression (Mandal & Pal, 2008). Atripla is a bi-layered tablet, with the first layer formed by wet granulation of efavirenz (EFV) and the second layer formed by dry granulation of emtricitabine (FTC) and tenofovir (TDF). It is critical to separate the granulation process in order to avoid API segregation. For example, the dose of EFV (600mg) per tablet is greater than that of TDF (245mg) and FTC (200 mg) (EMA, 2009).

1.7.3.3 Multi-particulate systems

This is an advanced FDC formulation method (**Figure 1.4**). The system combines multiple drugs with distinct release mechanisms into a single dosage form. When compared to the other two systems mentioned previously, this FDC system presents less difficulty during formulation

development. A multi-particulate FDC system may consist of film coated granules, pellets, or powder compressed into tablets with desired or tailored drug release profiles. A multi-particulate system can contain both immediate and delayed release granules/ microspheres. Wet granulation, spray-coating, spray drying, milling, roller compaction, and spheronization are some of the formulation methods used in the manufacturing of such systems (Desai *et al.*, 2013; Fernández-García *et al.*, 2020).

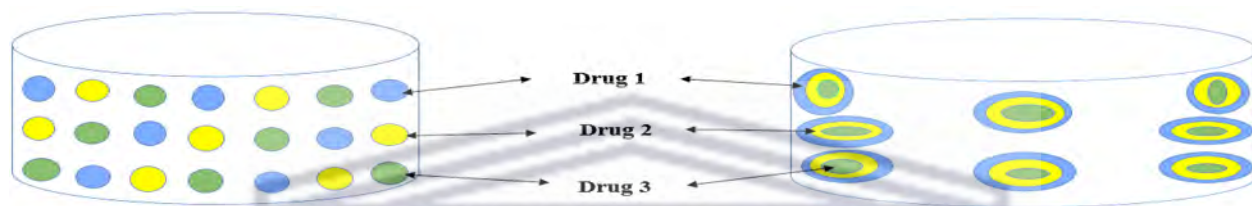


Figure 1.4: Multi-particulate fixed-dose combination system (Fernández-García *et al.*, 2020).

1.8 Microparticles (MPs) as multi-particulate drug delivery systems

Microparticles are small, round particles with diameter-dimension limits ranging from 1 to 1000 μm and typically exhibiting free-flowing behaviour with homogeneous or heterogeneous morphology. They are classified as microspheres (homogeneous) or microcapsules (heterogeneous) depending on the method of preparation and structure (**Figure 1.5**). The API is dissolved or homogeneously mixed with the excipients within microspheres, whereas API encapsulated into the core of a microparticle unit that is limited or surrounded by the excipients is referred to as a microcapsule (Campos *et al.*, 2013; Lengyel *et al.*, 2019; Padalkar *et al.*, 2011). The core of a microcapsule can be liquid, solid, semi-solid, or gas, and it can contain one or more APIs (Campos *et al.*, 2013).

Polymeric microparticles (P-MPs) are formed by incorporating a polymer into the formulation of microparticles or microcapsules. P-MPs have a polymer-based matrix with a known API concentration. The confinement of a given API in the polymer-based matrix can be caused by a uniform mixture with the polymer or by the polymer enveloping the API. The benefits of P-MPs, as summarised in **Table 1.1** below, explain why they are important in MDDS development (Bale *et al.*, 2016; Campos *et al.*, 2013; Deshmukh & Mohite, 2017; Farooq *et al.*, 2015; Lengyel *et al.*, 2019; Meghna *et al.*, 2017; Princely *et al.*, 2016; Vasir *et al.*, 2003).

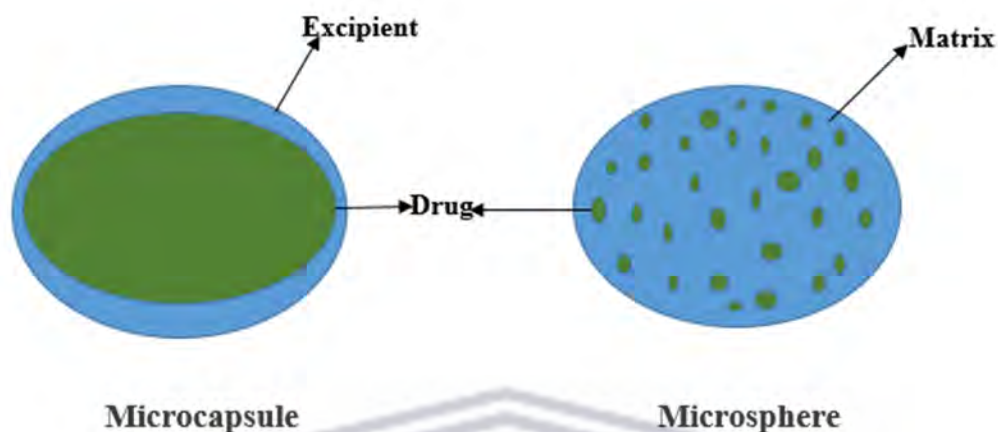


Figure 1.5: The two types of microparticles (microcapsule and microsphere) (Lengyel *et al.*, 2019).

The characteristics of the polymers used in the production of P-MPs determines the physicochemical characteristics of the formed P-MPs as well as how the loaded drug will be released from these particles (Vilos & Velasquez, 2012). Polymers perform numerous functions in a microparticle structure, the most important of which is to impart a matrix that shapes or forms the microparticle. As a result, the polymer must have mechanical strength, where the polymeric super-structure can maintain the integrity of the microparticle throughout manufacturing processes critical for particle development. Polymers are incorporated into P-MPs not only to control particle structure, but also to improve API adsorption and API stability in the GIT, thereby improving therapeutic efficacy (Andrianov & Payne, 1998; Meghna *et al.*, 2017).

Table 1.1: A summary of the advantages P-MPs may offer in terms of FDC formulation and to patients (Bale *et al.*, 2016; Campos *et al.*, 2013; Deshmukh & Mohite, 2017; Farooq *et al.*, 2015; Lengyel *et al.*, 2019; Meghna *et al.*, 2017; Princely *et al.*, 2016; Vasir *et al.*, 2003).

Advantages relating to the API or resulting dosage form	Advantages relating to the patient
<ul style="list-style-type: none"> • Protect the included API against degradation caused by heat, chemicals, UV exposure, dehydration, and oxidation during preformulation and formulation processes 	<ul style="list-style-type: none"> • Provide reduction in the dosing frequency brought forward through the possibility to control and extend drug release. <ul style="list-style-type: none"> ○ Bio-adhesive P-MPs based delivery systems are applied to prolong the dwelling time of drugs at the site of delivery
<ul style="list-style-type: none"> • Harmless handling of lethal encapsulated drugs within production facility 	<ul style="list-style-type: none"> • Effortlessly and precisely control drug release rates, targeting the API to a specific site in the body
<ul style="list-style-type: none"> • Effortless handling of fine particles thus reducing dust in production facility 	<ul style="list-style-type: none"> • Extending therapeutic concentration levels - enhancing patient adherence
<ul style="list-style-type: none"> • Concealing of unacceptable organoleptic characteristics 	<ul style="list-style-type: none"> • Decrease in the occurrence or intensity of adverse effects - enhancing patient adherence
<ul style="list-style-type: none"> • Integration into diverse therapeutic dosage forms like solids (capsules, tablets, sachets), semisolids (gels, creams, pastes), or fluids (solutions, suspensions, and including injections) 	<ul style="list-style-type: none"> • Enhanced drug delivery through non-invasive routes (ie. oral and nasal)

1.8.1 The design and formulation of polymeric microparticles (P-MPs) for oral drug delivery

1.8.1.1 Physical size of P-MPs

The preferred route of administration must be considered first when designing P-MPs. This will influence the particle size range that will be pursued. In comparison to other drug delivery routes, the useable particle size range for oral administration is much wider. Several studies have shown that decreasing the size of the microparticle increases gastrointestinal deposition or uptake by intestinal cells significantly (Eshrati *et al.*, 2018; Gaumet *et al.*, 2009; Leonard *et al.*, 2020; Tran *et al.*, 2011). Microparticles with large particle sizes have a lower surface area per unit volume, resulting in a slower rate of water penetration and matrix degradation than microparticles with smaller diameters. Therefore, during the design of P-MPs the resulting particle size is a significant consideration since the particle size will influence the drug release rate (Dawes *et al.*, 2009; Klose *et al.*, 2006). Given this, microspheres enable not only the ability to contain a sufficient quantity of drug(s), but also the ability to control the resulting particle size in order to achieve a specific drug release profile (Tran *et al.*, 2011). This is possible because the duration of action of drugs encapsulated in larger P-MPs may be extended due to increased drug loading capacity and a longer polymer matrix degradation period.

Using microparticles with particle sizes ranging from 10-200 μm typically results in ideal drug release profiles for drugs administered orally (Anderson & Shive, 2012). While microparticles less than 10 μm in diameter are at risk of being ingested by immune cells in the blood, immune reaction and inflammation may occur if microparticles larger than 200 μm are used as the delivery system for parenteral drug delivery (Dawes *et al.*, 2009; Klose *et al.*, 2006). As a result, a thorough understanding of the relationship between polymer component and properties, microparticle size, and structure is required for the customised fabrication of a microparticulate system with predetermined drug release reports (Cai *et al.*, 2009).

1.8.1.2 Physico-chemical properties of API to be incorporated into P-MPs

Melting point (thermal stability), partition coefficient, solubility in aqueous or organic solvents, chemical stability, hygroscopicity, and the specific solid-state form of a drug will all have an impact on the type of microparticle that can be prepared as well as the method of preparation. Prior to P-MP synthesis, it is important to investigate the solubility behaviour of the API that will

be included in P-MPs. The solubility of an API in specific solvents influences not only the method of preparation but also the polymers that can be used. Another aspect would be the API's thermal stability, which would determine not only the temperature ranges to be used during P-MP preparation but also which polymers would be able to withstand the same temperatures. Hygroscopicity and the solid-state form in which the drug exists will influence not only preparation methods but also post-preparation storage and subsequent formulation processes (Agnihotri *et al.*, 2004; Engelberg & Kohn, 1991; Vilos & Velasquez, 2012).

1.8.1.3 Typical polymers used for the preparation of P-MPs

Gelatin, chitosan, albumin, sodium alginate, locust bean gum, xanthan gum, okra gum, albumin, and acacia are well-known natural polymers used to produce P-MPs and have been extensively researched for their potential to aid in the development of microspheres (Farooq *et al.*, 2015; Vilos & Velasquez, 2012). Some natural polymers also impart muco-adhesive properties to the microparticles formed from them, allowing for the possibility of modified drug delivery. Poly(lactide-co-glycolide) (PLGA), (3-hydroxybutyrate-co-3-hydroxy valerate) (PHBV), poly(sebacic anhydride), poly(-caprolactone), and many other synthetic polymers are also used to make P-MPs (Vilos & Velasquez, 2012).

Polymers are well-known for their ability to improve the chemical and physical stability of drug molecules, as well as their bioavailability in some cases. As previously stated, a wide range of both natural and synthetic polymers exist as starting materials for P-MPs, and depending on the end goal of a specific P-MP, a combination of both natural and synthetic polymers may be used (Ngwuluka *et al.*, 2014; Swetha *et al.*, 2010). Furthermore, in order to effectively use these molecules in the synthesis of P-MPs, it is critical to have a thorough understanding of the bulk, surface, and intrinsic behaviour of the polymer(s) before selecting the most appropriate polymer(s) for a specific P-MP (Ngwuluka *et al.*, 2014). Polymers used in P-MP synthesis must have the desired mechanical, physical, and chemical properties while remaining cost-effective and biocompatible, ensuring human safety (Gavasane & Pawar, 2014). This must be linked to the intended route of administration and drug release, as well as the physicochemical properties of the APIs to be encapsulated in the P-MP(s) and the preferred synthesis method.

1.8.1.4 Polymeric microparticle (P-MP) synthesis methods in relation to processability

P-MPs can be prepared using a variety of methods (**Figure 1.6**), allowing for the creation of a wide range of microparticles with varying particle size, particle structure and surface chemistry (Campos *et al.*, 2013). The following section will be discussing the typical P-MP synthesis methods used in the pharmaceutical sector.

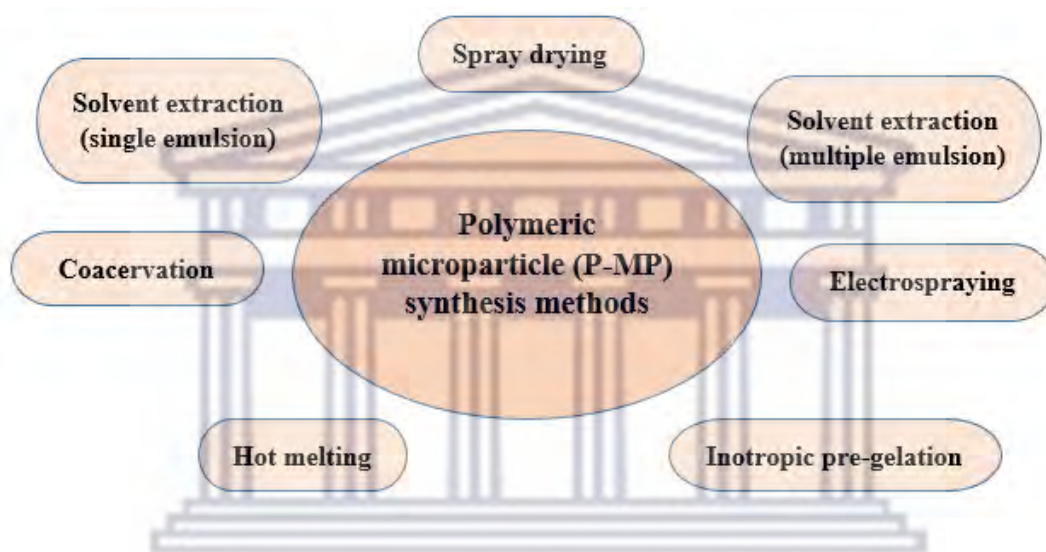


Figure 1.6: Typical methods used in the preparation of drug-loaded P-MPs (Das *et al.*, 2019; Fontes *et al.*, 2012; Li *et al.*, 2008; Shi *et al.*, 2020; Lin & Yu, 2000; Malik *et al.*, 2016; Timilsena *et al.*, 2017).

(a) Solvent extraction/evaporation involving a single emulsion process

The appropriate polymer is dissolved in a volatile organic solvent (dichloromethane, chloroform, ethyl acetate, ethyl formate) using this method. Following that, the API is dispersed or dissolved in the same organic phase. The resulting dispersion or solution is then emulsified in an immiscible aqueous phase, forming an oil in water (O/W) emulsion. The volatile organic solvent is then removed by evaporation, raising the temperature of the emulsion. As a result, solid, spherical particles float in the aqueous medium and are filtered out (Freiberg & Zhu, 2004; Li *et al.*, 2008).

(b) Solvent extraction/evaporation involving double (multiple) emulsion process

This method allows for the microencapsulation of hydrophilic APIs and is suitable for vaccines, peptides, and proteins (Das *et al.*, 2019; Jain, 2000). The API to be entrapped will be dissolved in an aqueous solution, either buffered or unbuffered. The aqueous phase is then vigorously mixed into the organic phase, which contains the polymer dissolved in a suitable organic solvent, to form the primary water in oil (W/O) emulsion. To form the secondary W/O/W emulsion, the primary emulsion is sonicated or homogenised before being dispersed in a high-volume stabilised (polyvinyl alcohol) aqueous medium. The process of evaporating or extracting the solvent from a W/O/W emulsion results in polymer solidification, API confinement, and microsphere formation (Campos *et al.*, 2013; Freiberg & Zhu, 2004). On the one hand, solvent evaporation is typically achieved by keeping the emulsion at a low pressure while continuously stirring, allowing the organic solvent to evaporate. The solvent extraction process, on the other hand, will involve the transfer of the emulsion to a large volume of water with stirring, causing the organic solvent to diffuse out, resulting in solid microparticles that can be washed and collected via filtration, sieving, or centrifugation (Jain, 2000).

(c) Spray drying method

Though spray drying is commonly thought of as a drying technique, it can also be used to encapsulate drugs within P-MPs (Bowey & Neufeld, 2010). Spray-drying can be used to convert biopharmaceuticals and biomacromolecules into nanoparticles and microparticles. Spray-drying materials include slurries, solutions, pastes, emulsions, melts, and suspensions, as well as heat-sensitive and heat-insensitive materials (Al-Khattawi *et al.*, 2018; I Ré, 1998; Santos *et al.*, 2018; Shi *et al.*, 2020). Among the many unit operations in the pharmaceutical industry, drying is one of the most important. Spray drying is the most widely used method for drying active agents and biological molecules such as protein, enzymes, extracts, and peptides. Spray drying has some advantages over other drying techniques in that the size, morphology, and density of the powder particles can be controlled. Powder properties such as particle size and density are critical for many drug delivery systems (for example, powders for suspension for the oral and dermal routes, inhalation for the nasal route) (Elverson & Millqvist-fureby, 2005).

In summary, during the formulation of P-MPs *via* spray drying, the polymer is dispersed in a suitable solvent. The API is then dissolved in the polymeric solution via high-speed homogenization to create the feedstock. In an atomizer, the feedstock is pressurized to form small droplets. These droplets are passed through a stream of hot air in a drying chamber, where the solvent quickly evaporates, resulting in the formation of microspheres with dimensions ranging from 1-100 μm . The filter bag or cyclone separator is used to separate the dried microparticles from the hot air, while vacuum drying is used to remove any remaining solvent (Das *et al.*, 2019). Polymers such as PLGA and chitosan, as well as film forming materials such as bovine serum albumin (BSA), are used to encapsulate APIs and achieve sustained drug release kinetics (Gavini *et al.*, 2002; Haswani *et al.*, 2006; Nettey *et al.*, 2006; Sun *et al.*, 2009). Spray-dried microparticles exhibited a variety of drug release profiles or bi-phase release profiles, including immediate burst release followed by delayed drug release that was sustained for an extended period of time (over 4 weeks) for DNA delivery (Kusonwiriawong *et al.*, 2004).

(d) Coacervation (phase separation) method

Coacervation is one of the oldest techniques for obtaining compound microencapsulation and can be classified as simple coacervation, which involves one colloidal solute such as gelatin or chitosan, or complex coacervation, which involves an aqueous polymeric solution prepared from two oppositely charged colloids (Deveci & Basal, 2009). A macromolecular solution separates into two immiscible liquid phases during the coacervation process: a dense coacervate phase and a dilute equilibrium phase. In a nutshell, this method consists of two consecutive steps: (1) dispersion of the compound to be encapsulated in a solution containing a surface-active hydrocolloid (gelatin, chitosan, ethylcellulose, alginate, pectin); (2) precipitation of the hydrocolloid onto the dispersed droplets by reducing the hydrocolloid's solubility, either by adding a non-solvent, changing the pH, temperature, or adding an electrolyte. In the case of complex coacervation, a second hydrocolloid solution is typically added to induce polymer-polymer complexation, followed by a final phase of cross-linking with formaldehyde or glutaraldehyde (Timilsena *et al.*, 2017).

(e) Hot melting method

Because of the associated toxicity of organic solvents commonly used in the previously mentioned P-MPs synthesis processes, solvent-free methods may be more advantageous in some cases (Lin & Yu, 2000). The drug particles are sieved to a size of less than 50 and then uniformly mixed with the melted polymer. The mixture is suspended in an immiscible solvent, such as silicone oil, and constantly stirred while being heated to 5 °C above the polymer melting point. After the emulsion has stabilized, it is cooled until the polymer particles harden. Decantation with petroleum ether cleans the resulting microparticles. Microparticles with sizes ranging from 1 µm to 1000 µm can be obtained, and the speed of stirring can be adjusted to easily control size distribution (Mathiowitz & Langer, 1987). The only limitation of this technique is the average heat to which the drug was subjected.

(f) Ionic gelation

The polymer, typically sodium alginate, is dissolved in distilled water before the API is added to the polymer solution. Maltodextrin, pectin, carboxymethylcellulose (CMC), and octenyl succinic anhydride (OSA) starch have all been reported to aid in the formation of microparticles (Fontes *et al.*, 2012). This solution is then dropped into a calcium chloride solution while being constantly stirred. The formed microspheres are immersed in a calcium chloride solution for 15 minutes to complete the curing reaction and form rigid spherical microparticles. The resulting microparticles are retrieved via decantation and then washed repeatedly with distilled water to remove any remaining calcium impurity on the surface of the microparticles before being dried at 45 °C for 12 hours. Chitosan microparticles can also be produced using the ionotropic gelation method, with several methods reporting minor differences. API was dispersed in the polymer solution after chitosan was dissolved in aqueous acetic acid. With constant stirring and sonication, a known amount of sodium tripolyphosphate (TPP) was dropped into the chitosan-API dispersion. Centrifugation at 3000 rpm for about 15 minutes yielded the chitosan microparticles (Jiang *et al.*, 2004).

(g) Electrospaying method

Electrospaying is a one-step method that uses an electric field's potential to destroy the cohesive forces of droplets, causing them to break up into smaller droplets with controlled size distributions, typically on the micro- or nanometer scale (Bock *et al.*, 2011). A suitable polymer and the drug are typically dispersed in a suitable solvent (such as chloroform). To increase the conductivity and stability of the polymer during spraying into the electric field, formic acid, emulsifier, and deionized water may be added to the solution. The solution is stirred continuously for 2 hours at room temperature with a magnetic stirrer, vortexed, and sonicated for 30 minutes in an ultrasonic bath to reduce the formation of microbubbles, forming the feed (Malik *et al.*, 2016). The feed solution is then injected into a glass syringe connected to the electrospaying apparatus and extruded at a constant rate using a syringe pump through a small but highly charged capillary (i.e. a 16-26 gauge stainless steel nozzle/needle) to form droplets or globules. A collector is placed 7 to 30 cm away from the capillary. To form a Taylor cone, a high voltage is applied between the needle and collector. Once the droplets have separated from the Taylor cone, the solvent evaporates, leaving compact and solid particles on the collector's surface (Bock *et al.*, 2011; Malik *et al.*, 2016).

1.8.2 Application of P-MPs in ARV delivery

FDC mucoadhesive microspheres were successfully prepared by Ekama *et al.* (2021). The ARVs encapsulated in this novel drug delivery system were maraviroc and tenofovir, and this loaded ARVs microsphere demonstrated excellent mucoadhesion at the vaginal wall for an extended period of time. This formulation was created as a preventative measure against HIV-1 infection. This mucoadhesive microsphere was created using the ionic gelation method (Ekama *et al.*, 2021). Princely *et al.* (2016) developed 3TC-loaded microspheres with controlled release. The ionic gelation technique was used to create these 3TC-loaded cross-linked polymeric microparticles. This formulation demonstrated controlled drug release with extended 3TC release for more than 24 hours. As a result, these 3TC microparticles will be able to overcome the shortcomings and limitations of traditional 3TC formulations (Princely *et al.*, 2016). Vilas & Thilagar (2021) created 3TC-loaded pectin microspheres as well. This formulation, a polymeric microparticle-colon-specific delivery system, was designed to deliver 3TC to the colon. To protect the pectin

microspheres from GIT degradation and to allow for controlled drug release, they were coated with Eudragit-S 100 polymer. These microspheres were created using a single water-in-oil emulsion solvent extraction/evaporation process (Vilas & Thilagar, 2021). Pandey *et al.* (2016) created an FDC of isoniazid and 3TC polymeric microparticles in another study. The formulation was created using a single oil-in-oil emulsion process and solvent extraction/evaporation. To achieve controlled drug release, two hydrophobic polymers, ethyl cellulose and Eudragit-S 100, were used, resulting in a biphasic drug release pattern. *In vitro*, the microspheres showed immediate drug release followed by sustained release for 12 hours (Pandey *et al.*, 2016). Venkatesh *et al.* (2019) prepared tenofovir microbeads using the ionotropic gelation method. Based on this study, a formulation was developed that maintained drug release for 24 hours. The drug's pharmacokinetic profile in the microbeads showed that it had a longer elimination half-life, a lower elimination rate, and a higher oral bioavailability when compared to pure drug sample. These tenofovir-loaded microbeads showed improved drug delivery for modified release, which lessens the negative effects of traditional therapy (Venkatesh *et al.*, 2019). Kim *et al.* (2020) successfully developed TDF-loaded enteric microspheres for improved duodenal delivery via the oral route. Two hydrophobic polymers, eudragit L-100 and ethyl cellulose, were used to ensure enteric-controlled release. *In vitro*, the microparticles released less than 10% of TDF from their matrix in 1 hour at pH 1.2, but over 85% was released in 1 hour at pH 6.5. As a result, these TDF microparticles are a promising formulation for targeted TDF delivery to the duodenum (Kim *et al.*, 2020).

1.9 Hypothesis on possible solutions

- The development of injectable long-acting ARVs will reduce frequent dosing, increasing adherence and ART efficacy. This dosage form will prevent gastric degradation and bypass hepatic metabolism of drugs, increasing ARV concentrations at HIV anatomical sites in the human body (Kim, 2021).
- The development of novel drug delivery systems (NDDS) for these ARVs will aid in drug targeting and tailored drug release mechanisms, increasing the bioavailability of ARVs with low aqueous solubility or permeability across epithelial cells and preventing degradation in the gastrointestinal tract (GIT) and through hepatic metabolism.

- The development of microsphere-based FDCs that can be reconstituted with water will make it easier for patients with HIV-related comorbidities to swallow.

1.10 Motivation for this study

Because HIV cannot be cured currently, it can only be treated or managed, HIV patients are left with no choice but to take ARVs every day of their lives in order to survive. As a result, proper and effective therapies are required for patients to build immunity and become resistant to other opportunistic diseases. The current first-line HIV treatment regimens formulated as FDC are usually fairly large in physical size and still requires patients to take medication every day. Previous studies suggest that it may lead to patient stigmatisation. Thus, a dosage form that can be ingested once and have sufficient therapeutic efficacy for more than 24 hours will be widely accepted by patients, increasing treatment adherence, decreasing drug resistance, and improving therapeutic efficacy. With a push toward patient-centered medicine development, formulation scientists must create dosage forms that provide not only better patient treatment but also a better patient experience.

1.11 Study aim

The rationale for this study was to investigate the development of 3TC- and TDF-loaded P-MPs exhibiting varying drug release profiles using various natural polymers in an effort to achieve a cost-effective solution for patient-centered HIV-treatment. The resulting drug loaded microspheres could then allow possible further formulation either into tablets, capsules or powders. Since 3TC and TDF still forms the cornerstone of several HIV treatment regimens a developed microsphere-based system could allow flexibility for the possible introduction of other ARVs or other drugs typically used in the treatment of HIV-associated co-infections as immediate release FDC constituents.

1.12 Objectives

- Physicochemical characterisation of the ARVs (3TC and TDF) using different analytical tools.

- Screening of several natural polymers to determine their useability in the formulation of 3TC- or TDF-loaded microspheres through determination of physicochemical properties and drug-excipient compatibility.
- Investigation of ionic gelation and spray drying as possible microsphere formulation processes.
- Preparation of drug-loaded polymeric microspheres utilising varying types of polymers and experimental parameters.
- Determination of 3TC and TDF release profiles from the drug-loaded polymeric microspheres.
- Complete physicochemical characterisation of the most optimal microsphere formulations.



1.13 References

- Abah, R.C. (2020). Achieving HIV targets by 2030: the possibility of using debt relief funds for sustainable HIV treatment in sub-Saharan Africa. *Journal of Public Health Policy*, 41(4), pp.421-435. Doi: <https://doi.org/10.1057/s41271-020-00238-x>.
- Agnihotri, S.A., Mallikarjuna, N.N. and Aminabhavi, T.M. (2004). Recent advances on chitosan-based micro-and nanoparticles in drug delivery. *Journal of Controlled Release*, 100(1), pp.5-28. Doi: <https://doi.org/10.1016/j.jconrel.2004.08.010>.
- Al-Khattawi, A., Bayly, A., Phillips, A. and Wilson, D. (2018). The design and scale-up of spray dried particle delivery systems. *Expert Opinion on Drug Delivery*, 15(1), pp.47-63. Doi: <https://doi.org/10.1080/17425247.2017.1321634>.
- Amidon, G.L., Lennernäs, H., Shah, V.P. and Crison, J.R. (1995). A theoretical basis for a biopharmaceutical drug classification: the correlation of in vitro drug product dissolution and in vivo bioavailability. *Pharmaceutical Research*, 12(3), pp.413-420. Doi: <https://doi.org/10.1023/A:1016212804288>.
- Anderson, A.M. and Bartlett, J.A. (2005). Fixed dose combination abacavir/lamivudine in the treatment of HIV-1 infection. *Expert Review of Anti-infective Therapy*, 3(6), pp.871-883. Doi: <https://doi.org/10.1586/14787210.3.6.871>.
- Anderson, J. M. and Shive, M. S. (2012). Biodegradation and biocompatibility of PLA and PLGA microspheres. *Advanced Drug Delivery Reviews*, 64, pp.72–82. Doi:10.1016/j.addr.2012.09.004.
- Andonova, V. (2017). Synthetic polymer-based nanoparticles: Intelligent drug delivery systems, in: Reddy, B (Ed.), *Acrylic Polymers in Healthcare*. *IntechOpen.*, London, pp.101-125. <http://dx.doi.org/10.5772/intechopen.69056>.
- Andrianov, A.K. and Payne, L.G. (1998). Polymeric carriers for oral uptake of microparticulates. *Advanced Drug Delivery Reviews*, 34(2-3), pp.155-170. Doi: [https://doi.org/10.1016/S0169-409X\(98\)00038-6](https://doi.org/10.1016/S0169-409X(98)00038-6).

Arya, N., Chakraborty, S., Dube, N. and Katti, D.S. (2009). Electrospraying: a facile technique for synthesis of chitosan-based micro/nanospheres for drug delivery applications. *Journal of Biomedical Materials Research Part B: Applied Biomaterials: An Official Journal of The Society for Biomaterials, The Japanese Society for Biomaterials, and The Australian Society for Biomaterials and the Korean Society for Biomaterials*, 88(1), pp.17-31. Doi: <https://doi.org/10.1002/jbm.b.31085>.

Aulton, M.E. and Taylor, K. eds. (2013). *Aulton's pharmaceuticals: the design and manufacture of medicines*. Elsevier Health Sciences.

Bale, S., Khurana, A., Reddy, A.S.S., Singh, M. and Godugu, C. (2016). Overview on therapeutic applications of microparticulate drug delivery systems. *Critical Reviews™ in Therapeutic Drug Carrier Systems*, 33(4). Doi: doi:10.1615/CritRevTherDrugCarrierSyst.2016015798.

Banakar, U.V. (1987). Drug delivery systems of the 90s: Innovations in controlled release. *American Pharmacy*, 27(2), pp.39-44. Doi: 10.1016/s0160-3450(15)32076-6.

Bangalore, S., Shahane, A., Parkar, S. and Messerli, F.H. (2007). Compliance and fixed-dose combination therapy. *Current Hypertension Reports*, 9(3), pp.184-189.

Bell, D.S.H. (2013). Combine and conquer: advantages and disadvantages of fixed-dose combination therapy. *Diabetes, Obesity and Metabolism*, 15(4), pp.291-300. Doi: <https://doi.org/10.1111/dom.12015>.

Bhatti, A.B., Usman, M. and Kandi, V. (2016). Current scenario of HIV/AIDS, treatment options, and major challenges with compliance to antiretroviral therapy. *Cureus*, 8(3). Doi: 10.7759/cureus.515.

Bock, N., Woodruff, M.A., Hutmacher, D.W. and Dargaville, T.R. (2011). Electrospraying, a reproducible method for production of polymeric microspheres for biomedical applications. *Polymers*, 3(1), pp.131-149. Doi: <https://doi.org/10.3390/polym3010131>.

Bowey, K. and Neufeld, R.J. (2010). Systemic and mucosal delivery of drugs within polymeric microparticles produced by spray drying. *BioDrugs*, 24(6), pp.359-377. Doi: <https://doi.org/10.2165/11539070-000000000-00000>.

Burger, J.J., Tomlinson, E., Mulder, E.M.A. and McVie, J.G. (1985). Albumin microspheres for intra-arterial tumour targeting. I. Pharmaceutical aspects. *International Journal of Pharmaceutics*, 23(3), pp.333-344. Doi: [https://doi.org/10.1016/0378-5173\(85\)90160-7](https://doi.org/10.1016/0378-5173(85)90160-7).

Cai, C., Mao, S., Germershaus, O., Schaper, A., Rytting, E., Chen, D. and Kissel, T. (2009). Influence of morphology and drug distribution on the release process of FITC-dextran-loaded microspheres prepared with different types of PLGA. *Journal of Microencapsulation*, 26(4), pp.334-345. Doi: <https://doi.org/10.1080/02652040802354707>.

Campbell, C., Skovdal, M., Madanhire, C., Mugurungi, O., Gregson, S. and Nyamukapa, C. (2011). “We, the AIDS people...”: how antiretroviral therapy enables Zimbabweans living with HIV/AIDS to cope with stigma. *American Journal of Public Health*, 101(6), pp.1004-1010.

Campos, E., Branquinho, J., Carreira, A.S., Carvalho, A., Coimbra, P., Ferreira, P. and Gil, M.H. (2013). Designing polymeric microparticles for biomedical and industrial applications. *European Polymer Journal*, 49(8), pp.2005-2021. Doi: <http://dx.doi.org/10.1016/j.eurpolymj.2013.04.033>.

Caplan, M.R., Daar, E.S. and Corado, K.C. (2018). Next generation fixed dose combination pharmacotherapies for treating HIV. *Expert Opinion on Pharmacotherapy*, 19(6), pp.589-596. Doi: <https://doi.org/10.1080/14656566.2018.1450866>.

Centers for Disease Control and Prevention (CDC). (2017). HIV among people aged 50 and over. [Online] Available at: <https://npin.cdc.gov/publication/hiv-among-people-aged-50-and-over> Accessed on August 14, 2022].

Clarke, S.M., Mulcahy, F.M., Tjia, J., Reynolds, H.E., Gibbons, S.E., Barry, M.G. and Back, D.J. (2001). Pharmacokinetic interactions of nevirapine and methadone and guidelines for use of nevirapine to treat injection drug users. *Clinical Infectious Diseases*, 33(9), pp.1595-1597. Doi: <https://doi.org/10.1086/322519>.

Cohen, C.J., Kubota, M., Brachman, P.S., Harley, W.B., Schneider, S., Williams, V.C., Sutherland-Phillips, D.H., Lim, M.L., Balu, R.B. and Shaefer, M.S. (2008). Short-term Safety and Tolerability of a Once-Daily Fixed-Dose Abacavir-Lamivudine Combination versus Twice-Daily Dosing of Abacavir and Lamivudine as Separate Components: Findings from the ALOHA

Study. *Pharmacotherapy: The Journal of Human Pharmacology and Drug Therapy*, 28(3), pp.314-322. Doi: <https://doi.org/10.1592/phco.28.3.314>.

Coovadia, H. (2004). Antiretroviral agents—how best to protect infants from HIV and save their mothers from AIDS. *New England Journal of Medicine*, 351(3), pp.289-292. Doi: [10.1056/NEJMe048128](https://doi.org/10.1056/NEJMe048128).

Das, M.K., Ahmed, A.B. and Saha, D. (2019). Microsphere a drug delivery system-a review. *International Journal of Current Pharmaceutical Research*, 11(4), 34-41. Doi: <https://doi.org/10.22159/ijcpr.2019v11i4.34941>.

Dasari, A. and Velmurugan, S.E. (2015). Formulation and evaluation of nevirapine mucoadhesive microspheres. *International Journal Pharmacy and Pharmaceutical Sciences*, 7(6), pp.342-348.

Dauda, R.S. (2018). Impact of HIV/aids epidemic on human capital development in W est Africa. *The International Journal of Health Planning and Management*, 33(2), pp.460-478. Doi: <https://doi.org/10.1002/hpm.2486>.

Dawes, G.J.S., Fratila-Apachitei, L.E., Mulia, K., Apachitei, I., Witkamp, G.J. and Duszczyk, J. (2009). Size effect of PLGA spheres on drug loading efficiency and release profiles. *Journal of Materials Science: Materials in Medicine*, 20(5), pp.1089-1094. Doi: <https://doi.org/10.1007/s10856-008-3666-0>.

De Clercq, E. (2002). Strategies in the design of antiviral drugs. *Nature Reviews Drug Discovery*, 1(1), pp.13-25.

Dellar, R. and Karim, Q.A. (2015). HIV/AIDS, food insecurity, and undernourishment: amplifying cycles of risk in vulnerable populations. In *Handbook of public health in natural disasters: Nutrition, food, remediation and preparation* (pp. 273-280). Wageningen Academic Publishers. Doi: <https://doi.org/10.3920/978-90-8686-806-3>.

Desai, D., Wang, J., Wen, H., Li, X. and Timmins, P. (2013). Formulation design, challenges, and development considerations for fixed dose combination (FDC) of oral solid dosage forms. *Pharmaceutical Development and Technology*, 18(6), pp.1265-1276.

Deshmukh, M.T. and Mohite, S.K. (2017). Preparation and evaluation of mucoadhesive microsphere of fluoxetine Hcl. *International Journal of Pharmaceutical Sciences and Research*, 8(9), pp.3776-3785.

Deveci, S.S. and Basal, G. (2009). Preparation of PCM microcapsules by complex coacervation of silk fibroin and chitosan. *Colloid and Polymer Science*, 287(12), pp.1455-1467. Doi: <https://doi.org/10.1007/s00396-009-2115-z>.

Devi, K.V. and Pai, R.S. (2006). Antiretrovirals: Need for an effective drug delivery. *Indian Journal of Pharmaceutical Sciences*, 68(1), p.1. Dio: 10.4103/0250-474X.22955.

Di Perri, G., Aguilar Marucco, D., Mondo, A., Gonzalez de Requena, D., Audagnotto, S., Gobbi, F. and Bonora, S. (2005). Drug-drug interactions and tolerance in combining antituberculosis and antiretroviral therapy. *Expert Opinion on Drug Safety*, 4(5), pp.821-836. Doi: <https://doi.org/10.1517/14740338.4.5.821>.

Eagling, V.A., Wiltshire, H., Whitcombe, I.W.A. and Back, D.J. (2002). CYP3A4-mediated hepatic metabolism of the HIV-1 protease inhibitor saquinavir in vitro. *Xenobiotica*, 32(1), pp.1-17. Doi: <https://doi.org/10.1080/00498250110085845>.

Ekama, S.O., Ilomuanya, M.O., Azubuike, C.P., Bamidele, T.A., Fowora, M.A., Aina, O.O., Ezechi, O.C. and Igwilo, C.I. (2021). Mucoadhesive Microspheres of Maraviroc and Tenofovir Designed for Pre-Exposure Prophylaxis of HIV-1: An in vitro Assessment of the Effect on Vaginal Lactic Acid Bacteria Microflora. *HIV/AIDS (Auckland, NZ)*, 13, p.399. Doi: [10.2147/HIV.S291065](https://doi.org/10.2147/HIV.S291065).

Elversson, J. and Millqvist-Fureby, A. (2005). Particle size and density in spray drying—effects of carbohydrate properties. *Journal of Pharmaceutical Sciences*, 94(9), pp.2049-2060. Doi: <https://doi.org/10.1002/jps.20418>.

Engelberg, I. and Kohn, J. (1991). Physico-mechanical properties of degradable polymers used in medical applications: a comparative study. *Biomaterials*, 12(3), pp.292-304. Doi: [https://doi.org/10.1016/0142-9612\(91\)90037-B](https://doi.org/10.1016/0142-9612(91)90037-B).

Eshrati, M., Amadei, F., Van de Wiele, T., Veschgini, M., Kaufmann, S. and Tanaka, M. (2018). Biopolymer-based minimal formulations boost viability and metabolic functionality of probiotics

Lactobacillus rhamnosus GG through gastrointestinal passage. *Langmuir*, 34(37), pp.11167-11175. <https://doi.org/10.1021/acs.langmuir.8b01915>.

European Medicine Agency (EMA). (2009). An overview of Atripla and why it is authorized in the EU. [Online] Available at: https://www.ema.europa.eu/en/documents/overview/atripla-epar-medicine-overview_en.pdf [Accessed on August 6, 2022].

Fahey, J.L., Taylor, J.M., Detels, R., Hofmann, B., Melmed, R., Nishanian, P. and Giorgi, J.V. (1990). The prognostic value of cellular and serologic markers in infection with human immunodeficiency virus type 1. *New England Journal of Medicine*, 322(3), pp.166-172. Doi: [10.1056/NEJM199001183220305](https://doi.org/10.1056/NEJM199001183220305).

Farooq, U., Malviya, R. and Sharma, P.K. (2015). Design and development of multi particulate system for targeted drug delivery using natural polymer. *Pharmaceutica. Analytica. Acta*, 6, p.366. Doi: <http://dx.doi.org/10.4172/2153-2435.1000366>.

Feder, A.F., Harper, K.N., Brumme, C.J. and Pennings, P.S. (2021). Understanding patterns of HIV multi-drug resistance through models of temporal and spatial drug heterogeneity. *Elife*, 10, p.e69032. Doi: <https://doi.org/10.7554/eLife.69032>.

Fernández-García, R., Prada, M., Bolás-Fernández, F., Ballesteros, M.P. and Serrano, D.R. (2020). Oral fixed-dose combination pharmaceutical products: Industrial manufacturing versus personalized 3D printing. *Pharmaceutical Research*, 37(7), pp.1-22. Doi: <https://link.springer.com/article/10.1007/s11095-020-02847-3>.

Fettiplace, A., Stainsby, C., Winston, A., Givens, N., Puccini, S., Vannappagari, V., Hsu, R., Fusco, J., Quercia, R., Aboud, M. and Curtis, L. (2017). Psychiatric symptoms in patients receiving dolutegravir. *Journal of Acquired Immune Deficiency Syndromes (1999)*, 74(4), p.423. Doi: <https://doi.org/10.1097%2FQAI.0000000000001269>.

Fontes, G.C., Finotelli, P.V., Rossi, A.M. and Rocha-Leão, M.H.Z. (2012). Optimization of penicillin G microencapsulation with OSA starch by factorial design. *Chemical Engineering Transactions*, 27, pp.85-90. Doi: 10.3303/CET1227015.

Freiberg, S. and Zhu, X.X. (2004). Polymer microspheres for controlled drug release. *International Journal of Pharmaceutics*, 282(1-2), pp.1-18. Doi: <https://doi.org/10.1016/j.ijpharm.2004.04.013>

Gaumet, M., Gurny, R. and Delie, F. (2009). Localization and quantification of biodegradable particles in an intestinal cell model: the influence of particle size. *European Journal of Pharmaceutical Sciences*, 36(4-5), pp.465-473. Doi: <https://doi.org/10.1016/j.ejps.2008.11.015>.

Gavasane, A.J. and Pawar, H.A. (2014). Synthetic biodegradable polymers used in controlled drug delivery system: an overview. *Clinical Pharmacology and Biopharmaceutics*, 3(2), pp.1-7. Doi: <http://dx.doi.org/10.4172/2167-065X.1000121>.

Gavini, E., Sanna, V., Juliano, C. and Giunchedi, P. (2003). Compressed biodegradable matrices of spray-dried PLGA microspheres for the modified release of ketoprofen. *Journal of Microencapsulation*, 20(2), pp.193-201. Doi: <https://doi.org/10.3109/02652040309178061>.

Gunaseelan, S., Gunaseelan, K., Deshmukh, M., Zhang, X. and Sinko, P.J. (2010). Surface modifications of nanocarriers for effective intracellular delivery of anti-HIV drugs. *Advanced Drug Delivery Reviews*, 62(4-5), pp.518-531. Doi: <https://doi.org/10.1016/j.addr.2009.11.021>.

Gupta, U. and Jain, N.K. (2010). Non-polymeric nano-carriers in HIV/AIDS drug delivery and targeting. *Advanced Drug Delivery Reviews*, 62(4-5), pp.478-490. Doi: <https://doi.org/10.1016/j.addr.2009.11.018>.

Haswani, D.K., Nettey, H., Oettinger, C. and D'Souza, M.J. (2006). Formulation, characterization and pharmacokinetic evaluation of gentamicin sulphate loaded albumin microspheres. *Journal of Microencapsulation*, 23(8), pp.875-886. Doi: <https://doi.org/10.1080/02652040601035093>.

Hogg, R.S., Yip, B., Kully, C., Craib, K.J., O'Shaughnessy, M.V., Schechter, M.T. and Montaner, J.S. (1999). Improved survival among HIV-infected patients after initiation of triple-drug antiretroviral regimens. *Canadian Medical Association Journal*, 160(5), pp.659-665.

I Ré, M. (1998). Microencapsulation by spray drying. *Drying Technology*, 16(6), pp.1195-1236. Doi: <https://doi.org/10.1080/07373939808917460>.

Jain, R.A. (2000). The manufacturing techniques of various drug loaded biodegradable poly (lactide-co-glycolide)(PLGA) devices. *Biomaterials*, 21(23), pp.2475-2490. Doi: [https://doi.org/10.1016/S0142-9612\(00\)00115-0](https://doi.org/10.1016/S0142-9612(00)00115-0).

Jiang, H.L., Park, I.K., Shin, N.R., Kang, S.G., Yoo, H.S., Kim, S.I., Suh, S.B., Akaike, T. and Cho, C.S. (2004). In vitro study of the immune stimulating activity of an atrophic rhinitis vaccine

associated to chitosan microspheres. *European Journal of Pharmaceutics and Biopharmaceutics*, 58(3), pp.471-476. Doi: <https://doi.org/10.1016/j.ejpb.2004.05.006>.

Kazmierski, W.M., Kenakin, T.P. and Gudmundsson, K.S. (2006). Peptide, peptidomimetic and small-molecule drug discovery targeting HIV-1 host-cell attachment and entry through gp120, gp41, CCR5 and CXCR4. *Chemical Biology & Drug Design*, 67(1), pp.13-26. Doi: <https://doi.org/10.1111/j.1747-0285.2005.00319.x>.

Kim, Y.S. (2021). Long-Acting Injectable Antiretroviral Agents for HIV Treatment and Prevention. *Infection & Chemotherapy*, 53(4), p.686. Doi: <https://doi.org/10.3947%2Fic.2021.0136>.

Kim, Y.H., Kim, Y.C., Kim, J.Y., Byeon, J., Maeng, H.J., Kim, S.T., Min, K.A., Jang, D.J. and Cho, K.H. (2020). Preparation and Characterization of Tenofovir Disoproxil-Loaded Enteric Microparticle. *Journal of Nanoscience and Nanotechnology*, 20(9), pp.5796-5799. Doi: <https://doi.org/10.1166/jnn.2020.17641>.

Klimas, N., Koneru, A. O., and Fletcher, M. A. (2008). Overview of HIV. *Psychosomatic Medicine*, 70(5), 523–530. Doi:10.1097/psy.0b013e31817ae69f.

Klose, D., Siepmann, F., Elkharraz, K., Krenzlin, S. and Siepmann, J. (2006). How porosity and size affect the drug release mechanisms from PLGA-based microparticles. *International Journal of Pharmaceutics*, 314(2), pp.198-206. Doi: <https://doi.org/10.1016/j.ijpharm.2005.07.031>.

Kumari, G. and Singh, R.K. (2012). Highly active antiretroviral therapy for treatment of HIV/AIDS patients: current status and future prospects and the Indian scenario. *HIV & AIDS Review*, 11(1), pp.5-14. Doi: <https://doi.org/10.1016/j.hivar.2012.02.003>.

Kusonwiriya Wong, C., Atuah, K., Alpar, O.H., Merkle, H.P. and Walter, E. (2004). Cationic stearylamine-containing biodegradable microparticles for DNA delivery. *Journal of Microencapsulation*, 21(1), pp.25-36. Doi: <https://doi.org/10.1080/02652040410001653777>.

Kwong, J. (2021). HIV and Ageing: Considerations for Older Adults Living with HIV. In *Providing HIV Care: Lessons from the Field for Nurses and Healthcare Practitioners* (pp. 151-165). Springer, Cham. [Online] Available at: https://link.springer.com/chapter/10.1007/978-3-030-71295-2_9 [Accessed on August 14, 2022].

- Lee, F.J., Amin, J. and Carr, A. (2014). Efficacy of initial antiretroviral therapy for HIV-1 infection in adults: a systematic review and meta-analysis of 114 studies with up to 144 weeks follow-up. *PloS One*, 9(5), p.e97482. Doi: <https://doi.org/10.1371/journal.pone.0097482>.
- Lengyel, M., Kállai-Szabó, N., Antal, V., Laki, A.J. and Antal, I. (2019). Microparticles, microspheres, and microcapsules for advanced drug delivery. *Scientia Pharmaceutica*, 87(3), p.20. Doi: <https://doi.org/10.3390/scipharm87030020>.
- Li, M., Rouaud, O. and Poncelet, D. (2008). Microencapsulation by solvent evaporation: State of the art for process engineering approaches. *International Journal of Pharmaceutics*, 363(1-2), pp.26-39. Doi: <https://doi.org/10.1016/j.ijpharm.2008.07.018>.
- Liao, L., Xing, H., Su, B., Wang, Z., Ruan, Y., Wang, X., Liu, Z., Lu, Y., Yang, S., Zhao, Q. and Vermund, S.H. (2013). Impact of HIV drug resistance on virologic and immunologic failure and mortality in a cohort of patients on antiretroviral therapy in China. *AIDS (London, England)*, 27(11), p.1815. Doi: <https://doi.org/10.1097%2FQAD.0b013e3283611931>.
- Lin, W.J. and Yu, C.C. (2000). Comparison of protein loaded poly(Σ -caprolactone) microparticles prepared by the hot-melt technique. *Journal of Microencapsulation*, 18(5), pp.585-592. Doi: 10.1080/02652040010019569.
- Littman, D.R. (1998). Chemokine receptors: keys to AIDS pathogenesis? *Cell*, 93(5), pp.677-680. Doi: [https://doi.org/10.1016/S0092-8674\(00\)81429-4](https://doi.org/10.1016/S0092-8674(00)81429-4).
- Leonard, F., Srinivasan, S., Liu, X., Collnot, E.M., Ferrari, M., Lehr, C.M. and Godin, B. (2020). Design and in vitro characterization of multistage silicon-PLGA budesonide particles for inflammatory bowel disease. *European Journal of Pharmaceutics and Biopharmaceutics*, 151, pp.61-72.
- Lucas, S. (2001). Update on the pathology of AIDS. *Intensive and Critical Care Nursing*, 17(3), pp.155-166.
- Malik, S.A., Ng, W.H., Bowen, J., Tang, J., Gomez, A., Kenyon, A.J. and Day, R.M. (2016). Electrospray synthesis and properties of hierarchically structured PLGA TIPS microspheres for use as controlled release technologies. *Journal of Colloid and Interface Science*, 467, pp.220-229. Doi: <https://doi.org/10.1016/j.jcis.2016.01.021>.

Mandal, U. and Pal, T.K. (2008). Formulation and in vitro studies of a fixed-dose combination of a bilayer matrix tablet containing metformin HCl as sustained release and glipizide as immediate release. *Drug Development and Industrial Pharmacy*, 34(3), pp.305-313. Doi: <https://doi.org/10.1080/03639040701657487>.

Marin, R.C., Streinu-Cercel, A., Moleriu, L.C. and Bungau, S.G. (2022). Analysis of virological response to therapy and resistance profile in treatment-experienced and naive HIV-1 infected Romanian patients receiving regimens containing darunavir boosted with ritonavir or cobicistat. *Biomedicine & Pharmacotherapy*, 150, p.113077. Doi: <https://doi.org/10.1016/j.biopha.2022.113077>.

Mathiowitz, E. and Langer, R. (1987). Polyanhydride microspheres as drug carriers I. Hot-melt microencapsulation. *Journal of controlled Release*, 5(1), pp.13-22. Doi: [https://doi.org/10.1016/0168-3659\(87\)90033-2](https://doi.org/10.1016/0168-3659(87)90033-2).

Mbonu, N.C., van den Borne, B. and De Vries, N.K. (2009). The stigma of people with HIV/AIDS in sub-Saharan Africa: a literature review. *Journal of Tropical Medicine*, 2009. Doi: <https://doi.org/10.1155/2009/145891>.

McCluskey, S.M., Siedner, M.J. and Marconi, V.C. (2019). Management of virologic failure and HIV drug resistance. *Infectious Disease Clinics*, 33(3), pp.707-742. DOI: <https://doi.org/10.1016/j.idc.2019.05.004>.

Meghna, K.S., Pillai, K., Giridas, S., Sreelakshmi, C. and Vijayakumar, B. (2017). Microsphere a drug delivery system—a review. *International Journal of Novel Trends in Pharmaceutical Sciences*, 7(4), pp.109-118.

Melikian, C., White, T.J., Vanderplas, A., Dezii, C.M. and Chang, E. (2002). Adherence to oral antidiabetic therapy in a managed care organization: a comparison of monotherapy, combination therapy, and fixed-dose combination therapy. *Clinical Therapeutics*, 24(3), pp.460-467. Doi: [https://doi.org/10.1016/S0149-2918\(02\)85047-0](https://doi.org/10.1016/S0149-2918(02)85047-0).

Miantezila Basilua, J., Mesia Kahunu, G., Pochart, P. and Tona Lutete, G. (2021). Overview of HIV treatment failure in Africa using the WHO Pharmacovigilance data. *Tropical Medicine & International Health*, 26(5), pp.530-534. Doi: <https://doi.org/10.1111/tmi.13556>.

- Miller, L.G., Huffman, H.B., Weidmer, B.A. and Hays, R.D. (2002). Patient preferences regarding antiretroviral therapy. *International Journal of STD & AIDS*, 13(9), pp.593-601. Doi: <https://doi.org/10.1258%2F09564620260216281>.
- Mirchandani, H. and Chien, Y.W (1993). Drug delivery approaches for anti-HIV drugs. *International Journal of Pharmaceutics*, 95(1-3), pp.1-21. Doi: [https://doi.org/10.1016/0378-5173\(93\)90385-S](https://doi.org/10.1016/0378-5173(93)90385-S).
- Mitra, A. and Wu, Y. (2012). Challenges and opportunities in achieving bioequivalence for fixed-dose combination products. *The American Association of Pharmaceutical Scientists Journal*, 14(3), pp.646-655. Doi: <https://doi.org/10.1208/s12248-012-9378-x>
- Moriarty, F., Bennett, K. and Fahey, T. (2019). Fixed-dose combination antihypertensives and risk of medication errors. *Heart*, 105(3), pp.204-209. Doi: <http://dx.doi.org/10.1136/heartjnl-2018-313492>.
- Nadia, R. and Elvira, D. (2022). HIV Drug Resistance Mutations. *Bioscientia Medicina: Journal of Biomedicine and Translational Research*, 6(7), pp.2006-2013. Doi: <https://doi.org/10.37275/bsm.v6i7.547>.
- Nettey, H., Haswani, D., Oettinger, C.W. and D'Souza, M.J. (2006). Formulation and testing of vancomycin loaded albumin microspheres prepared by spray-drying. *Journal of Microencapsulation*, 23(6), pp.632-642. Doi: <https://doi.org/10.1080/02652040600776564>.
- Ngwuluka, N.C., Ochekepe, N.A. and Aruoma, O.I. (2014). Naturapolyceutics: the science of utilizing natural polymers for drug delivery. *Polymers*, 6(5), pp.1312-1332. Doi: 10.3390/polym6051312.
- Odugbesan, J.A. and Rjoub, H. (2019). Relationship among HIV/AIDS prevalence, human capital, good governance, and sustainable development: Empirical evidence from Sub-Saharan Africa. *Sustainability*, 11(5), p.1348. Doi: <https://doi.org/10.3390/su11051348>.
- Padalkar, A.N., Shahi, S.R. and Thube, M.W. (2011). Microparticles: an approach for the betterment of the drug delivery system. *International Journal of Pharma. Research & Development* 3(1), 99 – 115.

- Panda, S., Pattnaik, S., Maharana, L., Teja, C.K. and Das, D. (2014). HIV and AIDS: Need of an Effective Drug Delivery. *Research Journal of Pharmacy and Technology*, 7(6), pp.686-694.
- Pandey, G., Yadav, S.K. and Mishra, B. (2016). Preparation and characterization of isoniazid and lamivudine co-loaded polymeric microspheres. *Artificial Cells, Nanomedicine, and Biotechnology*, 44(8), pp.1867-1877. Doi: <https://doi.org/10.3109/21691401.2015.1111229>.
- Peppas, N.A. and Buri, P.A. (1985). Surface, interfacial and molecular aspects of polymer bioadhesion on soft tissues. *Journal of Controlled Release*, 2, pp.257-275. Doi: [https://doi.org/10.1016/0168-3659\(85\)90050-1](https://doi.org/10.1016/0168-3659(85)90050-1).
- Podolsky, S.H. and Greene, J.A. (2011). Combination drugs—hype, harm, and hope. *New England Journal of Medicine*, 365(6), pp.488-491. Doi: 10.1056/NEJMp110616.
- Princely, S., Saleem basha, N., Nandhakumar S. and Dhanaraju Md. (2016). Controlled delivery of antiretroviral drug-loaded cross-linked microspheres by ionic gelation method. *Asian Journal of Pharmaceutical and Clinical Research*, 9(5), 264-271. Doi: <http://dx.doi.org/10.22159/ajpcr.2016.v9i5.13653>.
- Rankin, W.W., Brennan, S., Schell, E., Laviwa, J. and Rankin, S.H. (2005). The stigma of being HIV-positive in Africa. *PLoS Medicine*, 2(8), p.e247. Doi: <https://doi.org/10.1371/journal.pmed.0020247>.
- Ramana, L.N., Anand, A.R., Sethuraman, S. and Krishnan, U.M. (2014). Targeting strategies for delivery of anti-HIV drugs. *Journal of Controlled Release*, 192, pp.271-283. Doi: <https://doi.org/10.1016/j.jconrel.2014.08.003>.
- Rathbun, R.C., Lockhart, S.M. and Stephens, J.R. (2006). Current HIV treatment guidelines-an overview. *Current Pharmaceutical Design*, 12(9), pp.1045-1063. Doi: <https://doi.org/10.2174/138161206776055840>.
- Rehman, A.M., Simms, V., McHugh, G., Mujuru, H., Ngwira, L.G., Semphere, R., Moyo, B., Bandason, T., Odland, J.O. and Ferrand, R.A. (2022). Adherence to additional medication for management of HIV-associated comorbidities among older children and adolescents taking antiretroviral therapy. *Plos One*, 17(6), p.e0269229. Doi: <https://doi.org/10.1371/journal.pone.0269229>.

- Rintamaki, L.S., Davis, T.C., Skripkauskas, S., Bennett, C.L. and Wolf, M.S. (2006). Social stigma concerns and HIV medication adherence. *AIDS Patient Care & STDs*, 20(5), pp.359-368. Doi: <https://doi.org/10.1089/apc.2006.20.359>.
- Rosen, S. and Fox, M.P. (2011). Retention in HIV care between testing and treatment in sub-Saharan Africa: a systematic review. *PLoS Medicine*, 8(7), p.e1001056. Doi: <https://doi.org/10.1371/journal.pmed.1001056>.
- Sadia, M., Isreb, A., Abbadi, I., Isreb, M., Aziz, D., Selo, A., Timmins, P. and Alhnan, M.A. (2018). From 'fixed dose combinations' to 'a dynamic dose combiner': 3D printed bi-layer antihypertensive tablets. *European Journal of Pharmaceutical Sciences*, 123, pp.484-494. Doi: <https://doi.org/10.1016/j.ejps.2018.07.045>.
- Sampson, J. G., and Workman, M. L. (2016). Care of Patients with HIV Disease and Other Immune Deficiencies. Chapter 21. [Online] Available at: <https://nursekey.com/care-of-patients-with-hiv-disease-and-other-immune-deficiencies-2/> [Accessed on July 29, 2022].
- Santos, D., Maurício, A.C., Sencadas, V., Santos, J.D., Fernandes, M.H. and Gomes, P.S. (2018). Spray drying: an overview. *Biomaterials-Physics and Chemistry-New Edition*, pp.9-35. Doi: <http://dx.doi.org/10.5772/intechopen.72247>.
- Sayles, J.N., Wong, M.D., Kinsler, J.J., Martins, D. and Cunningham, W.E. (2009). The association of stigma with self-reported access to medical care and antiretroviral therapy adherence in persons living with HIV/AIDS. *Journal of General Internal Medicine*, 24(10), pp.1101-1108. Doi: <https://doi.org/10.1007/s11606-009-1068-8>.
- Sebaaly, J.C. and Kelley, D. (2017). Single-tablet regimens for the treatment of HIV-1 infection. *Annals of Pharmacotherapy*, 51(4), pp.332-344. Doi: <https://doi.org/10.1177/1060028016682531>.
- Schaecher, K.L. (2013). The importance of treatment adherence in HIV. *The American Journal of Managed Care*, 19(12 Suppl), pp.s231-7.
- Schlosser, R. (2019). Fixed-dose and fixed-ratio combination therapies in type 2 diabetes. *Canadian Journal of Diabetes*, 43(6), pp.440-444. Doi: <https://doi.org/10.1016/j.cjcd.2019.05.005>.

Scott Sutton, S., Magagnoli, J. and Hardin, J.W. (2016). Impact of pill burden on adherence, risk of hospitalization, and viral suppression in patients with HIV infection and AIDS receiving antiretroviral therapy. *Pharmacotherapy: The Journal of Human Pharmacology and Drug Therapy*, 36(4), pp.385-401. Doi: <https://doi.org/10.1002/phar.1728>.

Sierra, S., Kupfer, B. and Kaiser, R. (2005). Basics of the virology of HIV-1 and its replication. *Journal of Clinical Virology*, 34(4), pp.233-244. Doi: <https://doi.org/10.1016/j.jcv.2005.09.004>.

Shi, N.Q., Zhou, J., Walker, J., Li, L., Hong, J.K., Olsen, K.F., Tang, J., Ackermann, R., Wang, Y., Qin, B. and Schwendeman, A. (2020). Microencapsulation of luteinizing hormone-releasing hormone agonist in poly (lactic-co-glycolic acid) microspheres by spray-drying. *Journal of Controlled Release*, 321, pp.756-772. Doi: <https://doi.org/10.1016/j.jconrel.2020.01.023>.

Shiyani, B., Gattani, S. and Surana, S. (2008). Formulation and evaluation of bi-layer tablet of metoclopramide hydrochloride and ibuprofen. *The American Association of Pharmaceutical Scientists journal*, 9(3), pp.818-827. Doi: 10.1208/s12249-008-9116-y.

Sosnik, A. and Augustine, R. (2016). Challenges in oral drug delivery of antiretrovirals and the innovative strategies to overcome them. *Advanced Drug Delivery Reviews*, 103, pp.105-120. Doi: <https://doi.org/10.1016/j.addr.2015.12.022>.

Sun, Y., Cui, F., Shi, K., Wang, J., Niu, M. and Ma, R. (2009). The effect of chitosan molecular weight on the characteristics of spray-dried methotrexate-loaded chitosan microspheres for nasal administration. *Drug Development and Industrial Pharmacy*, 35(3), pp.379-386. Doi: <https://doi.org/10.1080/03639040802395185>.

Swetha, M., Sahithi, K., Moorthi, A., Srinivasan, N., Ramasamy, K. and Selvamurugan, N. (2010). Biocomposites containing natural polymers and hydroxyapatite for bone tissue engineering. *International Journal of Biological Macromolecules*, 47(1), pp.1-4. Doi: <https://doi.org/10.1016/j.ijbiomac.2010.03.015>.

Tadesse, W.T., Mekonnen, A.B., Tesfaye, W.H. and Tadesse, Y.T. (2014). Self-reported adverse drug reactions and their influence on highly active antiretroviral therapy in HIV infected patients:

a cross sectional study. *BMC Pharmacology and Toxicology*, 15(1), pp.1-9. Doi: <https://doi.org/10.1186/2050-6511-15-32>.

Timilsena, Y.P., Wang, B., Adhikari, R. and Adhikari, B. (2017). Advances in microencapsulation of polyunsaturated fatty acids (PUFAs)-rich plant oils using complex coacervation: A review. *Food Hydrocolloids*, 69, pp.369-381. Doi: <https://doi.org/10.1016/j.foodhyd.2017.03.007>.

Tran, V.T., Benoît, J.P. and Venier-Julienne, M.C. (2011). Why and how to prepare biodegradable, monodispersed, polymeric microparticles in the field of pharmacy?. *International Journal of Pharmaceutics*, 407(1-2), pp.1-11. Doi: <https://doi.org/10.1016/j.ijpharm.2011.01.027>.

Van Epps, P. and Kalayjian, R.C. (2017). Human immunodeficiency virus and aging in the era of effective antiretroviral therapy. *Infectious Disease Clinics*, 31(4), pp.791-810. Doi: <https://doi.org/10.1016/j.idc.2017.07.007>.

Venkatesh, D.N., Rao, P. and Rajeshkumar, R. (2019). Enhanced oral bioavailability of tenofovir from ionotropically gelled microbeads. *International Journal of Applied Pharmaceutics*, 11, pp.242-50. Dio: <http://dx.doi.org/10.22159/ijap.2019v11i4.32281>.

Vasir, J.K., Tambwekar, K. and Garg, S. (2003). Bioadhesive microspheres as a controlled drug delivery system. *International Journal of Pharmaceutics*, 255(1-2), pp.13-32. Doi: [https://doi.org/10.1016/S0378-5173\(03\)00087-5](https://doi.org/10.1016/S0378-5173(03)00087-5).

Vilas, S. and Thilagar, S. (2021). Formulation and optimisation of lamivudine-loaded Eudragit® S 100 polymer-coated pectin microspheres for colon-specific delivery. *IET Nanobiotechnology*, 15(1), pp.90-99. Doi: <https://doi.org/10.1049/nbt2.12010>.

Vilos, C. and Velasquez, L.A. (2012). Therapeutic strategies based on polymeric microparticles. *Journal of Biomedicine and Biotechnology*, 2012. Doi: 10.1155/2012/672760.

Vyas, T.K., Shah, L. and Amiji, M.M. (2006). Nanoparticulate drug carriers for delivery of HIV/AIDS therapy to viral reservoir sites. *Expert Opinion on Drug Delivery*, 3(5), pp.613-628. Doi: <https://doi.org/10.1517/17425247.3.5.613>.

Warr, G.W. and Šljivić, V.S. (1974). Origin and division of liver macrophages during stimulation of the mononuclear phagocyte system. *Cell Proliferation*, 7(6), pp.559-565. Doi: <https://doi.org/10.1111/j.1365-2184.1974.tb00439.x>.

Waziri, S.I., Nor, N.M., Abdullah, N.M.R. and Adamu, P. (2016). Effect of the prevalence of HIV/AIDS and the life expectancy rate on economic growth in SSA countries: Difference GMM approach. *Global Journal of Health Science*, 8(4), p.212. Doi: <https://doi.org/10.5539%2Fgjhs.v8n4p212>.

World Health Organization (2017). HIV drug resistance report 2017. Geneva: World Health Organization; 2017. [Online] Available at: <https://apps.who.int/iris/bitstream/handle/10665/255896/9789241512831-eng.pdf> [Accessed on July 29, 2022].

World Health Organization (2018a). Updated recommendations on first-line and second-line antiretroviral regimens and post-exposure prophylaxis and recommendations on early infant diagnosis of HIV: interim guidelines: supplement to the 2016 consolidated guidelines on the use of antiretroviral drugs for treating and preventing HIV infection. Geneva: World Health Organization; 2018. [Online] Available at: <https://apps.who.int/iris/handle/10665/277395> [Accessed on August 22, 2022].

World Health Organization (2018b). Dolutegravir (DTG) and the fixed-dose combination of tenofovir/lamivudine/dolutegravir (TLD). Briefing Note, April 2018. [Online] Available at: https://r.search.yahoo.com/_ylt=AwrFPh1WVOVi1jcaV31XNyoA;_ylu=Y29sbwNiZjEEcG9zAZlEdnRpZANEMTEyNV8xBHNIYwNzcg--/RV=2/RE=1659225302/RO=10/RU=https%3a%2f%2fwww.researchgate.net%2fprofile%2fMondli-Alfred%2fpost%2fWith-the-introduction-of-the-new-HIV-drug-it-would-make-the-immune-system-to-be-stronger-Wouldnt-it-trigger-other-hidden-infections-to-it-patients%2fattachment%2f5e8d010ff155db0001f37906%2fAS%253A877816417640448%25401586299151110%2fdownload%2fDTG-TLD-arv_briefing_2018.pdf/RK=2/RS=iaIIA21eUrIhJHSo64hvCiN.sU- [Accessed on July 30, 2022].

World Health Organization (2021). Consolidated guidelines on the use of antiretroviral drugs for treating and preventing HIV infection: recommendations for a public health approach. [Online] Available at: <https://www.who.int/publications/i/item/9789240031593>. [Accessed on 19 July 2022].

World Health Organization (2022). 'HIV/AIDS'. Summary of the global HIV epidemic, 2021. [Online] Available at: <https://www.who.int/data/gho/data/themes/hiv-aids>. [Accessed on July 29, 2022].

World Health Organization (2023). 'HIV/AIDS'. Summary of the global HIV epidemic, 2021. [Online] Available at: <https://www.who.int/data/gho/data/themes/hiv-aids>. [Accessed on July 29, 2022].

Xu, X., Yuan, M. and Nandy, P. (2012). Analysis of dose–response in flexible dose titration clinical studies. *Pharmaceutical Statistics*, 11(4), pp.280-286. Doi: <https://doi.org/10.1002/pst.1498>.

Yang, H.Y., Beymer, M.R. and Suen, S.C. (2019). Chronic disease onset among people living with HIV and AIDS in a large private insurance claims dataset. *Scientific Reports*, 9(1), pp.1-8. Doi: <https://doi.org/10.1038/s41598-019-54969-3>.



Chapter Two

The physicochemical characteristics of lamivudine and tenofovir disoproxil fumarate and an overview of natural polymers explored as part of polymeric microsphere formulation

2.1 Introduction

As described in Chapter 1 the physicochemical characteristics of drugs influences the outcome of any pharmaceutical formulation. This therefore stands also true for the formulation of drug-loaded microspheres. In order to allow informed decision making on microsphere formulation strategies and methodology it was necessary to conduct a literature review on the two active pharmaceutical ingredients, namely lamivudine (3TC) and tenofovir disoproxil fumarate (TDF) as well as on the polymers that were envisioned to be used in this study.

2.2 Lamivudine (3TC)

3TC is a well-known and frequently prescribed nucleoside analogue showing DNA polymerase activity (Kumari & Singh, 2012). As already discussed in Chapter 1, 3TC still forms part of the first-line HIV treatment regimens and is currently incorporated into the FDCs consisting of 3TC + TDF or 3TC + TDF + dolutegravir sodium (DTG), doravirine + TDF + 3TC, dolutegravir + 3TC, 3TC + raltegravir, abacavir + dolutegravir + 3TC, efavirenz + 3TC + TDF or 3TC + zidovudine (Anon, 2023; Casado & Banon, 2015; Li *et al.*, 2022; Sankaraiah *et al.*, 2022; Zamora *et al.*, 2019). From a molecular perspective (**Figure 2.1**), 3TC exhibits the following molecular formula ($C_8H_{11}N_3O_3S$) and according to IUPAC nomenclature is also termed 4-amino-1-[(2R,5S)-2-(hydroxymethyl)-1,3-oxathiolan-5-yl] pyrimidin-2-one (Strauch *et al.*, 2011).

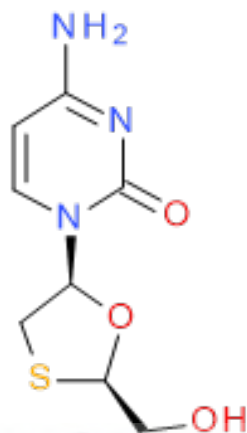


Figure 2.1: The chemical structure of 3TC (Harris *et al.*, 1998).

The molecule has a molecular weight of 229.26 g/mol and exists as a crystalline compound with a documented melting temperature of 160-162 °C (Johnson *et al.*, 1999; Pubchem, 2022b; Van Leeuwen *et al.*, 1992).

2.2.1 Physicochemical and pharmacokinetic properties of 3TC

The solid-state chemistry of this drug is of great pharmaceutical interest because it is claimed to exist in three polymorphic forms. The two crystalline forms (Form I and II) were first described by Jozwiakowski *et al.* in 1996, then Harris *et al.* researched them again in 1997. In 2007, Singh *et al.* published a patent demonstrating the presence of another crystalline form III. This new polymorphic form was characterised as a crystalline hemihydrate form exhibiting improved powder flow and bulk density in comparison with Form I and II. Interestingly, it was noted that Form I and II converts to Form III when slurried in water at ambient temperature for a period of 24 - 48 hours (Singh *et al.*, 2007). In terms of melting point characteristics it was noted that Form I melts at 135 °C followed by recrystallisation of the higher melting Form II at ≈ 150 °C. Thermal analysis revealed that Form II is the thermodynamically more stable form with a melting point of 178 °C. Form I further exhibits acicular morphology as rods or needle-shaped particles, Form II shows identifiable bipyramids whilst Form III presents as monoclinic crystals. A major drawback of the data reported for 3TC Form III is the fact that solubility data was not provided and further to this it was not possible to conclude on any differences in 3TC bioavailability between the

different solid-state forms. However, a more recent study investigated the polymorphic forms of 3TC even further. This study showed that 3TC Forms I and III are metastable forms and that Form II shows the lowest solubility in phosphate buffer whilst Form III is the most soluble (Chadha *et al.*, 2012).

Various reports on the solubility of 3TC Form II exist and reported aqueous solubility ranges from 70 - 84.9 mg/ml in distilled water maintained at ambient temperature (Brittain *et al.*, 2018; Jozwiakowski *et al.*, 1996; Strauch *et al.*, 2011). Furthermore, 3TC acts as a weak base with a pKa of 4.3 (Strauch *et al.*, 2011). The maximum 3TC daily dose is 300 mg, which can be divided into two doses of 150 mg twice daily, if not administered as part of a marketed FDC product. Based on the dose of 300 mg, which is the highest daily dose of 3TC as well as the reported water solubility it is evident that the dose volume is less than 250 ml, thereby classifying 3TC as a highly soluble drug. In terms of bioavailability, 3TC is still characterised as a variable drug with absolute bioavailability ranging from 68 to 88% and intracellular and elimination half-lives of 10.5–15.5 hours and 5–7 hours, respectively. It is however reported that systemic absorption is not significantly affected by food (Strauch *et al.*, 2011). In terms of intestinal permeability, 3TC is reported to be a BCS III class drug based on low gastrointestinal permeation which permeates through passive diffusion (Van Leeuwen, 1992; Strauch *et al.*, 2011).

2.3 Tenofovir disoproxil fumarate (TDF)

TDF is a pro-drug and the first reverse transcriptase inhibitor based on a nucleotide analogue to be authorised for the treatment of HIV. This drug is known as monophosphorylated nucleotide analogues, and it also has DNA polymerase activity (Fung *et al.*, 2002; Kearney *et al.*, 2004). TDF is a common once-daily backbone for use with other classes of ARVs due to its long intracellular and blood circulation half-lives of 60 and 17 hours, respectively. As a result, unless the goal is to develop TDF into a long-acting ARV, a modified drug delivery system is not required or cost-effective. Adults can take up to 300 mg per day (Kearney *et al.*, 2004; Tong *et al.*, 2007; Wassner *et al.*, 2020).

TDF (C₂₃H₃₄N₅O₁₄P), also termed [[(2R)-1-(6-aminopurin-9-yl)propan-2-yl]oxymethyl-(propan-2-yl)oxycarbonyloxymethoxy]phosphoryl]oxymethyl propan-2-yl carbonate;but-2-enedioic acid (**Figure 2.2**) has a molecular weight of 635.5g/mol, a crystalline particle morphology with an established melting point of 114–118 °C (Fung *et al.*, 2002; Pubchem, 2022a; Tong *et al.*, 2007).

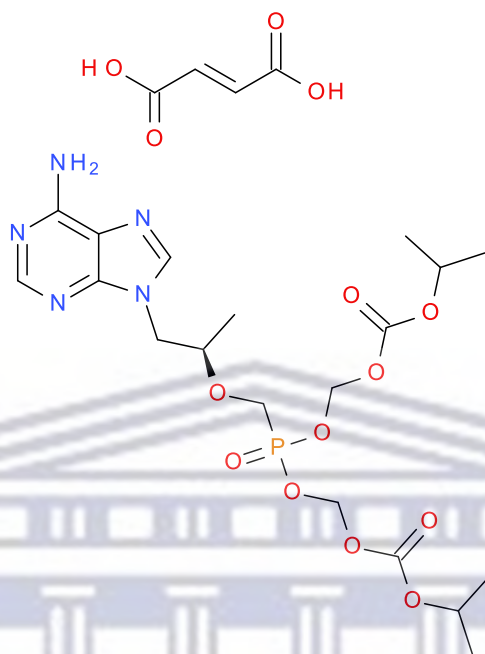


Figure 2.2: The chemical structure of TDF (Pubchem, 2022a).

2.3.1 Physicochemical and pharmacokinetic properties of TDF

From a physicochemical standpoint, TDF may exist in one of three solid-state forms (I, A, and B), with polymorphic Form I remaining unsolvated. Form A is not, however, a polymorph of the other two forms. Although Forms I and A appear to be polymorphic, fumaric acid content varies between the two forms. Form A is the cocrystal of tenofovir disoproxil, thus hemifumarate, whereas Form I is a salt, thus fumarate. Hence, they should be viewed as different compounds. Forms I and B are desolvated solvates, as shown by the physicochemical characterisation of TDF forms. The fact that the Fourier-transform infrared (FT-IR) spectra of Forms B and I of TDF are identical, while the solid-state NMR (ssNMR) data is very dissimilar, is another intriguing feature of this drug (Lee *et al.*, 2010; Sládková *et al.*, 2016). TDF is classified as a BCS Class III drug due to its substantial aqueous solubility (13.4 mg/mL at 25 °C) and low intestinal-wall permeability. As a result, the drug has low oral bioavailability; however, when administered with fatty-food, the oral bioavailability of TDF improves (Kearney *et al.*, 2004; Pubchem, 2022a; Tong *et al.*, 2007; Wassner *et al.*, 2020).

2.4 Natural polymers used in pharmaceutical preformulation and formulation

Since the aim of this study was to investigate the application of natural polymers in the formulation of drug-loaded microspheres to allow a more cost-effective formulation approach the subsequent section will focus on the characteristics and applications of natural polymers, typically used in pharmaceutical formulations.

Natural polymers are created in nature in the course of the growth phase of living organisms (Campos *et al.*, 2013). They are biogenic raw materials of high molecular weights from innate and renewable sources such as animals, micro-organisms, and plants with a carbon, oxygen, and nitrogen backbone. Typically, hydrophilic, biodegradable compounds, consisting of simple sugar units and linked by glucosidic bonds, possessing similar but non-identical repeating units with identical chain lengths (Ngwuluka *et al.*, 2014; Swetha *et al.*, 2010; Campos *et al.*, 2013).

Natural polymers can be classified into two categories; (a) polysaccharides and (b) proteins. Polysaccharides can be sourced from three origins; plants, marine, and microbes, whereas proteins are typically only sourced from plants and animals (Swetha *et al.*, 2010). Polysaccharides also display excellent biocompatibility and therefore they are appropriate materials when applied to extend systemic circulation and targeted drug delivery (Ngwuluka *et al.*, 2014). All natural polymers are biodegradable and considered non-toxic (Ngwuluka *et al.*, 2014; Shrivastava, 2018). Biodegradable polymeric substances have a temporary objective in the body and they are broken down to smaller molecular compounds with a regulated rate of degradation which can be broken down and or excreted; generally used for modified drug release, scaffolds in tissue engineering, and surgical sutures (Simionescu, 2015). It is because of all the above mentioned properties as well as the fact that natural polymers are cost-effective, easily accessible and easily modified that these molecules are more appealing than synthetic polymers within the area of pharmaceutical dosage form design (Ngwuluka *et al.*, 2014). Natural polymers can alter the release of a drug from a formulation. The drug release profile from a formulation consisting of natural polymers is influenced by the physicochemical characteristics of both the drug and polymer(s). Other factors that influence the release of drugs include; release mechanism of polymer, morphology, particle size, and shape of the pharmaceutical dosage form (Kumar & Gupta, 2012).

Based on various literature reports but also the cost-effectiveness and high level of availability it was decided that this study shall only focus on chitosan (CH), gelatin (GEL), xanthan gum (XG)

and sodium alginate (SA). The following paragraphs will provide an overview of the four polymers.

2.4.1 Chitosan (CH)

Due to its distinct physicochemical and functional properties, which captured the interest of a large number of pharmaceutical scientists, CH has stimulated the ongoing development of safe and effective drug delivery systems (Jana *et al.*, 2019; Patel *et al.*, 2010). CH is a polysaccharide that occurs naturally, and is generated by deacetylation of chitin *via* chemical (alkaline), enzymatic, or microwave-assisted methods (Berger *et al.*, 2004; Chatterjee *et al.*, 2022). Chitin is the major constituent of the exoskeleton of crustaceans used in the production of CH, such as shrimps. The degree of chitin deacetylation used to produce CH, as well as its molecular weight, have a significant impact on the physicochemical and functional properties of this polymer (Berger *et al.*, 2004; Patel *et al.*, 2010). It has amino and hydroxyl functional groups that can be easily modified for the intended purpose, specifically as controlled drug release carriers (Jana *et al.*, 2011; Jana *et al.*, 2019). CH's main chain contains an abundance of free amino groups, which become protonated in an acidic environment (Aranaz *et al.*, 2009). The muco-adhesive and absorption-increasing characteristics of CH make it a suitable polymeric vehicle for administering drugs to the mucosal tissue by increasing the *in vivo* contact time of the pharmaceutical formulation in the gastrointestinal tract, resulting in an improvement in the bioavailability of various drugs (He *et al.*, 1998; Patel *et al.*, 2010). CH's positively charged groups can easily interact with cross-linkers of negatively charged species to form interlinked polymeric structures, resulting in microspheres that can be used for targeted drug delivery (Patel *et al.*, 2010).

CH molecules (**Figure 2.3**) are made up of N-acetyl-2-amino-2-deoxy-D-glucopyranose (acetylated unit) and 2-amino-2-deoxyd-glucopyranose (deacetylated unit), which are linked by β -(1 \rightarrow 4)-glycosidic bonds (Berger *et al.*, 2004; Chatterjee *et al.*, 2022).

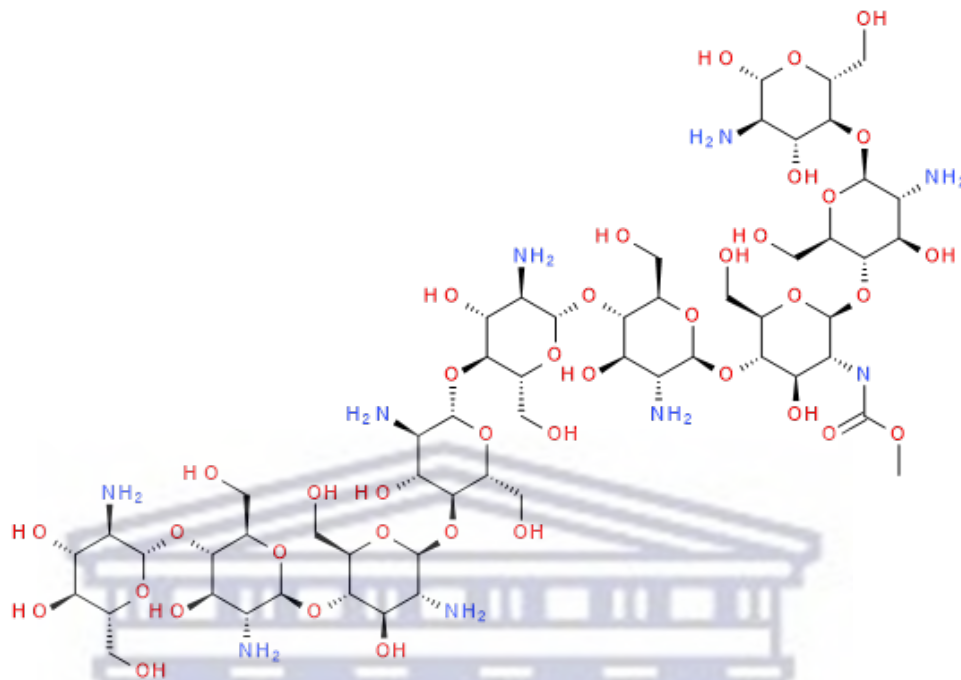


Figure 2.3: The chemical structure of chitosan (Pubchem, 2022c).

A summary of the physicochemical and functional properties of CH is provided in **Table 2.1**. Based on the ability of CH to effectively form polyelectrolyte complexes as well as the fact that it has a low toxicity profile makes it an ideal candidate for microsphere formulation aimed towards treatment of HIV-infected patients.

2.4.2 Gelatin (GEL)

For a very long time, GEL has been utilised as a wall material in the field of microencapsulation. It is a polypeptide that was created through the partial hydrolysis of collagen, which was taken from animals, as well as fish and insects, in acid, alkaline, or enzymatic solutions. Type A GEL is created using an acidic process, while Type B GEL is produced using an alkaline process (Djagny *et al.*, 2001; Foox & Zilberman, 2015; Xie *et al.*, 2006). GEL molecules (**Figure 2.4**) are made up of different polypeptide chains; α -chains (single or one polymer chain), β -chains (two covalently cross-linked α -chains), and γ -chains (three α -chains covalently cross-linked) (Alipa *et al.*, 2021; Rbi *et al.*, 2011).

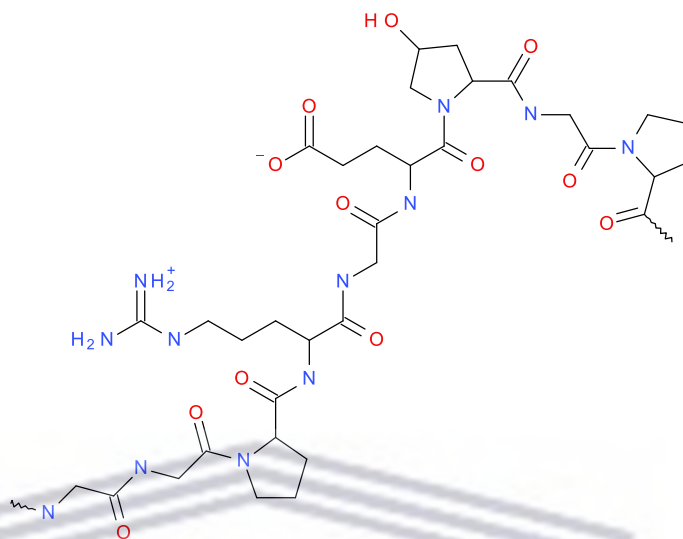


Figure 2.4: The chemical structure of Gelatin (Devi *et al.*, 2017).

Pure, dry commercial GEL typically has a very faint yellow to amber colour and is transparent, brittle, tasteless, and odourless. Commercial edible GEL has a molecular weight between 40,000 - 90,000 Daltons. The equilibria of GEL with acids and bases provides information about the nature of polypeptides and the amino acid composition. The electric charged groups and ionisation constant of a specific GEL determine its structural stability as well as the nature of its reaction with other substances. According to reports, GEL A has an isoelectric point (IEP) between pH 7 to 9, while GEL B has an IEP between pH 4.8 to 5.1 (Lengyel *et al.*, 2019; Qiao *et al.*, 2012). GEL is a protein that is water soluble. To ensure its dispersion, however, adequate precautions must be taken. GEL can be dissolved by briefly soaking the granules in a sufficient quantity of chilly water, then warming and mixing it while adding heated water to the dampened GEL until it reaches a concluding temperature of approximately 35 °C (Djagny *et al.*, 2001; Lengyel *et al.*, 2019). As outlined and summarised in **Table 2.1**, GEL is a highly versatile pharmaceutical excipient that may be cross-linked with other polymers to form an intricate polymeric structure.

2.4.3 Xanthan gum (XG)

XG is a microbial exopolysaccharide that occurs naturally (Elella *et al.*, 2021). The gram-negative bacterium *Xanthomonas campestris* ferments to produce it (Kumar & Gupta, 2012; Palaniraj & Jayaraman, 2011). Due to its exceptional physicochemical characteristics, biodegradability,

biocompatibility, immunogenicity, and non-toxicity, it has shown a significant potential in targeted applications like advanced drug delivery (Elella *et al.*, 2021; Kumar *et al.*, 2018). Additionally, XG is progressively being used for the development and improvement of pharmaceutical delivery systems (**Table 2.1**) due to its physicochemical characteristics, which include high molecular weight anionic polysaccharide with branched chains, high stability at pH 4–10, water solubility, hygroscopicity, temperature, and pH insensitivity (Cortes *et al.*, 2020; Kumar *et al.*, 2017; Kumar *et al.*, 2018; Kumar & Gupta, 2012; Lengyel *et al.*, 2019). When exposed to an aqueous medium, XG is soluble in both cold and hot water and requires vigorous agitation to prevent the formation of lumps (Kumar *et al.*, 2018).

As shown in **Figure 2.5**, XG is a branched polysaccharide with disaccharide as the repeating unit and side-chains made up of a trisaccharide consisting of D-mannose (-1,4), D-glucuronic acid (-1,2), and D-mannose that are linked to different glucose molecules in the backbone by -1,3 linkages. A pyruvic acid residue with an unknown distribution is connected to the 4th and 6th positions of the terminal D-mannose by a keto group. A position O-6 acetyl group is present in the D-mannose unit that is connected to the main chain (Jansson *et al.*, 1975; Petri, 2015).

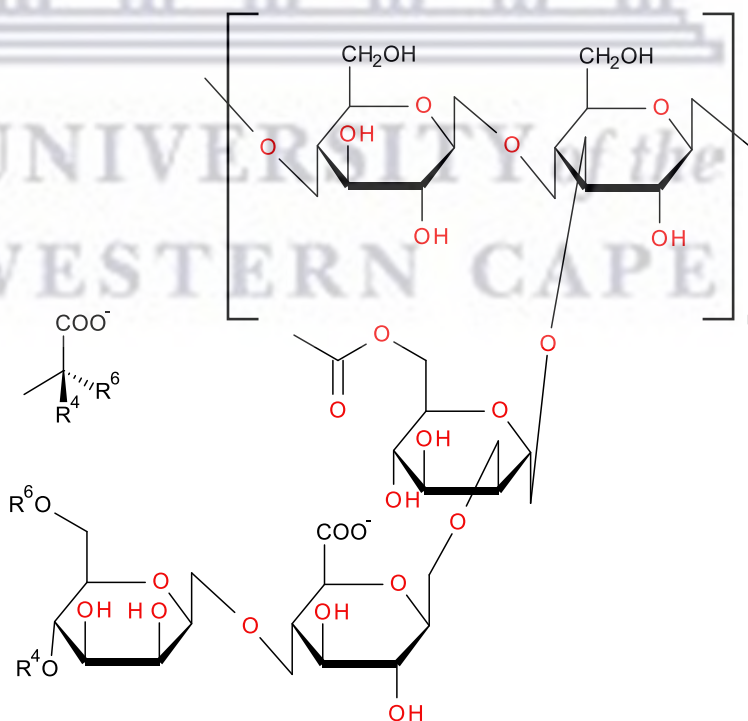


Figure 2.5: The chemical structure of Xanthan gum (Jansson *et al.*, 1975).

2.4.4 Sodium alginate (SA)

SA is a natural, linear, and anionic polysaccharide and it is one of the most commonly used polymers in the development of novel drug delivery systems. SA has been extensively employed as an encapsulating agent for peptides, drugs (antibiotics, acid-labile drugs), proteins, enzymes, and living cells (growth factors) because of its good biocompatibility, biodegradability, gelation in the mild state and chemical versatility (Agüero *et al.*, 2017; Bagheri *et al.*, 2014; Joye & McClements, 2014). SA molecules (**Figure 2.6**) are made up of 1, 4-linked β -D-mannuronic acid (M) and α -L-guluronic acid (G) monomers (Foroughi *et al.*, 2018).

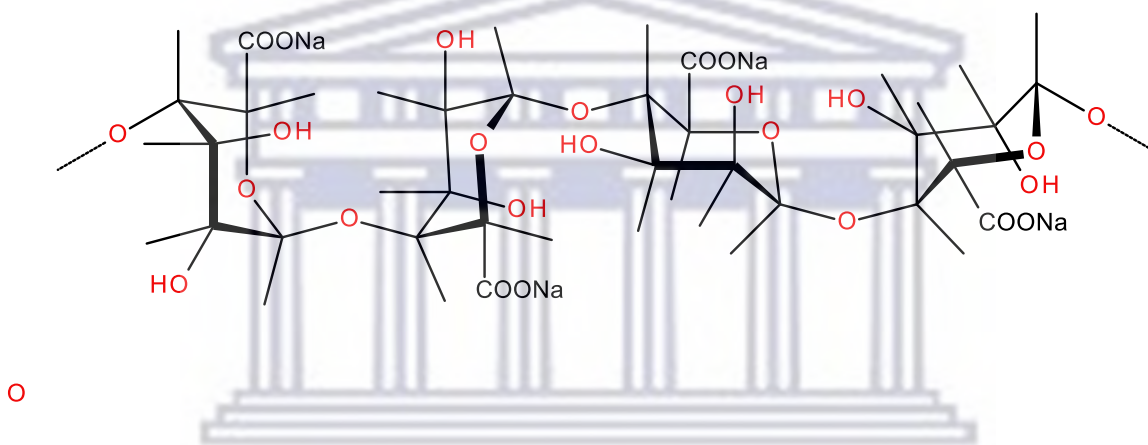


Figure 2.6: The chemical structure of Sodium alginate (Foroughi *et al.*, 2018).

SA-based microparticles are widely prepared by the ionotropic gelation method because the procedure is cheap, fast, and simple. The alginate microparticle morphology, particle shape, and size are influenced by formulation parameters such as; flow rate, SA concentration, the concentration of crosslinking agent (CaCl_2), and stirring speed when prepared by ionotropic gelation method (Joye & McClements, 2014). SA-based microparticles can break down when in contact with gastrointestinal fluids especially gastric juice because of the presence of acids and Na^+ -ions. This disintegration process is often random and this is the major reason why SA is often blended with one or more other polymer(s), with chitosan being commonly used with alginate.

Table 2.1: A summary of the physicochemical and functional properties playing significant roles in P-MP synthesis and possible drug release mechanisms for CH, GEL, XG and SA (Aguero *et al.*, 2017; Khan & Ram, 2014; Lengyel *et al.*, 2019; Mishra & Rautray, 2020).

Polymer	Physico-chemical properties	Functional properties	Drug release mechanism	Typical P-MP synthesis method	PMP synthesis challenges
Chitosan (Polysaccharide)	Positively charged (cationic) Water soluble (low pH) Hygroscopic (Jana <i>et al.</i> , 2011; Khan & Ram, 2014).	Formation of polyelectrolyte complexes Low toxicity profile High charge density Biocompatible Biodegradable Hypoallergenic Mucoadhesive Film-forming ability Permeation/absorption enhancement Antimicrobial, antibacterial and antifungal activity (Genta <i>et al.</i> , 1997; Jiang <i>et al.</i> , 2008;	First-order kinetics (Kumar & Gupta, 2012).	Emulsion techniques Spray drying Ionotropic gelation Coacervation (Genta <i>et al.</i> , 1997; Giunchedi <i>et al.</i> , 2002; Jaganathan <i>et al.</i> , 2005; Jiang <i>et al.</i> , 2004; Khan & Ram, 2014; Mitra & Dey, 2011; Saha <i>et al.</i> , 2006; Singh & Udupa, 1998).	P-MPs shape influenced by drug loading. Crosslinker type and concentration influence drug loading and P-MP size High aqueous solubility of chitosan limits the use for P-MPs for drug delivery to gastric environment. Drug content in the P-MPs and particle size depends on the

		Khan & Ram, 2014; Kumar & Gupta, 2012; Mitra & Dey, 2011; Pillai & Panchagnula, 2001; Varshosaz, 2007).			concentration of chitosan (Genta <i>et al.</i> , 1997; Giunchedi <i>et al.</i> , 2002; Jana <i>et al.</i> , 2011; Portero <i>et al.</i> , 2002 Saha <i>et al.</i> , 2006; Varshosaz <i>et al.</i> , 2004).
Gelatin (Protein)	Hydrophilic Hygroscopic Amphoteric gelatin A (isoelectric point (IEP) pH: 7–9 gelatin B (IEP: pH 4.8–5.0) pH dependent (Lengyel <i>et al.</i> , 2019).	Gelling agent Non-irritable, Biocompatible Biodegradable Non-toxic Non-carcinogenic, Low immunogenicity Low antigenicity High ability of crosslinking Emulsifier Binder	First-order release (Singh <i>et al.</i> , 2011).	Solvent evaporation single emulsion method Coacervation Spray-drying (Foux & Zilberman, 2015; Kawai <i>et al.</i> , 2000; Kimura <i>et al.</i> , 2003).	Unstable in aqueous medium – influencing drug release properties Concentration of crosslinking agents and duration of crosslinking influence drug release rate from P-MPs Swelling properties of gelatin P-MPs

		<p>Stabilizer</p> <p>Thermoreversible gelling</p> <p>Coating agent</p> <p>Film-forming agent</p> <p>Viscosity-increasing agent</p> <p>Suspending agent</p> <p>(Jana <i>et al.</i>, 2011; Lengyel <i>et al.</i>, 2019; Rowe <i>et al.</i>, 2009).</p>			<p>affected by crosslinker concentration (Del Gaudio <i>et al.</i>, 2017; Vandelli <i>et al.</i>, 2001).</p>
Xanthan Gum (Polysaccharide)	<p>Water soluble</p> <p>Hygroscopic</p> <p>Temperature and pH-insensitive</p> <p>High stability at pH 4 - 10</p> <p>(Kumar & Gupta, 2012; Lengyel <i>et al.</i>, 2019).</p>	<p>Mucoadhesive</p> <p>Suspending agent</p> <p>Stabilizer</p> <p>Pseudo plastic characteristics.</p> <p>Emulsifying agent</p> <p>Thickener</p> <p>Buoyancy/ floating properties. Drug release retarding characteristics.</p>	<p>Higuchi or zero-order kinetics</p> <p>(Andreopoulos & Tarantili, 2001; Kumar & Gupta, 2012)</p>	<p>Solvent evaporation w/o emulsion crosslinking</p> <p>Ionic crosslinking</p> <p>Spray drying (Al Mamun <i>et al.</i>, 2014; Bhattacharya <i>et al.</i>, 2013; Jain <i>et al.</i>, 2013; Mishra & Rautray, 2020;</p>	<p>Polymer concentration influences P-MP sizing, drug entrapment efficiency and release profile of loaded drug.</p> <p>The extent of crosslinking can</p>

		<p>GIT retention properties.</p> <p>Controlled release and targeted drug delivery. (Kumar & Gupta, 2012; Lengyel <i>et al.</i>, 2019).</p>		<p>Trombino <i>et al.</i>, 2019).</p>	<p>affect the particle size of P-MPs.</p> <p>Ionic strength of the medium can influence the release behaviour of drug loaded in the P-MPs. (Andreopoulos & Tarantili, 2001; Jain <i>et al.</i>, 2013).</p>
<p>Sodium alginate (Polysaccharide)</p>	<p>Water-soluble (at room temperature)</p> <p>Hygroscopic</p> <p>pH-sensitive</p> <p>Almost insoluble in ether and alcohol (Aguero <i>et al.</i>, 2017; Jana <i>et al.</i>, 2011; Lengyel <i>et al.</i>, 2019)</p>	<p>Biocompatible</p> <p>Biodegradable</p> <p>Low toxicity</p> <p>Thickening ability</p> <p>Viscosity increasing</p> <p>Mucoadhesive</p> <p>Binding ability</p> <p>Emulsion stabilizer</p> <p>Suspending ability</p> <p>Outstanding crosslinking ability</p>	<p>Burst release</p> <p>Diffusion Erosion (Kumar & Gupta, 2012; Lengyel <i>et al.</i>, 2019).</p>	<p>Ionotropic gelation</p> <p>Coacervation</p> <p>Spray drying</p> <p>Single or double emulsion method (Aguero <i>et al.</i>, 2017; Bowey & Neufeld, 2010; Lengyel <i>et al.</i>, 2019).</p>	<p>P-MPs show shrinking and poor stability in acidic environment.</p> <p>Osmotic changes result in uneven porosity, lower mechanical strength, weak wall-formation, and easy rupture.</p> <p>Formulation parameters</p>

		<p>(Aguero <i>et al.</i>, 2017; Bagheri <i>et al.</i>, 2014; Lengyel <i>et al.</i>, 2019; Kumar & Gupta, 2012).</p>		<p>such as alginate molecular weight, concentration, crosslinker concentration, stirring rate, needle internal diameter and flow speed affect the particle size, shape and structure of P-MPs prepared by ionotropic gelation (Aguero <i>et al.</i>, 2017; Lengyel <i>et al.</i>, 2019).</p>
--	--	---	--	--



2.5 Conclusion

The ultimate characteristics of ART-FDC are a low pill burden, patient tolerability, an elevated genetic barrier against viral resistance, a low ability for drug-drug interaction, decreased toxicity, low cost, the absence of laboratory safety monitoring, and expected clinical outcomes. Natural polymers have the potential to alter the release of API from a formulation. The physicochemical properties of both the drug and excipients influence how API is released from a formulation containing natural polymers. Other factors influencing drug release include polymer release mechanism, morphology, particle size, and the shape of the pharmaceutical dosage form (Kumar & Gupta, 2012; Singh *et al.*, 2011).

Great attempts have been made to create pharmaceutical formulations that either help drugs stay active longer in the body or help them target particular tissues or organs. The incorporation of these drugs into the appropriate matrix is one potential strategy for achieving these goals. Drug regulated-release carriers have many advantages over traditional pharmaceutical formulations, including increased efficacy, long-term maintenance of the desired drug concentration in the blood without exceeding lethal levels or dropping below the efficacious levels, decreased toxic effects, and increased patient adherence and comfort (Foux & Zilberman, 2015).



UNIVERSITY of the
WESTERN CAPE

2.6 References

- Agüero, L., Zaldivar-Silva, D., Peña, L. and Dias, M.L. (2017). Alginate microparticles as oral colon drug delivery device: A review. *Carbohydrate polymers*, 168, pp.32-43.
- Al Mamun, A., Bagchi, M., Amin, L., Sutradhar, K. and Huda, N. (2014). Development of natural gum based glipizide mucoadhesive microsphere. *Journal of Applied Pharmaceutical Science*, 4(1), pp.066-069. Doi: http://www.japsonline.com/admin/php/uploads/1160_pdf.pdf.
- Alipal, J., Pu'Ad, N.M., Lee, T.C., Nayan, N.H.M., Sahari, N., Basri, H., Idris, M.I. and Abdullah, H.Z. (2021). A review of gelatin: Properties, sources, process, applications, and commercialisation. *Materials Today: Proceedings*, 42, pp.240-250. Doi: <https://doi.org/10.1016/j.matpr.2020.12.922>.
- Andreopoulos, A.G. and Tarantili, P.A. (2001). Xanthan gum as a carrier for controlled release of drugs. *Journal of Biomaterials Applications*, 16(1), pp.34-46. Doi: <https://doi.org/10.1106%2FXBFG-FYFX-9TW9-M83U>.
- Anon. (2023). General Considerations When Using Fixed-Dose Combination Products. chrome-extension://efaidnbmnnnibpcajpcgclefindmkaj/https://clinicalinfo.hiv.gov/sites/default/files/guidelines/documents/pediatric-arv/drug-information-fixed-dose-combinations-tablets-minimum-body-weights-considerations-use-children-adolescents-pediatric-arv.pdf. Date of access: 01 August 2023.
- Aranaz, I., Mengibar, M., Harris, R., Paños, I., Miralles, B., Acosta, N., Galed, G. and Heras, Á. (2009). Functional characterization of chitin and chitosan. *Current Chemical Biology*, 3(2), pp.203-230. Doi: <https://doi.org/10.2174/187231309788166415>.
- Bagheri, L., Madadlou, A., Yarmand, M. and Mousavi, M.E. (2014). Spray-dried alginate microparticles carrying caffeine-loaded and potentially bioactive nanoparticles. *Food Research International*, 62, pp.1113-1119.
- Berger, J., Reist, M., Mayer, J.M., Felt, O., Peppas, N.A. and Gurny, R.J.E.J.O.P. (2004). Structure and interactions in covalently and ionically crosslinked chitosan hydrogels for biomedical applications. *European Journal of Pharmaceutics and Biopharmaceutics*, 57(1), pp.19-34. Doi: [https://doi.org/10.1016/S0939-6411\(03\)00161-9](https://doi.org/10.1016/S0939-6411(03)00161-9).

Bhattacharya, S.S., Mazahir, F., Banerjee, S., Verma, A. and Ghosh, A. (2013). Preparation and in vitro evaluation of xanthan gum facilitated superabsorbent polymeric microspheres. *Carbohydrate Polymers*, 98(1), pp.64-72. Doi: <https://doi.org/10.1016/j.carbpol.2013.05.011>.

Bowey, K. and Neufeld, R.J. (2010). Systemic and mucosal delivery of drugs within polymeric microparticles produced by spray drying. *BioDrugs*. 24(6), 359-377. Doi: <https://doi.org/10.2165/11539070-000000000-00000>.

Brittain, H.G., Grant, D.J. and Myrdal, P.B. (2018). 12 Effects of Polymorphism and Solid-State Solvation on Solubility and Dissolution Rate. *Polymorphism in pharmaceutical solids*, p.436.

Campos, E., Branquinho, J., Carreira, A.S., Carvalho, A., Coimbra, P., Ferreira, P. and Gil, M.H. (2013). Designing polymeric microparticles for biomedical and industrial applications. *Eur. Polym. J.*, 49(8), 2005-2021. Doi: <http://dx.doi.org/10.1016/j.eurpolymj.2013.04.033>.

Casado, J.L. and Banon, S. (2015). Dutrebis (lamivudine and raltegravir) for use in combination with other antiretroviral products for the treatment of HIV-1 infection. *Expert Review of Clinical Pharmacology*, 8(6), pp.709-718. Doi: <https://doi.org/10.1586/17512433.2015.1090873>.

Chadha, R., Arora, P. and Bhandari, S. (2012). Polymorphic forms of lamivudine: characterization, estimation of transition temperature, and stability studies by thermodynamic and spectroscopic studies. *International Scholarly Research Notices*. Doi: 10.5402/2012/671027.

Chatterjee, R., Maity, M., Hasnain, M.S. and Nayak, A.K. (2022). Chitosan: source, chemistry, and properties. In *Chitosan in Drug Delivery* (pp. 1-22). Academic Press. Doi: <https://doi.org/10.1016/B978-0-12-819336-5.00001-7>.

Cortes, H., Caballero-Florán, I.H., Mendoza-Muñoz, N., Escutia-Guadarrama, L., Figueroa-González, G., Reyes-Hernández, O.D., González-Del Carmen, M., Varela-Cardoso, M., González-Torres, M., Florán, B. and Del Prado-Audelo, M.L. (2020). Xanthan gum in drug release. *Cellular and Molecular Biology*, 66(4), pp.199-207.

Del Gaudio, C., Crognale, V., Serino, G., Galloni, P., Audenino, A., Ribatti, D. and Morbiducci, U. (2017). Natural polymeric microspheres for modulated drug delivery. *Materials Science and Engineering: C*, 75, pp.408-417. Doi: <https://doi.org/10.1016/j.msec.2017.02.051>.

Devi, N., Sarmah, M., Khatun, B. and Maji, T.K. (2017). Encapsulation of active ingredients in polysaccharide–protein complex coacervates. *Advances in colloid and interface science*, 239, pp.136-145. Doi: <https://doi.org/10.1016/j.cis.2016.05.009>.

Djagny, K.B., Wang, Z. and Xu, S. (2001). Gelatin: a valuable protein for food and pharmaceutical industries. *Critical Reviews in Food Science and Nutrition*, 41(6), pp.481-492. Doi: <https://doi.org/10.1080/20014091091904>.

Elella, M.H.A., Goda, E.S., Gab-Allah, M.A., Hong, S.E., Pandit, B., Lee, S., Gamal, H., ur Rehman, A. and Yoon, K.R. (2021). Xanthan gum-derived materials for applications in environment and eco-friendly materials: A review. *Journal of Environmental Chemical Engineering*, 9(1), p.104702. Doi: <https://doi.org/10.1016/j.jece.2020.104702>.

Foroughi, J., Mirabedini, A. and Warren, H. (2018). Hydrogels Fibers. In *Hydrogels* (pp. 121-139). IntechOpen. Doi: <http://dx.doi.org/10.5772/intechopen.74188>.

Foxx, M. and Zilberman, M. (2015). Drug delivery from gelatin-based systems. *Expert Opinion on Drug Delivery*, 12(9), pp.1547-1563. Doi: <https://doi.org/10.1517/17425247.2015.1037272>.

Fung, H.B., Stone, E.A. and Piacenti, F.J. (2002). Tenofovir disoproxil fumarate: a nucleotide reverse transcriptase inhibitor for the treatment of HIV infection. *Clinical Therapeutics*, 24(10), pp.1515-1548. Doi: [https://doi.org/10.1016/s0149-2918\(02\)80058-3](https://doi.org/10.1016/s0149-2918(02)80058-3).

Genta, I., Conti, B., Perugini, P., Pavanetto, F., Spadaro, A. and Puglisi, G. (1997). Bioadhesive microspheres for ophthalmic administration of acyclovir. *Journal of Pharmacy and Pharmacology*, 49(8), 737-742. Doi: 10.1111/j.2042-7158.1997.tb06103.x.

Giunchedi, P., Juliano, C., Gavini, E., Cossu, M. and Sorrenti, M. (2002). Formulation and in vivo evaluation of chlorhexidine buccal tablets prepared using drug-loaded chitosan microspheres. *European Journal Pharmaceutics and Biopharmaceutics*, 53(2), pp.233-239. Doi: 10.1016/s0939-6411(01)00237-5.

Harris, R., Yeung, R., áBrian Lamont, R., Lancaster, R., Lynn, S. and Staniforth, S. (1997). ‘Polymorphism’ in a novel anti-viral agent: Lamivudine. *Journal of the Chemical Society, Perkin Transactions 2*, (12), pp.2653-2660. Doi: <https://doi.org/10.1039/A704709F>.

Harris, R., Yeung, R., áBrian Lamont, R., Lancaster, R., Lynn, S. and Staniforth, S. (1998). CCDC 122714: Experimental Crystal Structure Determination. Doi: [10.5517/cc43pjf](https://doi.org/10.5517/cc43pjf).

He, P., Davis, S.S. and Illum, L. (1998). In vitro evaluation of the mucoadhesive properties of chitosan microspheres. *International Journal of Pharmaceutics*, 166(1), pp.75-88. Doi: [https://doi.org/10.1016/S0378-5173\(98\)00027-1](https://doi.org/10.1016/S0378-5173(98)00027-1).

Jaganathan, K.S., Rao, Y.U.B., Singh, P., Prabakaran, D., Gupta, S., Jain, A. and Vyas, S.P. (2005). Development of a single dose tetanus toxoid formulation based on polymeric microspheres: a comparative study of poly (D, L-lactic-co-glycolic acid) versus chitosan microspheres. *International Journal of Pharmaceutics*, 294(1-2), pp.23-32. Doi: 10.1016/j.ijpharm.2004.12.026.

Jana, S., Gandhi, A., Sen, K.K. and Basu, S.K. (2011). Natural polymers and their application in drug delivery and biomedical field. *Journal of Pharmaceutical Science and Technology*, 1(1), pp.16-27.

Jana, S., Sen, K.K. and Basu, S.K. (2011). Chitosan derivatives and their application in pharmaceutical fields. *International Journal of Pharmaceutical Sciences and Research*, 3(1).

Jana, S., Maiti, S., Sen, K.K. and Jana, S. (2019). Interpenetrating polysaccharide networks as oral drug delivery modalities. In *Polysaccharide Carriers for Drug Delivery*, pp. 319-338. Woodhead Publishing. Doi: <https://doi.org/10.1016/B978-0-08-102553-6.00011-8>.

Jain, A., Teja, M.R., Pariyani, L., Balamuralidhara, V. and Gupta, N.V. (2013). Formulation and evaluation of spray-dried esomeprazole magnesium microspheres. *Tropical Journal of Pharmaceutical Research*, 12(3), pp.299-304. Doi: <https://doi.org/10.4314/tjpr.v12i3.4>.

Jansson, P.E., Kenne, L. and Lindberg, B.J.C.R. (1975). Structure of the extracellular xanthomonas campestris *Carbohydrate Research*, 45, pp.275-82. Doi: [https://doi.org/10.1016/s0008-6215\(00\)85885-1](https://doi.org/10.1016/s0008-6215(00)85885-1).

Jiang, H.L., Park, I.K., Shin, N.R., Kang, S.G., Yoo, H.S., Kim, S.I., Suh, S.B., Akaike, T. and Cho, C.S. (2004). In vitro study of the immune stimulating activity of an atrophic rhinitis vaccine associated to chitosan microspheres. *European Journal Pharmaceutics and Biopharmaceutic*. 58(3), pp.471-476. Doi: [10.1016/j.ejpb.2004.05.006](https://doi.org/10.1016/j.ejpb.2004.05.006).

Jiang, H.L., Kang, M.L., Quan, J.S., Kang, S.G., Akaike, T., Yoo, H.S. and Cho, C.S. (2008). The potential of mannosylated chitosan microspheres to target macrophage mannose receptors in an adjuvant-delivery system for intranasal immunization. *Biomaterials*, 29(12), pp.1931-1939. Doi: 10.1016/j.biomaterials.2007.12.025.

Jozwiakowski, M.J., Nguyen, N.A.T., Sisco, J.M. and Spancake, C.W. (1996). Solubility behavior of lamivudine crystal forms in recrystallization solvents. *Journal of Pharmaceutical Sciences*, 85(2), pp.193-199. Doi: <https://doi.org/10.1021/js9501728>.

Johnson, M.A., Moore, K.H.P., Yuen, G.J., Bye, A. and Pakes, G.E. (1999). Clinical Pharmacokinetics of Lamivudine. drug disposition. *Clinical Pharmacokinetics*, Jan, 36 (1), pp. 41-66. Doi: <https://doi.org/10.2165/00003088-199936010-00004>.

Joye, I.J. and McClements, D.J. (2014). Biopolymer-based nanoparticles and microparticles: Fabrication, characterization, and application. *Current Opinion in Colloid & Interface Science*, 19(5), pp.417-427.

Kandel, C.E. and Walmsley, S.L. (2015). Dolutegravir—a review of the pharmacology, efficacy, and safety in the treatment of HIV. *Drug Design, Development and Therapy*, 9, p.3547. Doi: <https://doi.org/10.2147%2FDDDT.S84850>.

Kawai, K., Suzuki, S., Tabata, Y., Ikada, Y. and Nishimura, Y. (2000). Accelerated tissue regeneration through incorporation of basic fibroblast growth factor-impregnated gelatin microspheres into artificial dermis. *Biomaterials*, 21(5), pp.489-499. Doi: [https://doi.org/10.1016/S0142-9612\(99\)00207-0](https://doi.org/10.1016/S0142-9612(99)00207-0).

Kearney, B.P., Flaherty, J.F. and Shah, J. (2004). Tenofovir disoproxil fumarate. *Clinical Pharmacokinetics*, 43(9), pp.595-612. Doi: <https://doi.org/10.2165/00003088-200443090-00003>.

Khan, B.A. and Ram S.T. (2014). Formulation and evaluation of mucoadhesive microspheres of tenofovir disoproxil fumarate for intravaginal use. *Current Drug Delivery*, 11(1), 112-122. Doi: [10.2174/156720181000131028120709](https://doi.org/10.2174/156720181000131028120709).

Kimura, Y., Ozeki, M., Inamoto, T. and Tabata, Y. (2003). Adipose tissue engineering based on human preadipocytes combined with gelatin microspheres containing basic fibroblast growth factor. *Biomaterials*, 24(14), pp.2513-2521. Doi: [https://doi.org/10.1016/S0142-9612\(03\)00049-8](https://doi.org/10.1016/S0142-9612(03)00049-8).

Kumar, S. and Gupta, S.K. (2012). Natural polymers, gums and mucilages as excipients in drug delivery. *Polymer in Medicine*, 42(3-4), pp.191-197.

Kumar, A., Rao, K.M., Kwon, S.E., Lee, Y.N. and Han, S.S. (2017). Xanthan gum/bioactive silica glass hybrid scaffolds reinforced with cellulose nanocrystals: Morphological, mechanical and in vitro cytocompatibility study. *Materials Letters*, 193, pp.274-278. Doi: <https://doi.org/10.1016/j.matlet.2017.01.143>.

Kumar, A., Rao, K.M. and Han, S.S. (2018). Application of xanthan gum as polysaccharide in tissue engineering: A review. *Carbohydrate Polymers*, 180, pp.128-144. Doi: <https://doi.org/10.1016/j.carbpol.2017.10.009>.

Kumari, G. and Singh, R.K. (2012). Highly active antiretroviral therapy for treatment of HIV/AIDS patients: current status and future prospects and the Indian scenario. *HIV & AIDS Review*, 11(1), pp.5-14. Doi: <https://doi.org/10.1016/j.hivar.2012.02.003>.

Lee, E.H., Smith, D.T., Fanwick, P.E. and Byrn, S.R. (2010). Characterization and anisotropic lattice expansion/contraction of polymorphs of tenofovir disoproxil fumarate. *Crystal Growth & Design*, 10(5), pp.2314-2322. Doi: <https://doi.org/10.1021/cg1000667>.

Lengyel, M., Kállai-Szabó, N., Antal, V., Laki, A.J. and Antal, I. (2019). Microparticles, microspheres, and microcapsules for advanced drug delivery. *Scientia Pharmaceutica*, 87(3), p.20. Doi: <https://doi.org/10.3390/scipharm87030020>.

Li, G., Wang, Y. and De Clercq, E. (2022). Approved HIV reverse transcriptase inhibitors in the past decade. *Acta Pharmaceutica Sinica B*, 12(4), pp.1567-1590. Doi: <https://doi.org/10.1016/j.apsb.2021.11.009>.

Mishra, S. and Rautray, T.R. (2020). Fabrication of Xanthan gum-assisted hydroxyapatite microspheres for bone regeneration. *Materials Technology*, 35(6), pp.364-371. Doi: <https://doi.org/10.1080/10667857.2019.1685245>.

Mitra, A. and Dey, B. (2011). Chitosan microspheres in novel drug delivery systems. *Indian Journal of Pharmaceutical Sciences*, 73(4), 355 - 366. Doi: 10.4103/0250-474X.95607.

Ngwuluka, N.C., Ochekepe, N.A. and Aruoma, O.I. (2014). Naturapolyceutics: the science of utilizing natural polymers for drug delivery. *Polymers*. 6(5), pp.1312-1332. Doi:10.3390/polym6051312

Palaniraj, A. and Jayaraman, V. (2011). Production, recovery and applications of xanthan gum by *Xanthomonas campestris*. *Journal of Food Engineering*, 106(1), pp.1-12. Doi: <https://doi.org/10.1016/j.jfoodeng.2011.03.035>.

Patel, M.P., Patel, R.R. and Patel, J.K. (2010). Chitosan mediated targeted drug delivery system: a review. *Journal of Pharmacy & Pharmaceutical Sciences*, 13(4), pp.536-557. Doi: <https://doi.org/10.18433/J3JC7C>.

Petri, D.F. (2015). Xanthan gum: A versatile biopolymer for biomedical and technological applications. *Journal of Applied Polymer Science*, 132(23). Doi: <https://doi.org/10.1002/app.42035>.

Pillai, O. and Panchagnula, R. (2001). Polymers in drug delivery. *Current Opinion on Chemical Biology*, 5(4), 447-451. Doi: 10.1016/s1367-5931(00)00227-1.

Portero, A., Remunan-Lopez, C., Criado, M.T. and Alonso, M.J. (2002). eacetylated chitosan microspheres for controlled delivery of anti-microbial agents to the gastric mucosa. *Journal of Microencapsulation*, 19(6), pp.797-809. Doi: 10.1080/0265204021000022761.

PubChem. (2022a). National Center for Biotechnology Information. PubChem Compound Summary for CID 5486830, Tenofovir Disoproxil Fumarate. [Online] Available at: <https://pubchem.ncbi.nlm.nih.gov/compound/Tenofovir-Disoproxil-Fumarate>. [Accessed on February 19, 2022].

PubChem. (2022b). National Center for Biotechnology Information. PubChem Compound Summary for CID 60825, Lamivudine. [Online] Available at: <https://pubchem.ncbi.nlm.nih.gov/compound/Lamivudine>. [Accessed on February 19, 2022].

PubChem. (2022c). National Center for Biotechnology Information. PubChem Compound Summary for CID 71853, Chitosan. [Online] Available at: <https://pubchem.ncbi.nlm.nih.gov/compound/Chitosan>. [Accessed Nov. 10, 2022].

Qiao, C., Cao, X. and Wang, F. (2012). Swelling behavior study of physically crosslinked gelatin hydrogels. *Polymers and Polymer Composites*, 20(1-2), pp.53-58. Doi: <https://doi.org/10.1177/0967391112020001-210>.

Rowe, R.C., Sheskey, P. and Quinn, M. (2009). *Handbook of Pharmaceutical Excipients*. Libros Digitales-Pharmaceutical Press.

Rbii, K., Surel, O., Brambati, N., Buchert, A.M. and Violleau, F. (2011). Study of gelatin renaturation in aqueous solution by AFIFFF–MALS: Influence of a thermal pre-treatment applied on gelatin. *Food hydrocolloids*, 25(3), pp.511-514. Doi: <https://doi.org/10.1016/j.foodhyd.2010.08.001>.

Saha, T.K., Ichikawa, H. and Fukumori, Y. (2006). Gadolinium diethylenetriaminopentaacetic acid-loaded chitosan microspheres for gadolinium neutron-capture therapy. *Carbohydrate Research*, 341(17), pp.2835-2841. Doi: [10.1016/j.carres.2006.09.016](https://doi.org/10.1016/j.carres.2006.09.016).

Sankaraiah, J., Sharma, N. and Naim, M.J. (2022). Formulation and development of fixed-dose combination of bi-layer tablets of efavirenz, lamivudine and tenofovir disoproxil fumarate tablets 600 MG/300 MG/300 MG. *International Journal of Applied Pharmaceutics*, 14(1), pp.185-197.

Shrivastava, A. (2018). Introduction to plastics engineering, first ed. William, A. Publishing. <https://doi.org/10.1016/B978-0-323-39500-7.00001-0>.

Simionescu B.C. and Ivanov, D. (2015). Natural and synthetic polymers for designing composite materials, in: Antoniac, I. (Eds.), *Handbook of Bioceramics and Biocomposites*. Springer pp.1-54.

Singh, G.P., Srivastava, D., Saini, M.B. and Upadhyay, P.R., Lupin Limited. (2007). *A novel crystalline form of lamivudine*.

Singh, P., Prakash, D.E.V., Ramesh, B., Singh, N. and Mani, T.T. (2011). Biodegradable polymeric microspheres as drug carriers; A review. *Indian Journal of Novel Drug Delivery*, 3(2), pp.70-82.

Singh, U.V. and Udupa, N. (1998). Methotrexate loaded chitosan and chitin microspheres—in vitro characterization and pharmacokinetics in mice bearing Ehrlich ascites carcinoma. *Journal of Microencapsulation*, 15(5), 581-594. Doi: [10.3109/02652049809008242](https://doi.org/10.3109/02652049809008242).

Sládková, V., Dammer, O. and Kratochvíl, B. (2016). Solid forms of tenofovir disoproxil fumarate, their mutual conversion, and stabilization of form I in formulation. *Journal of Pharmaceutical Sciences*, 105(10), pp.3136-3142. Doi: <https://doi.org/10.1016/j.xphs.2016.07.002>.

Strauch, S., Jantratid E., Dressman, J.B., Junginger, H.E., Kopp, S., Midha, K.K., Shah, V.P., Stavchansky, S., Barends, D.M. (2011). Biowaiver monographs for immediate release solid oral dosage forms: lamivudine. *Journal of Pharmaceutical Sciences*, 100(6):2054-63. Doi: 10.1002/jps.22449.

Swetha, M., Sahithi, K., Moorthi, A., Srinivasan, N., Ramasamy, K. and Selvamurugan, N. (2010). Biocomposites containing natural polymers and hydroxyapatite for bone tissue engineering. *Int. J. Biol. Macromol.* 47(1), 1-4. Doi: 10.1016/j.ijbiomac.2010.03.015.

Tong, L., Phan, T.K., Robinson, K.L., Babusis, D., Strab, R., Bhoopathy, S., Hidalgo, I.J., Rhodes, G.R. and Ray, A.S. (2007). Effects of human immunodeficiency virus protease inhibitors on the intestinal absorption of tenofovir disoproxil fumarate in vitro. *Antimicrobial Agents and Chemotherapy*, 51(10), pp.3498-3504. Doi: <https://doi.org/10.1128/AAC.00671-07>.

Trombino, S., Serini, S., Cassano, R. and Calviello, G. (2019). Xanthan gum-based materials for omega-3 PUFA delivery: Preparation, characterization and antineoplastic activity evaluation. *Carbohydrate Polymers*, 208, pp.431-440. Doi: <https://doi.org/10.1016/j.carbpol.2019.01.001>.

Vandelli, M.A., Rivasi, F., Guerra, P., Forni, F. and Arletti, R. (2001). Gelatin microspheres crosslinked with D, L-glyceraldehyde as a potential drug delivery system: preparation, characterisation, in vitro and in vivo studies. *Int. J. Pharm.* 215(1-2), 175-184. Doi: 10.1016/s0378-5173(00)00681-5.

Van Leeuwen, R., Lange, J.M., Hussey, E.K., Donn, K.H., Hall, S.T., Harker, A.J., Jonker, P. and Danner, S.A. (1992). The safety and pharmacokinetics of a reverse transcriptase inhibitor, 3TC, in patients with HIV infection: a phase I study. *AIDS (London, England)*, 6(12), pp.1471-1475. Doi: <https://doi.org/10.1097/00002030-199212000-00008>.

Varshosaz, J., Sadrai, H. and Alinagari, R. (2004). Nasal delivery of insulin using chitosan microspheres. *Journal of Microencapsulation*, 21(7), pp.761-774. Doi: 10.1080/02652040400015403.

Varshosaz, J. (2007). The promise of chitosan microspheres in drug delivery systems. *Expert Opinion on Drug Delivery*, 4(3), pp. 263-273. Doi: 10.1517/17425247.4.3.263.

Wassner, C., Bradley, N. and Lee, Y. (2020). A review and clinical understanding of tenofovir: tenofovir disoproxil fumarate versus tenofovir alafenamide. *Journal of the International Association of Providers of AIDS Care*, 19, p.2325958220919231. Doi: <https://doi.org/10.1177%2F2325958220919231>.

Xie, Y.L., Zhou, H.M. and Qian, H.F. (2006). Effect of addition of peach gum on physicochemical properties of gelatin-based microcapsule. *Journal of Food Biochemistry*, 30(3), pp.302-312. Doi: <https://doi.org/10.1111/j.1745-4514.2006.00061.x>.

Zamora, F.J., Dowers, E., Yasin, F. and Ogbuagu, O. (2019). Dolutegravir and lamivudine combination for the treatment of HIV-1 infection. *HIV/AIDS-Research and Palliative Care*, pp.255-263. Doi: <https://doi.org/10.2147%2FHIV.S216067>.

Zhao, Y., Keene, C., Griesel, R., Sayed, K., Gwabe, Z., Jackson, A., Ngwenya, O., Schutz, C., Goliath, R., Cassidy, T. and Goemaere, E. (2021). AntiRetroviral Therapy In Second-line: investigating Tenofovir-lamivudine-dolutegravir (ARTIST): protocol for a randomised controlled trial. *Wellcome Open Research*, 6, p.33. Doi: <https://doi.org/10.12688/wellcomeopenres.16597.1>.

Chapter Three

Materials and Methodology

3.1 Introduction

The materials, techniques, and analytical tools used to determine the physicochemical properties and compatibility of 3TC, TDF, and the excipients (CH, GEL, XG, and SA) are discussed in detail in this chapter. In addition, the preparation of polymeric microspheres *via* ionic gelation and spray drying, with subsequent physicochemical characterisation and *in vitro* drug release profiles of drug-loaded microspheres, will be detailed.

3.2 Materials

3TC raw material was supplied by DB Fine Chemicals (Pty) Ltd. (Johannesburg, South Africa). TDF was an in-kind donation from Cipla in South Africa (Cape Town). Kimix Chemicals (Cape Town, South Africa) supplied chromatography-grade methanol (>99.9%). Analytical grade orthophosphoric acid, sodium hydroxide, 3% v/v hydrogen peroxide, glacial acetic acid, and 32% v/v hydrochloric acid, as well as acid-washed glass beads ($\leq 106 \mu\text{m}$) and gelatin Type B, were obtained from Sigma-Aldrich (Johannesburg, South Africa). Analytical grade sodium chloride, ammonium acetate, disodium hydrogen phosphate, citric acid, and potassium dihydrogen phosphate were purchased from LabChem (Johannesburg, South Africa). The distilled water for this study was provided by a Milli-Q Elix® Essential 3 water purification system (Merck, Johannesburg, South Africa). A Lasec® Purite laboratory water system provided ultrapure HPLC water with a resistivity of $18.2 \text{ M}\cdot\text{cm}^{-1}$ (Johannesburg, South Africa).

3.3 Methodology

3.3.1 Physicochemical characterisation of pure APIs, excipients and prepared microspheres

(a) Hot stage microscopy (HSM)

HSM, also known as thermal microscopy, is widely used as a foundation for the thermal analyses of compounds since it allows for the visual observation of changes in samples as a function of temperature and time. HSM is typically used to complement differential scanning calorimetry (DSC) and thermogravimetric analysis (TGA) results. Particle size and morphology, miscibility, melting, sublimation, evaporation, dehydration, decomposition, crystal growth, degradation,

incompatibility/interaction, desolvation, and polymorphism, are just a few of the physicochemical properties of active pharmaceutical ingredients and excipients that can be easily studied using HSM (Kumar *et al.*, 2020; Patel *et al.*, 2015; Stieger *et al.*, 2012).

In this study, a small amount of each sample was placed on a microscopic glass slide and heated on the Linkpad heating stage (Linkam Scientific Instruments Ltd., United Kingdom). A small amount of silicone oil was used to immerse the sample, which was then covered with a second microscope slide. Each sample was heated at a constant rate of 10 °C/min from 25 °C ± 2 °C until degradation was observed. Images were observed, captured, and temperatures recorded at each visible thermal event using Stream Essentials software and an Olympus UC30 camera attached to the microscope (Olympus Optical, Japan).

(b) Differential Scanning Calorimetry (DSC)

DSC is a thermal analysis method that determines the rate of heat flow and temperature in relation to sample changes, such as physical or chemical changes that occur due to temperature and time (Gill *et al.*, 2010). When heated at the same time and temperature, this apparatus can distinguish the amount of heat needed to raise the temperature of a sample against a known reference standard (Freire, 1995; Kodre *et al.*, 2014). Detecting phase transitions is one of the most essential applications of DSC. Inside the DSC, the sample to be analysed undergoes a physical change, requiring more or less heat to flow through the sample compared to the reference to maintain temperature equilibrium between them. An endothermic phase transition occurs when a sample requires more heat or energy to flow to equilibrate to the reference temperature. For example, more energy is absorbed by the sample during the transformation from solid to liquid. An exothermic phase transition occurs when less energy is required to raise the temperature of a sample (crystallization) (Gaisford *et al.*, 2019; Kodre *et al.*, 2014).

The samples were prepared by precisely weighing 2.0–3.0 mg of each sample into an aluminium pan, subsequently sealing it with an aluminium lid using a Perkin Elmer crimping device. A sealed, empty aluminium pan served as the reference sample. A Perkin Elmer DSC 8000 (Waltham, USA) was used. Each sample was heated from 30 to 300 °C at a heating rate of 10 °C/min at a flow rate of 20 mL/min. The equipment's melting temperature and heat flow accuracy were calibrated using indium (m.p. 156.6 °C, 28.62 J/g) and zinc (m.p. 419.5 °C). The obtained thermal data was processed using Pyris™ software (Perkin Elmer, Waltham, USA).

(c) Thermogravimetric analysis (TGA)

TGA is a thermal analysis procedure in which the sample mass is measured as temperature changes occur over time. This technique also provides information about physical (such as vaporization, adsorption, desorption, sublimation, fusion, crystalline transition, and absorption) and chemical (such as oxidation, chemisorption, dehydration, decomposition, and solid-state reactions) phenomena (Coats & Redfern, 1963; Law & Zhou, 2017). TGA can estimate the thermal stability of a specific sample over a specified temperature range. An advantage of TGA decomposition kinetics studies is that data may be obtained in a matter of hours, as opposed to the very long testing time required for oven-aged samples (Rajeswari *et al.*, 2020).

Each sample was prepared by zeroing an empty ceramic crucible on the Perkin Elmer 4000 (Waltham, USA) balance. Subsequently, about 2–4 mg of the sample was added to the crucible. The sample weight was recorded by the software, followed by heating from 30-600 °C at a controlled heating rate of 10 °C/min and a constant dry nitrogen gas purge of 20 mL/min. This instrument was periodically calibrated using the melting points of indium and aluminium, respectively, at 156.6 °C and 660.3 °C. The data was processed and retrieved using Pyris™ software (Perkin Elmer, Waltham, USA).

(d) Fourier-Transform infrared spectroscopy (FTIR)

FTIR is a procedure for collecting an infrared band of emission or absorption from a sample (Griffiths & James, 2007). When a sample is exposed to infrared radiation, the type of functional group in its molecular structure causes vibrational transitions like scissoring, bending, wiggling, contracting, rocking, stretching, wagging, and twisting of covalent bonds. This creates the sample's unique molecular fingerprint (Hou *et al.*, 2018; Law & Zhou, 2017). FTIR is typically used to determine how much light a sample can absorb at a specific wavelength range. The mid-infrared region was used in this study with a wavenumber of 4000 to 400 cm^{-1} , which corresponds to a wavelength between 2500 and 25000 nm (Hofko *et al.*, 2018). The solid-state behaviour of APIs and their pharmaceutical preparations can be determined using vibrational spectroscopy methods such as FTIR and Raman. These techniques can be used in compatibility studies to detect vibrational changes attributed to possible intermolecular interactions between mixture components. As a result, interactions that resulted in hydrate formation, dehydration, desalting, and the polymorphic transition of crystalline to amorphous states during pharmaceutical material

processing can be easily identified by these procedures. Regardless, overlapping peaks in the spectra can impede the investigation (Patel *et al.*, 2015).

Experimentally, a minute amount of the sample was placed on the cleaned crystal of the Perkin Elmer (Waltham, USA) Spectrum 400 spectrometer, and pressure was applied to a maximum of 60%. The sample was scanned four times at 2–4 cm⁻¹/sec resolutions. Each sample was analysed at a range of 650–4000 cm⁻¹. Spectrum[®] software version 6.3.5 (Perkin Elmer, Waltham, USA) was used to analyse, process, and retrieve the infrared spectra.

(e) Powder X-ray diffraction (PXRD)

PXRD is a quick and non-destructive method for quantifying a sample's diffraction pattern and determining the crystal morphology or crystallinity compared to a reference material. PXRD can quantify and qualitatively assess the degree of crystallinity of a pure drug. It is also used to investigate phase transitions and to characterise solvates and polymorphs (Law & Zhou, 2017; Rajeswari *et al.*, 2020; Tomoda *et al.*, 2020). PXRD is most commonly used for crystal identification and characterisation; each crystalline solid generates a unique diffraction configuration (each material will generate a distinctive pattern based on the structure of its crystal lattice). The lattice spacing and intensity of peaks in diffraction patterns reveal a sample's specific phases or components, resulting in an evaluation "fingerprint". In PXRD, crystalline samples show sharp peaks, whereas amorphous samples show broad, amorphous halos (Scrivens *et al.*, 2018; Tomoda *et al.*, 2020).

During sample analysis, a small amount of each sample was gently ground using an agate mortar and pestle. Subsequently, the samples were evenly distributed onto a suitable sample holder to form a thin layer. The PXRD pattern was obtained using a Bruker D8 Advance powder X-ray diffractometer (Karlsruhe, Germany) with radiation set at 40kV and 40mA. Diffraction patterns were collected between 4 and 40 °2 θ at room temperature.

(f) Scanning electron microscopy (SEM)

The morphology of powder particles and the formulated microspheres were determined by scanning electron microscopy. SEM analysis was done using an AURIGA Field Emission high-resolution scanning electron microscope (Zeiss, Germany). The sample to be analysed was mounted onto an aluminium stub using carbon tape. The mounted sample was subsequently coated

with a thin layer of gold-palladium. An accelerating voltage of 5 kV and a filament current of 2.350 ampere was applied.

(g) Particle size analysis

Particle size analysis of the spray dried drug-loaded microspheres were conducted using a PSA 1190 particle size analyser with a liquid dispersed particle size analysis range of 0.04 – 2500 µm (Anton Paar, Graz, Austria). All samples were analysed in liquid mode with the dispersant being distilled water. Approximately, 150 mg of sample was dispersed in 45 ml distilled water and the resulting dispersion was loaded into the instrument autosampler. A stirrer speed of 250 rpm and pump speed of 120 rpm at ambient temperature was utilised. The collected data was analysed by the Kalliope™ (Anton Paar, Graz, Austria) software. All measurements were conducted in triplicate (n = 3).

(h) High-performance liquid chromatography (HPLC)

At the onset of this study it was noted that the simultaneous HPLC analysis of 3TC and TDF was poorly documented and that most analytical methods reported simultaneous analysis from blood plasma samples but none considered the analysis of these drugs once incorporated into a polymeric matrix (Valluru *et al.*, 2013). It was therefore important to establish a suitably sensitive analytical method that would allow the accurate detection of the drugs with minimal to no interference by the polymers which were planned to be used in this study. To add multi-functionality to the HPLC method it was decided to develop and validate a suitable method which would also allow the detection and quantification of dolutegravir sodium (DTG). The rationale for this was based on the fact that DTG is often combined with 3TC and/or TDF. It was also considered that future studies might explore the combination of DTG with some of the polymers used in this study. This led to the development and validation of the following analytical method (Omoteso *et al.*, 2022).

The stationary phase of the reversed-phase HPLC procedure was a Kinetex®C₁₈, 250 x 4.6mm column. At 35 °C, the liquid chromatographic system ran isocratically with a mobile phase of 50:50 v/v methanol and water plus 1 mL orthophosphoric acid. The UV detection wavelength was set at 260 nm. The flow rate was 1.0 mL/min, with a sample injection volume of 10 µL/min. The method was validated using the International Conference on Harmonization of Technical Conditions for Pharmaceuticals for Human Use (ICH) recommendation Q2 (R1) (ICH Q2A, 1994;

ICH Q2B). The values of the following parameters were obtained: linearity and range, specificity, the limit of detection (LOD), the limit of quantification (LOQ), robustness, accuracy, and stability.

Appropriate correlation coefficients for linearity (R^2) of > 0.998 were obtained for 3TC, TDF and dolutegravir sodium (DTG). The LOD and LOQ were determined to be (40.27 $\mu\text{g/mL}$, 56.31 $\mu\text{g/mL}$, and 7.00 $\mu\text{g/mL}$ for TDF, 3TC, and DTG, respectively) and (134.22 $\mu\text{g/mL}$, 187.69 $\mu\text{g/mL}$, and 22.50 $\mu\text{g/mL}$ for TDF, 3TC, and DTG).

This method demonstrated precision, linearity, accuracy, recovery, ruggedness, and specificity in the detection and estimation of the three ARVs, separately or together, and when integrated within a polymeric matrix system. Furthermore, the degradation of the compounds can be easily detected using this method. The method development and validation was compiled into an already published research paper and will therefore not be discussed in detailed in this section (Omoteso *et al.*, 2022).

3.3.2 Preparation of microspheres

The formulation of microspheres was investigated using two techniques, namely: ionic gelation and spray drying.

(a) Formulation of drug-loaded microspheres *via* ionic gelation

This microspheres preparation approach used polymers such as XG, GEL, CH and SA. The ionic gelation preparation methods by Sharma *et al.* (2017), Shu & Zhu (2001), and Varma & Rao (2012) were used with modifications. Solutions consisting of XG, GEL or CH or combinations of these polymers and in various ratios were prepared in distilled water. Briefly, the relevant concentration(s) of polymer(s) was weighed using an analytical balance and subsequently transferred to a suitable size glass beaker containing distilled water. The resulting mixture was stirred constantly using a magnetic plate stirrer and magnetic stirrer bar until an homogeneous polymer solution was obtained. Subsequently, a specific concentration of the drug to be encapsulated into the microspheres were added to the polymer solution followed by continuous stirring until the polymer:drug solution was homogenous. Finally, the relevant crosslinker solution was prepared by weighing a suitable amount of calcium chloride which was subsequently transferred to a suitable glass beaker. The calcium chloride was dissolved in distilled water. This

study involved the investigation of various polymer, drug and crosslinker concentrations and the exact concentrations are specified in Chapter 4 as part of each relevant section.

After successful preparation of the polymer:drug and crosslinker solutions the polymer:drug solution was added dropwise to the crosslinker solution utilising a polypropylene syringe with an 18 gauge needle. After crosslinking, the resulting microspheres were allowed to cure for a period of time. The microspheres were collected and cleaned with distilled water. After washing, the spheres were carefully separated and dried on filter paper until a constant weight was achieved (Sharma *et al.*, 2017; Shu & Zhu, 2001; Varma & Rao, 2012).

(b) Formulation of drug-loaded microspheres by spray-drying

To make the microspheres, a Büchi B-290 spray dryer (Flawil, Switzerland) was utilised. For spray drying, a feed flow rate of 30 ml/min and an inlet temperature of 150 °C were used. These optimal processing parameters were determined after several trials with 15 g of GEL dissolved in a 10% v/v ethanol solution were spray dried using various instrument parameters. For the purpose of this study, various polymer:drug ratios were spray dried and characterised. The moisture content of the obtained microspheres was determined by desiccating for 60 minutes at 100 °C approximately 2g of each sample on an aluminium dish of the HR73 Halogen moisture analyser (Mettler-Toledo, Greifensee, Switzerland). The formulations were stored in a desiccator until needed.

3.3.2.1 Investigation of drug-loaded microspheres

(a) Percentage yield

This is the percentage of the total number of microspheres recovered after preparation and drying. Equation 3.1 was used to calculate the percentage yield after the formulation of drug-loaded microspheres.

Percentage yield (%) = ((Total mass of microspheres retrieved)/ (Total mass of drug and polymer))
X 100

Equation 3.1

(b) Content uniformity, drug loading and encapsulation efficiency (% EE)

The drug content uniformity, drug loading and encapsulation efficiency (% EE) were determined by weighing a known amount of microspheres (10 ± 5 mg) from different sections or portions of the formulation ($n = 9$). Subsequently, the samples were transferred into 10 ml volumetric flasks and diluted with distilled water. The resulting solutions were sonicated for 30 minutes, then filtered through $0.45 \mu\text{m}$ PVDF syringe filters into HPLC vials followed by HPLC analysis. Equations 3.2 – 3.4 were utilised to quantify content uniformity, drug loading and %EE.

$$\text{Content Uniformity (CU) (\%)} = \left(\frac{\text{Peak Area}_{(\text{sample})} \times \text{Concentration}_{(\text{standard})}}{\text{Peak Area}_{(\text{standard})} \times \text{Concentration}_{(\text{sample})}} \right) \times 100$$

Equation 3.2

$$\text{Encapsulation Efficiency (EE) (\%)} = \left(\frac{\text{total amount of drug in the microsphere yield from content uniformity}}{\text{amount of drug added during microsphere preparation}} \right) \times 100$$

Equation 3.3

$$\text{Drug loading (\%)} = \left(\frac{\text{weight of the drug in the sampled microspheres 'mg' from content uniformity}}{\text{weight of the sampled microspheres 'mg'}} \right) \times 100$$

Equation 3.4

(c) *In vitro* dissolution testing

All the formulated microspheres' *in vitro* dissolution studies were conducted using a Vankel VK700 dissolution bath (Varian, Palo Alto, USA). Microsphere dissolution experiments were performed in 0.1 M HCL buffer-pH-1.2, prepared as described in paragraph 3.3.2.1(e). The six dissolution vessels were filled with 900 ml of the dissolution medium, and the dissolution apparatus setup was kept at 37.5 ± 0.5 °C with a stirring speed or paddle rotation of 50 rpm. Before being dispersed into the vessels, the microspheres were suspended with glass beads. An aliquot (5 ml) of the dissolution medium was withdrawn from each of the six vessels at predetermined time intervals and filtered into HPLC vials for subsequent quantification through HPLC analysis using $0.22 \mu\text{m}$ PVDF syringe filters. After each withdrawal dissolution medium was replaced with the same volume (5 ml) of pre-heated, fresh dissolution medium to maintain the sink effect.

(d) Physicochemical and morphological investigation of drug-loaded microspheres

In order to gain a better understanding of the obtained drug release from the drug-loaded microspheres each formulation was further investigated using DSC, TGA, FTIR, PXRD, SEM and in some instances particle size analyses as already outlined in paragraphs 3.3.1 (a – g).

(e) Swelling behaviour

The swelling properties of drug-loaded polymeric microspheres were investigated to determine the fluid permeation rate through the formulation's matrix system and the swelling capacity. The swelling capacity was determined in pH 1.2 and pH 6.8 aqueous media to simulate what would happen to the formulations inside the GIT. The pH-1.2 acidic-buffered solution was made by combining 2 grams of sodium chloride and 7 ml of 0.1N hydrochloric acid in a 1 litre volumetric flask, then diluting it to 1000 ml with distilled water. The phosphate-buffered solution pH-6.8 was made by combining 77.3 ml of a 71.5 g/L disodium hydrogen phosphate solution with 22.7 ml of a 21 g/L citric acid solution in a 1 litre volumetric flask and diluting to 1000 ml with distilled water (USP, 2011). For this study, 50 mg of each formulation, drug:polymer physical mixture and GEL was added to 1 ml of the buffer solution (n = 3). After 24 hours the wet samples were blotted with filter paper and weighed immediately on an electronic balance. Equation 3.5 provides the calculation used to determine the percentage swelling of the microspheres in the buffer medium.

Percentage swelling (%) = $\frac{((\text{final weight of microspheres} - \text{initial dry weight of microspheres}) / (\text{initial dry weight of microspheres})) \times 100$

Equation 3.5

3.3.3 Drug-excipient compatibility studies

In pharmaceutical preparations, there are unavoidable direct contact between the drug(s) and excipient(s). Excipients are considered inactive since they are not eliciting any pharmacological action but these inert compounds can interact with drugs within dosage forms. To determine the presence or absence of dual or multiple drug-excipient interactions, extensive drug-drug and drug-excipient compatibility studies are required in the development of FDCs (Jeličić *et al.*, 2021). Drug-drug or drug-excipient interactions, also known as chemical, physical, or therapeutic incompatibilities, primarily result in unacceptable safety, efficacy, and stability. Physical

incompatibilities are changes in the organoleptic properties and/or solid-state form transformations caused by the combination of drugs or drugs and excipients. Chemical incompatibilities are the formation of inactive or toxic related substances as a result of chemical changes when drugs or drugs and excipients are combined (Jeličić *et al.*, 2020; Jeličić *et al.*, 2021). As a result, prior to formulation into any dosage form, a drug-drug and drug-excipient compatibility investigation is required. This would lead to information that would inform careful excipient selection and ultimately well-developed dosage forms. In a nutshell, determining drug-drug or drug-excipient compatibility is critical to ensure optimal drug bioavailability, acceptable shelf-life and ultimately positive patient treatment outcomes (Chadha & Bhandari, 2014; Chaves *et al.*, 2013; Patel *et al.*, 2015).

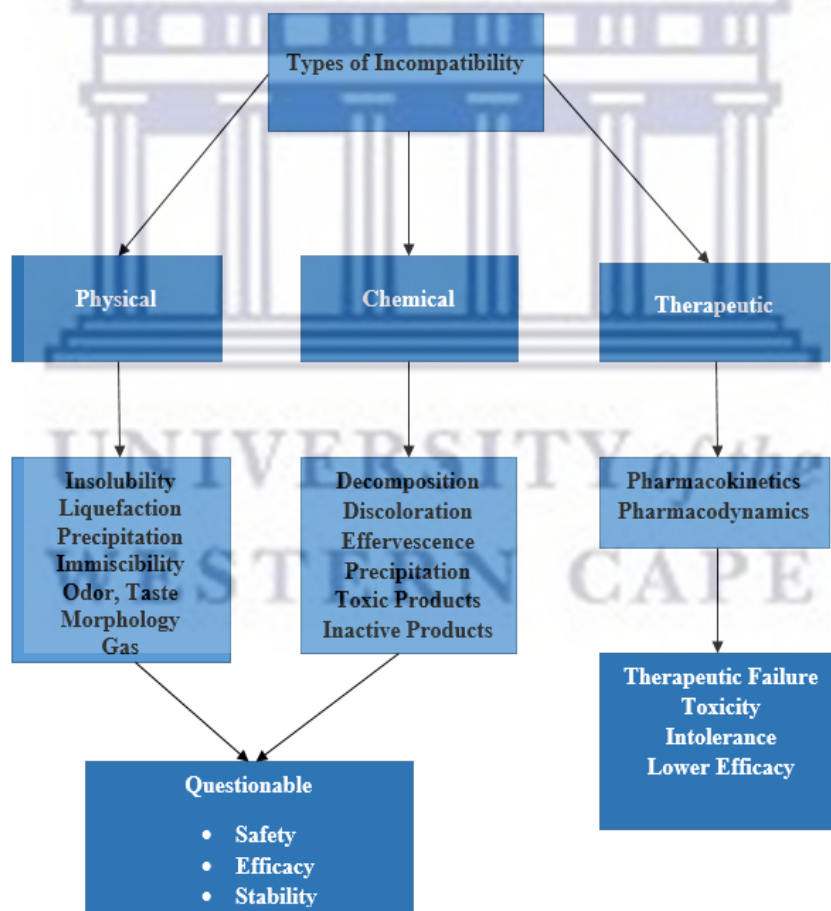


Figure 3.1: Summary of the types of drug-drug or drug-excipient incompatibilities (Di Perri *et al.*, 2005; Jeličić *et al.*, 2020; Jeličić *et al.*, 2021).

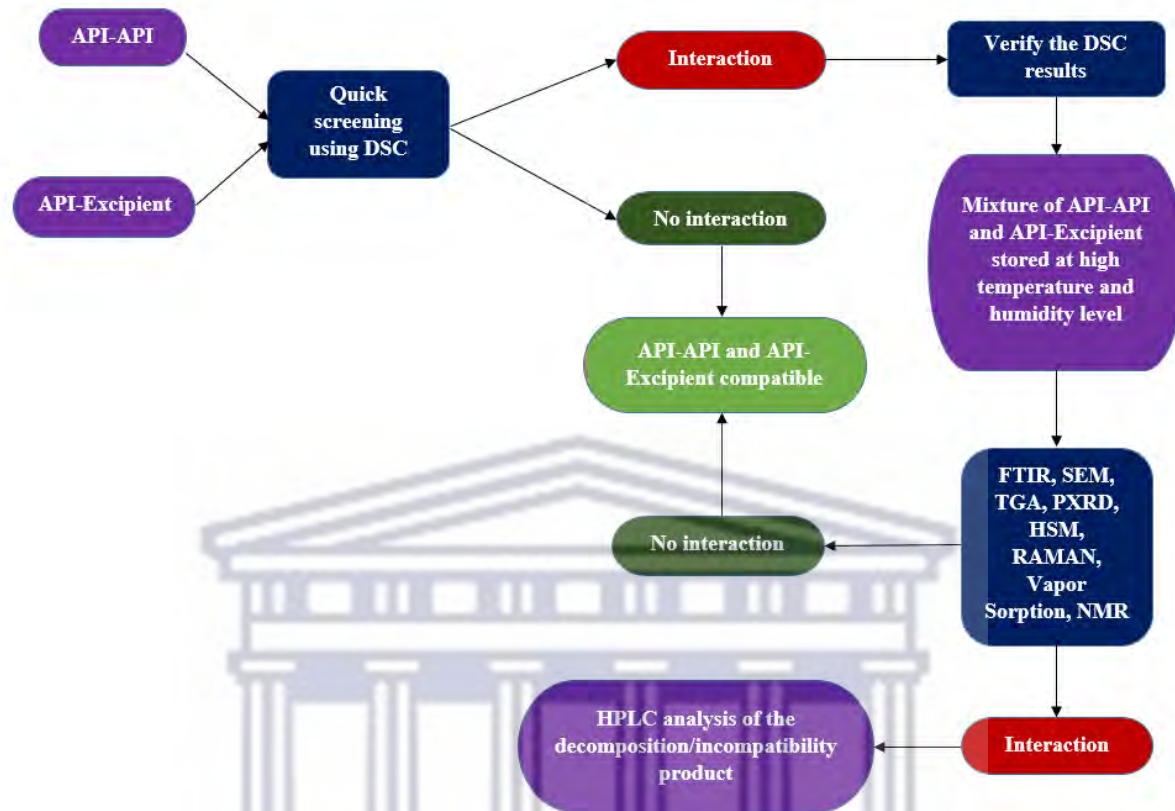


Figure 3.2: Decision tree for drug-drug and drug-excipient compatibility study (Chadha & Bhandari, 2014; Chaves *et al.*, 2013).

(a) Preparation of compatibility testing samples

Individual bulk powders of 3TC, TDF, and excipients were analysed using DSC, TGA, FTIR, and PXRD. The purity of each drug was also determined in comparison with the reference standards using HPLC analysis. The physical mixtures of each drug with excipient(s) in 1:1 wt/wt ratio were prepared by weighing the known amount of each drug into clearly labelled polytop vials, followed by the addition of the correctly weighed amount of excipient. The mixture was subsequently mixed for 5 minutes with a vortex mixer, then examined in the study.

(b) Examination of organoleptic properties

Samples were visually inspected for any physical changes that would suggest incompatibility, such as colour changes, odour, miscibility or textures, and liquefaction/melting or other physical alterations (Chadha & Bhandari, 2014).

(c) Isothermal Stress Testing (IST)

IST is typically used to assess the compatibility or interaction of two or more components. This method involves storing the multi-component blends (drug-drug or drug-excipient) in an oven at a temperature of 50-90 °C for a set period of time in the presence or absence of moisture. The drug content and physicochemical properties are then determined in order to establish the chemical and physical stability of the sample mixtures or to accelerate drug-drug and drug-excipient interaction (Gu *et al.*, 1990; Verma & Garg, 2005).

Isothermal stress testing was performed by exposure of the samples to extreme temperature of 60 °C ± 0.5 for 1 week in enclosed containers and stored inside a laboratory oven without added moisture. After the 1 week storing period, the samples were characterised using various analytical methods such as organoleptic property observation, DSC, TGA, FTIR, and PXRD to determine the physical compatibility or incompatibility of the drug-excipient mixtures.

3.4 Conclusion

This chapter detailed about the tools and methods utilised to carry out this study. Before analysing any sample, the instruments were calibrated to an acceptable standard to enable accurate and precise measurement. The outcomes of the experiments and data analysis were verified. A novel and simple HPLC method was designed, developed, and validated for the purpose of this study and the resulting, published research paper is attached as **Appendix I** to this thesis.

3.5 References

- Buckton, G. and Darcy, P. (1995). The use of gravimetric studies to assess the degree of crystallinity of predominantly crystalline powders. *International Journal of Pharmaceutics*, 123(2), pp.265-271. Doi: [https://doi.org/10.1016/0378-5173\(95\)00083-U](https://doi.org/10.1016/0378-5173(95)00083-U).
- Chadha, R. and Bhandari, S. (2014). Drug–excipient compatibility screening—role of thermoanalytical and spectroscopic techniques. *Journal of Pharmaceutical and Biomedical analysis*, 87, pp.82-97. Doi: <https://doi.org/10.1016/j.jpba.2013.06.016>.
- Chaves, L.L., Rolim, L.A., Gonçalves, M.L., Vieira, A.C., Alves, L.D., Soares, M.F., Soares-Sobrinho, J.L., Lima, M.C. and Rolim-Neto, P.J. (2013). Study of stability and drug-excipient compatibility of diethylcarbamazine citrate. *Journal of Thermal Analysis and Calorimetry*, 111(3), pp.2179-2186. Doi: <https://doi.org/10.1007/s10973-012-2775-7>.
- Coats, A.W. and Redfern, J.P. (1963). Thermogravimetric analysis. A review. *Analyst*, 88(1053), pp.906-924. Doi: <https://doi.org/10.1039/AN9638800906>.
- Di Perri, G., Aguilar Marucco, D., Mondo, A., Gonzalez de Requena, D., Audagnotto, S., Gobbi, F. and Bonora, S. (2005). Drug–drug interactions and tolerance in combining antituberculosis and antiretroviral therapy. *Expert Opinion on Drug Safety*, 4(5), pp.821-836. Doi: <https://doi.org/10.1517/14740338.4.5.821>.
- Egerton, R.F. (2016). The scanning electron microscope. In *Physical principles of electron microscopy* (pp. 121-147). Springer, Cham. Doi: https://doi.org/10.1007/978-3-319-39877-8_5.
- Freire, E. (1995). Differential scanning calorimetry. *Protein stability and folding*, pp.191-218. Doi: <https://doi.org/10.1385/0-89603-301-5:191>.
- Gaisford, S., Kett, V. and Haines, P. eds. (2019). *Principles of thermal analysis and calorimetry*. Royal society of chemistry.
- Gill, P., Moghadam, T.T. and Ranjbar, B. (2010). Differential scanning calorimetry techniques: applications in biology and nanoscience. *Journal of Biomolecular Techniques: JBT*, 21(4), p.167. Doi: <https://www.ncbi.nlm.nih.gov/pmc/articles/PMC2977967/>.

Gu, L., Strickley, R.G., Chi, L.H. and Chowhan, Z.T. (1990). Drug-excipient incompatibility studies of the dipeptide angiotensin-converting enzyme inhibitor, moexipril hydrochloride: dry powder vs wet granulation. *Pharmaceutical Research*, 7(4), pp.379-383. Doi: <https://doi.org/10.1023/A:1015871406549>.

Hassel, R.L. and Hesse, N.D. (2007). Investigation of pharmaceutical stability using dynamic vapor sorption analysis. New Castle (DE): TA Instruments Training Course.

Hofko, B., Porot, L., Falchetto Cannone, A., Poulikakos, L., Huber, L., Lu, X., Mollenhauer, K. and Grothe, H. (2018). FTIR spectral analysis of bituminous binders: Reproducibility and impact of ageing temperature. *Materials and Structures*, 51(2), pp.1-16. Doi: <https://doi.org/10.1617/s11527-018-1170-7>.

Hou, X., Lv, S., Chen, Z. and Xiao, F. (2018). Applications of Fourier transform infrared spectroscopy technologies on asphalt materials. *Measurement*, 121, pp.304-316. Doi: <https://doi.org/10.1016/j.measurement.2018.03.001>.

ICH Q2A, “Harmonised tripartite guideline, text on validation of analytical procedures, IFPMA,” in *Proceedings of the International Conference on Harmonization*, Geneva Switzerland, March 1994.

ICH Q2B, “Harmonised tripartite guideline, validation of analytical procedure: methodology, IFPMA,” in *Proceedings of the International Conference on Harmonization*, Geneva Switzerland, March 1996.

Jeličić, M.L., Brusač, E., Amidžić Klarić, D., Nigović, B., Keser, S. and Mornar, A. (2020). Physicochemical compatibility investigation of Mesalazine and folic acid using chromatographic and thermoanalytical techniques. *Pharmaceuticals*, 13(8), p.187. Doi: <https://doi.org/10.3390/ph13080187>.

Jeličić, M.L., Brusač, E., Kurajica, S., Cvetnić, M., Amidžić Klarić, D., Nigović, B. and Mornar, A. (2021). Drug–Drug Compatibility Evaluation of Sulfasalazine and Folic Acid for Fixed-Dose Combination Development Using Various Analytical Tools. *Pharmaceutics*, 13(3), p.400. Doi: <https://doi.org/10.3390/pharmaceutics13030400>.

Kodre, K., Attarde, S., Yendhe, P., Patil, R. and Barge, V. (2014). Research and reviews: *Journal of Pharmaceutical Analysis*. Research Review Journal of Pharmaceutical Analysis Differ, 3, pp.11-22.

Kontny, G. and Zografi, G. (1995). Physical characterization of pharmaceutical solids. Sorption of Water by Solids, 12, pp.387-418.

Kumar, A., Singh, P. and Nanda, A. (2020). Hot stage microscopy and its applications in pharmaceutical characterization. *Applied Microscopy*, 50(1), pp.1-11. Doi:

<https://doi.org/10.1186/s42649-020-00032-9>.

Mackin, L., Zanon, R., Park, J.M., Foster, K., Opalenik, H. and Demonte, M. (2002). Quantification of low levels (< 10%) of amorphous content in micronised active batches using dynamic vapour sorption and isothermal microcalorimetry. *International Journal of Pharmaceutics*, 231(2), pp.227-236. Doi: [https://doi.org/10.1016/S0378-5173\(01\)00881-X](https://doi.org/10.1016/S0378-5173(01)00881-X).

Murphy, B.M., Prescott, S.W. and Larson, I. (2005). Measurement of lactose crystallinity using Raman spectroscopy. *Journal of Pharmaceutical and Biomedical Analysis*, 38(1), pp.186-190. Doi: <https://doi.org/10.1016/j.jpba.2004.12.013>.

Omoteso, O.A., Milne, M. and Aucamp, M. (2022). The Validation of a Simple, Robust, Stability-Indicating RP-HPLC Method for the Simultaneous Detection of Lamivudine, Tenofovir Disoproxil Fumarate, and Dolutegravir Sodium in Bulk Material and Pharmaceutical Formulations. *International Journal of Analytical Chemistry*, 2022. Doi: <https://doi.org/10.1155/2022/3510277>.

Patel, P., Ahir, K., Patel, V., Manani, L. and Patel, C. (2015). Drug-Excipient compatibility studies: First step for dosage form development. *The Pharma Innovation*, 4(5, Part A), p.14. Doi: https://www.thepharmajournal.com/vol4Issue5/Issue_july_2015/4-4-9.1.pdf.

Rajeswari, A., Christy, E.J.S., Gopi, S., Jayaraj, K. and Pius, A. (2020). Characterization studies of polymer-based composites related to functionalized filler-matrix interface. *Interfaces in Particle and Fibre Reinforced Composites*, pp.219-250. Doi: <https://doi.org/10.1016/B978-0-08-102665-6.00009-1>.

- Scrivens, G., Ticehurst, M. and Swanson, J.T. (2018). Strategies for improving the reliability of accelerated predictive stability (APS) studies. In *Accelerated Predictive Stability* (pp. 175-206). Academic Press. Doi: <https://doi.org/10.1016/B978-0-12-802786-8.00007-3>.
- Sharma, M.A.Y.A., Choudhury, P.K. and Dev, S.K. (2017). Formulation and in-vitro-in-vivo evaluation of alginate-chitosan microspheres of glipizide by ionic gelation method. *Asian J Pharm Clin Res*, 10(7), pp.385-390. Doi: <http://dx.doi.org/10.22159/ajpcr.2017.v10i7.18725>.
- Shu, X.Z. and Zhu, K.J. (2001). Chitosan/gelatin microspheres prepared by modified emulsification and ionotropic gelation. *Journal of microencapsulation*, 18(2), pp.237-245. Doi: <https://doi.org/10.1080/02652040010000415>.
- Stieger, N., Aucamp, M., Zhang, S.W. and De Villiers, M.M. (2012). Hot-stage optical microscopy as an analytical tool to understand solid-state changes in pharmaceutical materials. *American Pharmaceutical Review*, 15(2).
- The United States Pharmacopeia (2011). USP 34; The national formulary: NF 29. [Online] Available at: <https://www.worldcat.org/title/united-states-pharmacopeia-2011-usp-34-the-national-formulary-nf-29/oclc/723055458> [Accessed on September 14, 2022].
- Valluru, R.K., Kumar, P. and Kilaru, N.B. (2013). High throughput LC–MS/MS method for simultaneous determination of tenofovir, lamivudine and nevirapine in human plasma. *Journal of Chromatography B*, 931, pp.117-126. Doi: <https://doi.org/10.1016/j.jchromb.2013.05.008>.
- Verma, R.K. and Garg, S. (2005). Selection of excipients for extended release formulations of glipizide through drug–excipient compatibility testing. *Journal of Pharmaceutical and Biomedical Analysis*, 38(4), pp.633-644. Doi: <https://doi.org/10.1016/j.jpba.2005.02.026>.
- Varma, M.M. and Rao, H.L.N. (2012). Evaluation of aceclofenac loaded alginate mucoadhesive spheres prepared by ionic gelation. *International Journal of Pharmaceutical Sciences and Nanotechnology*, 5(4), pp.1847-1857. Doi: <https://doi.org/10.37285/ijpsn.2012.5.4.4>.
- York, P. (1983). Solid-state properties of powders in the formulation and processing of solid dosage forms. *International Journal of Pharmaceutics*, 14(1), pp.1-28.

Chapter Four

The formulation of lamivudine- and tenofovir disoproxil fumarate-loaded microparticles

4.1 Introduction

As mentioned in Chapter 1, two of the most important treatment goals for ART are viral load suppression and improved quality of life in HIV-infected individuals (Rathbun *et al.*, 2006). For patients of all ages, the oral route of drug delivery is the most practical and universally acceptable. However, orally administered ARVs formulated as immediate release dosage forms may present with some shortcomings due to inherent pharmacokinetic features, resulting in drug concentration fluctuations in the systemic circulation (Eagling *et al.*, 2002; Ramana *et al.*, 2014). As also discussed in Chapter 1, it could be beneficial to reduce the frequency of dosing related to the current HIV-treatment regimens. In order to achieve this goal, the potential of formulating 3TC- and/or TDF-loaded microspheres were explored in this study.

4.2 Physicochemical characterisation of 3TC and TDF, and drug-excipient compatibility studies

Knowing and understanding the physicochemical properties of the drug(s) to be incorporated into a drug delivery system or final dosage form, forms the cornerstone of any pharmaceutical preformulation and formulation process. Therefore, for the purpose of this study the first step was to collect baseline data in terms of the physicochemical properties of 3TC and TDF.

Due to the direct contact and the potential for excipient and API interactions within the dosage form, a drug-excipient compatibility study between 3TC- or TDF-polymer(s) must be conducted before formulation into any dosage. In **Appendix II**, the drug-excipient compatibility or incompatibility findings are covered in great detail.

4.2.1 Thermal analyses of 3TC and TDF

Thermal analysis (HSM and DSC) confirmed that the purchased 3TC raw material existed as Form II. This conclusion was based on the observed bipyramidal morphology as well as the melting point of 179.67 °C (**Figure 4.1**). This was found to be in direct correlation with that reported in literature by Chadha *et al.* (2012), Harris *et al.* (1997), and Jozwiakowski *et al.* (2016).

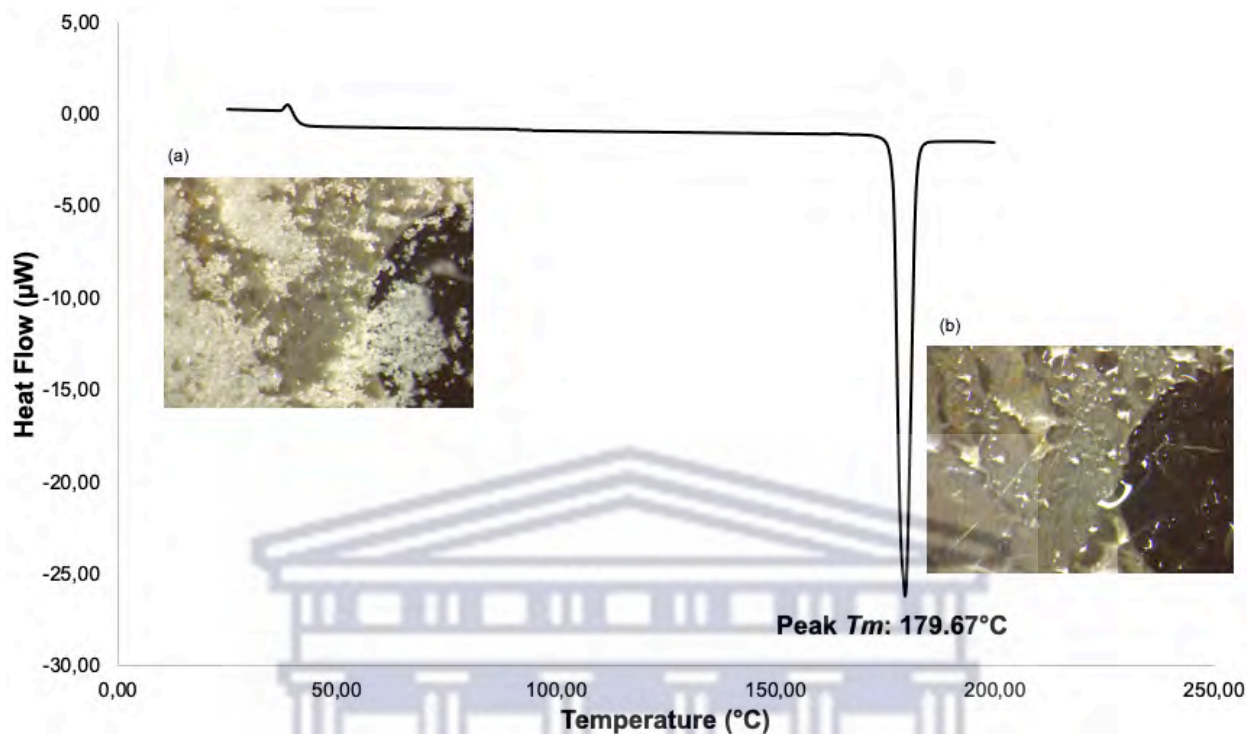


Figure 4.1: DSC thermogram obtained with 3TC with inset (a) depicting the morphology of 3TC raw material at ambient temperature and (b) micrograph captured of molten 3TC at $\approx 184.0^{\circ}\text{C}$.

TDF raw material exhibited a fine, white crystalline morphology (**Figure 4.2(a)**). During HSM analysis a melting point was observed at $\approx 110.9^{\circ}\text{C}$ followed by recrystallisation and a second melting event at $\approx 117^{\circ}\text{C}$ (**Figure 4.2(b)**). These visually observed events were confirmed from DSC analysis. **Figure 4.2** depicts the DSC thermogram obtained for TDF which shows two sharp thermal melting events at 111.83°C and 117.83°C . The presence of these endothermic peaks confirmed that the donated TDF raw material was crystalline. According to literature, TDF exists in three polymorphic forms, namely: Form A, Form B, and Form I (Lee *et al.*, 2010). The first endothermic peak observed was the melting of Form B, followed by the recrystallisation of molten Form B to Form I (Lee *et al.*, 2010; Tenghe, 2018).

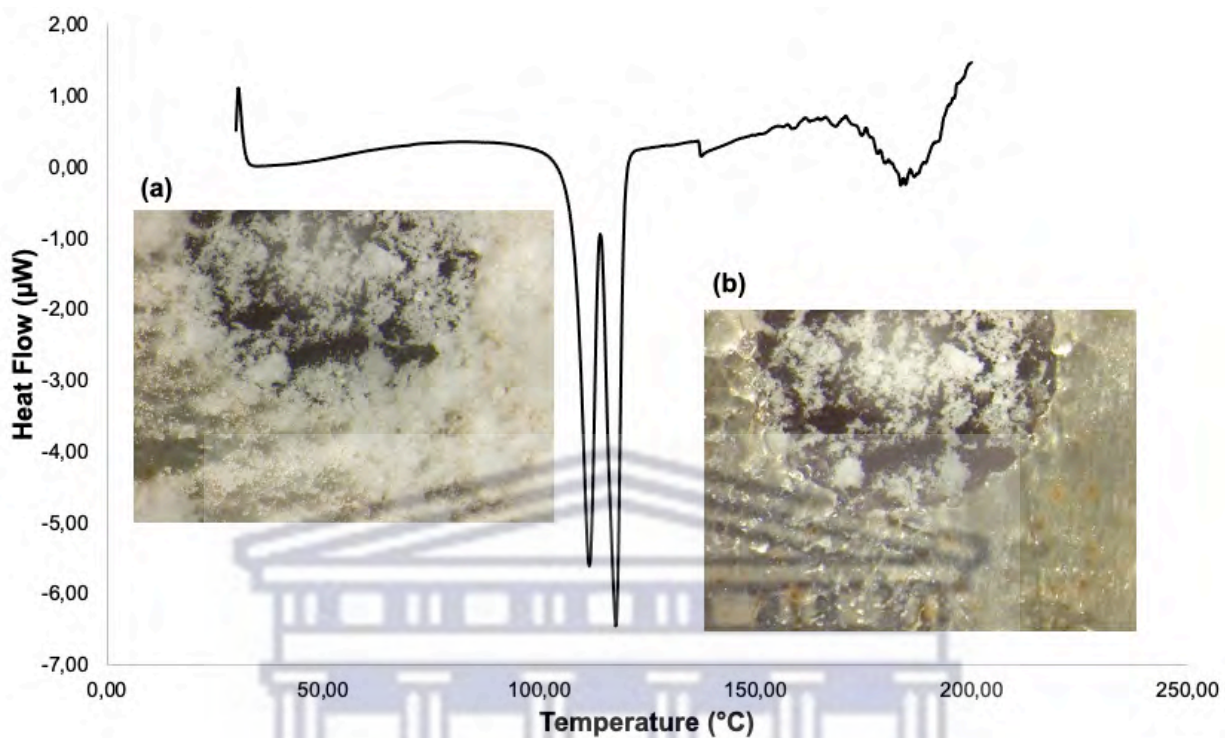


Figure 4.2: DSC thermogram obtained with TDF raw material with inset (a) depicting the onset of the first melting event of TDF raw material at $\cong 114.0$ $^{\circ}\text{C}$ and (b) micrograph captured of the onset of the second melting endotherm of TDF raw material at $\cong 118.0$ $^{\circ}\text{C}$.

TGA quantifies the mass loss of a sample upon exposure to heat. It may therefore be used to determine the thermal stability of a compound based on measured weight loss (Ebnesajjad, 2011; Scrivens *et al.*, 2018). **Figure 4.3** depicts an overlay of the TGA thermograms obtained with 3TC and TDF raw material and from the TGA traces it was concluded that 3TC shows thermal stability up to 231.83 $^{\circ}\text{C}$ and TDF raw material up to 172.67 $^{\circ}\text{C}$.

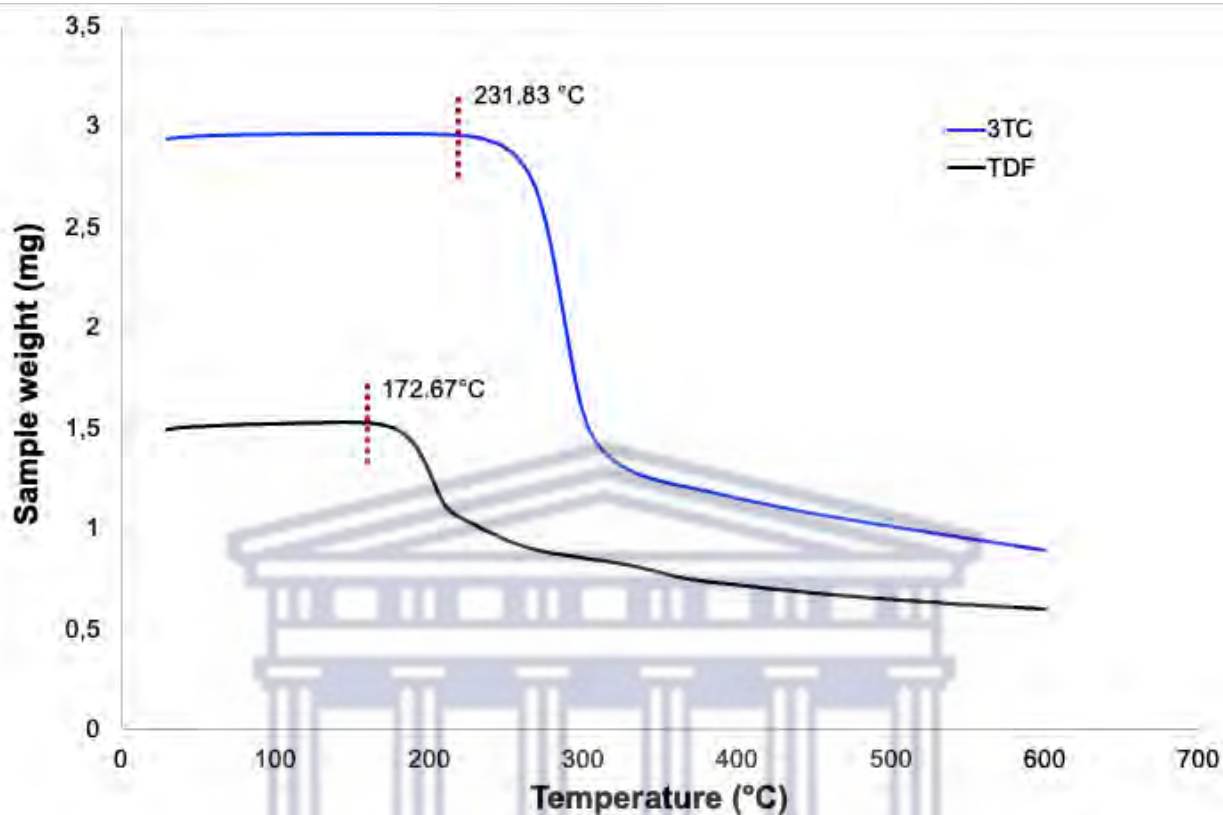


Figure 4.3: An overlay of the TGA traces obtained with 3TC and TDF raw material.

4.2.2 Fourier-Transform infrared spectroscopy of 3TC and TDF raw material

Fourier-transform infrared (FTIR) spectroscopy is used to identify functional groups in a sample as well as the presence of chemical bonds in a molecule. FTIR measures the intensity of the absorbance of the functional groups of a compound using the light absorption phenomenon (Khan *et al.*, 2018). **Figure 4.4** displays the FTIR spectra obtained for both 3TC and TDF raw material. Absorbance bands for 3TC were observed at 3327 cm^{-1} and 3198 cm^{-1} , corresponding to primary amino group (N-H₂)/ aromatic (1°) amine group stretching and alcohol (O-H) group stretching respectively. Absorbance bands were also observed at 3071 cm^{-1} and 2826 cm^{-1} as a result of vibration stretching of the aromatic sp² hybridized C-H bond and the aliphatic sp³ hybridized C-H bond. Peaks at 1641 cm^{-1} , 1636 cm^{-1} , and 1608 cm^{-1} were assigned to aromatic amide group (R-C=O-NR₂) vibration stretching, carbonyl group-cytidine carbonyl (NR₂-C=O-NR₂ -Cytosine) stretching, and an imine group (R₂C=NR) stretching, respectively (Chakraboarty *et al.*, 2014; Ngilirabanga *et al.*, 2021, Pandey *et al.*, 2016).

The IR spectrum of TDF revealed the presence of absorbance at 3202 cm^{-1} and 2979 cm^{-1} , respectively, corresponding to a primary amino group (N-H₂)/ aromatic (1°) amine group stretching and sp³ hybridized C-H bond of the aliphatic group. The vibration stretching of the ester (C=O) group was assigned from the absorbance band 1752 cm^{-1} . Stretching of the alkene/olefins (C=C) group and a bending N-H band were attributed to the bands at 1674 cm^{-1} and 1656 cm^{-1} , respectively (Silva *et al.*, 2017).

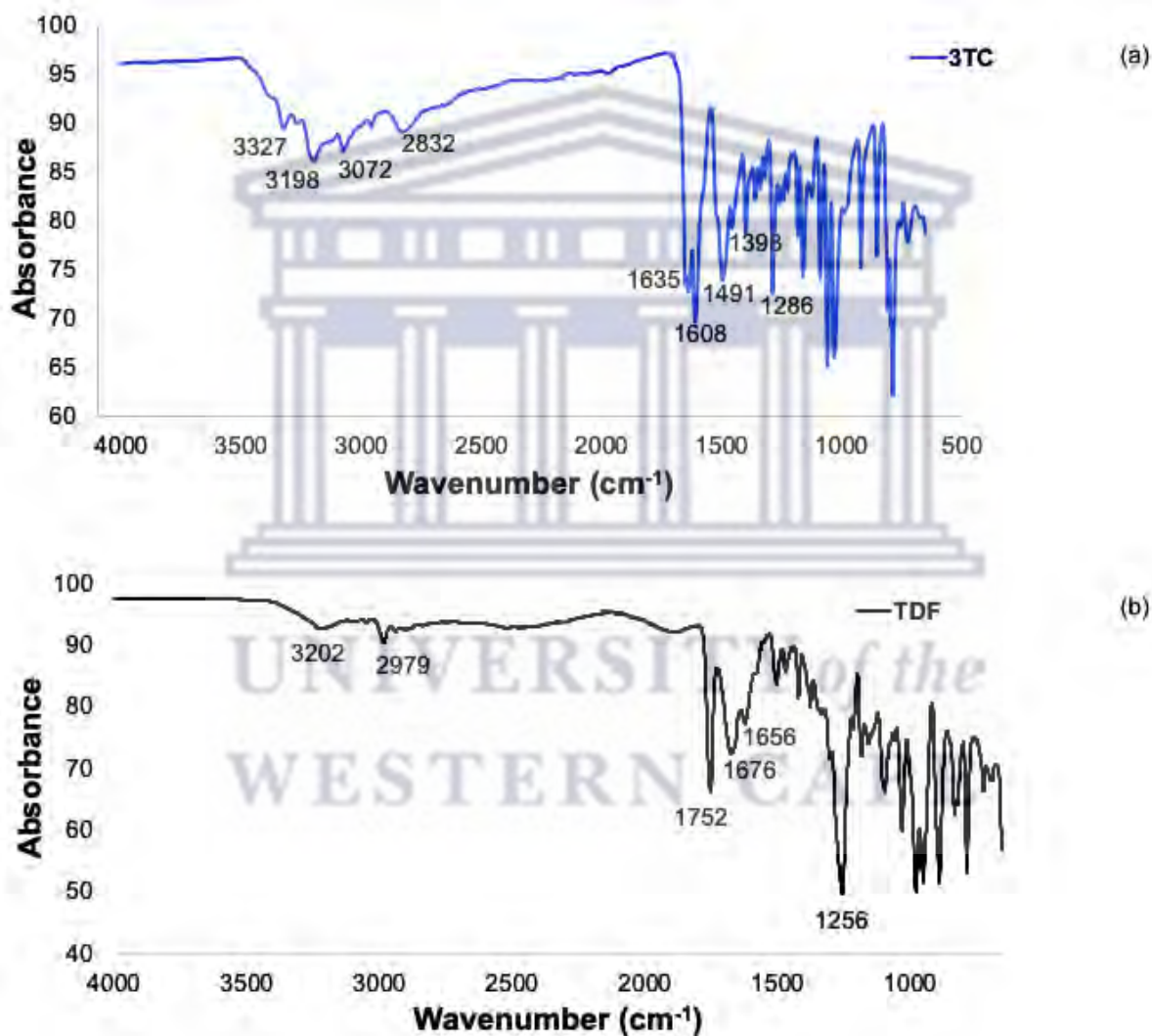


Figure 4.4: The FTIR spectra obtained for (a) 3TC raw material and (b) TDF raw material.

4.2.3 Powder X-ray diffraction of 3TC and TDF raw material

The PXRD pattern observed for 3TC was similar to that obtained in a previous study for crystalline anhydrous Form II (Harris *et al.*, 1997), confirming its crystallinity and purity. TDF exhibited a

crystalline PXRD pattern with a sharp distinctive peak at 5.03 °2θ and smaller diffraction peaks at 20.03, 25.13, and 30.23 °2θ. The PXRD patterns of TDF Form B and Form I were differentiated in a study by Lee *et al.* (2010) and based on this study it was confirmed that the TDF used in this study was Form I (**Figure 4.5**).

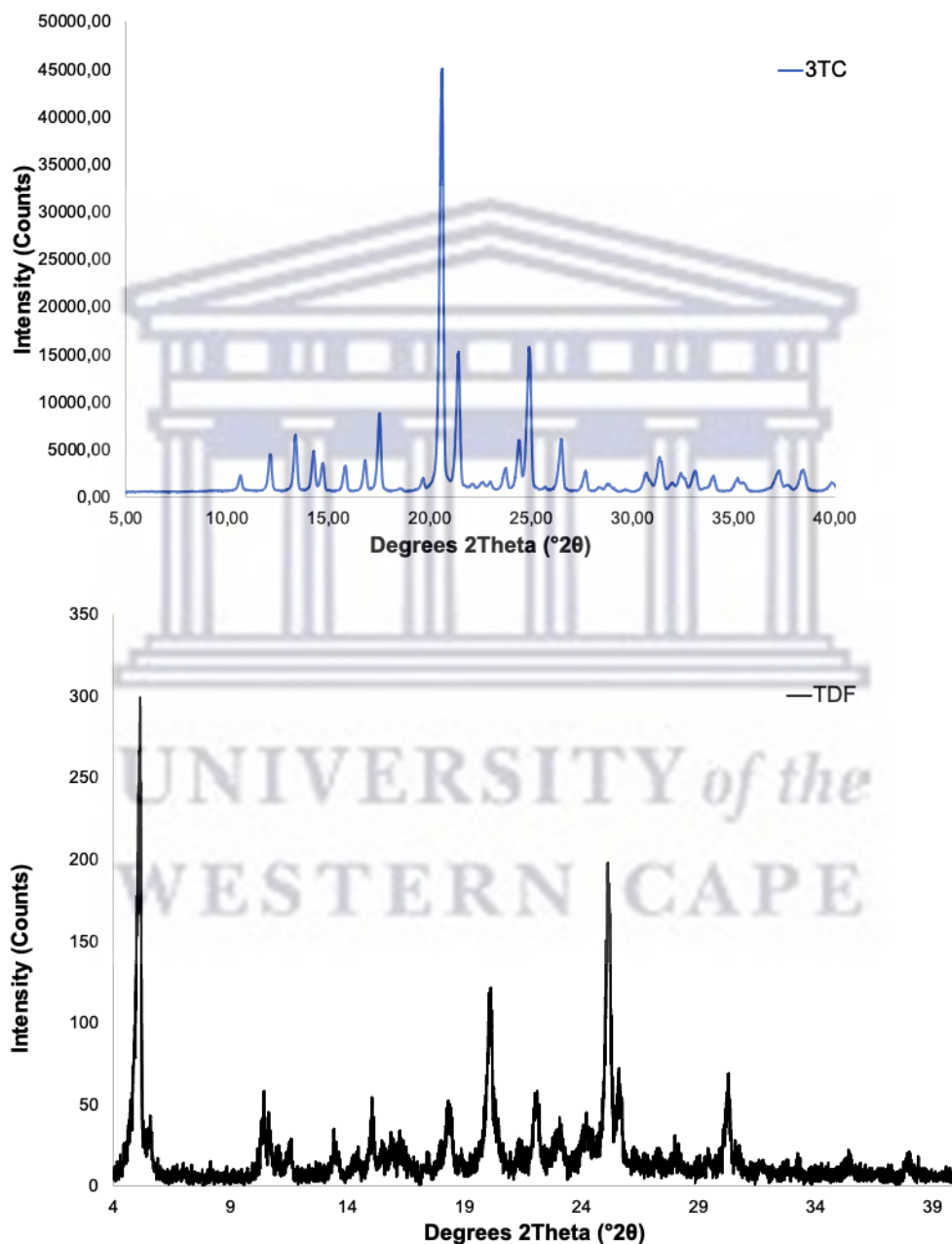


Figure 4.5: The PXRD diffractograms obtained for 3TC and TDF raw material.

From the collected physicochemical results it was concluded that 3TC and TDF raw materials were both crystalline in nature and it was confirmed that 3TC existed as Form II and TDF as Form I.

Since this study will involve various processing steps involving heating as part of the envisioned spray drying process it was important to conclude on the thermal stability of both compounds and therefore thermal analyses revealed that processing temperatures should not exceed $\cong 170$ °C. This conclusion was based on the onset of degradation observed for TDF raw material (**Figure 4.3**). From literature it was also noted that 3TC Form II may convert to Form III when slurried in water at ambient temperature for a period of 24 - 48 hours (Singh *et al.*, 2007) and therefore this aspect was considered as part of microsphere formulation strategies.

4.3 Investigation of ionic gelation as a potential formulation method for 3TC-loaded microspheres

As discussed in Chapter 2, 3TC is an ARV with a half-life of 5 - 7 hours which inevitably necessitates twice daily dosing. Although a highly soluble drug it is classified as a biopharmaceutical classification system (BCS) Class III drug due to low gastro-intestinal membrane permeation (Strauch *et al.*, 2011). Therefore, these drawbacks may be addressed by exploring the possibility to incorporate 3TC into a modified drug delivery system (MDDS), especially when not formulated as part of an FDC. It is a well-known fact that MDDS are designed to carry APIs effectively in the body while simultaneously regulating a specifically designed release mechanism for one or more of the included APIs (Vilos & Velasquez, 2012). The design and preparation of drug-loaded microparticles is one of the various drug carrier technologies that may assist in achieving this goal. Various excipients may be utilised to formulate such microparticles but this study focused on employing natural polymers which could potentially facilitate drug release over an extended period and increase drug permeation. As discussed in Chapter 1, several methods exist for formulating polymer-based microspheres, also termed polymeric microspheres (P-MPs) to facilitate modified-drug release mechanisms. It is also well-known that a plethora of polymers may be used to design such P-MPs. The severity, infection rate and the fact that HIV is more prevalent in socio-economically struggling regions necessitates the formulation and manufacturing of cost-effective treatment options. Therefore, utilising cost-effective excipients and preparation methods were the two major considerations in this study. Ionic gelation is reported to be an inexpensive, well-known technique which involves combining a polyelectrolyte (such as sodium alginate (SA)) with a multivalent ion (such as calcium salt) of opposite charge to form a calcium-alginate reticulate structure in the form of microspheres (Erten

Taysi *et al.*, 2019; Huang *et al.*, 2006; Raha *et al.*, 2018). Although there are some drawbacks associated with this technique, especially in terms of obtaining extended drug release (Almeida & Almeida, 2004; Chan *et al.*, 2006; Huang *et al.*, 2006; Kurozawa & Hubinger, 2017; Østberg *et al.*, 1994), it was considered as a preparation method for this study based on its simplicity and cost-effectiveness. Furthermore, previous studies reported on the successful preparation of 3TC-loaded P-MPs utilising ionic gelation (Gada & Setty, 2019; Parveen & Syed, 2014; Raj *et al.*, 2011) and it was decided to investigate ionic gelation of 3TC further. Furthermore, based on the fact that both 3TC and TDF are classified as BCS III drugs and both are highly soluble in aqueous media, it was decided to first focus on 3TC as part of the ionic gelation investigations.

Polymer mixtures used in the process of ionic gelation involving SA and calcium chloride have the potential to strengthen the P-MP structure by forming an interpenetrating polymer network. It is through such a polymeric network that controlled drug release could be obtained (Bulut, 2021; Raha *et al.*, 2018).

4.3.1 A screening study into formulation of 3TC-loaded microspheres

As a preliminary trial, SA, GEL, XG, CH and ethyl cellulose (EC) (**Table 4.1**) were investigated as polymers to establish the effect on 3TC release if cross-linked with calcium chloride. Since this was a preliminary trial the primary focus was on drug release rate followed by encapsulation efficiency (%EE) and yield. **Table 4.1** provides an outline of the initial ionic gelation formulations investigated. In all these formulations the concentrations of SA (2% w/v), calcium chloride (2% w/v) and 3TC (5% w/v) were kept constant. The curing time was also kept constant at 20 minutes.

Table 4.1: Outline of different polymers investigated in combination with SA and calcium chloride as crosslinkers in the first phase of the study on 3TC microencapsulation

Formulation code	Polymer concentration (% w/v)			3TC-loaded microsphere characteristics			
	Xanthan gum (XG)	Gelatin (GEL)	Chitosan (CH)	Yield (%)	Drug loading (%)	Encapsulation efficiency (%)	Percentage drug released in 2 hours in pH 1.2 (%)
F1	1.5	-	-	51.76	67.27 ± 0.58	59.19	78.32
F2	3	-	-	51.00	51.33 ± 0.08	52.36	97.77
F3	-	10	-	39.41	12.74 ± 0.18	17.07	53.69
F4	-	10	1	55.00	17.81 ± 0.46	35.26	49.74
F5		5	-	51.67	16.73 ± 0.61	20.75	72.48
F6		5	1	66.15	22.18 ± 1.29	38.15	65.29
F7	1.5	-	1	44.21	20.59 ± 0.59	17.29	71.41
F8	3	-	1	55.46	44.09 ± 2.70	53.79	68.10
F9	-	-	0.1	47.89	36.03 ± 0.81	24.50	91.10
F10	-	-	1	36.25	18.21 ± 0.68	10.56	112.89

The total 3TC concentration released in pH 1.2 dissolution medium after 2 hours was investigated and considered for F1 – F10. It was observed that the formulations containing only XG and only CH showed the most rapid 3TC release with F1 and F2 (XG only) exhibiting fairly high %EE of 59.19 % and 52.36 %, respectively. It was also observed that the higher the concentration of XG, the lower the %EE (F1 vs F2). F8 consisting of 3 %w/v XG and 1 %w/v CH showed %EE of 53.79 %, very similar to that obtained for F1 and F2, showing that the presence of CH in the cross-linking solution does not positively affect %EE and drug loading but brings forth a significant decrease in 3TC release from the microspheres. However, this conclusion becomes questionable upon considering F7 which contains less XG (1.5 % w/v) but the same concentration CH as F7 exhibited very poor drug loading and %EE and a sub-optimal 3TC release rate with 71.41% 3TC released within 2 hours. Theoretically, the higher the polymer ratio, the higher the drug loading and encapsulation are expected due to the higher density packing of the polymer's structure (Benavides *et al.*, 2016), however for XG the opposite effect was noted. From these results it was concluded that XG enhances %EE but also results in the rapid release of a high concentration 3TC, an undesired quality attribute since the aim was to obtain a slow and steady release rate. It is hypothesised that the high drug loading and %EE obtained with XG could be attributed to XG forming water-rich pockets within the polymer structure thereby allowing the solubility of a higher 3TC concentration in these water rich regions and thereby carrying more 3TC into the rigid polymer structure upon ionic cross-linking. Although this provides an excellent outcome in terms of %EE and drug loading it is also this attribute which results in rapid and almost complete 3TC release from the microspheres. From the perspective of drug release it is therefore hypothesised that XG does not facilitate the formation of a rigid polymeric structure when cross-linked with SA but rather forms a structure that facilitates the rapid diffusion of aqueous media into and out of the polymeric structure this being due to the hydrophilic nature of XG and its ability to absorb significant high levels of moisture (Verhoeven *et al.*, 2006).

F3 which constituted the use of only GEL showed very poor %EE and drug loading in comparison with the XG containing formulations but in contrast to F1 and F2 the released 3TC concentration was notably lower. Comparison of F3 with F5 (only GEL) indicated a slight increase in %EE and drug loading but a significant increase in 3TC release, thereby indicating that GEL possibly plays a role in the formation of a dense, rigid polymeric network upon crosslinking with SA in the presence of calcium chloride. In terms of drug release, it was noted that F4 which contains GEL

and CH showed the lowest concentration of 3TC released across a period of 2 hours in comparison to all other formulations. Comparison of F5 and F6 proved that the presence of CH affects 3TC release with F6 showing less released 3TC over a 2 hour period than F5. Interestingly, F9 and F10 which consisted only of CH cross-linked with SA showed complete and rapid 3TC release within the 2 hour drug release testing period. The %EE and drug loading was also noted to be poor and subsequently a conclusion was reached that in order to obtain a level of controlled drug release a combination of the tested natural polymers would be necessary.

From the obtained results it was concluded that the polymer network structure or matrix formed by combining a polymer with SA did not result in a sufficiently rigid or dense enough polymeric structure to prevent rapid drug release. From literature it was noted that poor encapsulation can be caused by weak ionic bonding or interaction between the polymer's hydroxyl, carbonyl, carboxyl, and amino functional groups and the divalent calcium ion of the crosslinker, or by poor electrostatic interactions and hydrogen bonding between the carboxyl or hydroxyl groups of alginate with the amide groups of GEL, carboxyl or hydroxyl groups of XG, and amino groups of CH (Derkach *et al.*, 2020; Jelvehgari *et al.*, 2014; Mirtič *et al.*, 2018; Pongjanyakul & Puttipipatkachorn, 2007). A major drawback observed during this initial trial was the aspect of high viscosity of the polymer solutions, which made it challenging to extrude through the syringe needle into the cross-linking solution, resulting in material loss due to sputtering and poor microsphere shape formation. With high viscosity solutions it was challenging to drop the solution in a drop-wise manner into the crosslinking solution, sometimes resulting in strings of polymer solution entering the crosslinking solution. This aspect negatively affected microsphere yield and was noted as a significant aspect which affects the final quality of the formulated microspheres.

4.3.2 Investigation of 3TC-loaded microsphere formulation using higher SA and crosslinker concentrations

Based on these results and taking guidance from previous studies reporting successful 3TC microsphere formulation *via* ionic gelation (Gada & Setty, 2019; Parveen & Syed, 2014; Raj *et al.*, 2011) it was decided to conduct a second formulation trial in which the concentrations of SA and calcium chloride were increased to 5 %w/v and 10 %w/v, respectively. Further to this the concentration of 3TC was reduced from 5% w/v to 1 %w/v. **Table 4.2** provides an outline of the second experimental trial conducted and throughout these formulations the curing time was kept

constant at 30 minutes. In this trial it was decided to include a control formulation with only SA as the polymer with no other polymer included. This was done to ascertain the %EE and 3TC release without the addition of other polymers.

During the second microsphere formulation trial it was decided to focus on 3TC release at different time periods and therefore *in vitro* dissolution studies were conducted with sampling at 10, 20, 40, 60, 120, 180, 240, 300 and 360 minutes. This was pursued to inform a better understanding of how 3TC is released from these microspheres and to conclude on possible modified drug release. It should be emphasised that in principle a 6 hour *in vitro* drug dissolution test in pH 1.2 dissolution medium does not align with human physiology, however the experiment was conducted in this manner since these formulations still formed part of the initial formulation trials. **Table 4.2** reports 3TC drug release (%) within the first 10 minutes of the *in vitro* dissolution study and **Figure 4.6** provides an overlay of the 3TC drug release profiles obtained for the six formulations.

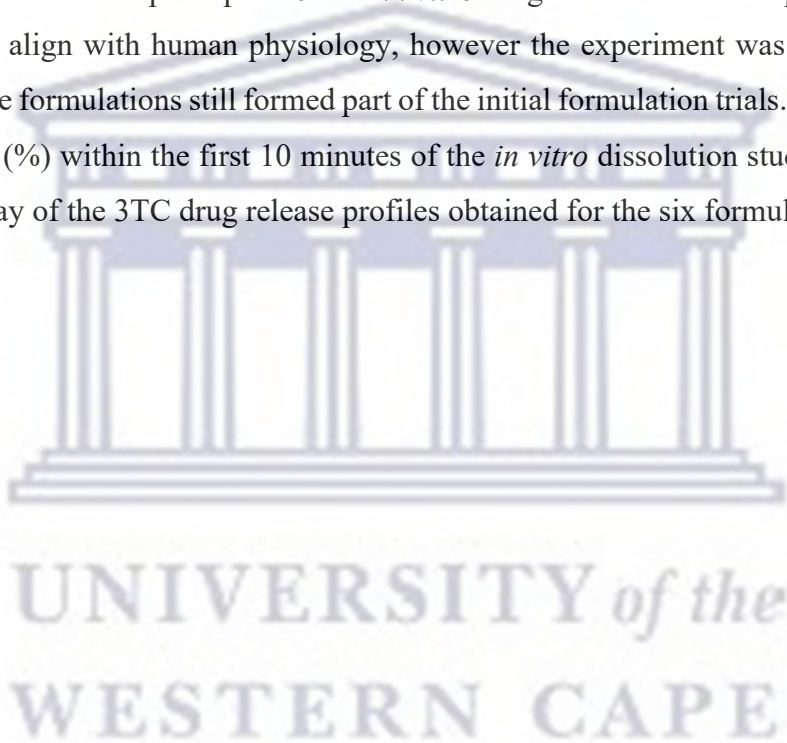


Table 4.2: Outline of different polymers investigated in combination with SA and calcium chloride as crosslinkers in the first phase of the study on 3TC microencapsulation

Formulation code	Polymer concentration (% w/v)			3TC-loaded microsphere characteristics		
	GEL	CH	XG	Yield (%)	EE (%)	% 3TC release in 10 minutes (pH 1.2)
F1b	-	-	-	31.16	42.39 ± 0.21	98.61 ± 4.41
F2b	1	-	-	26.34	64.10 ± 0.11	73.79 ± 2.97
F3b	-	1	-	20.58	87.85 ± 0.01	40.10 ± 1.70
F4b	-	-	1	27.46	43.11 ± 0.45	23.49 ± 1.55

For all formulations, F1b – F4b, the yield (%) was found to be low. Low yield can be attributed to the loss of the polymer-drug solution during the transfer process from the beaker containing the polymer-drug solution to the syringe (Benavides *et al.*, 2016). During the microsphere formulation process, in this study, it was noticed that the loss of the polymer-drug solution due to poor transferability to the syringe is a direct consequence of the high viscosity of the solutions. F1b, not containing any additional polymer other than SA was prepared in an effort to investigate the effect that polymer combinations could have on 3TC release, yield and %EE. This formulation showed rapid and complete drug release ($98.61 \pm 4.41\%$) within the first 10 minutes of *in vitro* dissolution testing. From this observation it was concluded that a mixture of polymers would be necessary to achieve a level of modified drug release. Upon evaluation of F2b (1 % w/v GEL) it was observed that it exhibited an %EE of $64.10 \pm 0.11\%$. In comparison with F3 (10 %w/v GEL) and F5 (5 %w/v GEL) which showed %EE of 17.07% and 20.75%, respectively it was concluded that a reduction in the GEL concentration have a significant effect on the ability to effectively encapsulate 3TC. Further, the drug release from F2b, within 2 hours, was found to be higher than with that previously quantified for F3 and F5 and therefore this observation further substantiated the conclusion that the higher the GEL concentration the more drug release retardation is possible.

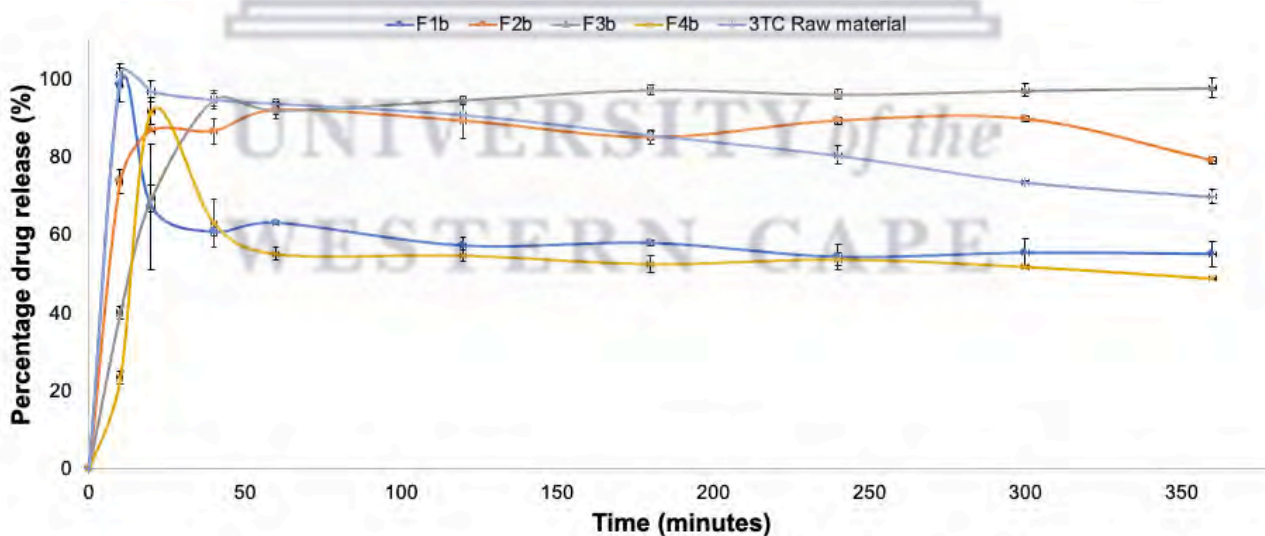


Figure 4.6: *In vitro* release profiles of 3TC from drug-loaded microspheres prepared *via* ionic gelation using various natural polymers.

F3b which consisted of 5 %w/v SA and 1 %w/v CH showed a slower onset of 3TC release in the first 10 minutes of dissolution testing (**Figure 4.7**), in comparison with F1b and F2b. However,

almost all loaded 3TC got released within 40 minutes ($94.73 \pm 1.51\%$) but it was noted that the concentration 3TC was maintained at $\cong 95.70\%$ over the 6 hour *in vitro* dissolution period (Figure 4.6).

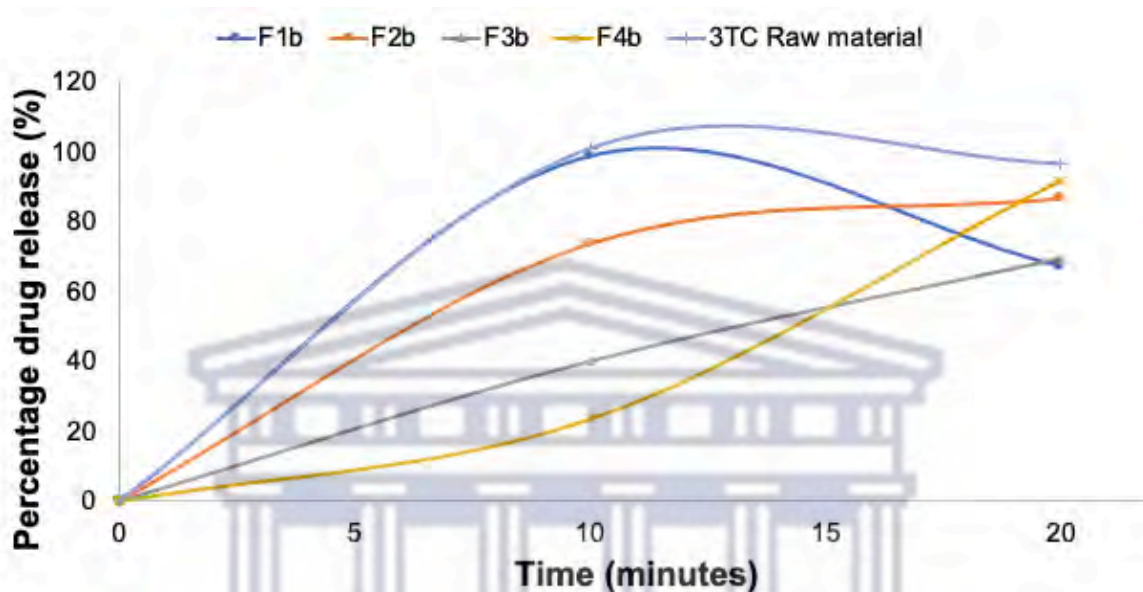


Figure 4.7: 3TC release from F1b - F6b microspheres formulation only depicting the 3TC concentrations quantified during the first 20 minutes of *in vitro* dissolution testing.

The 3TC release results (F3b) correlated well with that observed during the initial microsphere formulation trial (F9 and F10) and it informed a conclusion that the crosslinking of only CH with SA does not form a sufficiently rigid structure to facilitate a higher level of controlled drug release. It is hypothesised that this finding could be linked to the solubility of CH in acidic media. Therefore, although a cross-linked structure could have been formed the higher solubility of CH in the pH 1.2 dissolution media resulted in the formation of pores on the surface of the microspheres which subsequently led to enhanced penetration of dissolution medium into the microsphere and thereby release of the loaded drug. For F3b the %EE was found to be significantly higher in comparison with F9 and F10 (Table 4.1) and this was ascribed to the higher concentration of the calcium chloride as the crosslinker.

F4b consisted of 1 %w/v XG and although only $23.49 \pm 1.55\%$ 3TC was released in the first 10 minutes of *in vitro* dissolution testing, dose dumping was observed at 20 minutes ($91.83 \pm 3.48\%$) followed by a steady decline of released 3TC over the full 6 hour period. This result is in close

agreement with that observed with F1 and F2. The yield for F4b was significantly lower than that obtained during the formulation of F1 and F2 and the %EE was approximately 10% less than that quantified for F1 and F2.

4.3.3 Conclusion on ionic gelation as a microsphere formulation strategy

For GEL, the higher the GEL concentration the more 3TC release retardation is possible however the higher the GEL concentration the lower the product yield and %EE. From a process perspective it was also noted that the higher the GEL concentration the higher the solution viscosity which makes addition of the polymer solution to the crosslinker solution challenging. Thereby detrimentally affecting the scalability and cost-effectiveness of such a formulation. From the *in vitro* dissolution data obtained for F2b it became evident that GEL has the ability to provide sustained release of a highly hydrophilic drug with drug release sustained at +/- 85% for a period of 6 hours with a decline in dissolved 3TC observed only after 5 hours. The inclusion of CH in the polymeric network resulted in a slower onset of drug release but the complete drug load was released after 40 minutes of *in vitro* dissolution testing. It is however hypothesised that these 3TC microspheres could show an even slower onset of drug release in dissolution medium of higher pH values due to the solubility of CH in low pH solutions.

When XG is used as a polymer in the formulation of 3TC-loaded microspheres *via* ionic gelation a slower initial drug release rate comparative to F1b (SA only), F2b (SA and GEL) and F3b (SA and CH) was observed, however this modification in the drug release profile changed due to a clear dose dumping event at 20 minutes dissolution time. A major drawback of ionic gelation as a microsphere formulation strategy is the variable and in some instances poor yield. From the two conducted trials it became apparent that significant losses occur during the microsphere formation stage which undoubtedly lead to a less cost-effective formulation approach. From a process optimisation perspective it was therefore decided to investigate another commonly used microsphere formulation process, namely spray drying.

The next step was therefore to decide which polymers to include into the spray drying formulation phase. Based on the observations that significantly higher concentrations of GEL (5 - 10 % w/v) does lead to some level of modified release (**Table 4.1**) it was decided to explore GEL further. The dose dumping behaviour and lack of modified drug release upon incorporation of XG led to the decision to eliminate XG from further formulation studies. From the ionic gelation trials it

became apparent that a combination of GEL and CH does result in modified drug release (**Table 4.1**) and therefore CH was included in the next phase of the study.

4.4 Preparation of 3TC-loaded polymeric microparticles *via* spray drying

Spray drying is one of the most basic techniques for producing drug-loaded microspheres. In order to understand the effect that different formulation constituents could have on spray dried microspheres it is necessary to understand the process of spray drying. Spray drying is a continuous drying process that involves feed solution atomisation, droplet and air contact, evaporation and particle collection. The spray drying process starts with atomisation of the solution to be spray dried into fine droplets. These droplets then come into contact with a heated gas stream, most often this gas stream is air. Subsequently, the solvent is evaporated from the droplet through simultaneous heat and mass transfer, leaving behind dried particles which get separated and collected by a cyclone separator (Bowey and Nuefeld, 2010). Process parameters which directly affect the quality of the spray dried product includes the feed and air flow rates, viscosity of the feed solution and the surface tension (Masters, 1976). Throughout the following paragraphs the influence of these mentioned variables on the successful spray drying of 3TC-loaded microspheres will be discussed.

4.4.1 Optimisation of 3TC:polymer spray drying process

A literature search revealed only two published studies on spray dried 3TC using various polymers. It was noted that the study by Tshweu *et al.* (2013) followed a fairly complex double emulsion spray drying technique using poly(ϵ -caprolactone) (PCL) and polyvinyl alcohol (PVA) as the polymers. This reported spray drying process included the use of the preparation of a water-in-oil-in-water nano-emulsion which was subsequently spray dried. This study did however not report on the percentage yield (%) achieved. Another study by Mohaweb *et al.* (2014) reported the spray drying of 3TC in combination with 1 %w/v CH dissolved in 1 %v/v acetic acid followed by mixing the resulting solution with various 3TC concentrations dissolved in 96 %v/v ethanol or 1 %w/w hydroxymethyl propyl cellulose (HPMC) with a 3TC solution consisting of ethanolic solution (2:3 v/v) ethanol (96 %v/v): water. It was noted that a product yield ranging from 22.43 - 38.60% was achieved. The strategy to incorporate CH in the spray drying feed solution was found to be interesting and something that requires exploration based on the results obtained in the ionic gelation phase of the study (**Table 4.1**). However, due to the Büchi B-290 spray dryer

setup available at the time of this study the use of an acetic acid solution to solubilise CH followed by feeding the acetic acid solution through the affixed nozzle was not feasible since the nozzle was not constructed from anti-corrosive material.

Based on the information gathered from these two studies it was therefore decided to firstly focus on GEL as the polymer to be incorporated into the 3TC spray drying feed solution and to aim to obtain sufficiently high product yield. The spray drying of GEL with various drugs in an effort to either achieve controlled drug release or to enhance drug solubility and dissolution rate have been reported (Jeevana *et al.*, 2009; Leucuta, 1990; Panizzon *et al.*, 2014; Tran *et al.*, 2014; Yousaf *et al.*, 2015), but none focused on the effect of GEL on the formulation of 3TC-loaded microspheres. Previous studies demonstrated that the drug-polymer ratio, and the drug-polymer interaction can all affect the properties of GEL-based drug-loaded microspheres (Foux & Zilberman, 2015).

To investigate the effect of GEL on the drug release of spray dried 3TC-loaded microspheres, varying drug-polymer ratios were investigated. It is a well-known fact that the higher the concentration of dissolved or suspended solids in the feed solution the better the spray dried product yield. Therefore 3TC-GEL combinations were prepared to have a 15% w/v concentration. Based on the observation that a high concentration GEL could facilitate modified 3TC release (**Table 4.1**) the aim was to obtain the highest possible GEL concentration in the feed solution. Initial feed solutions were tested and it should be noted that the initial trial solutions were prepared using only distilled water. It was noticed that the higher the GEL concentration the higher the viscosity. The spraying of a 1:1 (3TC:GEL) solution, consisting of 7.5 %w/v 3TC and 7.5 %w/v GEL resulted in unacceptable pumping of the feed solution with blockage of the spraying nozzle and poor formation of the droplet spraying cone with intermittent sputtering of the feed solution into the drying chamber. Also, the drying process was found to be poor with a significant portion of the feed solution remaining adhered as a sticky mass either in the drying chamber or on the glassware linking the drying chamber and cyclone separator (**Figure 4.8**).

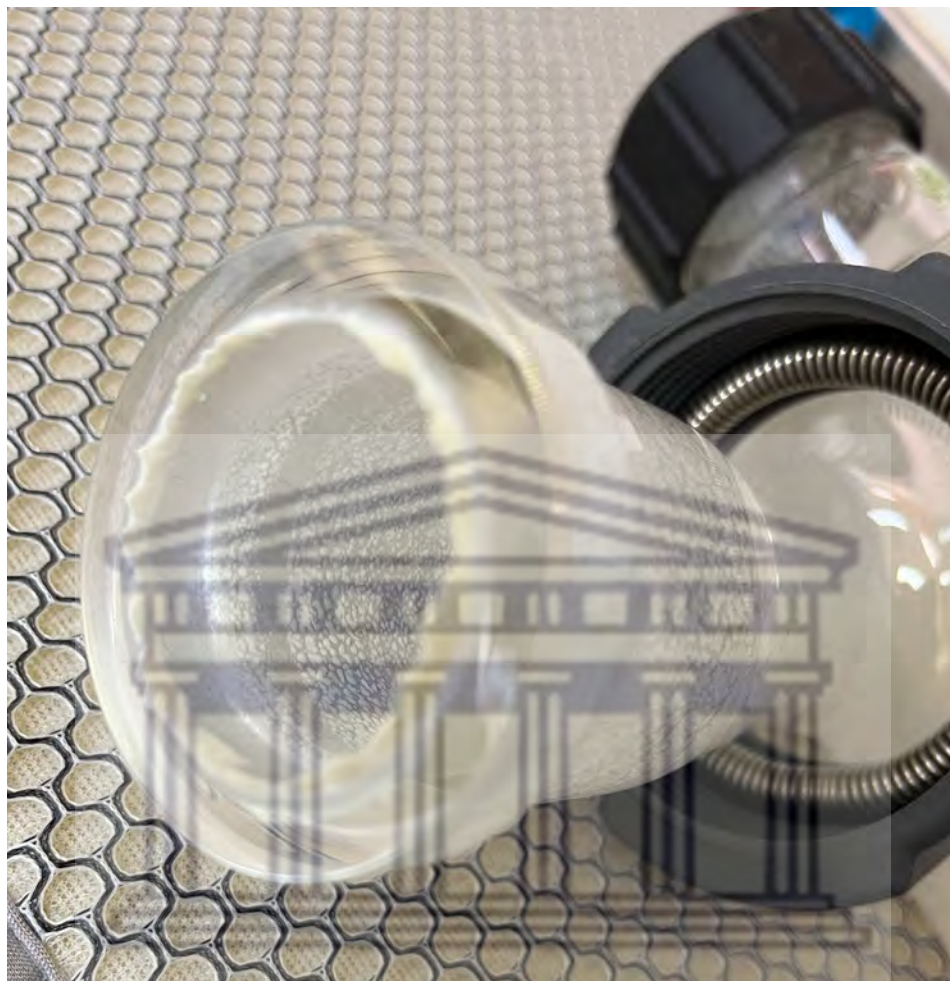


Figure 4.8: A picture indicating remaining residue on the spray dryer glassware post spray drying of a 1:1 3TC:GEL feed solution with 3TC and GEL solubilised in distilled water.

Based on this outcome it was decided to reduce the viscosity of the 3TC:GEL feed solutions through the addition of 10 %v/v ethanol (99.9 %v/v). The concentration ethanol which could be added to the feed solutions was limited by the spray dryer setup not being connected to an inert loop. Due to safety considerations a maximum concentration of 10 % v/v organic phase in aqueous feed solutions were adhered to. The reduction in the viscosity resulted in easy pumping of the feed solution, the formation of a well-shaped spraying cone with visibly fine droplet formation. Several inlet temperatures were also tested and an inlet temperature of 150 °C showed to yield a sufficiently dry powder. From the spray drying optimisation trials three final feed solutions, as outlined in **Table 4.3**, were investigated further. To achieve an acceptable droplet drying and subsequent product yield, a feed flow rate of 30 % and an inlet temperature of 150 °C, were utilised.

Table 4.3: The 3TC and polymer concentration, percentage yield (%), moisture content, drug loading (%) and encapsulation efficiency (%EE) obtained with the three 3TC:polymer feed solutions as obtained from optimisation efforts

Formulation code	3TC (%w/v)	GEL (%w/v)	Yield (%)	Moisture content (%)	Drug loading (%)	%EE	Mean particle size (µm)
F1SD	7.5	7.5	47.52	1.35	69.97 ± 0.14	66.49 ± 0.56	98.67 ± 1.21
F2SD	5	10	64.50	3.05	53.10 ± 0.21	102.74 ± 1.67	97.23 ± 1.49
F3SD	3	12	40.71	7.75	10.07 ± 0.07	17.70 ± 0.55	95.95 ± 1.49

The higher polymer ratio in F3SD increased the viscosity of the feed solution, however the viscosity was still sufficiently low to allow adequate pumping and atomisation thereof. However, upon consideration of the resulting moisture content it could be hypothesised that the drying of the atomised droplets was not sufficient. Upon further review of the post spray drying results obtained for F3 poor drug loading and %EE was also noted. This could also be attributed to poor drug and polymer loss during spray drying due to insufficient drying. In terms of processing efficiency, F2SD proved to be superior due to a high yield percentage and excellent %EE.

4.4.2 Determination of *in vitro* drug release from spray dried 3TC-loaded microspheres

The dissolution rates of 3TC from F1SD - F3SD were tested and compared to 3TC raw material as well as the physical mixture of the corresponding 3TC:polymer ratio. The physical mixtures constituted the exact same 3TC:GEL ratios as per **Table 4.3** and the preparation method of these powder mixtures are described in Chapter 3, paragraph 3.3.2 (b). The *in vitro* dissolution rate was determined in pH 1.2 for 120 minutes at 37 ± 0.5 °C. This study aimed to replicate or determine the behaviour of 3TC-loaded gelatin-based microspheres in the stomach. In acidic conditions, the high intrinsic dissolution property of 3TC was confirmed by a quick dissolution rate of 100% in 5 minutes (Dezani *et al.*, 2013).

The dissolution profile of F1SD revealed, as depicted in **Figure 4.9** that $73.81 \pm 0.77\%$ of the 3TC was released from the microspheres in the first 5 minutes of dissolution testing. This result

demonstrated rapid burst release of 3TC followed by a very slow but steady decline in drug release over the 2 hour period. Given that this formulation had a 66.49% encapsulation efficiency, the burst release could be attributed to drug particles on the microsphere surface (Jelvehgari *et al.*, 2011). Just 69.5% of 3TC was liberated from this formulation at the end of the dissolution testing. This formulation demonstrated biphasic drug release. However, although the drug release showed a rapid onset the total 3TC concentration released over time was significantly lower than that quantified for 3TC raw material and the physical powder mixture of 3TC:GEL. In comparison with 3TC raw material the released 3TC concentration was 27.00% lower than that obtained with F1SD and the dissolution concentration difference between F1SD and the physical mixture (F1SD(PM)) was quantified as 20.16%.

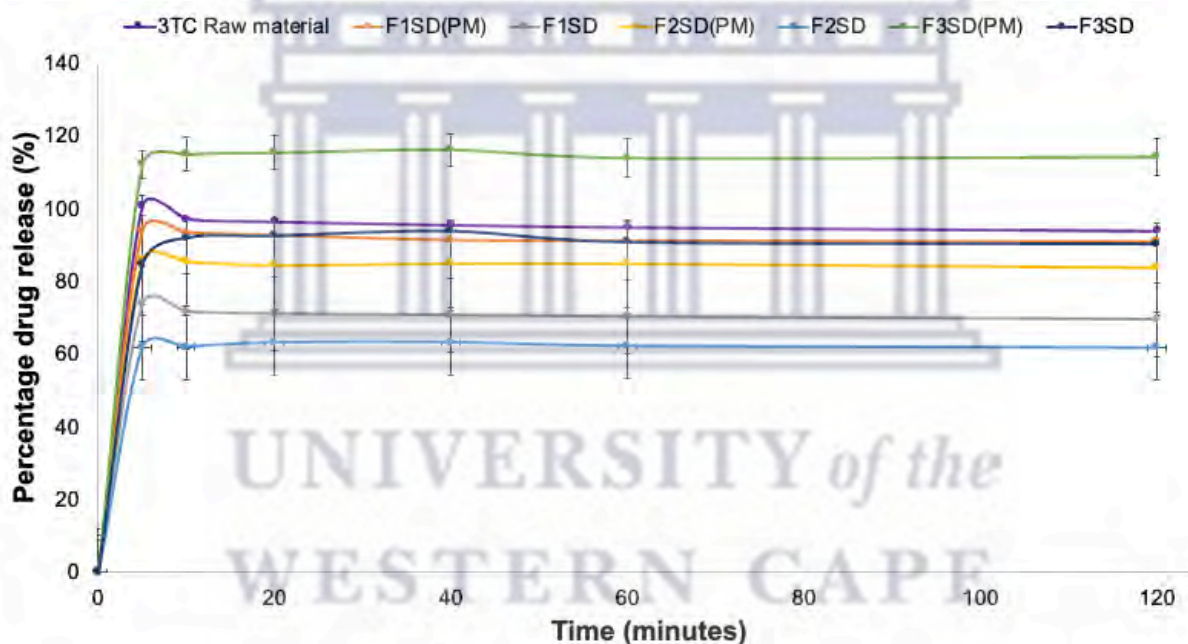


Figure 4.9: An overlay of the *in vitro* dissolution results obtained with 3TC raw material, F1SD(PM), F1SD, F2SD(PM), F2SD, F3SD(PM) and F3SD in pH 1.2 dissolution medium at 37 ± 0.5 °C.

F2SD showed a similar pattern of drug release (**Figure 4.9**), with approximately $61.63 \pm 1.36\%$ of the 3TC released from the microspheres in the first 5 minutes. The highest concentration 3TC released from these microspheres was quantified after 40 minutes ($63.05 \pm 1.10\%$) and this was followed by a very slow and steady decline in 3TC released concentration. This result showed that a 3.5% w/v increase in GEL concentration resulted in reduced 3TC drug release, by about 9%.

Despite this, an increase in GEL concentration is associated with a decrease in drug loading ($53.10 \pm 0.21\%$) but excellent %EE. A difference of 39.18% drug release was quantified between 3TC raw material and F2SD whilst a 15.02% difference was observed between 3TC raw material and the physical mixture, F2SD(PM), thereby showing that microsphere formation did possibly result in the encapsulation of 3TC in a GEL-based microsphere which slows drug release.

The dissolution profile comparison of F3SD with that of 3TC raw material and F3SD(PM) shows that $84 \pm 3.55\%$ of the 3TC was released in 5 minutes, and at the end of the dissolution test almost all of the 3TC was released. This dissolution behaviour is understandable given the poor %EE and determined drug loading. While comparing the dissolution rate of F3SD with that of F3SD(PM) it was noted that drug release from the physical mixture was 12% higher. At the end of the 2-hour dissolution testing, $114.22 \pm 5.15\%$ of the entire 3TC concentration was released. This observed phenomenon may be ascribed to the wettability of GEL and the fact that large concentrations of GEL has the ability to enhance the drug dissolution rate when in close contact with drug molecules (Kallinteri & Antimisiaris, 2001). It should be noted that the swelling ability of a polymer can also affect the pace of dissolution of a drug contained in a matrix. Polymer networks with strong swelling power in an aqueous medium can enhance drug release from such a network. GEL has a low swelling ability but high solubility in water (Dolci *et al.*, 2020) and therefore it can be hypothesised that 3TC release from GEL-based microspheres prepared by spray drying is governed by the solubility of GEL and not the swelling behaviour thereof. In order to confirm this hypothesis the swelling behaviour of the 3TC-loaded spray dried microspheres were investigated.

4.4.3 Determination of the swelling behaviour of 3TC-loaded spray dried microspheres

To determine swelling behaviour and strength in physiological media, the swelling properties of F1SD, F2SD and F3SD were determined in comparison with pure GEL and the drug-polymer physical mixtures (F1SD(PM), F2SD(PM) and F3SD(PM)). This investigation was performed by exposing the mentioned samples to acidic buffer solution (pH 1.2) and phosphate buffer solution (pH 6.8) at room temperature (25 ± 2 °C) and 37 ± 1 °C, respectively. All of the samples showed gelling at room temperature. After 24 hours, the increase in weight was determined for each sample (n=3) and the obtained data is depicted in **Figure 4.10**. It was observed that, in comparison, swelling of GEL exposed to pH 1.2 and pH 6.8 does not differ significantly ($p > 0.05$). Evaluating the swelling capacity of the physical mixtures in pH 1.2 medium, it was only F1SD(PM) that

showed a statistically significant lower swelling compared to GEL only. The swelling behaviour of F1SD(PM) was significantly lower in pH 1.2 than that quantified for F3SD(PM) ($p < 0.05$). Overall, the spray dried microspheres showed less swelling capacity than the physical mixture counterparts, with F3SD showing the overall highest level of swelling in pH 1.2 medium. However, comparison between the three spray dried formulations revealed no statistically significant difference in swelling capacity upon exposure to acidic medium.

In the alkaline solution, it was observed that the swelling of the physical mixture (F2SD(PM)) was significantly higher than that quantified for F1SD(PM) and F3SD(PM). It was also evident that the swelling of the F1SD microspheres was less than that quantified for F2SD and F3SD ($p < 0.05$). In contrast, at 37 ± 1 °C, the formulations in the acidic buffer solution dissolved rather than swell. The formulations exposed to the phosphate buffer solution solubilised in 20 minutes.

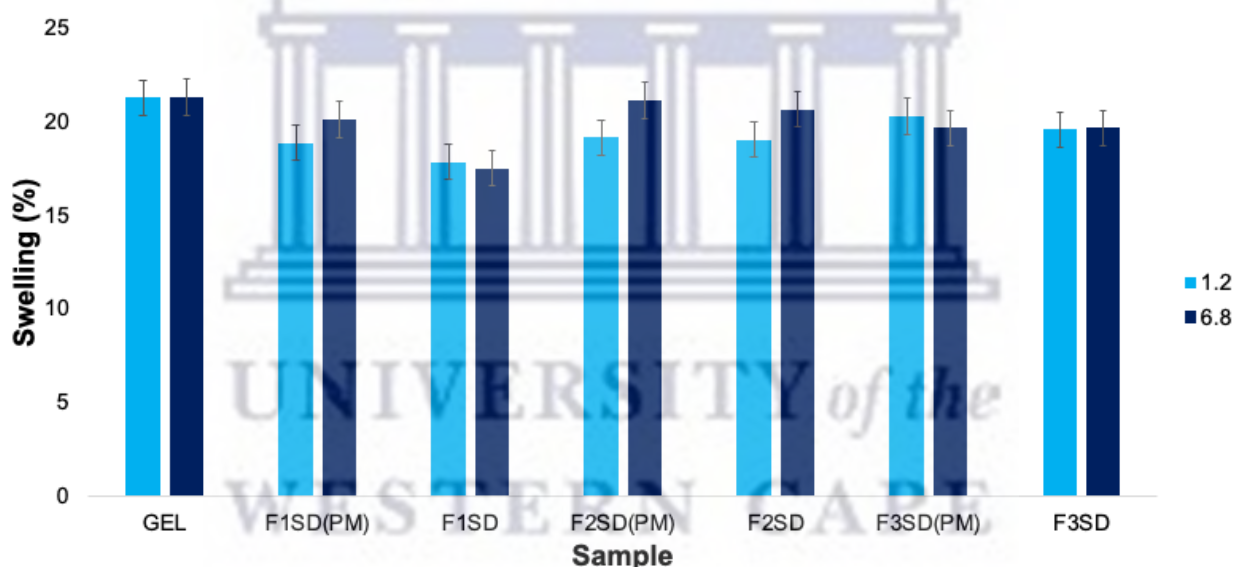


Figure 4.10: The swelling behavior of 3TC-loaded GEL-based microspheres formulations at pH-1.2 and pH-6.8 at ambient temperature over a period of 24 hours.

Overall, these findings indicated that the swelling of the GEL-based spray dried formulations are heat and pH sensitive. However, the observed swelling capacity is different from that reported by Qiao *et al*, (2012). In their study it was reported that GEL Type B shows higher swelling capability at low pH in comparison with very poor swelling at pH 6. This is due to the isoelectric point of GEL being at pH 6 and the fact that GEL is a polyampholytic molecule, thereby consisting of positively and negatively charged monomer subunits. Due to its polyampholytic characteristics

the swelling of GEL-based particles could be affected by the pH of the aqueous medium it is exposed to as well as the temperature. Therefore, considering that, a higher level of swelling of the spray dried microspheres was expected in pH 1.2 and lesser swelling in pH 6.8. Furthermore, a higher degree of swelling was expected at 37 °C. As depicted in **Figure 4.10**, the complete opposite was observed in the current study. It is therefore firstly hypothesised that the salt content in the pH 1.2 buffer solution detrimentally affected the swelling capacity of the GEL-based microspheres when exposed to the more acidic aqueous buffer. This hypothesis is based on results reported by Qiao et al, (2012), showing that the higher the salt content of a solution the lower the swelling capacity. Secondly, it is hypothesised that since these microspheres did not consist of only GEL but that a highly soluble drug was incorporated into the polymeric network the GEL polymer network was exceedingly fragile, leading to more solubilisation occurring rather than swelling. It was also noted that other studies reported the improved solubilisation of GEL as the temperature rises and that GEL has low structural integrity at physiological conditions (Djabourov & Papon, 1983; Xiao *et al.*, 2001; Dolci *et al.*, 2020). From the swelling studies it was apparent that GEL alone swells more than when it is combined with 3TC, thereby substantiating the hypothesis that 3TC diminishes the swelling capacity of GEL.

In summary, it was evident that the swelling capacity of GEL is affected by the pH and temperature but in this case the combination of GEL with 3TC showed unexpected swelling behaviour. At this point in time of the study it was therefore concluded that the rapid 3TC release from the spray dried particles is governed more by the hydrophilicity of 3TC and that the high aqueous solubility thereof drives the observed dissolution behaviour rather than a lack of swelling capability. It was furthermore deduced that cross-linking or modification of GEL would be needed to improve the rigidity and interlinked structure of the polymeric network to further influence the release of 3TC (Ahmady & Samah, 2021; Dolci *et al.*, 2020; Foux & Zilberman, 2015; Santoro *et al.*, 2014; Wang *et al.*, 2012).

4.4.4 The physicochemical properties of F2SD in comparison with 3TC, GEL and F2SD(PM)

As described in Chapter 1, a microsphere is a polymeric matrix system in which a drug is uniformly mixed with the wall-forming component or polymeric matrix. The drug-polymer interaction, the physical state of the drug in the polymeric matrix, and modifications during the microencapsulation process can all have an impact on the physicochemical, morphological, and

drug release features of the microspheres formulation (Dubernet, 1995; Sipos *et al.*, 2008; Tran *et al.*, 2014; Yousaf *et al.*, 2015). Based on the 3TC release profiles obtained (Figures 4.9) it was concluded that GEL does provide a level of modified drug release and even more so when microspheres were formed. However, it also became apparent that 3TC dissolution behaviour, especially a retardation in 3TC dissolution is highly dependent on the GEL concentration with a 10 %w/v GEL concentration providing some modified drug release in all instances investigated thus far in this study. It was therefore decided to characterise the F2SD GEL-based microspheres further in terms of physicochemical characteristics. This was done to enable an understanding of the GEL-based microsphere structure and the effect thereof on 3TC dissolution.

The physicochemical characterisation was conducted by DSC, TGA, FTIR, PXRD and SEM studies. DSC analysis of F2SD and F2SD(PM) revealed an absence of the crystalline 3TC melting peak in the drug-loaded GEL-based microspheres (Figure 4.11). The absence of the crystalline 3TC peak in the F2SD can be attributed to the amorphous dispersion of 3TC in the gelatine matrix (Tran *et al.*, 2014; Sipos *et al.*, 2008).

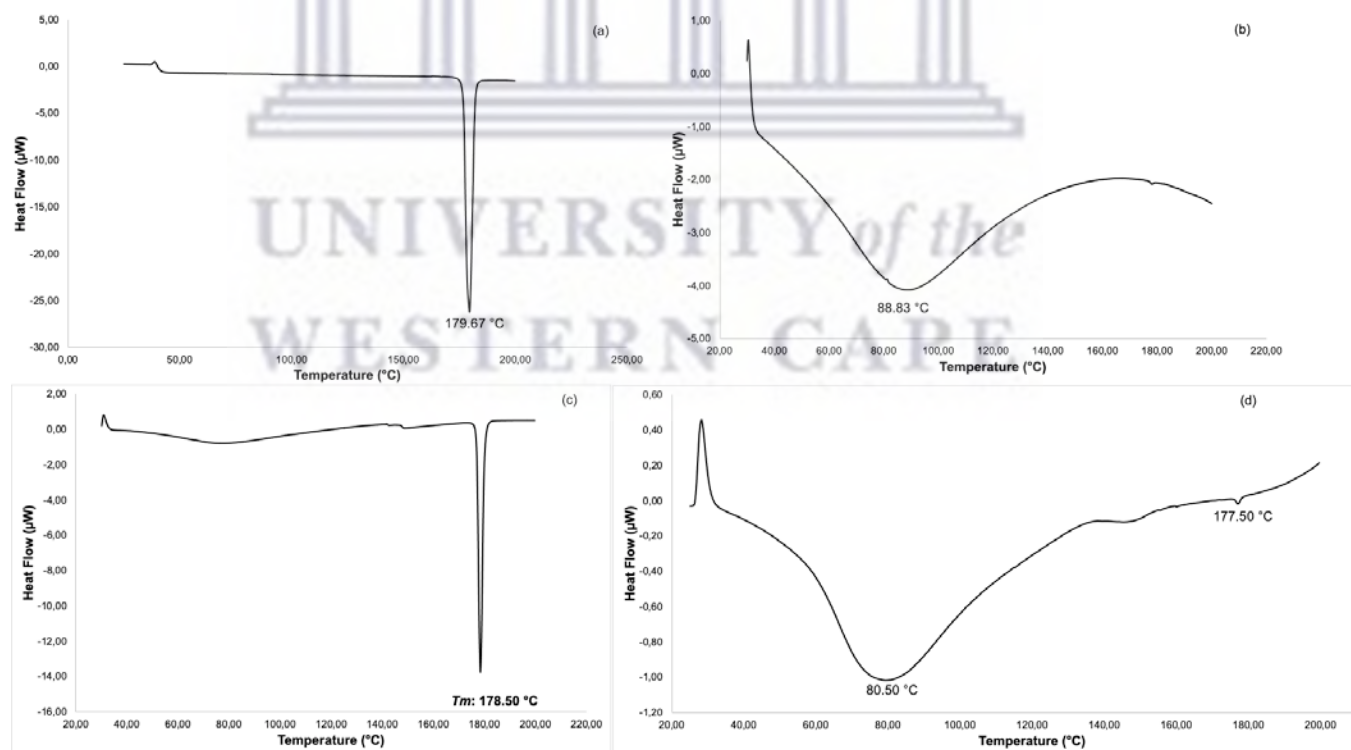
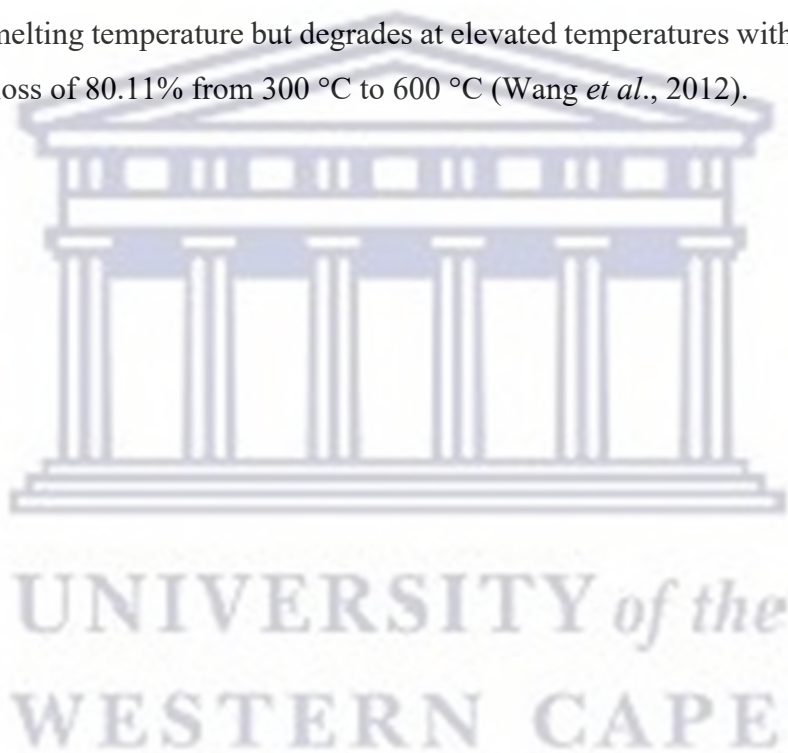


Figure 4.11: DSC thermograms of (a) pure 3TC, (b) GEL, (c) F2SD(PM) and (d) F2SD.

TGA was used to determine the thermal stability of F2SD and to ascertain whether 3TC and GEL are compatible with one another upon mixing and whether the subsequent spray drying process resulted in significant changes in terms of drug and/or polymer stability. **Figure 4.12** depicts an overlay of the TGA traces obtained for 3TC, GEL, F2SD and F2SD(PM). The obtained result for 3TC demonstrates a one-step mass loss of 69.97%, supported by various literature sources (Chadha *et al.*, 2012; Gomes *et al.*, 2013; Jozwiakowski *et al.*, 1996). Compared to pure 3TC, the thermal degradation of F2SD and F2SD(PM) corresponded well with that observed with 3TC and GEL alone (**Table 4.4**). The TGA thermogram obtained for GEL confirms the DSC results, indicating that GEL has no melting temperature but degrades at elevated temperatures with a significant one-step total weight loss of 80.11% from 300 °C to 600 °C (Wang *et al.*, 2012).



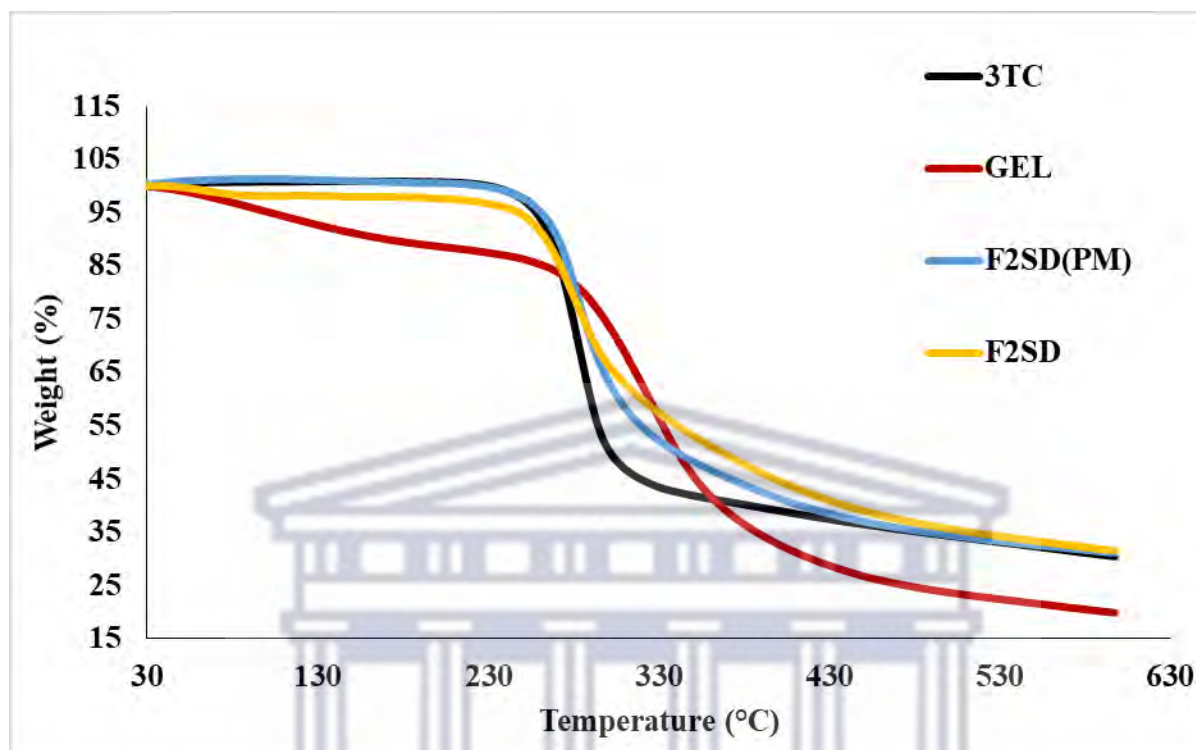


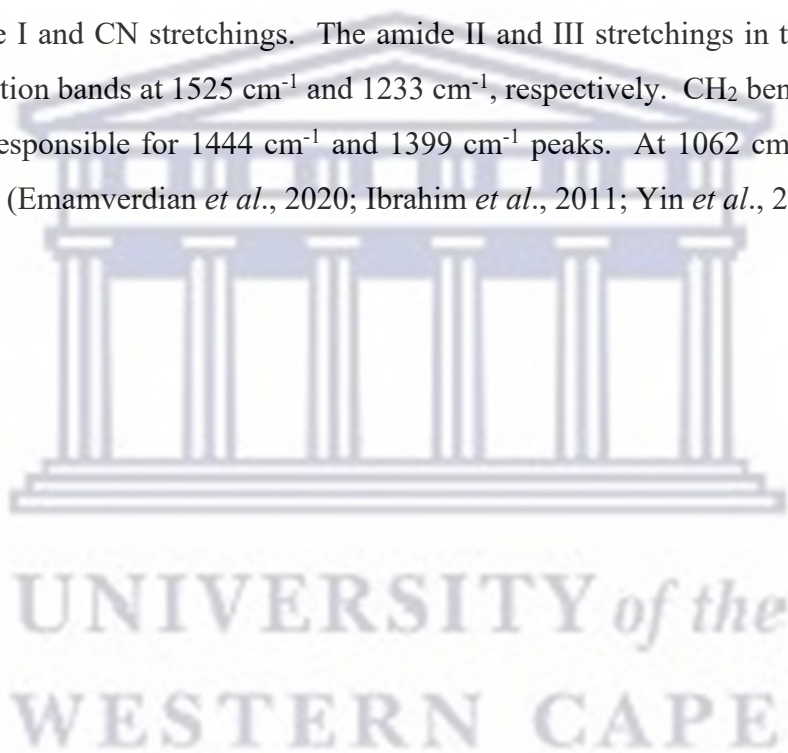
Figure 4.12: The overlay of TGA thermograms obtained for 3TC raw material, GEL, F2SD(PM) compared to F2SD during heating at a rate of 10°C/min from 30 to 600 °C.

Table 4.4: The summary table for pure 3TC, GEL, F2SD and F2SD(PM) outlining the onset of degradation temperatures and percentage mass losses acquired between 30 to 600 °C at 10°C/min.

SAMPLE	Onset of Degradation (°C)	Percentage Weight Loss (%)
3TC	269.37	69.57
GEL	313.09	80.11
F2SD(PM)	293.30	74.82
F2SD	299.69	67.60

FTIR spectroscopy can investigate the alteration of solid-state drug characteristics and their interactions with polymers following the production of microspheres (Bertoni *et al.*, 2020). **Figure**

4.13 illustrates the FTIR spectra obtained for the pure 3TC, GEL, F2SD and F2SD(PM). All of the prominent functional groups reported in the literature for 3TC bulk powder, such as the primary amino group, alcohol group, C-H bonds, aromatic amide group, carbonyl group, imine group, C-O-C groups, ring mode, ring breathing mode, were shown in the 3TC sample used for this study (Chakraboarty *et al.*, 2014; Ngilirabanga *et al.*, 2021; Pandey *et al.*, 2016; Singh & Nath, 2012). The IR spectrum obtained with GEL, (**Figure 4.13(b)**) revealed distinctive peaks at 3279 cm^{-1} and 2936 cm^{-1} , corresponding to amide group N-H and CH_2 stretching, respectively. The peak at 1634 cm^{-1} was assigned to ester (C=O) vibration stretching; this absorption band was also assigned to amide I and CN stretchings. The amide II and III stretchings in the GEL structure, caused the absorption bands at 1525 cm^{-1} and 1233 cm^{-1} , respectively. CH_2 bending and wagging vibrations were responsible for 1444 cm^{-1} and 1399 cm^{-1} peaks. At 1062 cm^{-1} , the CH_3 amide group was visible (Emamverdian *et al.*, 2020; Ibrahim *et al.*, 2011; Yin *et al.*, 2009).



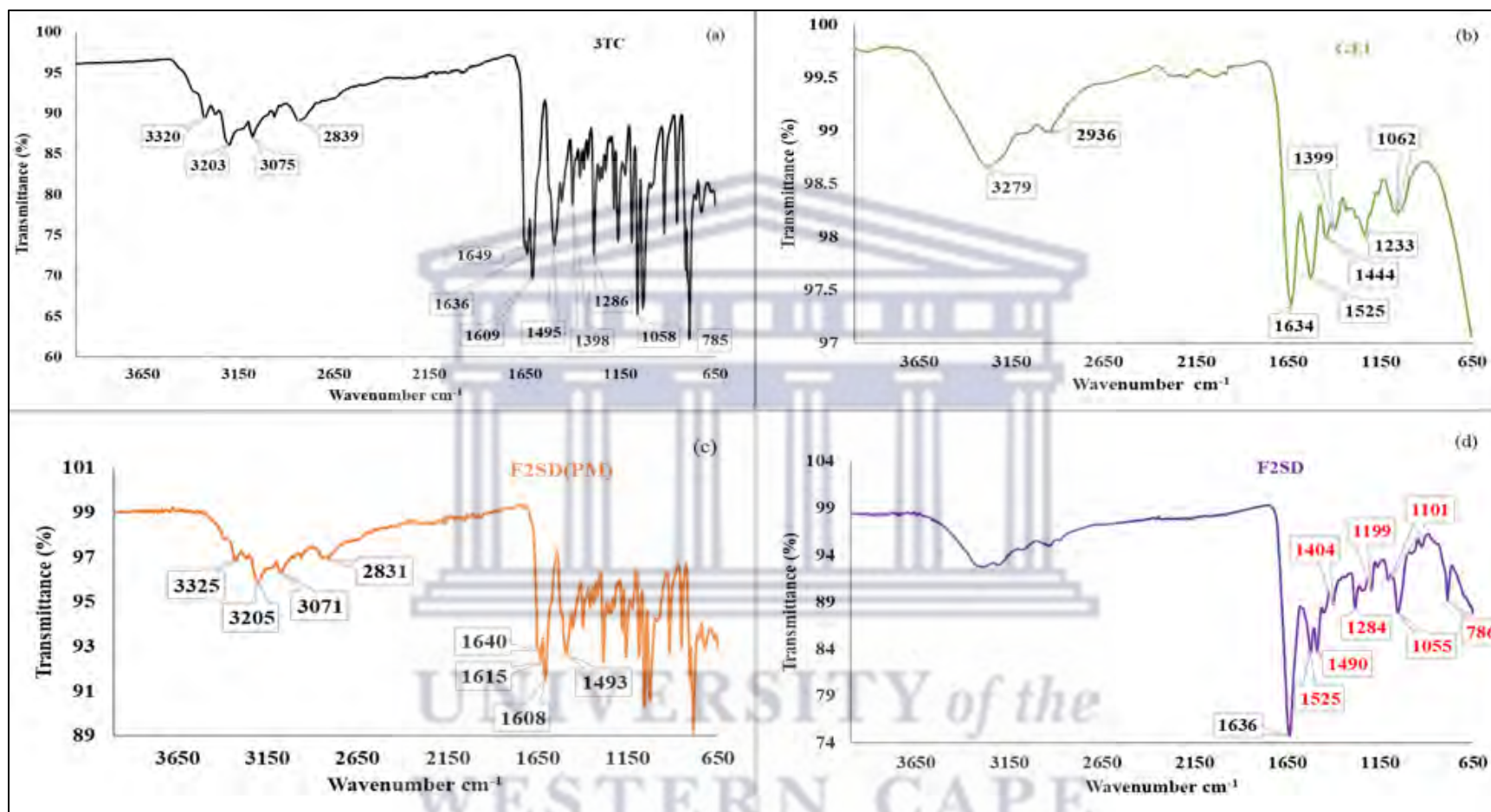


Figure 4.13: FTIR spectrum pure of (a) 3TC, (b) GEL, (c) F2SD(PM) compared to (d) F2SD obtained at ambient temperature within a scanning range of 650 - 4000 cm⁻¹.

The IR spectrum of the physical combination (**Figure 4.13 (c)**) shows significant absorption bands of pure 3TC with slight shifts in wavenumber and peak intensities. This finding indicates no interaction between 3TC and GEL in their physical combination, indicating that these pharmaceutical ingredients are compatible (see also **Appendix II**). The IR spectrum of F2SD (**Figure 4.13 (d)**) showed significant broadening of peaks and the disappearance of all prominent absorption bands associated with 3TC in the 2800 - 3400 cm^{-1} range. The disappearance of these typical peaks can be deduced that the drug molecules were incorporated into the matrix of the polymer. This result support F2SD excellent %EE. These findings in correlation with DSC results confirm the presence of a drug-polymer interaction. The absorption bands at 1636 cm^{-1} for the microsphere formulation may be attributed to 3TC or GEL. Compared to pure 3TC or GEL, this carbonyl or ester (C=O) vibration peak has a different shape, higher intensity, and is positioned at a higher wavenumber to GEL. According to Fini *et al.*, (2008) alterations in the carbonyl absorption spectrum band are critical for interpreting the molecular state of a drug in a polymer matrix. The occurrence of doublet peaks at 1490 cm^{-1} and 1525 cm^{-1} related to the 3TC ring mode and GEL amide II stretching was also identified (Chakraborty *et al.*, 2014; Emamverdian *et al.*, 2020; Ibrahim *et al.*, 2011; Yin *et al.*, 2009).

These results support the high %EE obtained with this formulation. It could therefore be concluded that an interaction between 3TC and GEL occurred. Compared to the pure drug at 1495 cm^{-1} , the ring mode of the drug embedded in the GEL at 1525 cm^{-1} was moved to a lower wavenumber (1490 cm^{-1}). Due to the disappearance of the polymer's doublet peaks at 1444 cm^{-1} and 1399 cm^{-1} , which were attributable to CH₂ bending and wagging vibrations, a new sharp singlet peak at 1404 cm^{-1} related to CH₂ vibration was introduced (Ibrahim *et al.*, 2011). GEL contributed absorption bands at 1199 cm^{-1} and 1055 cm^{-1} , corresponding to amide III stretching and the CH₃ amide group, respectively. However, the shape of these two peaks in the formulation differs, and they were pushed to lower wavenumbers when compared to pure polymer (1233 cm^{-1} and 1062 cm^{-1}) (Emamverdian *et al.*, 2020; Ibrahim *et al.*, 2011). The drug's absorption band at 1087 cm^{-1} was likewise embedded in the GEL at 1062 cm^{-1} , moved to a higher wavenumber, and found in the formulation at 1101 cm^{-1} . All of these alterations point to a reduction in drug-drug intermolecular hydrogen bonding, and the creation of hydrogen bonds between drug molecules and the polymer chain (Bertoni *et al.*, 2020). Finally, changes in the shape, intensity, and

wavenumber of distinctive peaks at 1495 cm^{-1} , 1286 cm^{-1} , and 785 cm^{-1} of 3TC to medium or weak in the formulation, indicates a decrease in the drug's degree of crystallinity (Li *et al.*, 2021).

In summary, the broadening of peaks around the $2800 - 3400\text{ cm}^{-1}$ region, as well as the increase or decrease in the intensities and wavenumbers of the absorption bands of amide I, II, and III bonds seen in F2SD compared to GEL (**Table 4.5**), indicates a decrease in intermolecular hydrogen bonding between 3TC molecules and the presence of hydrogen bonding between drug molecules and polymer chains (Yin *et al.*, 2009).



Table 4.5: Table of 3TC and GEL chemical structures describing the wavenumbers depicted in FTIR analysis with corresponding functional groups when compared to F2SD(PM) and F2SD' absorption spectra.

3TC	GEL	F2SD(PM)	F2SD	Functional group
Wavenumber (cm ⁻¹)				
3320	3279	3325	-	N-H ₂
3203	-	3205	-	O-H
3075	2936	3071	-	CH-SP ²
2839	-	2831	-	CH-SP ³
1649	-	1640	-	R-C=O-NR ₂
1636	1634	1615	1636	C=O/Amide I
1609	-	1608	-	R ₂ -C=NR
	1525	-	1525	Amide II
1495	-	1493	1490	Ring mode
	1444	-	-	CH ₂
	1399	-	1404	CH ₂
1286	-	1284	1284	C-O-C
	1233	-	1199	Amide III
1159	-	1160	-	C-O-C
	1062	-	1055	CH ₃
785	-	785	786	Ring breathing mode

Figure 4.14 show PXRD patterns of 3TC, GEL, F2SD(PM) and F2SD recorded at room temperature (25 °C) throughout a scanning range of 4 - 40 °2 θ . Similar to prior research, the PXRD pattern of pure 3TC showed a diffraction contour of crystalline material (Harris *et al.*, 1997; Ngilirabanga *et al.*, 2021). The PXRD pattern of GEL showed a diffraction profile with no sharp or narrow symmetric peaks, confirming its amorphous nature (Yousaf *et al.*, 2015). The physical mixture exhibited PXRD patterns similar to pure 3TC, with sharp symmetric peaks.

The PXRD pattern of F2SD revealed diffused spectra typical of amorphous materials. Because GEL is mainly amorphous, the polymer matrix's drug for spray-dried formulations is made amorphous by the polymer. The absence of crystalline peaks of 3TC in the PXRD patterns of this formulation suggested that the drug and GEL interacted. This interaction is most likely molecular and may result in the drug forming a solid solution in the polymer(s) matrix (Yüksel *et al.*, 1996). In other words, the absence of typical peaks in PXRD pattern of F2SD indicates that 3TC is entirely amorphous, encapsulated, and bonded with GEL polymer in the microspheres formulation (Panizzon *et al.*, 2014).

The formation of microspheres were confirmed from SEM (**Figure 4.14, insets (e) and (f)**), with the crystalline morphology of 3TC mixed with GEL clearly visible in comparison with a microspherical morphology exhibited by F2SD. It was however noted that the microspheres were not formed as completely separate microspheres but a rather fused morphology was evident. This could be due to the effect of GEL as a wall forming polymer or that the spray drying parameters were not sufficiently optimised. It is hypothesised that the spraying of the feed solution was probably too fast thereby resulting in the formation of poorly formed droplets which dried in a fused mass rather than independent, well-shaped microspheres. It is also hypothesised that the relative high viscosity of the feed solution could have affected poor droplet formation during the spraying process.

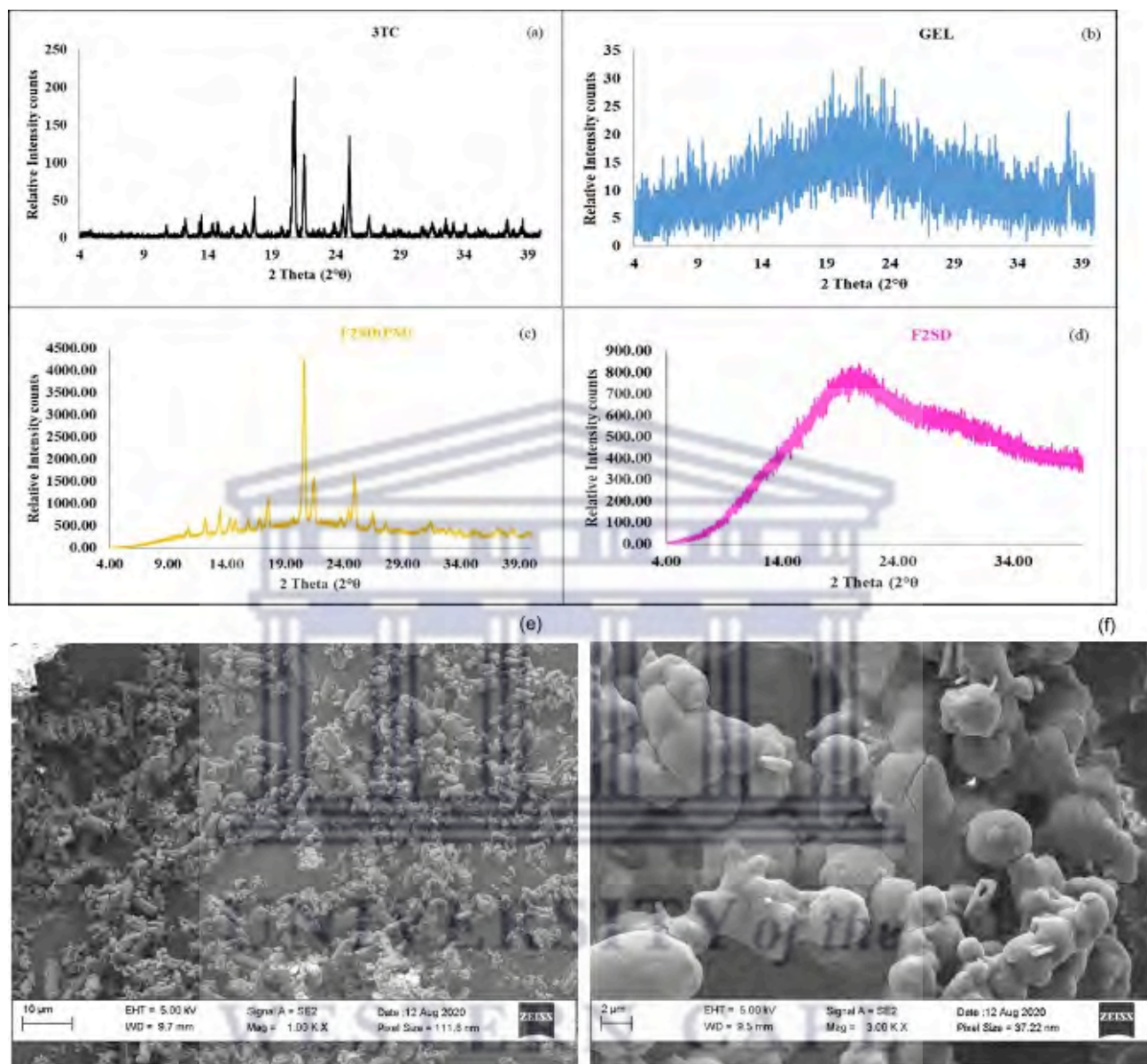


Figure 4.14: The PRXD patterns obtained for (a) 3TC, (b) GEL, (c) F2SD(PM) compared to (d) F2SD at room temperature within a scanning limit of 4 - 40° 2θ and inset (e) depicting the SEM micrograph obtained with F2SD(PM) versus the SEM micrograph obtained with F2SD (inset (f)).

4.4.5 Combination of GEL and CH as polymers for the formulation of 3TC-loaded microspheres by spray drying

As discussed in paragraph 4.4.1 the initial incorporation of CH in the spray drying formulations was not feasible due to the fact that from literature reports it was understood that CH should be

dissolved in diluted acetic acid. Something that was a limiting factor due to the spray dryer not being equipped with an anti-corrosive spraying nozzle. However, from a more in-depth literature search it was observed that it is possible to dissolve CH in various solutions that consist of either citric acid, lactic acid or formic acid (Parize, *et al.*, 2008; Chinta *et al.*, 2008). From this knowledge formulations in which CH is to be incorporated was investigated. In order to test the solubilisation of CH in a citric acid (CA) solution a 1% w/v CA solution was prepared. The solubility of CH in this solution was tested and it was noted that if a concentration of 2 %w/v CH is reached the solution starts to show precipitation. By increasing the CA concentration to 2% w/v the CH concentration could be increased. It was noted that Parize and co-workers (2008) successfully dissolved 3% w/v CH in a 5% w/v CA solution. However, CA is a highly water soluble compound and for the purpose of a modified drug release system it was decided to limit the CA concentration to only 1% w/v thereby limiting the maximum concentration CH to be incorporated to 2% w/v. The feed solutions through which F1SD - F3SD microspheres were spray dried contained 10% v/v ethanol, however the incorporation of ethanol in the 2% w/v CH-CA solution resulted in the formation of an insoluble fibre like structure which was hypothesised to be the precipitation of the CH-polymeric network. Therefore ethanol could not be used to reduce the viscosity of the feed solution in CH-based feed solutions. This resulted in the investigation of the maximum concentration GEL to be incorporated to achieve a feed solution with a viscosity that would allow successful pumping thereof. Various concentrations of GEL were incorporated into the CH-CA solution and formulations as outlined in **Table 4.6.** were subsequently spray dried. The same spray drying parameters as discussed in paragraph 4.4.1 were utilised.

Table 4.6: Outline of CH-GEL combinations dissolved in a 1% w/v CA-solution spray dried for the formulation of 3TC-loaded microspheres

Formulation code	CA (% w/v)	CH (% w/v)	GEL (% w/v)	3TC (% w/v)
F1cSD	1	2	3	5
F2cSD	1	2	5	5
F3cSD	1	2	7	5
F4cSD	1	2	10	5

From the spray drying process only formulation F1cSD provided a sufficient yield of 64.53% with a determined moisture content of 3.21% and a mean particle size of $95.98 \pm 1.91 \mu\text{m}$, whilst F2SD provided a very poor yield of only 12.28%, a moisture content of 6.55% and mean particle size of $160.56 \pm 1.49 \mu\text{m}$. With F3SD a production outcome similar to that depicted in **Figure 4.8** was achieved with a thin ‘sticky’ film adhered to the collection vessel and no dried powder particles. F4cSD did not spray dry successfully due to clogging of the spray nozzle and ultimately ceasing of the spraying process due to a complete blockage of the spray nozzle.

4.4.6 *In vitro* dissolution testing and physicochemical characterisation of F1cSD

Figure 4.15 depicts the 3TC drug release profiles obtained with F1cSD and the physical mixture of F1cSD(PM) in comparison with 3TC raw material in pH 1.2 for a period of 7 hours. In comparison with 3TC raw material and the physical mixture containing CA, CH, GEL and 3TC in the same ratio as in F1cSD it was observed that F1cSD shows a significantly reduced onset of 3TC release. The onset of 3TC release from the microspheres is followed by a steady and controlled release profile with the highest concentration 3TC being $97.63 \pm 1.59 \%$. This was noted as a significant delay in drug release especially since this drug release study was performed in pH 1.2, a dissolution medium in which CH is soluble in. From these results it was deduced that a strongly linked polymeric network was formed between CH and GEL during the spray drying process and therefore physicochemical characterisation of this formulation followed.

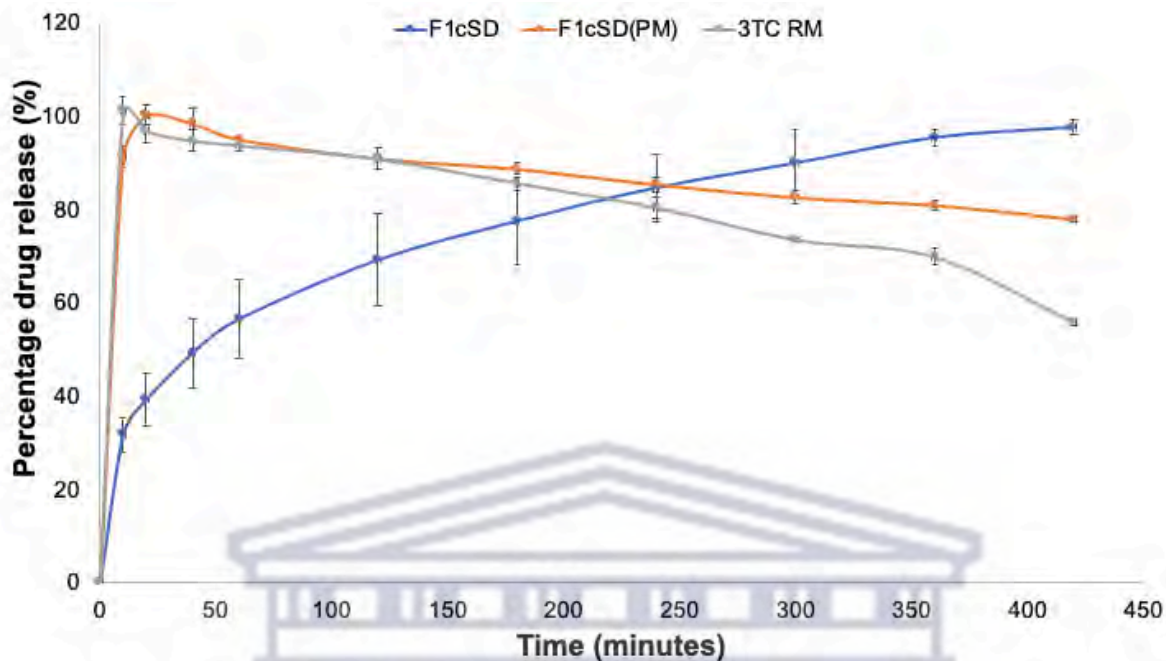


Figure 4.15: Overlay of the dissolution profiles obtained for 3TC raw material in comparison with F1cSD and F1cSD(PM).

The DSC thermograms obtained with F1cSD(PM) and F1cSD are shown in **Figure 4.16**. The DSC result of F1cSD(PM) (**Figure 4.16(a)**) revealed that the physical mixture contained a sharp endothermic peak associated with the 3TC. The DSC thermogram of F1cSD (**Figure 4.16(b)**) revealed the absence of the crystalline 3TC melting peak in the drug-loaded CH-GEL-based microspheres. The absence of the crystalline 3TC peak in the F1cSD can be attributed to the amorphous dispersion of 3TC in the CH-GEL matrix (Tran *et al.*, 2014; Sipos *et al.*, 2008). The two broad endothermic peaks at 79.23 °C and 145.88 °C may be due to the glass transition (T_g) temperatures of GEL and CH, respectively. However, as natural polymers, properties like molecular weight, crystallinity or amorphicity, and deacetylation degree often cause variations in polymer T_g . (Altınışık *et al.*, 2009; Ogunjimi *et al.*, 2020; Yousaf *et al.*, 2015).

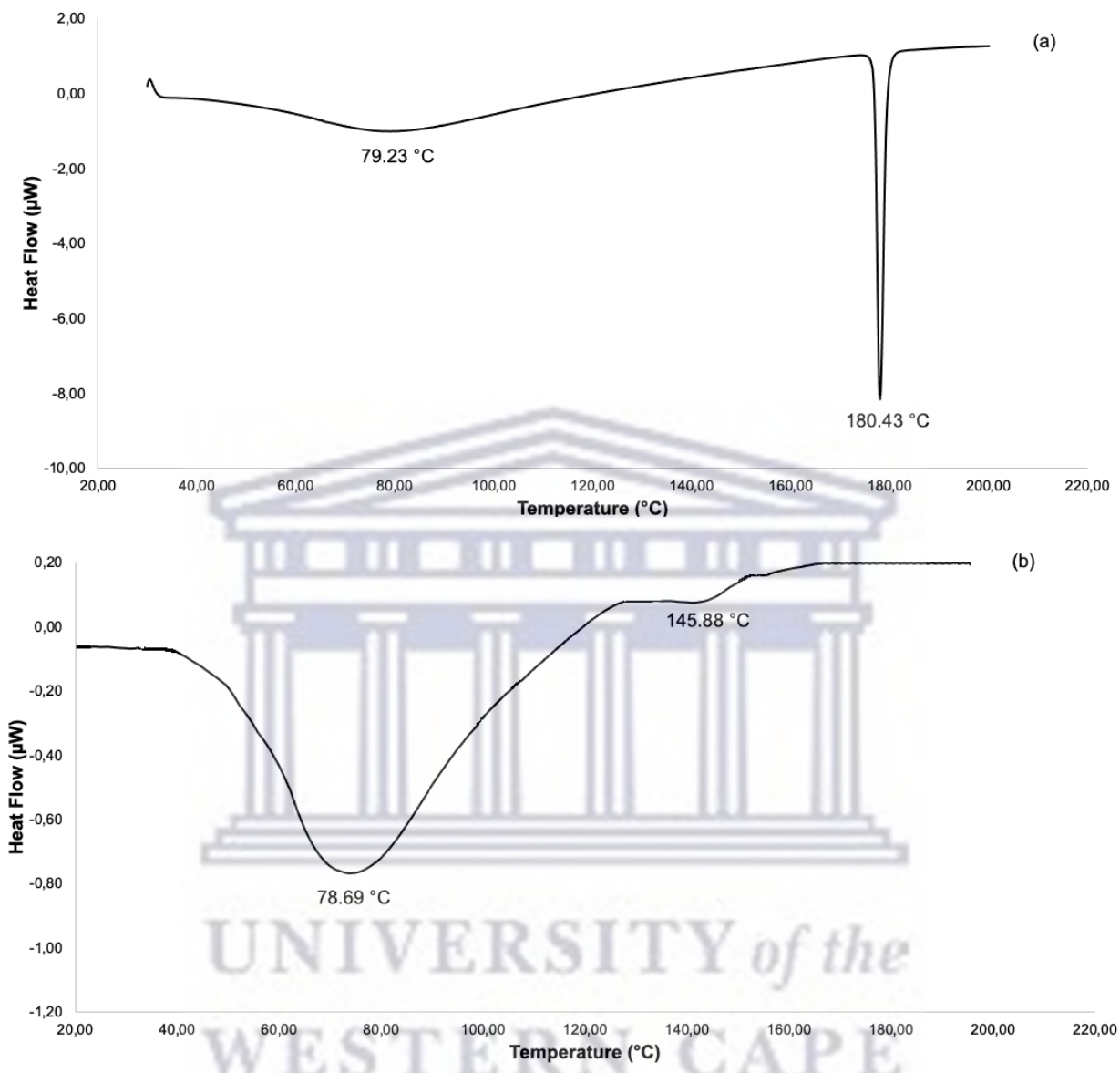


Figure 4.16: DSC thermograms obtained for (a) F1cSD(PM) and (b) F1cSD.

Figure 4.17 depicts the FTIR spectra of pure 3TC, F1cSD, and F1cSD(PM). The physical combination's IR spectrum (**Figure 4.17(d)**) shows significant absorption bands of pure 3TC with slight shifts in wavenumber and peak intensities. As a result, there are no chemical interactions between the API and polymers *via* a physical mixture.

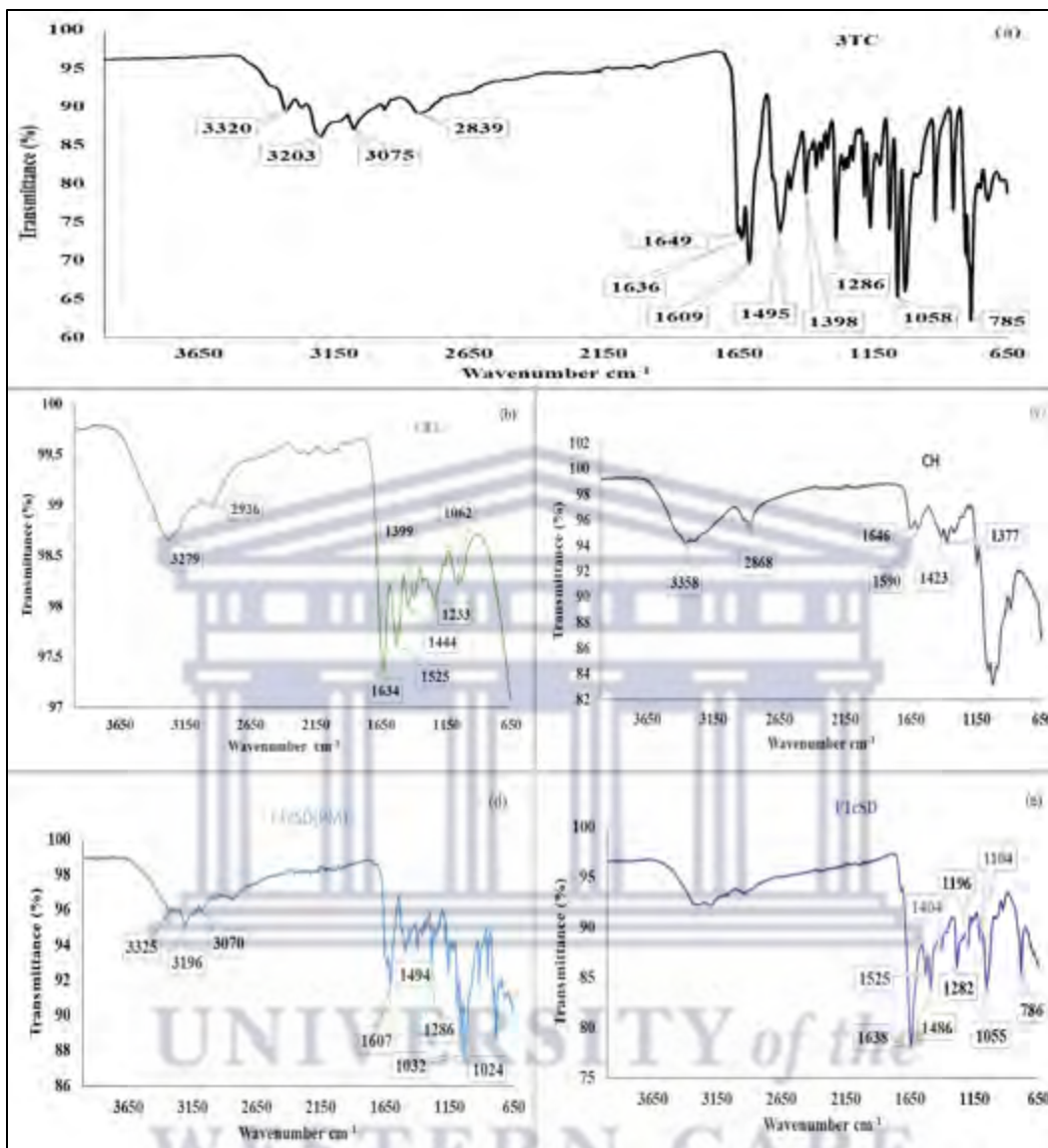


Figure 4.17: FTIR spectrum pure of (a)3TC, (b) GEL, (c) CH, (d) F1cSD(PM) compared to (e) F1cSD obtained at ambient temperature within a scanning range of 650 - 4000 cm^{-1} .

The IR spectrum of F1cSD (**Figure 4.17 (e)**) showed significant broadening of peaks and the disappearance of all prominent absorption bands associated with 3TC in the 2800 - 3400 cm^{-1} range. The disappearance of these typical peaks can be deduced that the drug molecules were incorporated into the matrix of the polymer. These findings with DSC results confirms the presence of drug-polymer interaction. The absorption bands at 1638 cm^{-1} for the microsphere formulation could have come from 3TC or GEL. Compared to pure 3TC or GEL, this carbonyl or ester (C=O) vibration peak has a different shape, higher intensity, and is positioned at a higher

wavenumber. According to Fini *et al.*, (2008) alterations in the carbonyl absorption spectrum band are critical for interpreting the molecular state of a drug in a polymer matrix. The occurrence of doublet sharp peaks at 1486 cm^{-1} and 1525 cm^{-1} related to 3TC ring mode and GEL amide II stretching was found (Chakraborty *et al.*, 2014; Emamverdian *et al.*, 2020; Ibrahim *et al.*, 2011; Yin *et al.*, 2009).

It could therefore be concluded that an interaction between 3TC and GEL occurred. Compared to the pure drug at 1495 cm^{-1} , the ring mode of the drug embedded in the GEL at 1525 cm^{-1} was moved to a lower wavenumber (1486 cm^{-1}). Due to the disappearance of the polymer's doublet peaks at 1444 cm^{-1} and 1399 cm^{-1} , which were attributable to CH₂ bending and wagging vibrations, a new sharp singlet peak at 1404 cm^{-1} related to CH₂ vibration was introduced (Ibrahim *et al.*, 2011). GEL contributed absorption bands at 1282 cm^{-1} and 1055 cm^{-1} , corresponding to amide III stretching and the CH₃ amide group, respectively. However, the shape of these two peaks in the formulation differs, and they were pushed to lower wavenumbers when compared to pure GEL-polymer (1233 cm^{-1} and 1062 cm^{-1}) (Emamverdian *et al.*, 2020; Ibrahim *et al.*, 2011). The drug's absorption band at 1087 cm^{-1} was likewise embedded in the GEL at 1062 cm^{-1} , moved to a higher wavenumber, and found in the formulation at 1104 cm^{-1} . All of these alterations point to a reduction in drug-drug intermolecular hydrogen bonding, and the creation of hydrogen bonds between drug molecules and the polymer chain (Bertoni *et al.*, 2020). Finally, changes in the shape, intensity, and wavenumber of distinctive peaks at 1495 cm^{-1} , 1286 cm^{-1} , and 785 cm^{-1} of 3TC to medium or weak in the formulation, indicates a decrease in the drug's degree of crystallinity (Li *et al.*, 2021).

In summary, the broadening of peaks around the $2800\text{-}3400\text{ cm}^{-1}$ region, as well as the increase or decrease in the intensities and wavenumbers of the absorption bands of amide I, II, and III bonds seen in F1cSD compared to GEL, indicates a decrease in intermolecular hydrogen bonding between 3TC molecules and the presence of hydrogen bonding between drug molecules and polymer chains (Yin *et al.*, 2009).

The IR spectrum of F1cSD (**Figure 5.17(e)**) is slightly different from that of F2SD (**Figure 5.13(d)**) at distinctive peaks at 1638 cm^{-1} , 1486 cm^{-1} , 1282 cm^{-1} , 1196 cm^{-1} , and 1104 cm^{-1} demonstrating that the small amount of CH added to this formulation had effect.

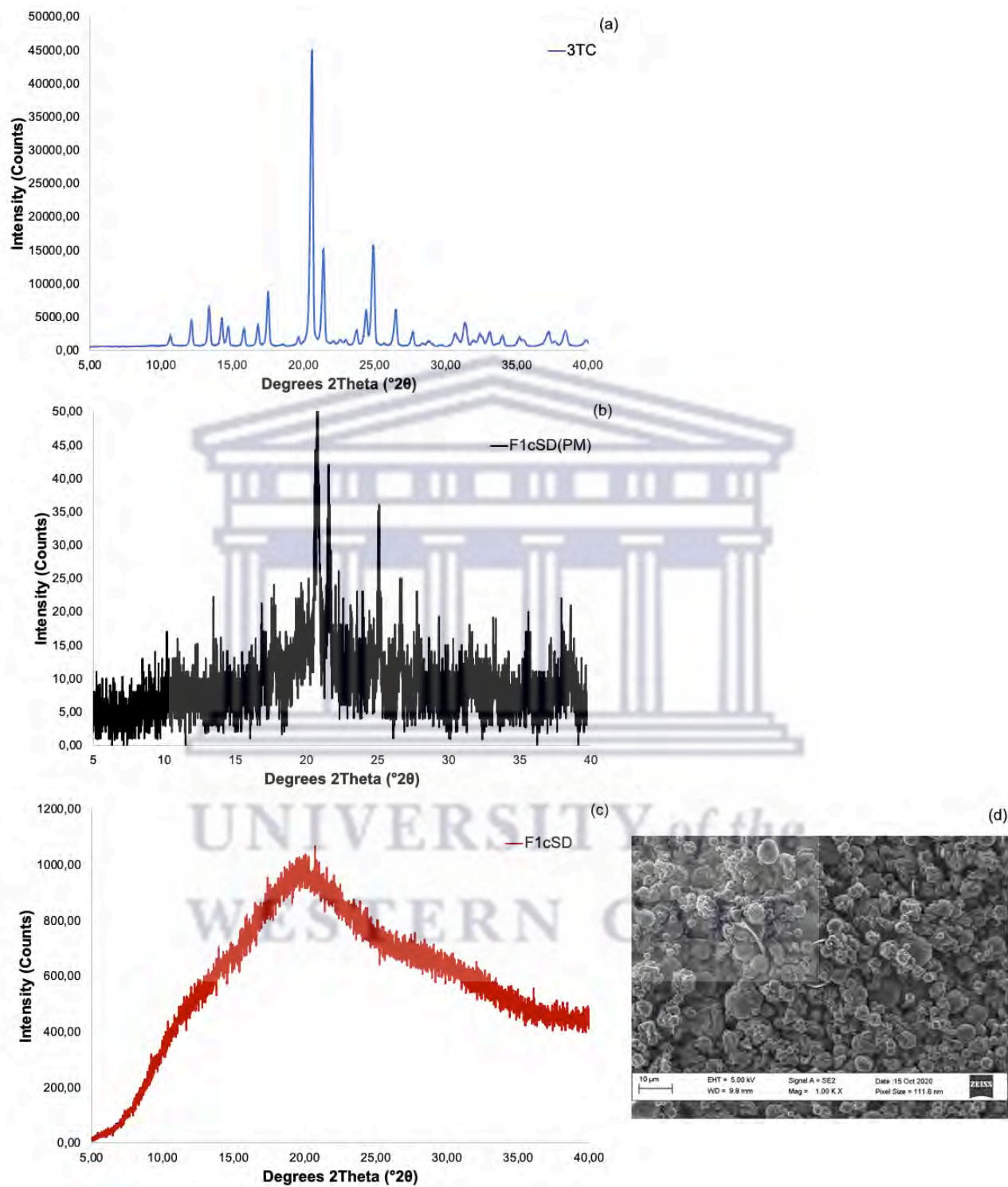


Figure 4.18: PXR D diffractograms obtained with (a) 3TC raw material, (b) F1cSD(PM) and (c) F1cSD with inset (d) depicting the SEM micrograph obtained with F1cSD.

Figure 4.18 show PXRD patterns of 3TC, F1cSD(PM) and F1cSD recorded at room temperature (25 °C) throughout a scanning range of 4 - 40 °2 θ . The physical mixtures of the spray-dried formulation (**Figure 4.18(b)**) exhibited PXRD patterns similar to pure 3TC, with sharp symmetric peaks but at lower intensities due to the presence of amorphous GEL and CH. The PXRD pattern of F1cSD (**Figure 4.18(c)**) revealed diffused spectra typical of amorphous solids. The absence of crystalline peaks of 3TC in the PXRD patterns of this formulation suggested that the drug and CH-GEL interacted. This interaction is most likely molecular and may result in the drug forming a solid solution in the polymer(s) matrix (Yüksel *et al.*, 1996). In other words, the absence of typical peaks in PXRD pattern of F1cSD indicates that 3TC is entirely amorphous, encapsulated, and bonded with CH-GEL polymers in the microspheres formulation (Panizzon *et al.*, 2014). From Figure 4.18(d) it became apparent that the spray drying of 3TC using both GEL and CH as polymers resulted in well-defined drug-loaded microspheres with almost no fused microparticles visible.

4.4.7 Conclusion on the formulation of 3TC-loaded microspheres by incorporating CH into the polymeric network

The results of the physicochemical characterisation of F1cSD compared to 3TC raw material and F1cSD(PM) using DSC, FTIR, PXRD and SEM revealed that the physical state of 3TC changed in the CH-GEL matrix system during the spray drying process from crystalline to amorphous, 3TC was well encapsulated or incorporated into the wall-forming materials, and there was strong intramolecular hydrogen bonding or interaction between 3TC molecules and the CH-GEL side chains in the spray dried formulation.

During the *in vitro* dissolution study in the same pH 1.2 dissolution medium and testing conditions, the strong interaction between 3TC:CH-GEL (5:2:3% w/v) and dense polymer-polymer complexation of CH-GEL (2:3% w/v) ensured a significantly reduced onset of 3TC release or burst release from F1cSD compared to F1SD, F2SD, and F3SD. Therefore, adding CH to the polymeric network significantly decreased the early start of drug release seen in F1SD, F2SD, and F3SD. It can be deduced that 3TC was more encapsulated into the matrix system of CH-GEL than GEL only during the spray drying process.

4.5 Formulation of TDF-loaded microspheres *via* spray drying

TDF, as previously discussed in Chapter 2, is a BCS Class III tenofovir prodrug (Patil *et al.*, 2017; Pubchem, 2022; Wassner *et al.*, 2020). As a result, low permeability is the rate-limiting step, which directly affects gastro-intestinal tract absorption and oral bioavailability in the systemic circulation (Amidon *et al.*, 1995; Patil *et al.*, 2017). TDF also has a low oral availability (around 25%) due to its conversion to the monoester form during absorption (Shailender *et al.*, 2017; Van Gelder *et al.*, 2002). The formulation development of such a class of drugs may be complex. TDF's high aqueous solubility (13.4 mg/mL) reduces loading efficiency into polymeric microparticles due to easy leaching out of the carrier, making it difficult to formulate this drug into a controlled drug delivery system (Kaur *et al.*, 2018; Patil *et al.*, 2017; Pubchem, 2022). However, once-daily administration is sufficient because TDF has long plasma and intracellular half-lives of 17 and 60 hours, respectively. As a result, a potential modified drug delivery system in which TDF is also incorporated as part of a FDC should be able to maintain plasma stability and the desired therapeutic level of TDF for an extended period but formulation of TDF into a modified drug delivery system would not be considered a cost-effective approach. Therefore it would make sense to investigate the effect a spray drying process, as described in paragraph 4.4, would have on TDF in terms of *in vitro* dissolution so as to ascertain whether it would be a possibility to incorporate TDF in a microsphere-based formulation, without necessarily modifying TDF drug release. Based on the microsphere formulation studies conducted for 3TC, the fact that TDF is also a BCS Class III drug and the fact that the spray drying process resulted in the best 3TC-loaded microsphere formulation outcome in terms of yield, it was decided to combine TDF in exactly the same GEL combinations (paragraphs 4.4.1) for spray drying purposes, in the event 3TC and TDF have to be co-processed into drug-loaded microspheres. **Table 4.7** provides an outline of the TDF:GEL concentrations utilised in the formulation of GEL-based TDF-loaded microspheres. The spray drying process followed is as described in paragraph 4.4.1 and Chapter 3, paragraph 3.3.2(b).

Table 4.7: Outline of TDF:GEL ratios which were dissolved in 10 %v/v ethanolic solution and subsequently spray dried

Formulation code	TDF (% w/v)	GEL (% w/v)	Yield (%)	Moisture content (%)	Drug loading (%)	%EE
F5SD	7.5	7.5	31.06	2.49	41.04 ± 1.29	25.50 ± 0.56
F6SD	5	10	41.95	2.23	32.98 ± 1.53	41.50 ± 1.67
F7SD	3	12	43.75	3.31	25.75 ± 2.01	56.32 ± 0.55

From the results it was clear that TDF's %EE increases as polymer concentration increases. The highest TDF %EE (56.32 ± 0.55%) was obtained with a 1.6-fold increase in GEL concentration (F7SD). This result could be due to improved TDF solubility or dispersion in the polymeric matrix at higher GEL concentrations (Wang & Wang, 2002). The low yield (Table 4.7) of F5SD microspheres can be attributed to their poor encapsulation efficiency (25.50% ± 0.56), as less drug was solubilised and efficiently entrapped in the polymer matrix compared to F6SD and F7SD microspheres. According to Yeo & Park, polymer solubility in water-miscible co-solvents can affect the encapsulation efficiency of polymeric microparticles. These researchers also discovered an increase in %EE of microspheres when the drug and polymer interact more strongly *via* hydrogen and van der Waals bonding forces (Yeo & Park, 2004). As a result, it could be expected that F7SD has a more solid drug-polymer interaction than the other two microsphere formulations.

According to Shu *et al.* (2006), increasing the inlet temperature from 170 to 210 °C during spray drying increased production yield and encapsulation efficiency. A previous study on the spray drying encapsulation of hydrophilic etanidazole revealed a low production yield and lower drug loading of the hydrophilic drug was associated with higher encapsulation efficiency. According to the study, formulations with lower drug loading had a higher percentage of their drug content dissolved in a given solvent volume. Their lower drug-polymer ratio resulted in more remarkable drug encapsulation into the polymer matrix (Wang & Wang, 2002). Tran *et al.* (2014) also reported that decreasing the GEL-drug ratio increased drug loading capacity but did not affect encapsulation efficiency. However, from the results obtained in this study it was observed that

%EE was significantly affected by an increase in GEL concentration. According to Ogunjimi *et al.* (2020), increasing polymer concentration may result in increased viscosity and polymer availability to entrap hydrophilic drugs. The best microspheres formulation should have a high drug encapsulation efficiency and loading capacity (Ogunjimi *et al.*, 2020).

4.5.1 Drug release determination from spray-dried TDF loaded microspheres

The dissolution rate of the three TDF-loaded microsphere formulations were determined and compared to that of pure TDF and the corresponding physical mixtures in pH 1.2 (acidic buffer solution) for 120 minutes at 37 ± 0.5 °C. **Figure 4.19** depicts the dissolution profiles of all the samples used in this analysis. This study aimed to replicate or determine the behaviour of water-soluble drug-loaded GEL-based microspheres in the stomach. The effect of polymer concentration, drug-polymer interaction, TDF solid-state properties in the GEL matrix, and drug modification in the polymer matrix during the spray drying process on the dissolution rate of formulations F5SD, F6SD and F7SD were investigated.

Pure TDF dissolved completely (102 ± 1.02 %) within 10 minutes. TDF is a weak base drug that ionises readily in an aqueous acidic medium, resulting in high solubility and dissolution rate in simulated gastric fluid (Bazzo *et al.*, 2019; Patil *et al.*, 2017). In 10 minutes, 97 ± 4.34 % of the TDF was released from the microspheres, according to the dissolution profile of F5SD. This result showed that almost all TDF was released from the polymer matrix in a short time period. Given the formulation's encapsulation efficiency of 25.50%, the rapid TDF release could be attributed to most drug particles on the microsphere's surface in their loosely associated state or free-state (Jelvehgari *et al.*, 2011; Yeo & Park, 2004; Patil *et al.*, 2017). The total drug released from F5SD at the end of the two-hour testing period was 93%, demonstrating that the polymer concentration used was insufficient to slow the dissolution rate of TDF from its matrix. The dissolution profiles of F5SD and the corresponding physical mixture are very similar, demonstrating the weak drug-polymer interactions in F5SD.

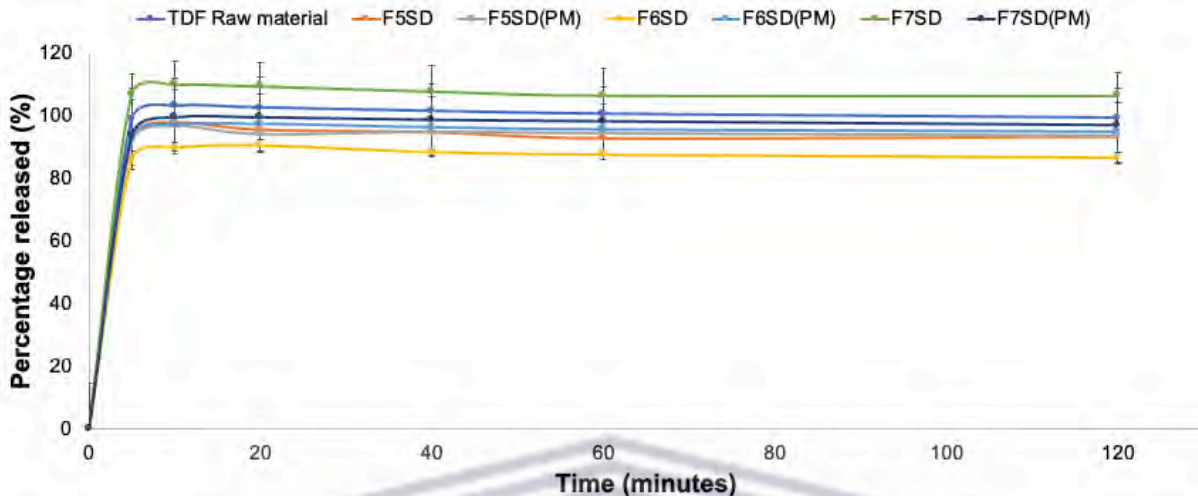


Figure 4.19: Overlay of the dissolution profiles obtained for TDF raw material in comparison with F5SD, F5SD(PM), F6SD, F6SD(PM), F7SD and F7SD(PM) in pH 1.2 dissolution medium at 37 ± 0.5 °C.

The dissolution profile of F6SD is similar to that of F5SD. Approximately $89 \pm 1.68\%$ of the TDF was released from the GEL matrix in 10 minutes. As a result, F6SD demonstrated rapid TDF release similar to F5SD, but increasing the polymer concentration reduced TDF release by 8%. Comparing the dissolution profiles of F6SD with that of F5SD demonstrates that higher concentrations of GEL can be used to control the release of TDF to a certain level. F6SD demonstrated superior TDF %EE in comparison with F5SD (25.50%), implying that the drug-polymer interactions are more substantial in F6SD, more drug is entrapped in the polymer matrix, and dissolution rates are delayed with insignificant differences.

F7SD improved the release of TDF in the pH 1.2 dissolution medium. In 10 minutes, $109 \pm 1.87\%$ of the TDF was released. This is an increase of 7% in comparison with pure TDF release. Given that this formulation had a low drug loading capacity (25.75%) but a high encapsulation efficiency (56.32%), it is possible that a high concentration of GEL could be used to improve drug bioavailability (Yousaf *et al.*, 2015). This faster dissolution rate of TDF from F7SD compared to pure TDF, F5SD, F6SD, and their corresponding physical mixtures suggests that spray drying of the drug in combination with a high concentration of GEL could have resulted in a change in solid-state form of TDF. The possibility that TDF converted to an amorphous solid-state form could be a clarification for the enhanced rate of drug dissolution. However, the increase in the dissolution

concentration of TDF could also be attributed to improved wetting caused by intimate contact between the drug molecules and GEL (Kallinteri & Antimisiaris, 2001).

Due to the poor swelling properties observed in the 3TC-loaded GEL microspheres, the swelling behaviour of the TDF-loaded GEL-based microspheres were not investigated. According to previous research, non-cross-linked GEL microspheres prepared by spray drying swell poorly in both acidic and alkaline buffer solutions at room temperature. This can be ascribed to the fact that GEL has low structural integrity under physiological conditions (Dolci *et al.*, 2020). Therefore, GEL must be physically or chemically modified to ensure structural integrity or stability under physiological conditions due to its high solubility in aqueous environments (Dolci *et al.*, 2018; Vandelli *et al.*, 2001).

Based on the fact that spray drying of TDF with varying concentrations GEL did not significantly alter the drug release rate of TDF, except in the instance where TDF was combined with 12% w/v GEL it was decided to investigate F7SD further to ascertain whether the GEL concentration and spray drying process resulted in the amorphisation of TDF. Considering the insignificant difference in TDF release rate, whether spray dried with GEL or just mixed with GEL in a physical mixture allowed the conclusion that should TDF be co-formulated with F2SD, for example, no significant modification in the TDF release rate would be observed. DSC, FTIR, and PXRD were used to determine the solid state characteristics of TDF in combination with 12% w/v of GEL.

Figure 4.20 depicts the DSC thermograms obtained with TDF raw material, GEL, F7SD(PM) and F7SD. The broad glass transition temperature (T_g) of GEL was 88.53 °C, with no endothermic event, showing that GEL is amorphous (Yousaf *et al.*, 2015). From **Figure 4.20(c)** the sharp endothermic peaks associated with the TDF was present in the physical mixture, however upon spray drying **Figure 4.20(d)** the first endothermic peak disappeared with only the second melting peak of TDF present at 116.78 °C.

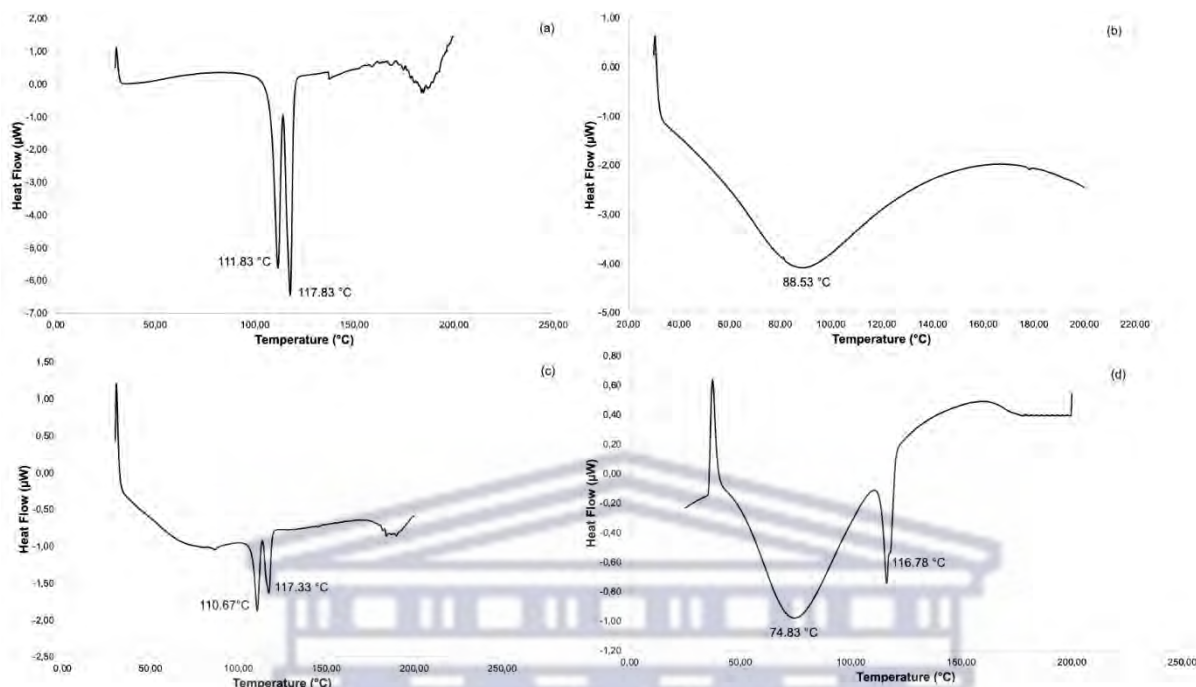


Figure 4.20: DSC traces obtained for (a) TDF raw material, (b) GEL, (c) F7SD(PM) and (d) F7SD.

The FTIR spectrum of TDF displayed prominent functional groups like aromatic (1°) amine, sp^3 C-H bond, ester (C=O), alkene/olefins (C=C), N-H band, aromatic (C=N) pairs, P=O bond, primary aromatic C=N, N-H wagging and C-H deformation bands (Bazzo *et al.*, 2019; Gomes *et al.*, 2015; Patil *et al.*, 2017; Silva *et al.*, 2017). The IR spectrum of the physical mixture (**Figure 4.21(c)**) showed IR pattern similar to the distinct peaks of pure TDF with minor band shifts. These findings show that TDF and GEL have no interaction in their pure physical combination, proving that these pharmaceutical ingredients are compatible.

The IR spectrum of F7SD mixture showed distinct bands seen in the IR spectra of TDF and GEL but with some significant band shifts and lower peak intensities (**Figure 4.21 (d)**). Although the intensities absorbance bands obtained with F7SD were reduced and located at slightly different wavenumbers (**Table 4.8**), no new peaks were formed in the formulation's spectrum. These findings confirmed that the drug and polymer interacted via intermolecular hydrogen bonding, TDF was physically entrapped in the GEL matrix, and thereby a tightly formed polymeric network with TDF did not occur (Ogunjimi *et al.*, 2020; Patil *et al.*, 2017).

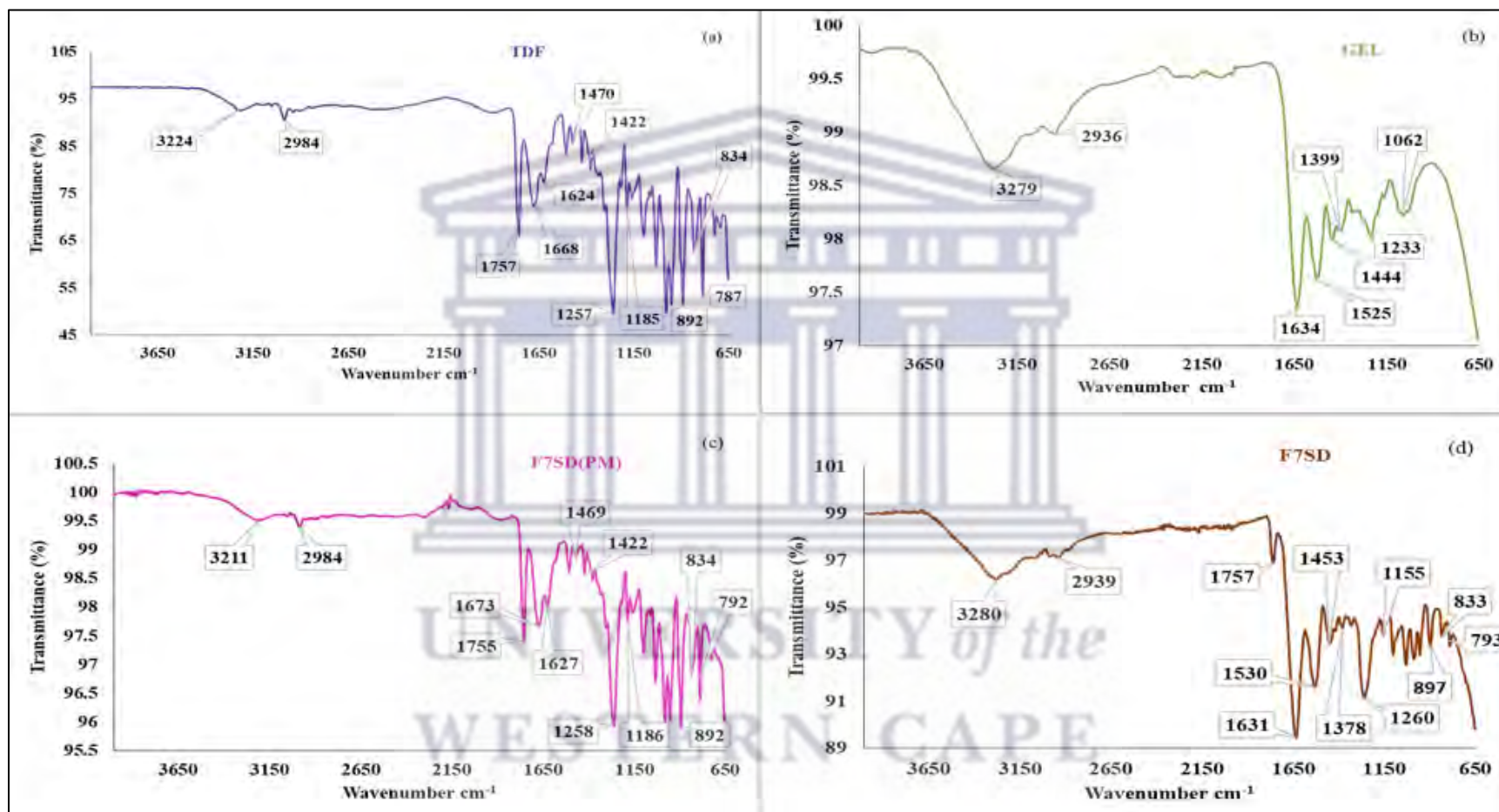
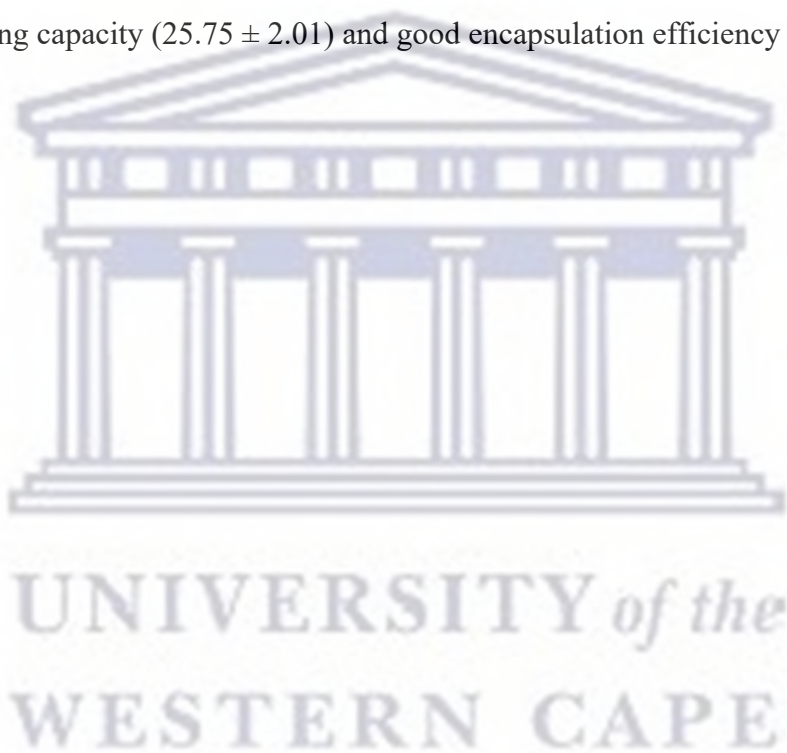


Figure 4.21: FTIR spectrum pure of (a)TDF, (b) GEL, (c) F7SD(PM) compared to (d) F7SD obtained at ambient temperature within a scanning range of 650 - 4000 cm^{-1} .

Table 4.8: Table of TDF and GEL chemical structures describing the wavenumbers depicted in FTIR analysis with corresponding functional groups when compared to F7SD(PM) and F7SD' absorption spectra.

TDF	GEL	F2SD(PM)	F2SD	Functional group
Wavenumber (cm ⁻¹)				
-	3279	-	3280	N-H ₂
3224	-	3211	-	N-H ₂
2984	-	2984	-	CH-SP ³
-	2936	-	2939	CH-SP ²
1757	-	1755	1757	C=O
1668	-	1673	-	C=C
-	1634	-	1631	C=O/Amide I
1624	-	1627	-	N-H
-	1525	-	1530	Amide II
1470	-	1469	-	C=N
-	1444	-	1453	CH ₂
1422	-	1422	-	C=N
-	1399	-	1378	CH ₂
1257	-	1258	1260	C-N
-	1233	-	-	Amide III
1185	-	1186	1155	P=O
-	1062	-	-	CH ₃
892	-	892	897	N-H/C-H
834	-	834	833	N-H/C-H
787	-	792	793	N-H/C-H

The PXRD diffraction pattern obtained for F7SD (**Figure 4.22 (d)**) revealed diffused spectra typical of amorphous materials. The absence of crystalline TDF peaks in the PXRD pattern obtained for F7SD indicates strong intermolecular hydrogen bonding or interaction between the molecules of TDF and GEL in this formulation. This molecular interaction may result in the drug forming a solid solution in the polymer matrix which would clarify the increase in TDF dissolution rate (Yüksel *et al.*, 1996). In another word, the absence of typical peaks in PXRD patterns of F7SD microspheres indicates that TDF is entirely amorphous, well encapsulated or entrapped within the gelatin polymer matrix (Panizzon *et al.*, 2014; Patil *et al.*, 2017). This F7SD PXRD result confirms its low drug loading capacity (25.75 ± 2.01) and good encapsulation efficiency (56.32 ± 0.55).



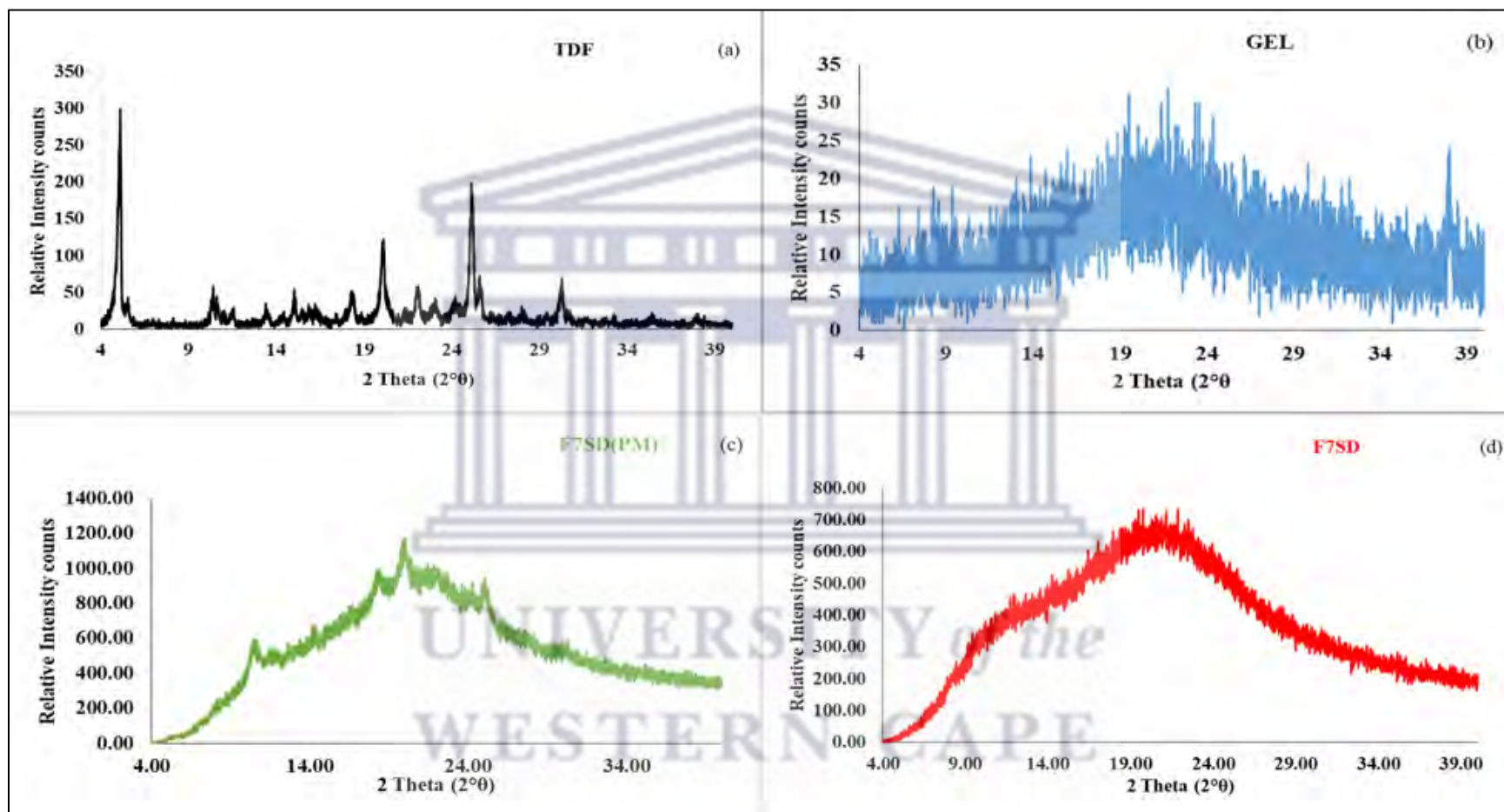


Figure 4.22: The PRXD patterns obtained for (a) TDF, (b) GEL, (c) F7SD(PM) compared to (d) F7SD at room temperature within a scanning limit of 4 - 40° 2 θ .

4.6 Conclusion

The preparation of 3TC-microspheres using ionic gelation methods with natural polymers such as SA, CH, GEL, EC, IN, and XG with calcium chloride to improve the mechanical strength and stability of the polymeric network structure surrounding the drug (Huang *et al.*, 2006) demonstrates that polyelectrolyte complexation with GEL provided the best formulation and has the ability to provide sustained release of a highly hydrophilic drug with drug release sustained at +/- 85% for a period of 6 hours with a decline in dissolved 3TC observed only after 5 hours. The best-modified drug release system 3TC-microspheres (F4) at pH 1.2 prepared by ionic gelation method was from SA, GEL (high concentration-10% w/v), CH (1% w/v) and calcium chloride polyelectrolyte complexation with only 49.74% of 3TC released in 2 hours. Therefore, the polymer mixtures of GEL and CH enabled the modified release of hydrophilic 3TC. The coating of this GEL-CH microspheres can lead to the production of modified drug delivery system for delayed or extended drug release. The use of an automated syringe instead of the manual syringe needle that can easily extrude the viscous polymer solution into the cross-linker solution will improve the production yield during microspheres preparation using ion gelation method.

This study successfully used spray drying to produce formulations encapsulating 3TC and TDF. When compared to previous studies (Mohaweb *et al.* (2014) and Patil *et al.* (2017), the optimised process parameters/variables (such as feed concentration, polymer concentration, inlet temperature, drug-polymer ratio, feed flow rate, air flow rate, outlet temperature, and co-solvent system) were sufficient for the production yield and encapsulation efficiency of 3TC with GEL only or in combination with CH, and TDF with GEL.

The dissolution profile of the 3TC-loaded spray dried microspheres in the pH 1.2 dissolution medium for F2SD showed modified release of 3TC from the GEL matrix due to good encapsulation efficiency; as result of substantial drug-polymer interactions or intermolecular hydrogen bonding and reduction in the crystallinity of 3TC in the polymeric matrix. By utilising cost-effective and up-scalable processing method such as the coating of F2SD with a hydrophobic polymer or stearic acid should prevent or reduces the first burst effect, improve gastroprotection, and may lead to the development of extended drug delivery microspheres systems for 3TC. Additionally, GEL's mechanical properties will be improved by cross-linking, which will improve the modified release of 3TC (Dolci *et al.*, 2020). The spray-dried microspheres prepared from

3TC: CH-GEL (5:2:3% w/v) dissolved in a 1% w/v CA solution demonstrated reduced initial burst release followed by a steady and controlled release profile for 3TC for 7 hours at pH 1.2, with the highest concentration of 3TC being $97.63 \pm 1.59\%$.

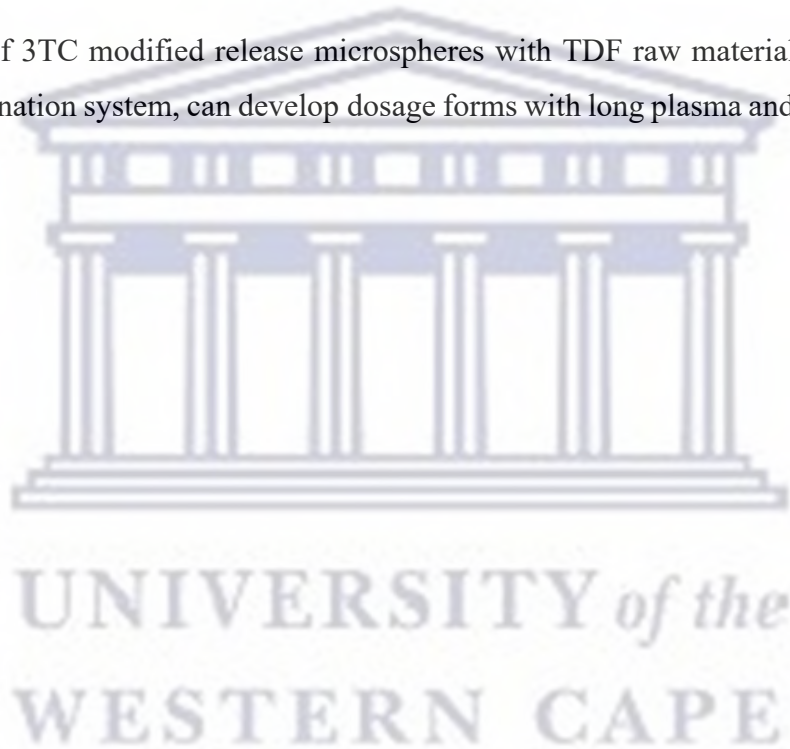
The *in vitro* dissolution testing of TDF-loaded spray-dried GEL microspheres in the pH 1.2 dissolution medium for F5SD and F6SD revealed that the release of TDF from the GEL matrix was modified to a certain level as a result of low encapsulation efficiency and weak drug-polymer interactions. This finding supported previous research studies by Kaur *et al.* (2018), Patil *et al.* (2017), and Pubchem (2022), that TDF's high aqueous solubility (13.4 mg/mL) reduces loading efficiency into polymeric microparticles due to easy leaching out of the carrier, making it difficult to formulate this drug into a modified drug delivery system. These two formulations can be optimised by; (a) Polymeric Coating: Apply a polymeric coating to the microparticles to control drug release. This coating can help to reduce the leaching of TDF from the carrier while providing a controlled and sustained release of the drug. (b) Hydrophobic Excipients: Incorporating hydrophobic excipients or polymers that can interact with TDF and reduce its solubility. This can enhance the drug loading efficiency and stability within the microparticles. (c) Use of Solid Lipid Nanoparticles (SLNs): SLNs are lipid-based nanoparticles that can encapsulate hydrophobic drugs like TDF. These particles provide controlled drug release and minimize leaching due to the lipid matrix.

The dissolution profile of F7SD in the pH 1.2 dissolution medium revealed a faster dissolution rate of TDF from the polymeric matrix than TDF raw material and the other two formulations due to improved wetting caused by intimate contact between the drug molecules and higher GEL concentration. Thus, a high concentration of hydrophilic polymer GEL may be used to improve TDF bioavailability (Bruschi *et al.*, 2003; Dolci *et al.*, 2018; Piao *et al.*, 2008; Yousaf *et al.*, 2015).

In conclusion, this study demonstrated that the drug-polymer ratio and drug-polymer interaction could all impact the properties of GEL (plus CH)-based drug-loaded microspheres. Therefore, depending on the physical state of the drug in the polymeric matrix, drug-polymer interaction, and polymer concentration, GEL-based drug-loaded microspheres can either enhance or retard the dissolution rate of the drug contained in its matrix. Despite belonging to the same BCS Class III, the co-processing of 3TC and TDF as modified release microspheres by spray drying method will be complex due to their different dissolution profiles and drug-polymer interactions. Because 3TC

still forms part of the first-line HIV treatment regimens and is currently incorporated into the FDCs consisting of 3TC + TDF or 3TC + TDF + dolutegravir sodium (DTG), doravirine + TDF + 3TC, dolutegravir + 3TC, 3TC + raltegravir, abacavir + dolutegravir + 3TC, efavirenz + 3TC + TDF or 3TC + zidovudine (Anon, 2023; Casado & Banon, 2015; Li *et al.*, 2022; Sankaraiah *et al.*, 2022; Zamora *et al.*, 2019), a modified drug delivery system is necessary due to its known short intracellular and blood circulation half-lives. Whereas, since TDF is a common once-daily backbone for use with other classes of ARVs due to its long intracellular and blood circulation half-lives, a modified drug delivery system is not necessary.

Co-formulation of 3TC modified release microspheres with TDF raw materials as a multi-layer fixed-dose combination system, can develop dosage forms with long plasma and intracellular half-lives.



4.7 References

Ahmady, A. and Samah, N.H.A. (2021). A review: Gelatine as a bioadhesive material for medical and pharmaceutical applications. *International Journal of Pharmaceutics*, 608, p.121037. Doi: <https://doi.org/10.1016/j.ijpharm.2021.121037>.

Almeida, P.F. and Almeida, A.J. (2004). Cross-linked alginate–gelatine beads: a new matrix for controlled release of pindolol. *Journal of Controlled Release*, 97(3), pp.431-439. Doi: <https://doi.org/10.1016/j.jconrel.2004.03.015>.

Al-Muhanna, M.K., Rub, M.A., Azum, N., Khan, S.B. and Asiri, A.M. (2015). Effect of gelatin on micellization and microstructural behavior of amphiphilic amitriptyline hydrochloride drug solution: A detailed study. *The Journal of Chemical Thermodynamics*, 89, pp.112-122. Doi: <https://doi.org/10.1016/j.jct.2015.05.007>.

Amidon, G.L., Lennernäs, H., Shah, V.P. and Crison, J.R. (1995). A theoretical basis for a biopharmaceutic drug classification: the correlation of in vitro drug product dissolution and in vivo bioavailability. *Pharmaceutical Research*, 12, pp.413-420. Doi: <https://doi.org/10.1023/A:1016212804288>.

Andonova, V. (2017). Synthetic polymer-based nanoparticles: Intelligent drug delivery systems, in: Reddy, B (Ed.), *Acrylic Polymers in Healthcare. IntechOpen.*, London, pp.101-125. Doi: <http://dx.doi.org/10.5772/intechopen.69056>.

Andrianov, A.K. and Payne, L.G. (1998). Polymeric carriers for oral uptake of microparticulates. *Advanced Drug Delivery Reviews*, 34(2-3), pp.155-170. Doi: [https://doi.org/10.1016/S0169-409X\(98\)00038-6](https://doi.org/10.1016/S0169-409X(98)00038-6).

Anon. (2023). General Considerations When Using Fixed-Dose Combination Products. chrome-extension://efaidnbmnnnibpcajpcglclefindmkaj/https://clinicalinfo.hiv.gov/sites/default/files/guidelines/documents/pediatric-arv/drug-information-fixed-dose-combinations-tablets-minimum-body-weights-considerations-use-children-adolescents-pediatric-arv.pdf. Date of access: 01 August 2023.

Altınışık, A., Seki, Y. and Yurdakoc, K. (2009). Preparation and characterization of chitosan/KSF biocomposite film. *Polymer Composites*, 30(8), pp.1035-1042. Doi: <https://doi.org/10.1002/pc.20651>.

Bazzo, G.C., Mostafa, D., França, M.T., Pezzini, B.R. and Stulzer, H.K. (2019). How tenofovir disoproxil fumarate can impact on solubility and dissolution rate of efavirenz?. *International Journal of Pharmaceutics*, 570, p.118597. Doi: <https://doi.org/10.1016/j.ijpharm.2019.118597>.

Benavides, S., Cortés, P., Parada, J. and Franco, W. (2016). Development of alginate microspheres containing thyme essential oil using ionic gelation. *Food Chemistry*, 204, pp.77-83. Doi: <https://doi.org/10.1016/j.foodchem.2016.02.104>.

Bertoni, S., Albertini, B. and Passerini, N. (2020). Different BCS class II drug-gelucire solid dispersions prepared by spray congealing: Evaluation of solid state properties and in vitro performances. *Pharmaceutics*, 12(6), p.548. Doi: <https://doi.org/10.3390/pharmaceutics12060548>.

Bowey, K. and Neufeld, R.J. (2010). Systemic and mucosal delivery of drugs within polymeric microparticles produced by spray drying. *BioDrugs*, 24, pp.359-377. Doi: <https://doi.org/10.2165/11539070-000000000-00000>.

Bulut, E. (2021). Development and optimization of Fe³⁺-crosslinked sodium alginate-methylcellulose semi-interpenetrating polymer network beads for controlled release of ibuprofen. *International Journal of Biological Macromolecules*, 168, pp.823-833. Doi: <https://doi.org/10.1016/j.ijbiomac.2020.11.147>.

Bruschi, M.L., Cardoso, M.L.C., Lucchesi, M.B. and Gremião, M.P.D. (2003). Gelatin microparticles containing propolis obtained by spray-drying technique: preparation and characterization. *International Journal of Pharmaceutics*, 264(1-2), pp.45-55. Doi: [https://doi.org/10.1016/S0378-5173\(03\)00386-7](https://doi.org/10.1016/S0378-5173(03)00386-7).

Casado, J.L. and Banon, S. (2015). Dutrebis (lamivudine and raltegravir) for use in combination with other antiretroviral products for the treatment of HIV-1 infection. *Expert Review of Clinical Pharmacology*, 8(6), pp.709-718. Doi: <https://doi.org/10.1586/17512433.2015.1090873>.

Chadha, R., Arora, P. and Bhandari, S. (2012). Polymorphic forms of lamivudine: characterization, estimation of transition temperature, and stability studies by thermodynamic and spectroscopic studies. *International Scholarly Research Notices*. Doi: 10.5402/2012/671027.

Chakraborty, S., Ganguly, S. and Desiraju, G.R. (2014). Synthon transferability probed with IR spectroscopy: cytosine salts as models for salts of lamivudine. *CrystEngComm*, 16(22), pp.4732-4741. Doi: <https://doi.org/10.1039/C3CE42156B>.

Chinta, D.D., Graves, R.A., Pamujula, S., Praetorius, N., Bostanian, L.A., Mandal, T.K. (2009). Spray-Dried Chitosan as a Direct Compression Tableting Excipient. *Drug Development and Industrial Pharmacy*, 35:1, 43-48, DOI: [10.1080/03639040802149053](https://doi.org/10.1080/03639040802149053).

Dahan, A., Beig, A., Lindley, D. and Miller, J.M. (2016). The solubility–permeability interplay and oral drug formulation design: Two heads are better than one. *Advanced drug delivery reviews*, 101, pp.99-107. Doi: <https://doi.org/10.1016/j.addr.2016.04.018>.

Derkach, S.R., Voron'ko, N.G., Sokolan, N.I., Kolotova, D.S. and Kuchina, Y.A. (2020). Interactions between gelatin and sodium alginate: UV and FTIR studies. *Journal of Dispersion Science and Technology*, 41(5), pp.690-698. Doi: <https://doi.org/10.1080/01932691.2019.1611437>.

Dezani, A.B., Pereira, T.M., Caffaro, A.M., Reis, J.M. and Serra, C.H.D.R. (2013). Equilibrium solubility versus intrinsic dissolution: characterization of lamivudine, stavudine and zidovudine for BCS classification. *Brazilian Journal of Pharmaceutical Sciences*, 49, pp.853-863. Doi: <https://doi.org/10.1590/S1984-82502013000400026>.

Djabourov, M. and Papon, P. (1983). Influence of thermal treatments on the structure and stability of gelatin gels. *Polymer*, 24(5), pp.537-542. Doi: [https://doi.org/10.1016/0032-3861\(83\)90101-5](https://doi.org/10.1016/0032-3861(83)90101-5).

Dolci, L.S., Liguori, A., Panzavolta, S., Miserocchi, A., Passerini, N., Gherardi, M., Colombo, V., Bigi, A. and Albertini, B. (2018). Non-equilibrium atmospheric pressure plasma as innovative method to crosslink and enhance mucoadhesion of econazole-loaded gelatin films for buccal drug delivery. *Colloids and Surfaces B: Biointerfaces*, 163, pp.73-82. Doi: <https://doi.org/10.1016/j.colsurfb.2017.12.030>.

Dolci, L.S., Albertini, B., Di Filippo, M.F., Bonvicini, F., Passerini, N. and Panzavolta, S. (2020). Development and in vitro evaluation of mucoadhesive gelatin films for the vaginal delivery of econazole. *International Journal of Pharmaceutics*, 591, p.119979. Doi: <https://doi.org/10.1016/j.ijpharm.2020.119979>.

Dubernet, C. (1995). Thermoanalysis of microspheres. *Thermochimica Acta*, 248, pp.259-269.

Eagling, V.A., Wiltshire, H., Whitcombe, I.W.A. and Back, D.J. (2002). CYP3A4-mediated hepatic metabolism of the HIV-1 protease inhibitor saquinavir in vitro. *Xenobiotica*, 32(1), pp.1-17. Doi: <https://doi.org/10.1080/00498250110085845>.

Ebnesajjad, S. (2011). Surface and material characterization techniques. In *Handbook of Adhesives and Surface Preparation* (pp. 31-48). William Andrew Publishing. Doi: <https://doi.org/10.1016/B978-1-4377-4461-3.10004-5>.

Emamverdian, P., Kia, E.M., Ghanbarzadeh, B. and Ghasempour, Z. (2020). Characterization and optimization of complex coacervation between soluble fraction of Persian gum and gelatin. *Colloids and Surfaces A: Physicochemical and Engineering Aspects*, 607, p.125436. Doi: <https://doi.org/10.1016/j.colsurfa.2020.125436>.

Erten Taysi, A., Cevher, E., Sessevmez, M., Olgac, V., Mert Taysi, N. and Atalay, B. (2019). The efficacy of sustained-release chitosan microspheres containing recombinant human parathyroid hormone on MRONJ. *Brazilian Oral Research*, 33. Doi: <https://doi.org/10.1590/1807-3107bor-2019.vol33.0086>.

Fini, A., Cavallari, C. and Ospitali, F. (2008). Raman and thermal analysis of indomethacin/PVP solid dispersion enteric microparticles. *European Journal of Pharmaceutics and Biopharmaceutics*, 70(1), pp.409-420. Doi: <https://doi.org/10.1016/j.ejpb.2008.03.016>.

Foxx, M. and Zilberman, M. (2015). Drug delivery from gelatin-based systems. *Expert Opinion on Drug Delivery*, 12(9), pp.1547-1563. Doi: <https://doi.org/10.1517/17425247.2015.1037272>.

Gada, S., Anandkumar, Y. and Setty, C.M. (2019). Preparation, evaluation and stability of lamivudine loaded alginate-tamarind mucilage microspheres. *International Journal of Applied Pharmaceutics*, pp.365-370.

Gomes, E.C.D.L., Mussel, W.N., Resende, J.M., Fialho, S.L., Barbosa, J. and Yoshida, M.I. (2013). Chemical interactions study of antiretroviral drugs efavirenz and lamivudine concerning the development of stable fixed-dose combination formulations for AIDS treatment. *Journal of the Brazilian Chemical Society*, 24, pp.573-579. Doi: <https://doi.org/10.5935/0103-5053.20130071>.

Gomes, E.C.D.L., Mussel, W.N., Resende, J.M., Fialho, S.L., Barbosa, J., Carignani, E., Geppi, M. and Yoshida, M.I. (2015). Characterization of tenofovir disoproxil fumarate and its behavior under heating. *Crystal Growth & Design*, 15(4), pp.1915-1922. Doi: <https://doi.org/10.1021/acs.cgd.5b00089>.

Harris, R., Yeung, R., áBrian Lamont, R., Lancaster, R., Lynn, S. and Staniforth, S. (1997). 'Polymorphism' in a novel anti-viral agent: Lamivudine. *Journal of the Chemical Society, Perkin Transactions 2*, (12), pp.2653-2660. Doi: <https://doi.org/10.1039/A704709F>.

Huang, H.J., Yuan, W.K. and Chen, X.D. (2006). Microencapsulation based on emulsification for producing pharmaceutical products: A literature review. *Developments in Chemical Engineering and Mineral Processing*, 14(3-4), pp.515-544.

Ibrahim, M., Mahmoud, A.A., Osman, O., Abd El-Aal, M. and Eid, M. (2011). Molecular spectroscopic analyses of gelatin. *Spectrochimica Acta Part A: Molecular and Biomolecular Spectroscopy*, 81(1), pp.724-729. Doi: <https://doi.org/10.1016/j.saa.2011.07.012>.

Jeevana, J.B. and Sunitha, G. (2009). Development and evaluation of gelatin microspheres of tramadol hydrochloride. *Journal of Young Pharmacists*, 1(1), p.24. Doi: 10.4103/0975-1483.51871.

Jelvehgari, M., Hassanzadeh, D., Kiafar, F., Loveym, B.D. and Amiri, S. (2011). Preparation and determination of drug-polymer interaction and in-vitro release of mefenamic acid microspheres made of celluloseacetate phthalate and/or ethylcellulose polymers. *Iranian Journal of Pharmaceutical Research: IJPR*, 10(3), p.457.

Jelvehgari, M., Barghi, L. and Barghi, F. (2014). Preparation of chlorpheniramine maleate-loaded alginate/chitosan particulate systems by the ionic gelation method for taste masking. *Jundishapur Journal of Natural Pharmaceutical Products*, 9(1), p.39. Doi: <https://doi.org/10.17795%2Fjjnpp-12530>.

Jozwiakowski, M.J., Nguyen, N.A.T., Sisco, J.M. and Spancake, C.W. (1996). Solubility behavior of lamivudine crystal forms in recrystallization solvents. *Journal of Pharmaceutical Sciences*, 85(2), pp.193-199. Doi: <https://doi.org/10.1021/js9501728>.

Kallinteri, P. and Antimisiaris, S.G. (2001). Solubility of drugs in the presence of gelatin: effect of drug lipophilicity and degree of ionization. *International Journal of Pharmaceutics*, 221(1-2), pp.219-226. Doi: [https://doi.org/10.1016/S0378-5173\(01\)00688-3](https://doi.org/10.1016/S0378-5173(01)00688-3).

Kaur, G., Grewal, J., Jyoti, K., Jain, U.K., Chandra, R. and Madan, J. (2018). Oral controlled and sustained drug delivery systems: Concepts, advances, preclinical, and clinical status. In *Drug targeting and stimuli sensitive drug delivery systems* (pp. 567-626). William Andrew Publishing.

Khan, S.A., Khan, S.B., Khan, L.U., Farooq, A., Akhtar, K. and Asiri, A.M. (2018). Fourier transform infrared spectroscopy: fundamentals and application in functional groups and nanomaterials characterization. In *Handbook of materials characterization* (pp. 317-344). Springer, Cham. Doi: https://doi.org/10.1007/978-3-319-92955-2_9

Kurozawa, L.E. and Hubinger, M.D. (2017). Hydrophilic food compounds encapsulation by ionic gelation. *Current Opinion in Food Science*, 15, pp.50-55. Doi: <https://doi.org/10.1016/j.cofs.2017.06.004>.

Lee, E.H., Smith, D.T., Fanwick, P.E. and Byrn, S.R. (2010). Characterization and anisotropic lattice expansion/contraction of polymorphs of tenofovir disoproxil fumarate. *Crystal Growth & Design*, 10(5), pp.2314-2322. Doi: <https://doi.org/10.1021/cg1000667>.

Leucuta, S.E. (1990). Controlled release of nifedipine from gelatin microspheres and microcapsules: in vitro kinetics and pharmacokinetics in man. *Journal of Microencapsulation*, 7(2), pp.209-217. Doi: <https://doi.org/10.3109/02652049009021834>.

Li, L., Li, Y., Wu, Z., Chen, J. and Chen, J. (2021). Spray-Dried Quercetin-Lactose Powders for Oral Tablets with Improved Dissolution Rates and Modified Material Properties. *Journal of Nanomaterials*, 2021, pp.1-6. Doi: <https://doi.org/10.1155/2021/2365353>.

Li, G., Wang, Y. and De Clercq, E. (2022). Approved HIV reverse transcriptase inhibitors in the past decade. *Acta Pharmaceutica Sinica B*, 12(4), pp.1567-1590. Doi: <https://doi.org/10.1016/j.apsb.2021.11.009>.

Masters K. (1976). Spray-drying: an introduction to principles, operational practice and applications. 2nd ed. New York: John Wiley & Sons.

Mirtič, J., Ilaš, J. and Kristl, J. (2018). Influence of different classes of crosslinkers on alginate polyelectrolyte nanoparticle formation, thermodynamics and characteristics. *Carbohydrate Polymers*, 181, pp.93-102. Doi: <https://doi.org/10.1016/j.carbpol.2017.10.040>.

Mohaweb, O.A.M., El-Ashmoony, M.M., Essam, T., Elgazayerly, O.N. (2014). Spray-dried lamivudine microspheres. *Journal of Pharmaceutical Research and Opinion*, 4, pp. 1-7.

Ngilirabanga, J.B., Aucamp, M. and Samsodien, H. (2021). Mechanochemical synthesis and characterization of Zidovudine-lamivudine solid dispersion (binary eutectic mixture). *Journal of Drug Delivery Science and Technology*, 64, p.102639. Doi: <https://doi.org/10.1016/j.jddst.2021.102639>.

Ogunjimi, A.T., Fiegel, J. and Brogden, N.K. (2020). Design and characterization of spray-dried chitosan-naltrexone microspheres for microneedle-assisted transdermal delivery. *Pharmaceutics*, 12(6), p.496. Doi: <https://doi.org/10.3390/pharmaceutics12060496>.

Østberg, T., Lund, E.M. and Graffner, C. (1994). Calcium alginate matrices for oral multiple unit administration: IV. Release characteristics in different media. *International Journal of Pharmaceutics*, 112(3), pp.241-248. Doi: [https://doi.org/10.1016/0378-5173\(94\)90360-3](https://doi.org/10.1016/0378-5173(94)90360-3).

Pandey, G., Yadav, S.K. and Mishra, B. (2016). Preparation and characterization of isoniazid and lamivudine co-loaded polymeric microspheres. *Artificial Cells, Nanomedicine, and Biotechnology*, 44(8), pp.1867-1877. Doi: <https://doi.org/10.3109/21691401.2015.1111229>.

Panizzon, G.P., Bueno, F.G., Ueda-Nakamura, T., Nakamura, C.V. and Dias Filho, B.P. (2014). Preparation of spray-dried soy isoflavone-loaded gelatin microspheres for enhancement of dissolution: formulation, characterization and in vitro evaluation. *Pharmaceutics*, 6(4), pp.599-615. Doi: <https://doi.org/10.3390/pharmaceutics6040599>.

Parveen, A. and Syed, I.A. (2014). Formulation and evaluation of mucoadhesive microspheres of Lamivudine. *International Journal of Pharmaceutical Sciences and Drug Research*, 6(2), pp.102-108.

Parize, A.L., de Souza, T.C.R., Brighente, I.M.C., de Fávère, V.T., Laranjeira, M.C.M., Spinelli, A., Longo, E. (2008). Microencapsulation of the natural urucum pigment with chitosan by spray drying in different solvent. *African Journal of Biotechnology*, 7(17), pp. 3107-3114.

Patil, S., Kadam, C. and Pokharkar, V. (2017). QbD based approach for optimization of Tenofovir disoproxil fumarate loaded liquid crystal precursor with improved permeability. *Journal of Advanced Research*, 8(6), pp.607-616. Doi: <https://doi.org/10.1016/j.jare.2017.07.005>.

Piao, M.G., Yang, C.W., Li, D.X., Kim, J.O., Jang, K.Y., Yoo, B.K., Kim, J.A., Woo, J.S., Lyoo, W.S., Han, S.S. and Lee, Y.B. (2008). Preparation and in vivo evaluation of piroxicam-loaded gelatin microcapsule by spray drying technique. *Biological and Pharmaceutical Bulletin*, 31(6), pp.1284-1287. Doi: <https://doi.org/10.1248/bpb.31.1284>.

Pongjanyakul, T. and Puttipipatkachorn, S. (2007). Xanthan–alginate composite gel beads: molecular interaction and in vitro characterization. *International Journal of Pharmaceutics*, 331(1), pp.61-71. Doi: <https://doi.org/10.1016/j.ijpharm.2006.09.011>.

PubChem. (2022). National Center for Biotechnology Information. PubChem Compound Summary for CID 5486830, Tenofovir Disoproxil Fumarate. [Online] Available at: <https://pubchem.ncbi.nlm.nih.gov/compound/Tenofovir-Disoproxil-Fumarate>. [Accessed on February 19, 2022].

PubChem. (2023). National Center for Biotechnology Information. PubChem Compound Summary for CID 24832091, Ethyl cellulose. <https://pubchem.ncbi.nlm.nih.gov/compound/Ethyl-cellulose>. Accessed July 25, 2023.

Qiao, C., Cao, X. and Wang, F. (2012). Swelling behavior study of physically crosslinked gelatin hydrogels. *Polymers and Polymer Composites*, 20(1-2), pp.53-58. Doi: <https://doi.org/10.1177/0967391112020001-210>.

Raha, A., Bhattacharjee, S., Mukherjee, P., Paul, M. and Bagchi, A. (2018). Design and characterization of ibuprofen loaded alginate microspheres prepared by ionic gelation method. *International Journal of Pharmaceutical Research and Health Sciences*, 6, pp.2713-2729.

Rajinikanth, P.S., Karunagaran, L.N., Balasubramaniam, J. and Mishra, B. (2008). Formulation and evaluation of clarithromycin microspheres for eradication of *Helicobacter pylori*. *Chemical and Pharmaceutical Bulletin*, 56(12), pp.1658-1664. Doi: <https://doi.org/10.1248/cpb.56.1658>.

Ramana, L.N., Anand, A.R., Sethuraman, S. and Krishnan, U.M. (2014). Targeting strategies for delivery of anti-HIV drugs. *Journal of Controlled Release*, 192, pp.271-283. Doi: <https://doi.org/10.1016/j.jconrel.2014.08.003>.

Rathbun, R.C., Lockhart, S.M. and Stephens, J.R. (2006). Current HIV treatment guidelines-an overview. *Current Pharmaceutical Design*, 12(9), pp.1045-1063. Doi: <https://doi.org/10.2174/138161206776055840>.

Sankaraiah, J., Sharma, N. and Naim, M.J. (2022). Formulation and development of fixed-dose combination of bi-layer tablets of efavirenz, lamivudine and tenofovir disoproxil fumarate tablets 600 MG/300 MG/300 MG. *International Journal of Applied Pharmaceutics*, 14(1), pp.185-197.

Santoro, M., Tatara, A.M. and Mikos, A.G. (2014). Gelatin carriers for drug and cell delivery in tissue engineering. *Journal of Controlled Release*, 190, pp.210-218. Doi: <https://doi.org/10.1016/j.jconrel.2014.04.014>.

Scrivens, G., Ticehurst, M. and Swanson, J.T. (2018). Strategies for improving the reliability of accelerated predictive stability (APS) studies. In *Accelerated Predictive Stability* (pp. 175-206). Academic Press. Doi: <https://doi.org/10.1016/B978-0-12-802786-8.00007-3>.

Shailender, J., Ravi, P.R., Saha, P., Dalvi, A. and Myneni, S., 2017. Tenofovir disoproxil fumarate loaded PLGA nanoparticles for enhanced oral absorption: Effect of experimental variables and in vitro, ex vivo and in vivo evaluation. *Colloids and Surfaces B: Biointerfaces*, 158, pp.610-619. Doi: <https://doi.org/10.1016/j.colsurfb.2017.07.037>.

Silva, J.P.A., Figueirêdo, C.B.M., de Medeiros Vieira, A.C.Q., de Lyra, M.A.M., Rolim, L.A., Rolim-Neto, P.J., de La Roca Soares, M.F., Albuquerque, M.M. and Soares-Sobrinho, J.L. (2017). Thermal characterization and kinetic study of the antiretroviral tenofovir disoproxil fumarate. *Journal of Thermal Analysis and Calorimetry*, 130(3), pp.1643-1651. Doi: <https://doi.org/10.1007/s10973-017-6477-z>.

Sipos, P., Szűcs, M., Szabó, A., Erős, I. and Szabó-Révész, P. (2008). An assessment of the interactions between diclofenac sodium and ammonio methacrylate copolymer using thermal analysis and Raman spectroscopy. *Journal of Pharmaceutical and Biomedical Analysis*, 46(2), pp.288-294. Doi: <https://doi.org/10.1016/j.jpba.2007.10.008>.

Shu, B., Yu, W., Zhao, Y. and Liu, X. (2006). Study on microencapsulation of lycopene by spray-drying. *Journal of Food Engineering*, 76(4), pp.664-669. Doi: <https://doi.org/10.1016/j.jfoodeng.2005.05.062>.

Singh, G.P., Srivastava, D., Saini, M.B. and Upadhyay, P.R., Lupin Limited. (2007). *A novel crystalline form of lamivudine*.

Singh, A.V. and Nath, L.K. (2012). Evaluation of compatibility of tablet excipients and novel synthesized polymer with lamivudine. *Journal of Thermal Analysis and Calorimetry*, 108(1), pp.263-267. Doi: <https://doi.org/10.1007/s10973-011-1650-2>.

Strauch, S., Jantratid, E., Dressman, J.B., Junginger, H.E., Kopp, S., Midha, K.K., Shah, V.P., Stavchansky, S. and Barends, D.M. (2011). COMMENTARY: biowaiver monographs for immediate release solid oral dosage forms: lamivudine. *Journal of Pharmaceutical Sciences*, 100(6), pp.2054-2063.

Tenghe, L.A., (2018). Formulation and evaluation of polymeric micelles for improved oral delivery of tenofovir disoproxil fumarate and zidovudine using poly-lactic-co-glycolic acid nanoparticles.

Tran, T.H., Ramasamy, T., Poudel, B.K., Marasini, N., Moon, B.K., Cho, H.J., Choi, H.G., Yong, C.S. and Kim, J.O. (2014). Preparation and characterization of spray-dried gelatin microspheres encapsulating ganciclovir. *Macromolecular Research*, 22, pp.124-130. Doi: <http://dx.doi.org/10.1007/s13233-014-2018-9>.

Tshweu, L., Katata, L., Kalombo, L. and Swai, H. (2013). Nanoencapsulation of water-soluble drug, lamivudine, using a double emulsion spray-drying technique for improving HIV treatment. *Journal of Nanoparticle Research*, 15, pp.1-11.

Vandelli, M.A., Rivasi, F., Guerra, P., Forni, F. and Arletti, R. (2001). Gelatin microspheres crosslinked with D, L-glyceraldehyde as a potential drug delivery system: preparation,

characterisation, in vitro and in vivo studies. *International Journal of Pharmaceutics*, 215(1-2), pp.175-184. Doi: [https://doi.org/10.1016/S0378-5173\(00\)00681-5](https://doi.org/10.1016/S0378-5173(00)00681-5).

Van Gelder, J., Deferme, S., Naesens, L., De Clercq, E., Van den Mooter, G., Kinget, R. and Augustijns, P. (2002). Intestinal absorption enhancement of the ester prodrug tenofovir disoproxil fumarate through modulation of the biochemical barrier by defined ester mixtures. *Drug Metabolism and Disposition*, 30(8), pp.924-930. Doi: <https://doi.org/10.1124/dmd.30.8.924>.

Verhoeven, E., Vervaeke, C., Remon, J.P. (2006). Xanthan gum to tailor drug release of sustained-release ethylcellulose mini-matrices prepared via hot-melt extrusion: in vitro and in vivo evaluation. *European Journal of Pharmaceutics and Biopharmaceutics*, 63, pp.320-330.

Vilos, C. and Velasquez, L.A. (2012). Therapeutic strategies based on polymeric microparticles. *Journal of Biomedicine and Biotechnology*, 2012. Doi: 10.1155/2012/672760.

Wang, F.J. and Wang, C.H. (2002). Effects of fabrication conditions on the characteristics of etanidazole spray-dried microspheres. *Journal of Microencapsulation*, 19(4), pp.495-510. Doi: <https://doi.org/10.1080/02652040210140483>.

Wang, W., Wang, Z., Liu, Y., Li, N., Wang, W. and Gao, J. (2012). Preparation of reduced graphene oxide/gelatin composite films with reinforced mechanical strength. *Materials Research Bulletin*, 47(9), pp.2245-2251. Doi: <https://doi.org/10.1016/j.materresbull.2012.05.060>.

Wassner, C., Bradley, N. and Lee, Y. (2020). A review and clinical understanding of tenofovir: tenofovir disoproxil fumarate versus tenofovir alafenamide. *Journal of the International Association of Providers of AIDS Care*, 19, p.2325958220919231. Doi: <https://doi.org/10.1177/2325958220919231>.

Xiao, C., Liu, H., Lu, Y. and Zhang, L. (2001). Blend films from sodium alginate and gelatin solutions. Doi: <https://doi.org/10.1081/MA-100103352>.

Yin, R., Huang, Y., Huang, C., Tong, Y. and Tian, N. (2009). Preparation and characterization of novel gelatin/cerium (III) fiber with antibacterial activity. *Materials Letters*, 63(15), pp.1335-1337. Doi: <https://doi.org/10.1016/j.matlet.2009.03.014>.

Yousaf, A.M., Kim, D.W., Kim, J.K., Kim, J.O., Yong, C.S. and Choi, H.G. (2015). Novel fenofibrate-loaded gelatin microcapsules with enhanced solubility and excellent flowability:

preparation and physicochemical characterization. *Powder Technology*, 275, pp.257-262. Doi: <https://doi.org/10.1016/j.powtec.2015.02.004>.

Yüksel, N., Tinçer, T. and Baykara, T. (1996). Interaction between nicardipine hydrochloride and polymeric microspheres for a controlled release system. *International Journal of Pharmaceutics*, 140(2), pp.145-154. Doi: [https://doi.org/10.1016/0378-5173\(96\)04560-7](https://doi.org/10.1016/0378-5173(96)04560-7).

Zamora, F.J., Dowers, E., Yasin, F. and Ogbuagu, O. (2019). Dolutegravir and lamivudine combination for the treatment of HIV-1 infection. *HIV/AIDS-Research and Palliative Care*, pp.255-263. Doi: <https://doi.org/10.2147%2FHIV.S216067>.



Chapter Five

Concluding remarks

5.1 General conclusion

In Chapter 1 of this thesis, it was extensively discussed how HIV infection poses several burdens, including comorbidities, economic, social, and therapeutic limitations (Abah, 2020; Bhatti *et al.*, 2016; Campbell *et al.*, 2011; Devi & Pai, 2006; Kwong, 2021; Waziri *et al.*, 2016). Since poverty and a lack of readily available, affordable medicine contribute to the continued prevalence of HIV/AIDS in developing nations, formulation scientists must create ARVs that are affordable, adaptable, discrete, and effective, as well as those that can increase therapeutic adherence and lessen pill burden. However, the World Health Organisation has recommended an FDC of ARVs (TDF, 3TC, and DTG) that is both affordable and effective, especially in low-income countries (Bhatti *et al.*, 2016; Dellar & Karim, 2015; Lee *et al.*, 2014; WHO, 2021). Currently, the FDC for these three drugs and several 3TC-based FDCs on the market is an oral immediate-release formulation; they are associated with several advantages, but they will still be subject to some of the shortcomings of conventional ARV formulations administered *via* the oral route. All of these issues prompted this research.

Developing an inexpensive modified drug delivery system (microsphere-based formulation) for these drugs as a single FDC is critical to improving patient treatment efficacy. The two ARVs, 3TC and TDF, which are among the cornerstones of several HIV treatment regimens, were investigated in this study in order to develop 3TC- and TDF-loaded P-MPs with varying drug release profiles using various readily accessible natural polymers (CH, GEL, XG, and SA) with simple and inexpensive preparation methods (ionic gelation and spray drying) to achieve a cost-effective solution for patient-centered HIV treatment. Aside from the availability and cost-effectiveness of CH, GEL, XG, and SA as wall-forming materials, this study focused on these four natural polymers as wall-forming materials due to their known biodegradability, non-toxicity, biocompatibility, and ability to modify drug release from their matrix system and also improve drug bioavailability (Ngwuluka *et al.*, 2014; Simionescu, 2015; Shrivastava, 2018).

The physicochemical properties of the drug(s) and drug-excipient(s) compatibility were studied before the preparation of 3TC- and TDF-loaded P-MPs using different analytical techniques such

as HSM, DSC, TGA, FTIR, PXRD, and HPLC to determine the physical and chemical properties of drugs before incorporating them into a drug delivery system and the useability of natural polymers in the formulation of 3TC- or TDF-loaded microspheres. The drug release profile of a formulation consisting of natural polymers is influenced by the physicochemical characteristics of both the drug and the polymer(s). The APIs' thermal and spectroscopic analyses confirmed that they were both crystalline and 3TC-Form II and TDF-Form I were used in this study. The drug-excipient (s) compatibility studies revealed no interaction between 3TC- or TDF- polymer(s) in their physical combinations or seven days (7) isothermal stress testing (**Appendix II**). Because the HPLC method found in the literature was complex (Omoteso *et al.*, 2022), an HPLC method for the simultaneous detection of 3TC, TDF, and DTG was developed and published as a research article during this study (**Appendix I**).

The ionic gelation method was used to investigate the use of CH, GEL, XG, and SA to modify the release of highly soluble ARVs. The dissolution testing results of the first batch (F1-F10) of 3TC-loaded microspheres revealed that formulations made solely of SA-CH- or SA-XG-calcium chloride polyelectrolyte complexation without any form of polymer coating could not demonstrate significantly modified drug release. The cumulative amount of drug released in 2 hours from SA-XG-calcium chloride microspheres revealed that the higher the XG concentration, the higher the %EE and drug loading, resulting in an unexpected increase in drug release. As a result of the formation of a weak polymeric structure with SA, high XG ratio microspheres prepared by ionic gelation will enhance the fast release rather than the sustained release of 3TC at pH 1.2. Due to the rigid polymeric structure formed with SA, microspheres prepared from high concentrations of GEL in both GEL-SA- and GEL-SA (plus 1% CH)-calcium chloride polyelectrolyte complexation can significantly retain 3TC in their matrix. The yield, %EE, and release profiles of the second batch (F1b-F6b) of 3TC-loaded microspheres prepared at higher SA and cross-linker concentrations confirmed that polymer mixtures can result in successful modified drug release. Furthermore, a lower GEL ratio can increase %EE, drug loading, and production yield but enhances drug release. The best-modified drug release system 3TC-microspheres (F4) at pH 1.2 prepared by ionic gelation method was from SA, GEL (high concentration-10% w/v), CH (1% w/v) and calcium chloride polyelectrolyte complexation with only 49.74% of 3TC released in 2 hours. Therefore the physicochemical properties and concentration of natural polymer are essential factors to consider when preparing a modified drug delivery system using the ionic gelation

method. Some of the measures that can be taken to improve the polymeric structure of the mixtures of the polymer include (a) the use of an internal gelation method rather than the typical external-extrusion/ syringe dropping ionic gelation method (Belščak-Cvitanović *et al.*, 2016; Silva *et al.*, 2006; Uyen *et al.*, 2020), and (b) the cross-linking of sodium alginate or calcium-alginate beads with other cross-linkers such as polyphosphate, glutaraldehyde, or Fe³⁺ (Almeida & Almeida, 2004; Bulut, 2021; Choudhary *et al.*, 2018; Wang *et al.*, 2016). Furthermore, using an automated syringe instead of the manual syringe needle that can easily extrude the viscous polymer solution into the cross-linker solution will improve the production yield and microsphere quality. Future studies should be done to investigate if the coating of the 3TC-loaded microsphere will build a sufficient diffusion barrier layer that prevents the migration of hydrophilic 3TC to the surrounding medium when the formulation is hydrated in the acid medium (pH 1.2-stimulated stomach condition) and can ensure highly sustained or extended-release of 3TC from natural polymeric matrix system.

Spray drying of 3TC with natural polymers (GEL and CHI-GEL) was successful in the production of 3TC-loaded microspheres using optimised process parameters, as evidenced by the high production yield (64.50%), drug loading ($53.10\% \pm 0.213.05$), low moisture content (3.05%), and excellent %EE (102.74 ± 1.67), particularly for formulation F2SD. The dissolution profiles of 3TC-loaded spray-dried microsphere formulations revealed that the modified release of 3TC from the GEL/ CHI-GEL polymeric matrix system is dependent on %EE, which can be related to the strength of the drug-polymer (s) interaction and polymer concentration. Due to the superior %EE of this formulation, a two-fold increase in polymer-to-drug ratio resulted in both immediate and significantly modified release of 3TC in the stimulated acidic condition. Notably, a four-fold polymer-to-drug ratio formulated microspheres failed to sustain 3TC release from the polymeric matrix due to low %EE ($17.70\% \pm 0.55$). The poor swelling behaviour of the spray-dried GEL microspheres revealed that 3TC was released from these formulations based on the polymeric matrix system's solubility rather than swelling in the aqueous medium. Because of the strong drug-polymer and polymer-polymer interactions, the polymer mixtures of CH-GEL resulted in the production of 3TC-loaded spray-dried microspheres (F1cSD) with significantly reduced initial burst release and steady and sustained release of 3TC for 7 hours (in pH 1.2). DSC, TGA, FTIR, and PXRD results revealed that natural polymers (GEL and CH-GEL) were successful in microencapsulating 3TC, that the drug's crystalline solid state was changed to amorphous, and that

drug-polymer(s) interactions were strong in spray-dried formulations. Because of the known sensitivity of these wall-forming materials at lower pH, additional studies such as scanning electron microscopy, particle size analysis to determine the surface morphology and particle size of the microspheres, as well as dissolution testing in pH 4.5, 6.8, and possibly 7.4 should be investigated to determine more drug release profiles. F2SD and F1cSD formulation optimisation is required by either coating with hydrophobic polymer or stearic acid to ensure extended drug delivery of more than 24 hours or cross-linking of the natural polymer to achieve a delay or predetermined modified release of 3TC.

Spray drying TDF with GEL resulted in the formation of TDF-loaded microspheres, which enhanced TDF release rather than the desired modified release in pH 1.2. Though the release of TDF from F5SD and F6SD into the stimulated acidic environment was modified to some extent, not significantly, the two formulations can be optimised with the incorporation of other polymers or coating to prevent the easy leaching out of TDF from the carrier. These two formulation upgrades require an impenetrable diffusion barrier layer that is not ionised or sensitive to acidic environments. Compared to the TDF raw material, the formulation F7SD demonstrated a promising dissolution profile due to the superior release rate of TDF in pH 1.2 ($109 \pm 1.87\%$ of TDF released in 10 minutes). This TDF-loaded spray-dried microsphere could help improve TDF's known low oral bioavailability. This formulation's pharmacokinetic parameters and permeability should be investigated to determine whether TDF's oral bioavailability and plasma stability have improved. Given that improved TDF bioavailability in F7SD could lead to dose reductions for HIV, and with or without renal impairment, this medication's long-term toxicity could be reduced. According to DSC, FTIR, and DSC results, the physical state of TDF was changed from crystalline to amorphous, the drug-polymer interaction was weak, which reduced the modified release of TDF.

The drug-loaded microspheres created in this study will allow for further formulation into tablets, capsules, or powders. Because 3TC still forms part of the first-line HIV treatment regimens and is currently incorporated into the FDCs consisting of 3TC + TDF or 3TC + TDF + dolutegravir sodium (DTG), 3TC + raltegravir, dolutegravir + 3TC, abacavir + dolutegravir + 3TC or 3TC + zidovudine (Anon, 2023; Casado & Banon, 2015; Zamora *et al.*, 2019), a modified drug delivery system is necessary due to its known short intracellular and blood circulation half-lives. Whereas,

since TDF is a common once-daily backbone for use with other classes of ARVs due to its long intracellular and blood circulation half-lives, a modified drug delivery system is not necessary or cost-effective.

In conclusion, spraying drying is the superior manufacturing method to ionic gelation in terms of simplicity, scalability, and cost-effectiveness. However, it is critical to remember that spray-dried natural polymer (s)-based drug-loaded microspheres can either boost or retard the dissolution rate of drug of the same BCS Class contained in their matrix, depending on drug and polymer properties, solid-state of the drug in the polymeric matrix, drug-polymer interaction, polymer-polymer interaction, and polymer concentration.



5.2 References

- Abah, R.C. (2020). Achieving HIV targets by 2030: the possibility of using debt relief funds for sustainable HIV treatment in sub-Saharan Africa. *Journal of Public Health Policy*, 41(4), pp.421-435. Doi: <https://doi.org/10.1057/s41271-020-00238-x>.
- Almeida, P.F. and Almeida, A.J. (2004). Cross-linked alginate–gelatine beads: a new matrix for controlled release of pindolol. *Journal of Controlled Release*, 97(3), pp.431-439. Doi: <https://doi.org/10.1016/j.jconrel.2004.03.015>.
- Anon. (2023). General Considerations When Using Fixed-Dose Combination Products. chrome-extension://efaidnbmnnnibpcajpcglclefindmkaj/https://clinicalinfo.hiv.gov/sites/default/files/guidelines/documents/pediatric-arv/drug-information-fixed-dose-combinations-tablets-minimum-body-weights-considerations-use-children-adolescents-pediatric-arv.pdf. Date of access: 01 August 2023.
- Belščak-Cvitanović, A., Bušić, A., Barišić, L., Vrsaljko, D., Karlović, S., Špoljarić, I., Vojvodić, A., Mršić, G. and Komes, D. (2016). Emulsion templated microencapsulation of dandelion (*Taraxacum officinale* L.) polyphenols and β -carotene by ionotropic gelation of alginate and pectin. *Food Hydrocolloids*, 57, pp.139-152. Doi: <https://doi.org/10.1016/j.foodhyd.2016.01.020>
- Bhatti, A.B., Usman, M. and Kandi, V. (2016). Current scenario of HIV/AIDS, treatment options, and major challenges with compliance to antiretroviral therapy. *Cureus*, 8(3). Doi: 10.7759/cureus.515.
- Bulut, E. (2021). Development and optimization of Fe³⁺-crosslinked sodium alginate-methylcellulose semi-interpenetrating polymer network beads for controlled release of ibuprofen. *International Journal of Biological Macromolecules*, 168, pp.823-833. Doi: <https://doi.org/10.1016/j.ijbiomac.2020.11.147>.
- Campbell, C., Skovdal, M., Madanhire, C., Mugurungi, O., Gregson, S. and Nyamukapa, C. (2011). “We, the AIDS people...”: how antiretroviral therapy enables Zimbabweans living with HIV/AIDS to cope with stigma. *American Journal of Public Health*, 101(6), pp.1004-1010.

Casado, J.L. and Banon, S. (2015). Dutrebis (lamivudine and raltegravir) for use in combination with other antiretroviral products for the treatment of HIV-1 infection. *Expert Review of Clinical Pharmacology*, 8(6), pp.709-718. Doi: <https://doi.org/10.1586/17512433.2015.1090873>.

Choudhary, S., Reck, J.M., Carr, A.J. and Bhatia, S.R. (2018). Hydrophobically modified alginate for extended release of pharmaceuticals. *Polymers for Advanced Technologies*, 29(1), pp.198-204. Doi: <https://doi.org/10.1002/pat.4103>.

Dellar, R. and Karim, Q.A. (2015). HIV/AIDS, food insecurity, and undernourishment: amplifying cycles of risk in vulnerable populations. In *Handbook of public health in natural disasters: Nutrition, food, remediation and preparation* (pp. 273-280). Wageningen Academic Publishers. Doi: <https://doi.org/10.3920/978-90-8686-806-3>.

Devi, K.V. and Pai, R.S. (2006). Antiretrovirals: Need for an effective drug delivery. *Indian Journal of Pharmaceutical Sciences*, 68(1), p.1. Dio: 10.4103/0250-474X.22955.

Kwong, J. (2021). HIV and Ageing: Considerations for Older Adults Living with HIV. In *Providing HIV Care: Lessons from the Field for Nurses and Healthcare Practitioners* (pp. 151-165). Springer, Cham. [Online] Available at: https://link.springer.com/chapter/10.1007/978-3-030-71295-2_9 [Accessed on August 14, 2022].

Lee, F.J., Amin, J. and Carr, A. (2014). Efficacy of initial antiretroviral therapy for HIV-1 infection in adults: a systematic review and meta-analysis of 114 studies with up to 144 weeks follow-up. *PloS One*, 9(5), p.e97482. Doi: <https://doi.org/10.1371/journal.pone.0097482>.

Ngwuluka, N.C., Ochekepe, N.A. and Aruoma, O.I. (2014). Naturapolyceutics: the science of utilizing natural polymers for drug delivery. *Polymers*. 6(5), pp.1312-1332. Doi:10.3390/polym6051312.

Omoteso, O.A., Milne, M. and Aucamp, M. (2022). The Validation of a Simple, Robust, Stability-Indicating RP-HPLC Method for the Simultaneous Detection of Lamivudine, Tenofovir Disoproxil Fumarate, and Dolutegravir Sodium in Bulk Material and Pharmaceutical Formulations. *International Journal of Analytical Chemistry*, 2022. Doi: <https://doi.org/10.1155/2022/3510277>.

Shrivastava, A., 2018. Introduction to plastics engineering, first ed. William, A. Publishing. <https://doi.org/10.1016/B978-0-323-39500-7.00001-0>.

Silva, C.M., Ribeiro, A.J., Figueiredo, I.V., Gonçalves, A.R. and Veiga, F. (2006). Alginate microspheres prepared by internal gelation: Development and effect on insulin stability. *International Journal of Pharmaceutics*, 311(1-2), pp.1-10. Doi: <https://doi.org/10.1016/j.ijpharm.2005.10.050>.

Simionescu B.C. and Ivanov, D. (2015). Natural and synthetic polymers for designing composite materials, in: Antoniac, I. (Eds.), Handbook of Bioceramics and Biocomposites. Springer pp.1-54. <https://doi.org/10.3109/10837459809028495>.

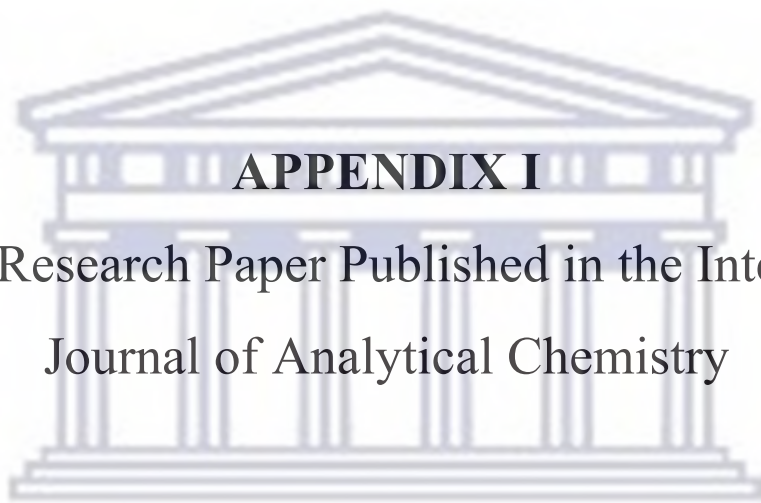
Uyen, N.T.T., Hamid, Z.A.A., Tram, N.X.T. and Ahmad, N. (2020). Fabrication of alginate microspheres for drug delivery: A review. *International Journal of Biological Macromolecules*, 153, pp.1035-1046.

Wang, Q.S., Wang, G.F., Zhou, J., Gao, L.N. and Cui, Y.L. (2016). Colon targeted oral drug delivery system based on alginate-chitosan microspheres loaded with icariin in the treatment of ulcerative colitis. *International Journal of Pharmaceutics*, 515(1-2), pp.176-185. Doi: <https://doi.org/10.1016/j.ijpharm.2016.10.002>.

Waziri, S.I., Nor, N.M., Abdullah, N.M.R. and Adamu, P. (2016). Effect of the prevalence of HIV/AIDS and the life expectancy rate on economic growth in SSA countries: Difference GMM approach. *Global Journal of Health Science*, 8(4), p.212. Doi: <https://doi.org/10.5539%2Fgjhs.v8n4p212>.

World Health Organization (2021). Consolidated guidelines on the use of antiretroviral drugs for treating and preventing HIV infection: recommendations for a public health approach. [Online] Available at: <https://www.who.int/publications/i/item/9789240031593>. [Accessed on 19 July 2022].

Zamora, F.J., Dowers, E., Yasin, F. and Ogbuagu, O. (2019). Dolutegravir and lamivudine combination for the treatment of HIV-1 infection. *HIV/AIDS-Research and Palliative Care*, pp.255-263. Doi: <https://doi.org/10.2147%2FHIV.S216067>.



APPENDIX I

Original Research Paper Published in the International
Journal of Analytical Chemistry

UNIVERSITY *of the*
WESTERN CAPE

Research Article

The Validation of a Simple, Robust, Stability-Indicating RP-HPLC Method for the Simultaneous Detection of Lamivudine, Tenofovir Disoproxil Fumarate, and Dolutegravir Sodium in Bulk Material and Pharmaceutical Formulations

Omobolanle Ayoyinka Omoteso ¹, Marnus Milne ², and Marique Aucamp ¹

¹School of Pharmacy, University of the Western Cape, Bellville, Cape Town, 7530, South Africa

²School of Pharmacy, Sefako Makgatho Health Sciences University, Ga-Rankuwa, Pretoria 0208, South Africa

Correspondence should be addressed to Marique Aucamp; maucamp@uwc.ac.za

Received 20 September 2021; Revised 30 December 2021; Accepted 8 January 2022; Published 4 February 2022

Academic Editor: Mohamed Abdel-Rehim

Copyright © 2022 Omobolanle Ayoyinka Omoteso et al. This is an open access article distributed under the Creative Commons Attribution License, which permits unrestricted use, distribution, and reproduction in any medium, provided the original work is properly cited.

An effective analytical method is requisite to ensure the accurate identification and quantification of drug(s), either in bulk material or in complex matrices, which form part of finished pharmaceutical products. For the purpose of a pharmaceutical formulation study, it became necessary to have a simple, yet robust and reproducible reversed-phase HPLC method for the simultaneous detection and quantification of lamivudine (3TC), tenofovir disoproxil fumarate (TDF), and dolutegravir sodium (DTG) in bulk form, complex polymeric matrices, and during drug release studies. A suitable method was developed using a Kinetex[®] C₁₈, 250 × 4.6 mm column as stationary phase and a mobile phase consisting of 50 : 50 v/v methanol and water with 1 mL orthophosphoric acid, with a flow rate of 1.0 mL/min and column temperature maintained at 35°C. A detection wavelength of 260 nm and an injection volume of 10 µL were used. The method was validated according to the International Conference on Harmonization (ICH) guideline Q2 (R₁), and the parameters of linearity and range, accuracy, precision, specificity, limit of detection (LOD), limit of quantification (LOQ), robustness, and stability were all determined. Acceptable correlation coefficients for linearity (R₂) of >0.998 for each of the three drugs were obtained. The LOD was quantified to be 56.31 µg/mL, 40.27 µg/mL, and 7.00 µg/mL for 3TC, TDF, and DTG, respectively, and the LOQ was quantified as 187.69 µg/mL, 134.22 µg/mL, and 22.5 µg/mL for 3TC, TDF, and DTG, respectively. In relation to all the determined validation parameters, this method proves to be suitable for the accurate identification and quantification of the three ARVs, either alone or in combination, as well as when incorporated into polymeric matrices. Furthermore, the method proves to be suitable to detect degradation of the compounds.

1. Introduction

Lamivudine (3TC) is a nucleoside analog reverse transcriptase inhibitor (NRTI), used for the treatment of HIV-1, HIV-2, and hepatitis B infection (Figure 1(a)) [1, 2]. Tenofovir disoproxil fumarate (TDF) was the first nucleotide analog reverse transcriptase inhibitor (NtRTI) (Figure 1(b)), approved for the treatment of HIV infection [3]. A combination of TDF with other NRTIs and different classes of antiretroviral drugs (ARVs) causes synergistic effects showing activity against all subtypes of HIV-1 and certain strains of HIV-2 [4].

Dolutegravir (DTG) is a unique second-generation integrase strand transfer inhibitor (INSTI) (Figure 1(c)), developed as a result of the limitations of the first-generation INSTIs, which includes potency, resistance by the virus, dosing frequency, dosing weight, and drug genetic barrier [5–7]. It is effective against numerous HIV-1 and HIV-2 clinical isolates [8]. The 2016 WHO Consolidated Guidelines recommended the combination of the mentioned three ARVs as the first-line regimen mainstay of HIV treatment. Currently, the combination of 3TC, TDF, and DTG is formulated as a fixed-dose combination (FDC) oral tablet.

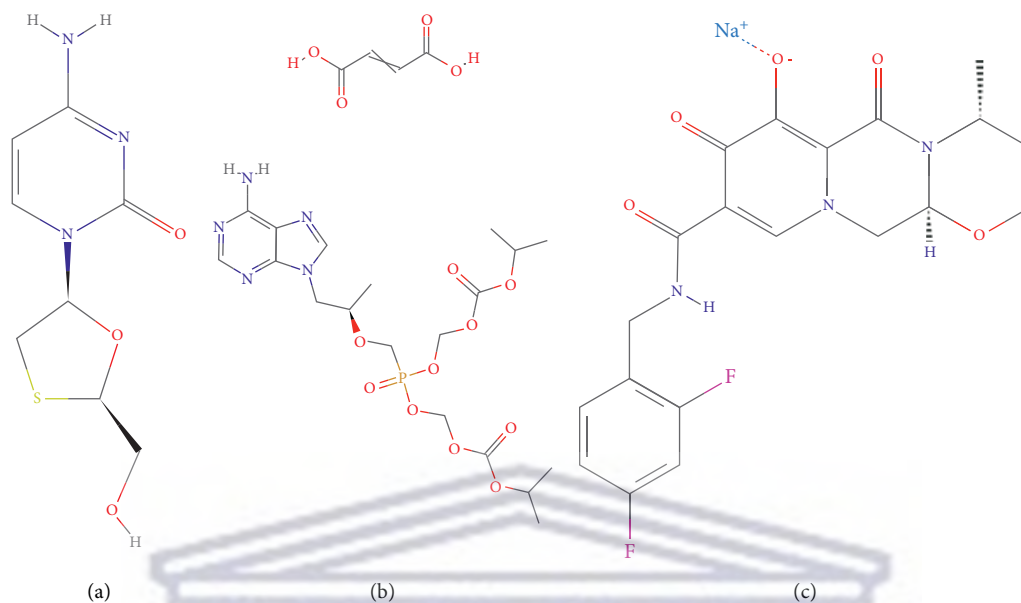


FIGURE 1: Chemical structure of (a) 3TC, (b) TDF, and (c) DTG [10–12].

Although a few FDC formulations, containing these three compounds, have already been developed and marketed, the combination of these ARVs into novel and more patient-orientated dosage forms is steadily emerging. This is mostly attributed to the biopharmaceutical classification system (BCS) classes to which these ARVs belong and the ever-present challenge of reducing the “pill burden” experienced by HIV-positive patients. A previous study has reported the successful development and validation of an RP-HPLC method for the simultaneous detection and quantification of the three mentioned ARVs [9]. Reviewing of this mentioned study revealed chromatographic conditions, which utilised a fairly complex mobile phase gradient, consisting of two mobile phases, as well as the utilisation of two different diluents. However, for the purpose of a pharmaceutical preformulation study, which involved the combination and processing of the three ARVs into complex polymeric matrices, the need was identified to be able to identify and quantify all three compounds simultaneously using a much simpler and more cost-effective method. The rationale for developing this RP-HPLC method was to allow the detection and quantification of 3TC, TDF, and DTG simultaneously across a wide concentration range. Furthermore, the RP-HPLC method should be sufficiently robust and sensitive to detect low drug concentrations in typical drug release media. A thorough literature review did not reveal the availability and reporting of an RP-HPLC method for the simultaneous detection and quantification of 3TC, TDF, and DTG in typical pharmaceutical dissolution media.

In this presented work, the authors describe a simple, yet robust and reproducible RP-HPLC method for the simultaneous detection and quantification of 3TC, TDF, and DTG. This method was validated by proving acceptable limits in terms of concentration range, linearity, precision, accuracy, and specificity of the method towards the accurate

identification and quantification of the three ARVs when incorporated into polymeric matrices and typical drug release media as well as the ability to detect unknown degradation products or identify the degradation of the compounds.

2. Materials and Methods

2.1. Materials and Reagents. Lamivudine (3TC) and tenofovir disoproxil fumarate (TDF) reference standards with certified purities of 99.7% and 99.8%, respectively, were purchased from Industrial Analytical (Johannesburg, South Africa). 3TC bulk raw material was purchased from DB Fine Chemicals (Pty) Ltd (Johannesburg, South Africa), whilst dolutegravir sodium (DTG) certified reference standard (purity of 99.4%), and DTG and TDF bulk raw material was in-kind donations from Cipla South Africa. Chromatography grade methanol (>99.9%) was purchased from Kimix Chemical (Cape Town, South Africa). Ultrapure HPLC water with resistivity of $18.2 \text{ M}\Omega \cdot \text{cm}^{-1}$ was produced by a Lasec® Purite Laboratory Water System (Johannesburg, South Africa). Analytical grade orthophosphoric acid was purchased from Sigma-Aldrich Chemie GmbH (Darmstadt, Germany).

Pharmaceutical grade gelatin and medium molecular weight chitosan were purchased from Sigma-Aldrich Chemie GmbH (Darmstadt, Germany), and pharmaceutical grade xanthan gum was purchased from Savannah Fine Chemicals (Pty) Ltd (Milnerton, South Africa). Distilled water was obtained from a Milli-Q Elix® Essential 3 Water Purification System (Merck, Johannesburg, South Africa). For forced degradation studies, hydrochloric acid (HCl) (32%), sodium hydroxide (NaOH), and 3% v/v hydrogen peroxide (H_2O_2), all of the analytical grades were purchased from Sigma-Aldrich (Darmstadt, Germany). All reference and sample

solutions were prepared using A-grade volumetric glassware and were filtered into HPLC vials using PVDF 0.22 μm syringe filters.

2.2. HPLC Instrumentation and Chromatographic Conditions. The method development was performed using a KNAUER AZURA DAD (Berlin, Germany) HPLC system equipped with an autosampler, quaternary pump, photodiode array detector, and column thermostat. The ClarityChrom software package was used for data processing purposes. A column with end-capped octadecylsilyl silica gel, Kinetex[®] C₁₈, 250 \times 4.6 mm (Phenomenex[®], Torrance, USA), was used as stationary phase. The chromatographic system was set to run isocratically with a mobile phase consisting of 50 : 50 v/v methanol and water with 1 mL orthophosphoric acid. The flow rate was set at 1.0 ml/min, and an injection volume of 10 μL and detection wavelength of 260 nm were used.

2.3. Preparation of Standard Stock and Sample Solutions. A standard stock solution consisting of all three drugs containing 1200.0 $\mu\text{g/ml}$ 3TC, TDF, and 200.0 $\mu\text{g/ml}$ DTG using a 50 : 50 v/v methanol and water mixture was prepared. Several dilutions were made from this stock solution, using the same diluent, and used as working standard solutions for the validation of the analytical method. Sample solutions containing all three ARVs alone and combined with the natural polymers such as gelatin, xanthan gum, and chitosan were prepared in the same concentration range as that of the standard stock solution. These solutions were used in the determination of the specificity and recovery of the analytical method in the instances where the ARVs were incorporated into polymeric matrices.

2.4. Method Validation. The method was validated according to the International Conference on Harmonization (ICH) of Technical Requirements for Registration of Pharmaceuticals for Human Use guideline Q2 (R1) and the parameters of linearity and range, accuracy, specificity, limit of detection (LOD), limit of quantification (LOQ), robustness, and stability [13, 14].

2.4.1. Linearity and Range. Linearity and range were measured through the analysis of five serial dilutions of the stock solution ranging between 150.0 and 1200.0 $\mu\text{g/mL}$ for 3TC and TDF and 1.5–210 $\mu\text{g/ml}$ for DTG. For each ARV, the relevant calibration curve was constructed followed by the calculation of the slope, y -intercept, and associated correlation coefficient (R^2).

2.4.2. Accuracy. The accuracy of this analytical method was determined by preparing a standard solution of a mixture of the three ARVs having a concentration of 600 $\mu\text{g/ml}$ 3TC and TDF and 100 $\mu\text{g/ml}$ DTG. From this solution, three concentration levels of 50%, 100%, and 150% were analysed followed by the quantification of the recovered ARV concentration.

2.4.3. Precision. The precision of this method was determined on two levels, which included repeatability (intra-assay precision) and intermediate precision (ruggedness). Repeatability data for each compound were obtained by analysing six replicates of solutions containing 600 $\mu\text{g/mL}$ 3TC, TDF, and 105 $\mu\text{g/mL}$ DTG. Intermediate precision was determined through the analysis of six replicates of solutions at the same concentration level used during repeatability testing but prepared on varying days and by various analysts.

2.4.4. Limit of Detection (LOD) and Limit of Quantification (LOQ). The LOD and LOQ concentrations for 3TC, TDF, and DTG when analysed simultaneously were determined following ICH guideline Q2 (R1) by applying the following equations:

$$\text{LOD} = \frac{3.3\sigma}{b},$$
$$\text{LOQ} = \frac{10\sigma}{b},$$
(1)

where σ is the standard deviation of the response values across the concentration range used to determine linearity and range of the analytical method and b is the slope of the calibration curve.

2.4.5. Specificity. Since this method was developed to allow identification and quantification of all three ARVs combined into polymeric matrices followed by drug loading quantification, drug release, and stability testing, it was also considered imperative to validate this method through the combination of the three ARVs with polymers such as gelatin, xanthan gum, and chitosan by adding these polymers to a working solution containing 600 $\mu\text{g/mL}$ 3TC, TDF, and 105 $\mu\text{g/mL}$ DTG. Furthermore, the influence of typical drug release media on the separation and elution of the ARVs was tested by preparing solutions containing all three drugs using pH 1.2 (HCl), pH 4.5 (acetate buffer), pH 6.8 (phosphate buffer), and distilled water as diluents.

Forced degradation studies were performed as per ICH guideline Q1A (R2) stability testing of new drug substances and products [13, 14]. To study possible degradation of 3TC, TDF, and DTG when exposed to an acidic environment, 1 mL of a 1N HCl solution was added to 1 mL of a working solution of an initial concentration of 601.71 $\mu\text{g/ml}$ 3TC, 603.33 $\mu\text{g/ml}$ TDF, and 105.00 $\mu\text{g/ml}$ DTG. This solution was mixed thoroughly and incubated at $60.0 \pm 2.0^\circ\text{C}$ for a 30 minute period, followed by the subsequent injection of 10 μL . The same procedure was applied to investigate the possible degradation of 3TC, TDF, and DTG when exposed to alkaline and oxidative conditions, where either 1 mL of a 1N NaOH or 3% H₂O₂ solution was added to 1 mL of the stock solution, following the same procedure as described for acidic degradation. In all instances of specificity testing, the obtained chromatography was compared with a standard solution consisting of 600 $\mu\text{g/ml}$ 3TC and TDF and 100 $\mu\text{g/ml}$ DTG.

2.4.6. Robustness. The robustness of this analytical method was performed by doing minor modifications towards the method parameters, which included variation in the column thermostat temperature, different C_{18} column types and manufacturers, mobile phase organic solvent concentration, and detection wavelength.

2.4.7. Solution Stability. The stability of the standard working solution was investigated by storing the solution in the fridge ($2^{\circ}\text{C} \pm 0.5^{\circ}\text{C}$) and in ambient conditions ($25^{\circ}\text{C} \pm 0.5^{\circ}\text{C}$) to determine how stable this solution will remain in the diluent. The standard working solution was stored in the specified temperature conditions for a period of 4 months and was analysed at 0, 1, and 4 months.

2.4.8. Statistical Analysis. All investigated method validation parameters were either performed in triplicate or in sixfold. This allowed the expression of the data as average values with calculated relative standard deviations (%RSD). Regression statistics were calculated using Excel software and applying the Analysis ToolPak.

3. Results and Discussion

3.1. Linearity and Range. The linearity of the method was established from a regression plot of peak response area against the concentration level of each drug. The linearity was demonstrated across the range of 150.0–1200.0 $\mu\text{g}/\text{mL}$ for 3TC and TDF and 1.5–210 $\mu\text{g}/\text{mL}$ for DTG, which was evident from the correlation coefficients (R^2) of >0.998 (Table 1), proving that there exists a good correlation between method responses across the concentration range. Further to this, the slope and y -intercept were also calculated and are presented in Table 1.

3.2. Accuracy. The accuracy of the proposed method was conducted through recovery studies, which were performed by preparing samples at three concentration levels, 50%, 100%, and 150% as outlined in Table 1, falling within the concentration range of 300–900 $\mu\text{g}/\text{mL}$ for 3TC and TDF and 53–158 $\mu\text{g}/\text{mL}$ for DTG. These solutions were analysed against a reference standard solution of known concentration, and the recovered concentration was quantified and reported.

3.3. Precision. On both levels, the analytical method proved to be precise and repeatable with intra-assay precision calculated for 3TC, TDF, and DTG well below %RSD of 2% (Table 1). Intermediate precision, determined across multiple days and by multiple analysts, showed the method to exhibit acceptable intermediate precision with %RSD values less than 2%.

3.4. LOD and LOQ. The limit of detection is the lowest concentration of a drug that will be detectable but will not produce repeatable quantification of the specific compound, whilst the limit of quantification is the lowest concentration

of the drug that will still be quantifiable with acceptable repeatability. For this method, the LOD and LOQ for 3TC were determined to be 56.31 $\mu\text{g}/\text{mL}$ and 187.69 $\mu\text{g}/\text{mL}$, respectively; for TDF, 40.27 $\mu\text{g}/\text{mL}$ and 134.22 $\mu\text{g}/\text{mL}$, respectively; and lastly for DTG, 6.77 $\mu\text{g}/\text{mL}$ and 22.5 $\mu\text{g}/\text{mL}$, respectively (Table 1).

3.5. Specificity. The specificity was determined using the diluent, polymers, and typical dissolution media as blank solutions followed by the comparison of these blank injections with the injections of solutions containing the three ARVs. Figure 2 depicts the chromatography obtained during the simultaneous analysis of 3TC, TDF, and DTG when solubilised in the diluent. During the analysis, it was observed that none of the polymeric materials interfered with the elution of either of the ARVs. The determination of the specificity of the method when buffered aqueous media were used showed no peak interferences when pH 1.2 (Figure 3), pH 4.5 (Figure 4), and pH 6.8 (Figure 5) buffered media and distilled water (Figure 6) are used as solvents. This suggests that this method will be suitable for use as an analytical method during drug release studies in pH 1.2, pH 4.5, and pH 6.8 buffered media and distilled water) of dosage forms containing all three ARVs.

Forced degradation of the 3TC, TDF, and DTG containing standard solution revealed that this method is suitable and sensitive for the detection of degradation of the three ARVs. After the treatment of the standard solution with 1N HCl, it was observed that 3TC remains quantifiable, but a significant shift in the retention times of TDF and DTG was observed (Figure 7), thus affecting the accurate identification and quantification of these two ARVs. A chromatogram obtained with the standard solution of 3TC, TDF, and DTG is depicted in Figure 8 and shows that none of the ARVs are quantifiable after alkaline hydrolysis. Furthermore, it became evident that of the three drugs, 3TC is sensitive towards oxidation with only TDF and DTG remaining identifiable and quantifiable after treatment of the standard solution with 3% hydrogen peroxide (Figure 9).

Bench top stability of the standard working solution was also conducted, and it indicated the stability of the solution across a four-month period stored at either $2^{\circ}\text{C} \pm 0.5^{\circ}\text{C}$ or $25^{\circ}\text{C} \pm 0.5^{\circ}\text{C}$ (Table 2). This stability study proved that all three ARVs remain stable in the diluent for a period of 4 months when stored at $2^{\circ}\text{C} \pm 0.5^{\circ}\text{C}$, but when stored at $25^{\circ}\text{C} \pm 0.5^{\circ}$ for the same period of time only 3TC and DTG remained stable with a 47.05% reduction in the purity of TDF during the storage period. In terms of stability when the solution is exposed to sunlight for a period of 4 months, the potency of both TDF and DTG reduced significantly, as provided in Table 2, thus proving that these ARV containing solutions should preferably be stored at $2^{\circ}\text{C} \pm 0.5^{\circ}\text{C}$ if intended for analysis across long periods of time.

3.6. Robustness. The robustness of the method was investigated by applying deliberate changes to the chromatographic system and included changes in the mobile phase

TABLE 1: Summary of the validation parameters investigated during the validation of the proposed HPLC method for the simultaneous identification and quantification of 3TC, TDF, and DTG.

Validation parameters	3TC	TDF	DTG
Linearity ($R^2 > 0.998$)	0.999	0.999	0.999
Slope	12236.13	11357.99	29030.74
y -intercept	242.59	-100.76	-43.92
LOD ($\mu\text{g/mL}$)	56.31	40.27	6.77
LOQ ($\mu\text{g/mL}$)	187.69	134.22	22.5
Accuracy (recovery 98–102%)			
50% level	100.31	101.56	101.27
100% level	100.67	101.33	104.94
150% level	101.57	100.41	100.78
Precision (%RSD <2%)	0.08	0.13	0.17

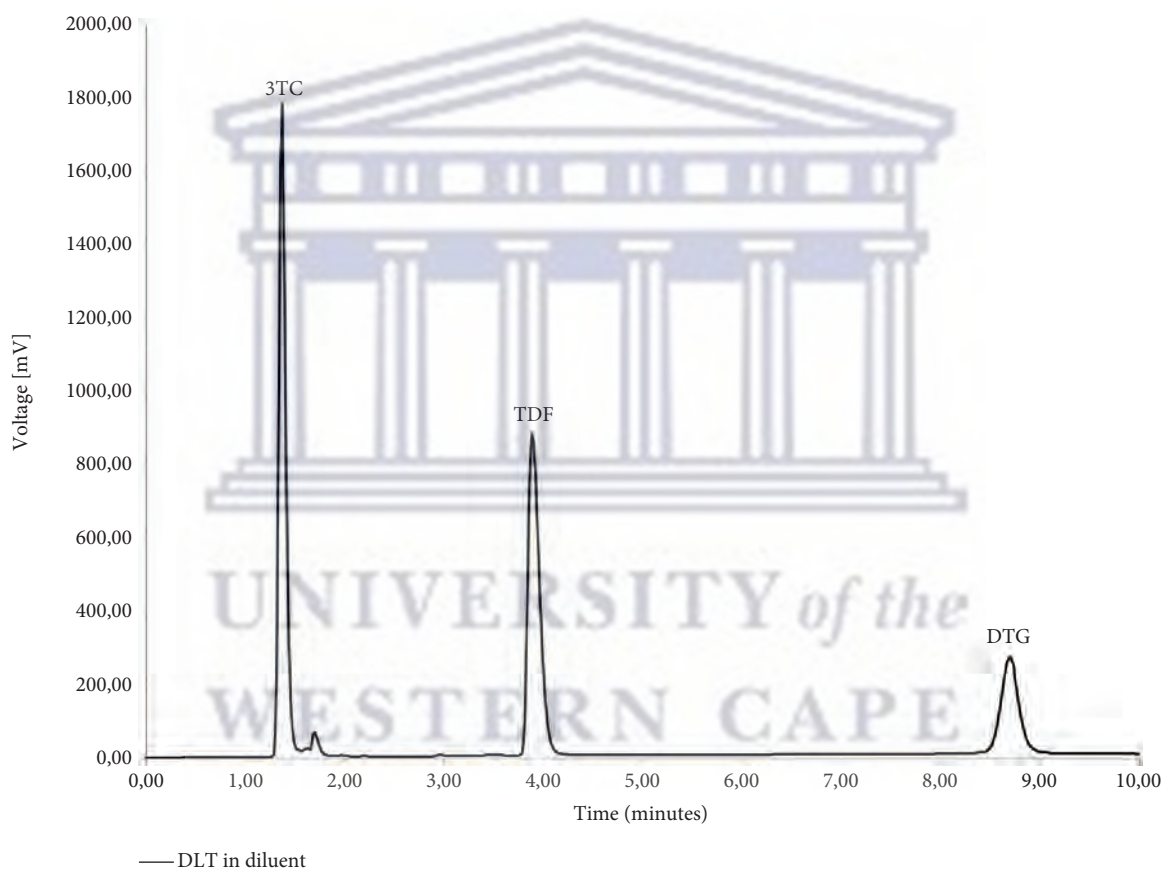


FIGURE 2: HPLC obtained with 3TC, TDF, and DTG dissolved in the diluent of 50 : 50 v/v methanol:ultrapure water.

flow rate, mobile phase composition, column temperature, and variation between different column lengths. The stability of the analytical solution was also established across a 48-hour period. Throughout robustness testing, a solution at a

concentration level of 600 $\mu\text{g/mL}$ 3TC, TDF, and 105 $\mu\text{g/mL}$ DTG was used and an injection volume of 10 μL was used. Table 3 summarises the results obtained during the robustness testing.

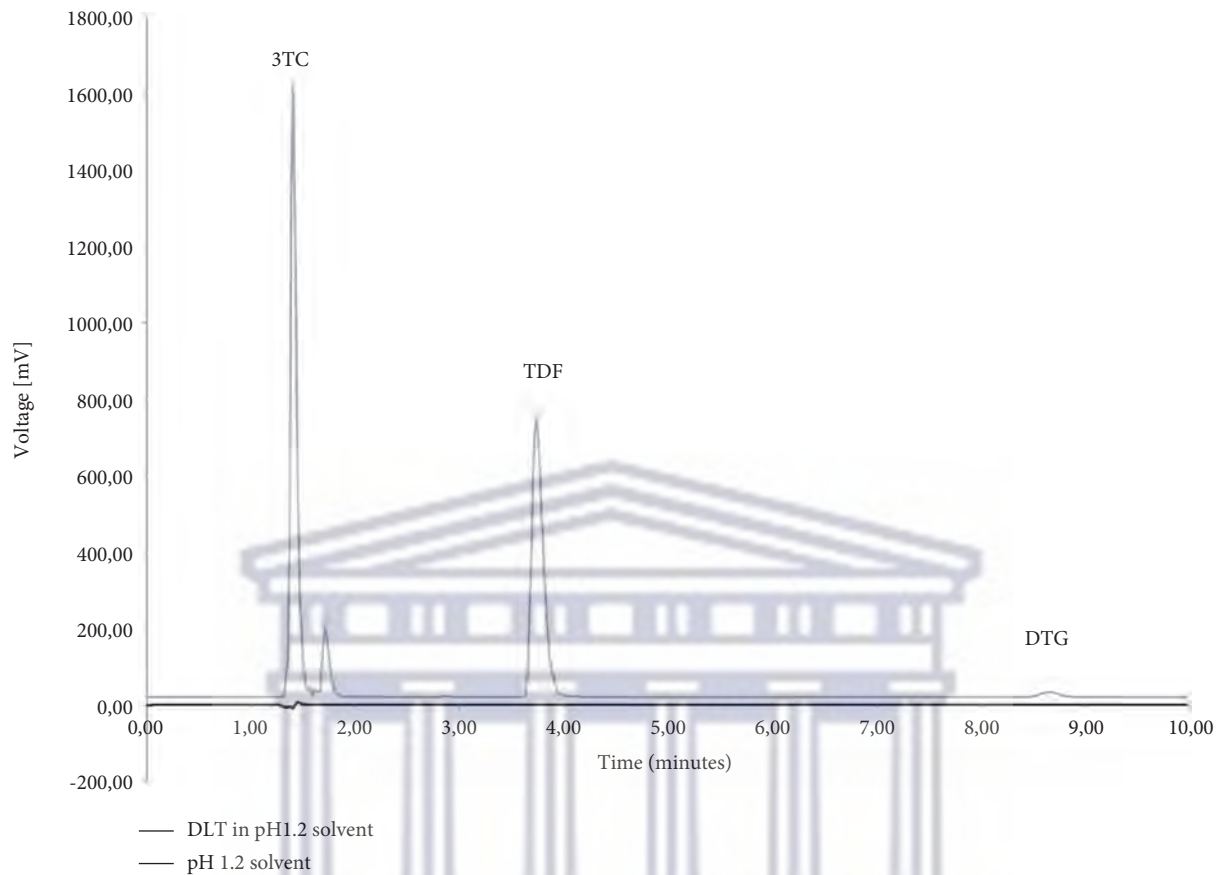


FIGURE 3: Overlay of HPLC obtained with 3TC, TDF, and DTG (denoted as DLT) dissolved in pH 1.2 buffered aqueous medium and an injection of only pH 1.2 buffered medium.

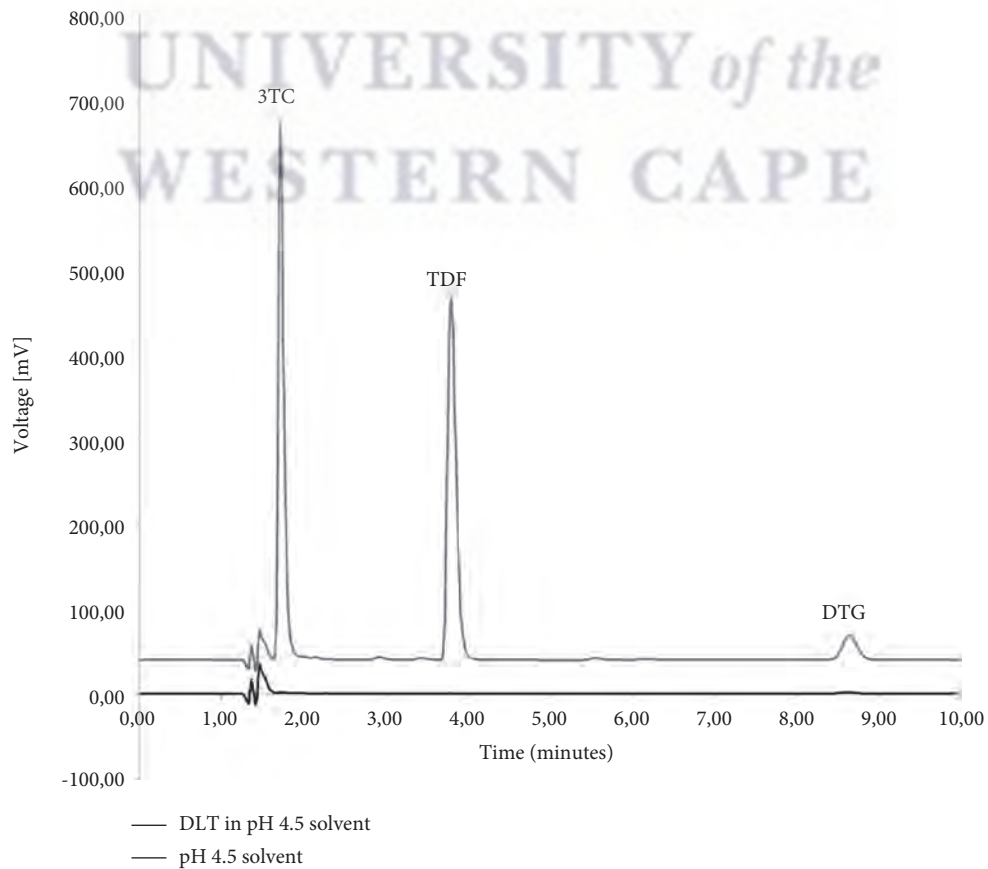


FIGURE 4: Overlay of HPLC obtained with 3TC, TDF, and DTG (denoted as DLT) dissolved in pH 4.5 buffered aqueous medium and an injection of only pH 4.5 buffered medium.

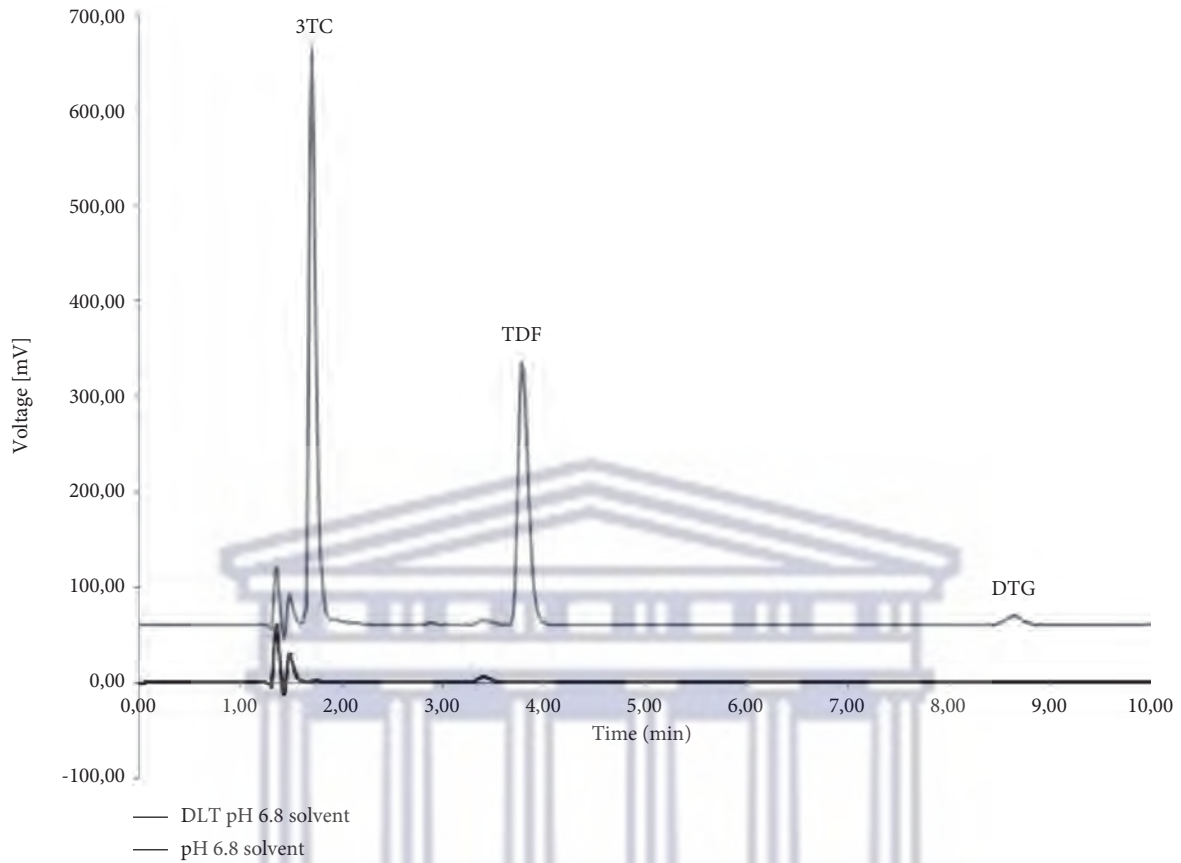


FIGURE 5: Overlay of HPLC obtained with 3TC, TDF, and DTG (denoted as DLT) dissolved in pH 6.8 buffered aqueous medium and an injection of only pH 6.8 buffered medium.

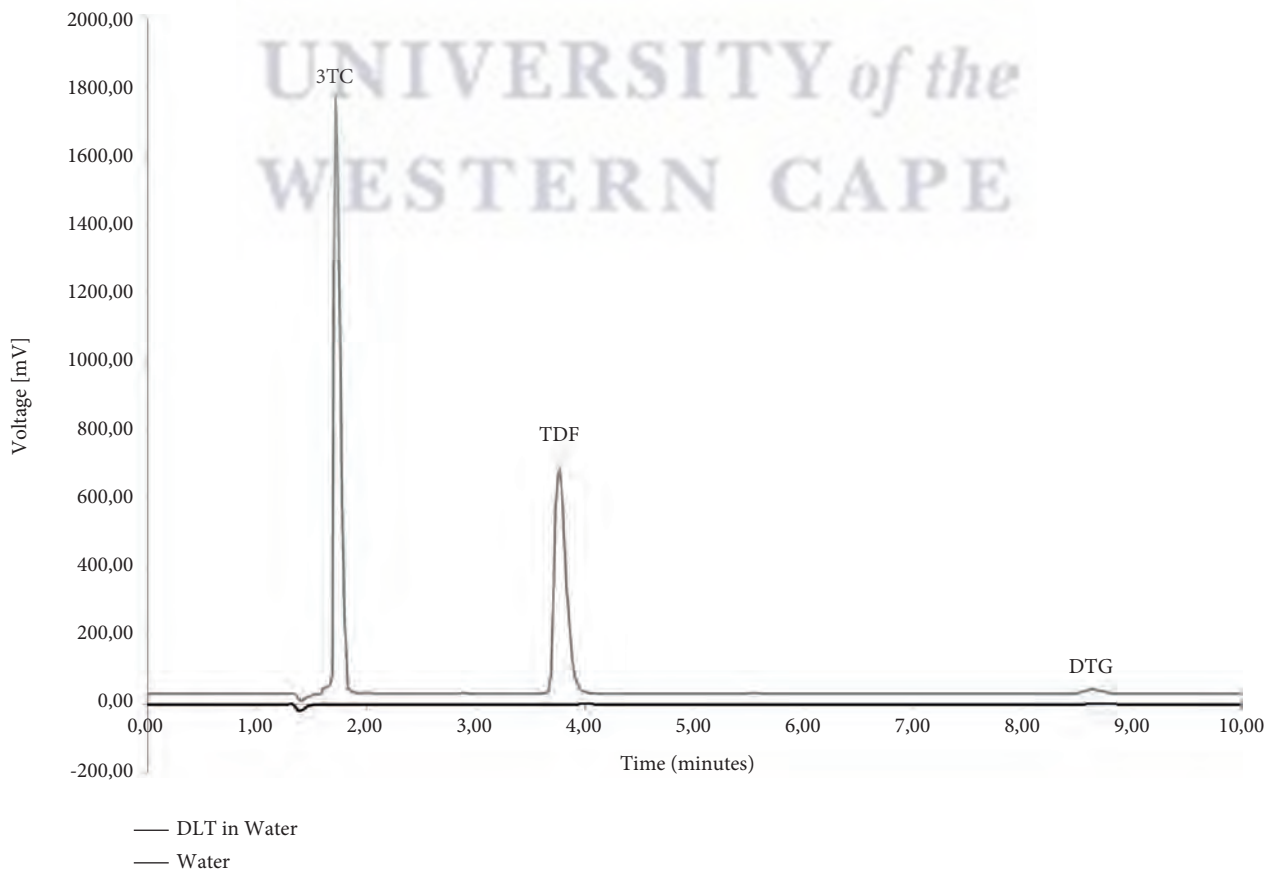


FIGURE 6: Overlay of HPLC obtained with 3TC, TDF, and DTG (denoted as DLT) dissolved in distilled water and an injection of only distilled water.

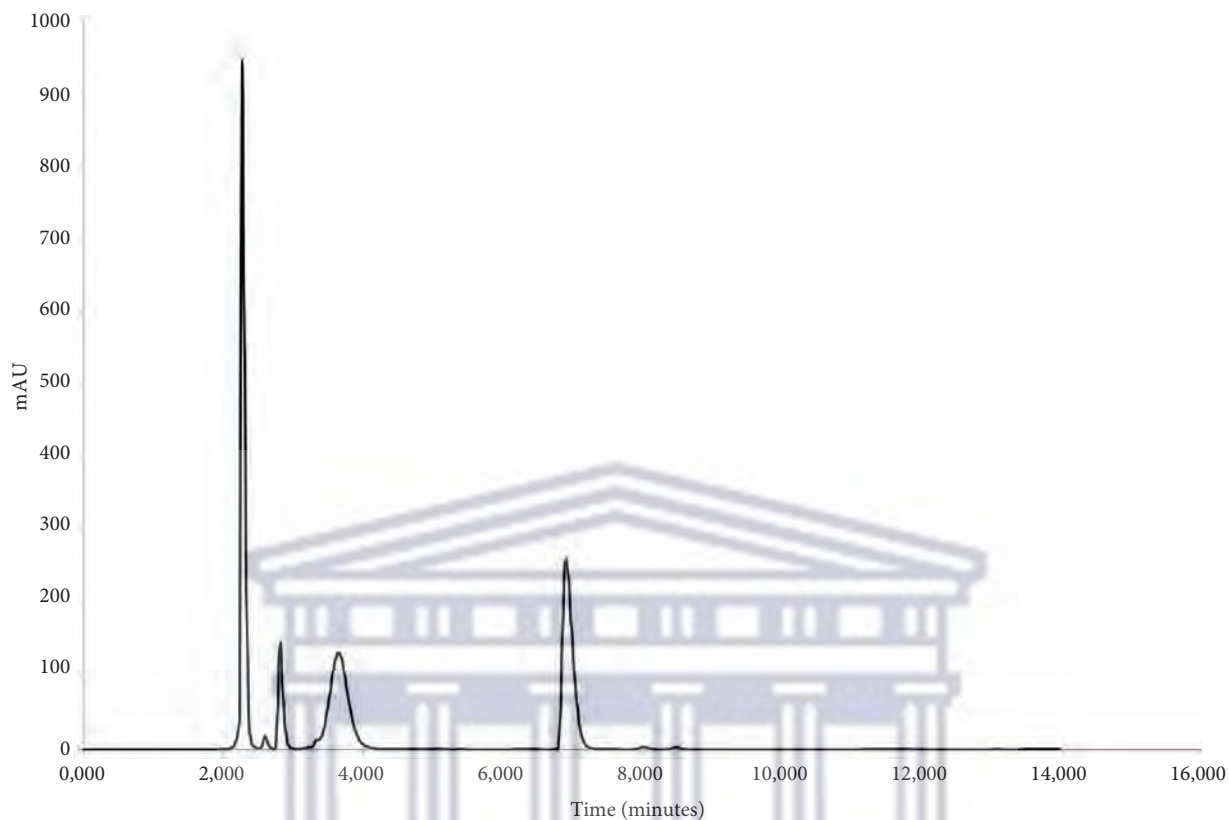


FIGURE 7: HPLC obtained with 3TC, TDF, and DTG standard solution after treatment with 1N HCl for 30 minutes at 60°C.

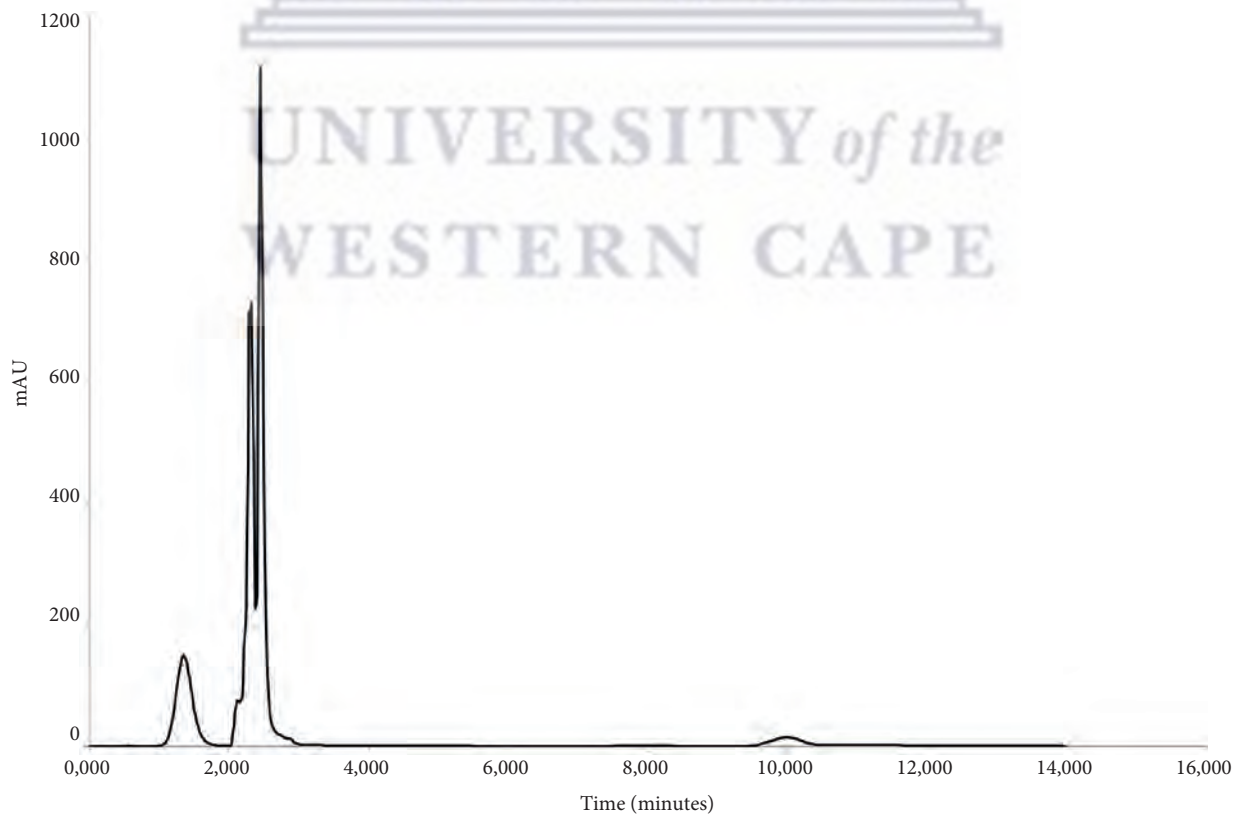


FIGURE 8: HPLC obtained with 3TC, TDF, and DTG standard solution after treatment with 1N NaOH solution for 30 minutes at 60°C.

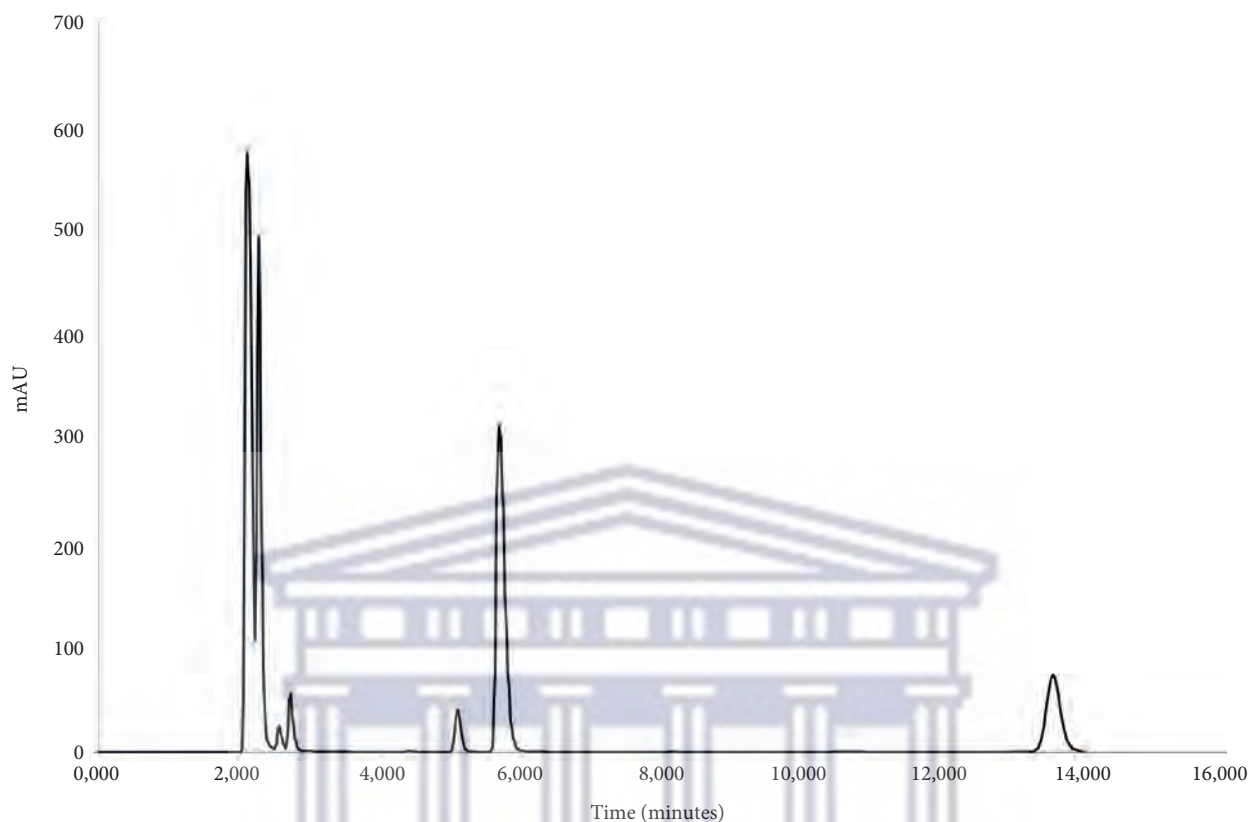


FIGURE 9: HPLC obtained with 3TC, TDF, and DTG standard solution after treatment with 3%v/v hydrogen peroxide solution for 30 minutes at 60°C.

TABLE 2: Quantification of the percentage (%) purity of each drug after exposure of the working standard solution to 1N HCl, 1N NaOH, and 3% v/v hydrogen peroxide for a period of 30 minutes at 60°C and to storage in 2°C ± 0.5°C, 25°C ± 0.5°C, and normal UV light in ambient conditions for a period of 4 months.

Degradation type	% assay of active ingredient		
	3TC	TDF	DTG
Acid hydrolysis	53.17	36.99	59.21
Alkaline hydrolysis	0.00	0.00	19.92
Oxidation	86.31	38.80	41.26
2°C ± 0.5°C	95.71	101.33	115.31
25°C ± 0.5°C	101.59	52.95	121.01
UV light	101.79	43.22	35.96

TABLE 3: Summary of the effect of deliberate chromatographic variations on the retention time (minutes) and peak symmetry of the peak responses for 3TC, TDF, and DTG.

Chromatographic condition	3TC		TDF		DTG	
	Retention time (min)	Peak symmetry	Retention time (min)	Peak symmetry	Retention time (min)	Peak symmetry
Column temperature (°C)						
35	1.33	1.4	3.35	1.5	7.70	0.8
40	1.35	1.3	3.17	1.4	6.39	1.1
50	1.32	1.4	2.95	1.4	5.36	0.98
Different column types						
Phenomenex® Kinetex® C ₁₈ 250 × 4.6 mm	1.45	1.4	4.87	1.3	12.08	0.8
Phenomenex® Kinetex® C ₁₈ 150 × 4.6 mm	1.35	1.3	3.35	1.6	8.20	1.0
Discovery HS C ₁₈ 150 × 4.6 mm	1.43	1.4	4.85	1.33	12.07	0.8
Mobile phase composition (% v/v)						

TABLE 3: Continued.

Chromatographic condition	3TC		TDF		DTG	
	Retention time (min)	Peak symmetry	Retention time (min)	Peak symmetry	Retention time (min)	Peak symmetry
90:10	1.48	1.40	ND	ND	ND	ND
85:15	1.32	3.0	ND	ND	ND	ND
80:20	1.51	1.25	ND	ND	ND	ND
70:30	1.32	1.38	1.68	1.38	2.30 (0.00)	1.29 (9.61)
60:40	1.33	1.25	2.08	1.38	3.63	1.16
50:50	1.33	1.4	3.35	1.5	7.70	0.8
40:60	1.36	1.5	7.23	2.3	8.42	1.0
Detection wavelength (nm)						
250	1.33	1.25	3.68	1.70	8.60	1.30
260	1.33	1.25	3.68	1.70	8.60	1.30
270	1.33	1.50	3.68	2.00	8.60	1.30
280	1.33	1.50	3.68	2.00	8.60	1.20

ND denotes no peak detected.

4. Conclusion

Based on the precision, linearity, accuracy, recovery, robustness, and specificity results, which includes the investigation into the use of various pharmaceutically relevant solvents and the forced degradation of 3TC, TDF, and DTG obtained using this new RP-HPLC method, showed that this method is suitable for the accurate identification and quantification of the three ARVs. Specificity testing conducted using typical pharmaceutically related drug release media proved that the simultaneous detection and quantification of all three ARVs are not negatively affected when combined with these solvent systems. Since this method is intended for the analysis of 3TC, TDF, and DTG during typical pharmaceutical preformulation and dosage form formulation processes, it was also important to ascertain the suitability of the analytical method when unknown and potential process-induced degradation products form part of the analytical matrix. The specificity and thus suitability of the analytical method to distinguish between 3TC, TDF, DTG, and any unknown degradation products were also proven during method validation. The determination of LOD and LOQ also proved that this method is suitable for the simultaneous detection and quantification of all three ARVs, with significantly low drug concentrations being identifiable and quantifiable.

Data Availability

All chromatographic data and methodology used to support the findings of this study are available from the corresponding author upon request.

Conflicts of Interest

The authors declare that they have no conflicts of interest.

Acknowledgments

The authors wish to acknowledge the Royal Society/African Academy of Sciences FLAIR Fellowship (Grant Number:

FLR\R1\191360) for the granted funding that facilitated the successful completion of the research presented in this study.

References

- [1] J. A. Coates, N. Cammack, H. J. Jenkinson et al., "(-)-2'-Deoxy-3'-thiacytidine is a potent, highly selective inhibitor of human immunodeficiency virus type 1 and type 2 replication in vitro," *Antimicrobial Agents and Chemotherapy*, vol. 36, no. 4, pp. 733-739, 1992.
- [2] H. Soudeyns, X. I. Yao, Q. Gao et al., "Anti-human immunodeficiency virus type I activity and in vitro toxicity of 2'-deoxy-3'-thiacytidine (BCH-189), a novel heterocyclic nucleoside analog," *Antimicrobial Agents and Chemotherapy*, vol. 35, no. 7, pp. 1386-1390, 1991.
- [3] K. Squires, A. L. Pozniak, G. Pierone et al., "Tenofovir DF in antiretroviral experienced, nucleoside-resistant HIV-1 infected patients with complete viral suppression," *Annals of Internal Medicine*, vol. 139, no. 5_Part_1, pp. 313-320, 2003.
- [4] B. L. Robbins, R. V. Srinivas, C. Kim, N. Bischofberger, and A. Fridland, "Antihuman immunodeficiency virus activity and cellular metabolism of a potential prodrug of the acyclic nucleoside phosphonate 9-R-(2-phosphonomethoxypropyl) adenine (PMPA), Bis(isopropylxymethylcarbonyl) PMPA," *Antimicrobial Agents and Chemotherapy*, vol. 42, no. 3, pp. 612-617, 1998.
- [5] M. L. Cottrell, T. Hadzic, and A. D. M. Kashuba, "Clinical pharmacokinetic, pharmacodynamic and drug-interaction profile of the integrase inhibitor dolutegravir," *Clinical Pharmacokinetics*, vol. 52, no. 11, pp. 981-994, 2013.
- [6] D. J. Hazuda, P. Felock, M. Witmer et al., "Inhibitors of strand transfer that prevent integration and inhibit HIV-1 replication in cells," *Science*, vol. 287, no. 5453, pp. 646-650, 2000.
- [7] J. C. C. Lenz and J. K. Rockstroh, "S/GSK1349572, a new integrase inhibitor for the treatment of HIV: promises and challenges," *Expert Opinion on Investigational Drugs*, vol. 20, no. 4, pp. 537-548, 2011.
- [8] M. Kobayashi, T. Yoshinaga, T. Seki et al., "In vitro anti-retroviral properties of S/GSK1349572, a next-generation HIV integrase inhibitor," *Antimicrobial Agents and Chemotherapy*, vol. 55, no. 2, pp. 813-821, 2011.
- [9] N. Mallikarjuna Rao and D. Gowri Sankar, "Development and validation of stability-indicating HPLC method for simultaneous determination of Lamivudine, tenofovir, and

- Dolutegravir in bulk and their tablet dosage form,” *Future Journal of Pharmaceutical Sciences*, vol. 1, no. 2, pp. 73–77, 2015.
- [10] National Center for Biotechnology Information, *PubChem Compound Summary for CID 60825, Lamivudine* National Center for Biotechnology Information, Bethesda, Maryland, 2021.
- [11] National Center for Biotechnology Information, *PubChem Compound Summary for CID 5486830, Tenofovir Disoproxil Fumarate*, National Center for Biotechnology Information, Bethesda, Maryland, 2021.
- [12] National Center for Biotechnology Information, *PubChem Compound Summary for CID 46216142, Dolutegravir Sodium*, National Center for Biotechnology Information, Bethesda, Maryland, 2021.
- [13] ICH Q2A, “Harmonised tripartite guideline, text on validation of analytical procedures, IFPMA,” in *Proceedings of the International Conference on Harmonization*, Geneva Switzerland, March 1994.
- [14] ICH Q2B, “Harmonised tripartite guideline, validation of analytical procedure: methodology, IFPMA,” in *Proceedings of the International Conference on Harmonization*, Geneva Switzerland, March 1996.



APPENDIX II



UNIVERSITY *of the*
WESTERN CAPE

Appendix II

Drug-excipient compatibility testing results

II.1 Introduction

Chapter 3 discussed the significance of drug-drug or drug-excipient compatibility research. Formulation incompatibilities can affect the stability and bioavailability of drugs, negatively impacting their safety and efficacy (Gomes *et al.*, 2013). As a result, before developing dosage forms, a compatibility study must be conducted to determine the compatibility of the drugs and excipients (Jeličić *et al.*, 2021).

This study aimed to assess the physicochemical compatibility of 3TC, TDF with the polymers used in this study when combined at equal ratio. The drug-excipient compatibility results reported in this section are for only drugs and excipients physical mixture (PM) that gave the promising formulations. Therefore only the compatibility results of 3TC-GEL (1:1 wt/wt), 3TC-CHI (1:1 wt/wt), TDF-GEL (1:1 wt/wt), and TDF-CHI (1:1 wt/wt) were reported.

II.2 Drug-excipient compatibility testing under ambient conditions

For accurate compatibility testing, it is necessary to first and foremost determine the physicochemical characteristics of the individual compounds and compare that with the corresponding PM. The following section will describe the investigated properties which facilitated the compatibility study.

II.2.1 Examination of organoleptic properties

The organoleptic properties of all the samples showed no discernible visual changes (**Tables A1 and A2**) over 24 hours. All raw materials (3TC, TDF, GEL, and CH) retained their original colors under storage at ambient temperature for 24 hours. After being mixed at equal ratio, the PM of these samples (3TC-GEL (1:1 wt/wt), 3TC-CHI (1:1 wt/wt), TDF-GEL (1:1 wt/wt), and TDF-CHI (1:1 wt/wt)) had no traces of discoloration or odour. The samples did not liquefy during storage at room temperature (25 °C).

Table A1: Organoleptic properties of 3TC-GEL (1:1) and 3TC-CH (1:1) at ambient temperature (25 °C).

ORGANOLEPTIC PROPERTIES	3TC-GEL (1:1) PM	3TC-CHI (1:1) PM
Discoloration	No	No
Odor	Odourless	Odourless
Melting	No	No

Table A2: Organoleptic properties of TDF-GEL (1:1) PM and TDF-CH (1:1) PM at ambient temperature (25 °C).

ORGANOLEPTIC PROPERTIES	TDF-GEL (1:1) PM	TDF-CHI (1:1) PM
Discoloration	No	No
Odor	Odourless	Odourless
Melting	No	No

III.2.2 Thermal Analyses

Thermal analysis may determine or provide information about basic physical and chemical processes such as melting point, decomposition, dehydration, enthalpy and entropy, stability, phase transition, crystallisation, glass transition, percentage crystallinity, desolvation, and chemical reaction. These changes are typically associated with thermal properties such as heat or heat capacity (Fortunato, 2013; Law & Zhou, 2017; Rajeswari *et al.*, 2020). The individual drugs and excipients and drug-excipient combinations were investigated for this compatibility study using DSC and TGA. **Figures A1** and **A2** depicts the DSC thermograms of pure 3TC, GEL, CH, 3TC:GEL (1:1)PM, 3TC:CH (1:1)PM and pure TDF, GEL, CH, TDF:GEL (1:1)PM, and TDF:CH (1:1)PM, respectively, during heating ranges of 30 to 350 °C at a heating rate of 10 °C/min.

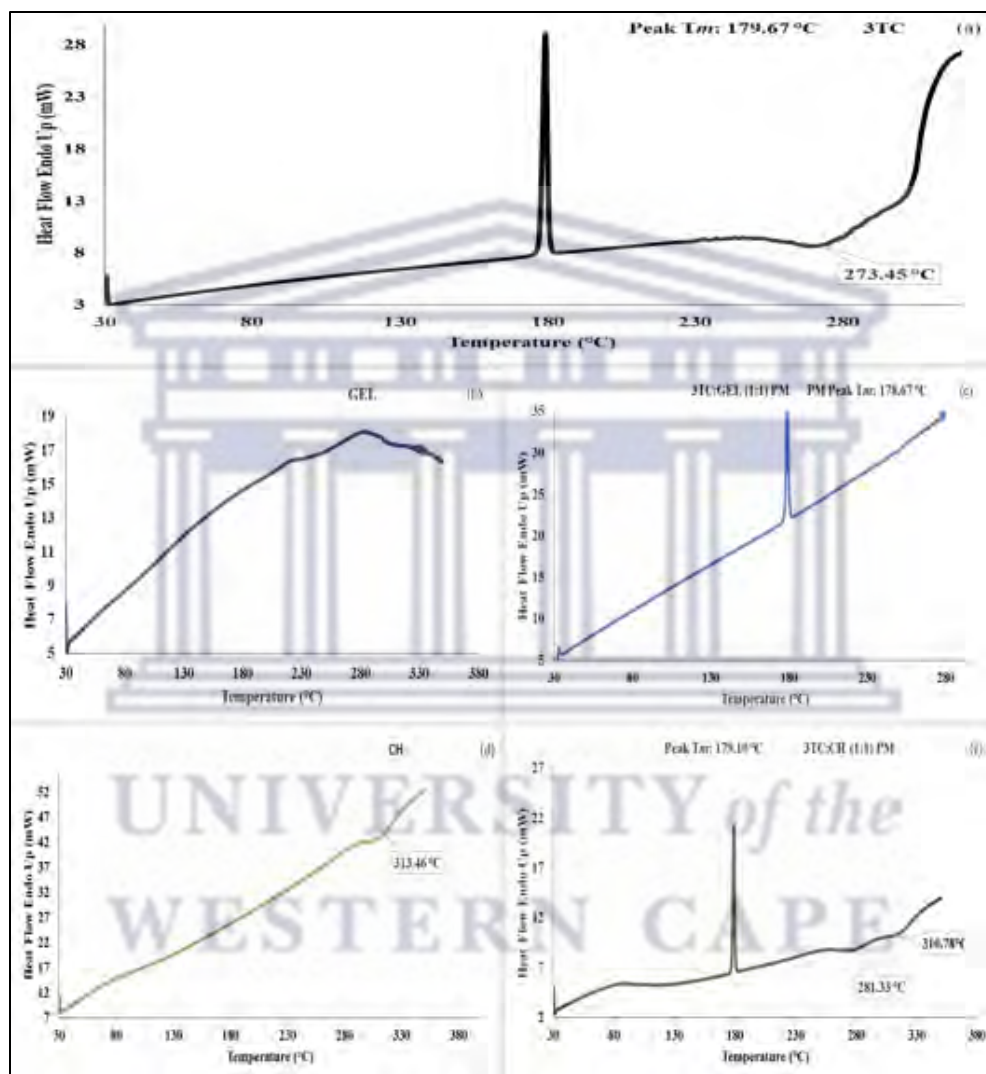


Figure A1: DSC thermograms of pure (a) 3TC, (b) GEL, (c) 3TC-GEL (1:1) PM, (d) CH, and (e) 3TC-CH (1:1) PM, during a heating range of 30 to 350 °C at a heating rate of 10 °C/min.

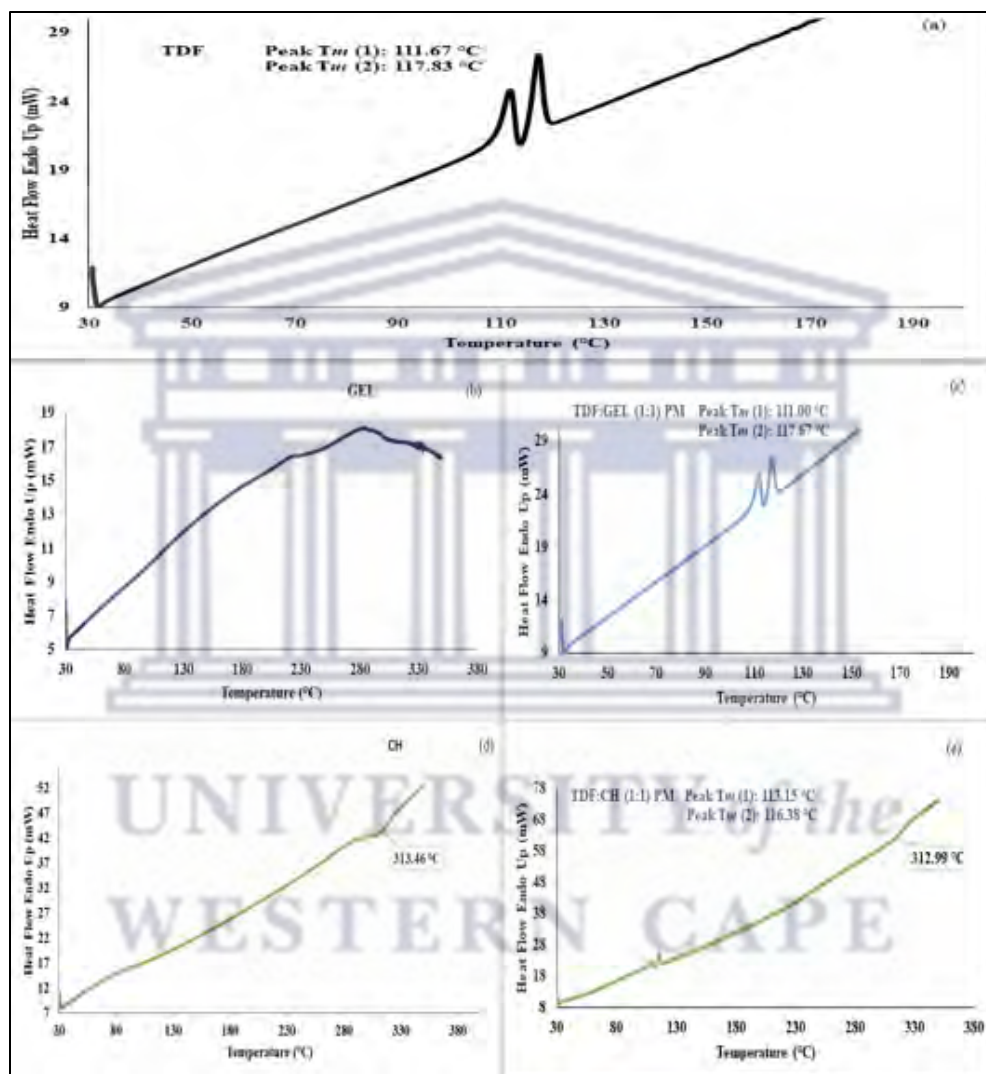


Figure A2: DSC thermograms of pure (a) TDF, (b) GEL, (c) TDF-GEL (1:1) PM, (d) CH, and (e) TDF-CH (1:1) PM, during a heating range of 30 to 350 °C at a heating rate of 10 °C/min.

The DSC results of 3TC (**Figure A1 (a)**) and TDF (**Figure A2 (a)**) were already reported in chapter 4, paragraph 4.2.1. After melting, a very broad exothermic event occurs at approximately 273.45 °C, characteristic of the 3TC (**Figure A1 (a)**) decomposition process (Gomes *et al.*, 2013). GEL (**Figure A1(b)/ A2(b)**) exhibited a broad glass transition temperature (T_g) at 89.33 °C and no endothermic event, indicating that GEL is amorphous (Yousaf *et al.*, 2015). The DSC thermogram of CH (**Figure A1(d)/ A2(d)**) demonstrated broad endothermic peak at 303.46 °C. The same sharp endothermic peak of pure 3TC was observed in the 3TC-GEL (1:1)PM (**Figure A1(c)**) and 3TC-CH (1:1)PM (**Figure A1(e)**) at 178.67 °C and 179.10 °C, respectively, with reduced intensity. The DSC thermogram of TDF-GEL (1:1)PM (**Figure A2(c)**) and TDF-CH (1:1)PM (**Figure A2(e)**) revealed the two endothermic peaks of the polymorphic TDF (**Figure A2(a)**). The decrease in the sizes of the two endothermic melting peaks of TDF-GEL (1:1) PM (**Figure A2(c)**) and TDF-CH (1:1) PM (**Figure A2(e)**) compared to the pure TDF sample are due to the component mixing of TDF with GEL or CH (Scrivens *et al.*, 2018). Therefore, these thermograms demonstrates the existence of the crystalline 3TC and TDF outside the polymer, confirming the compatibility and stability of the drug-polymer physical mixtures (Singh & Nath, 2012).

TGA quantifies the mass loss of a sample upon exposure to heat. It may be used to determine a substance's thermal stability based on measured weight loss (Ebnesajjad, 2011; Scrivens *et al.*, 2018). **Figures A3** and **A4** showed the overlay of TGA thermograms obtained for pure 3TC, GEL, 3TC-GEL (1:1)PM, CH, and 3TC-CH (1:1)PM and pure TDF, GEL, TDF-GEL (1:1)PM, CH, and TDF-CH (1:1)PM, during heating at a rate of 10°C/min from 30 to 600 °C.

The TGA curves of 3TC (**Figure A1(a)**) and TDF (**Figure A2(a)**) were already reported in chapter 4, paragraph 4.2.1. GEL has no melting temperature but degrades at elevated temperature with a drastic one-step total weight loss of 80.11% from approximately 300 °C to 600 °C (Wang *et al.*, 2012). The onset of thermal degradation around 313.09 °C, was ascribed to degradation of intermolecular side-chains (Xiao *et al.*, 2001).

CH also degraded at elevated temperature 303.22 °C, which was very close to the endothermic event observed on DSC thermogram at 303.46 °C (**Figure A1(d)/ A2(d)**). CH demonstrated one-step total weight loss of 54.02% from approximately 280 °C to 600 °C.

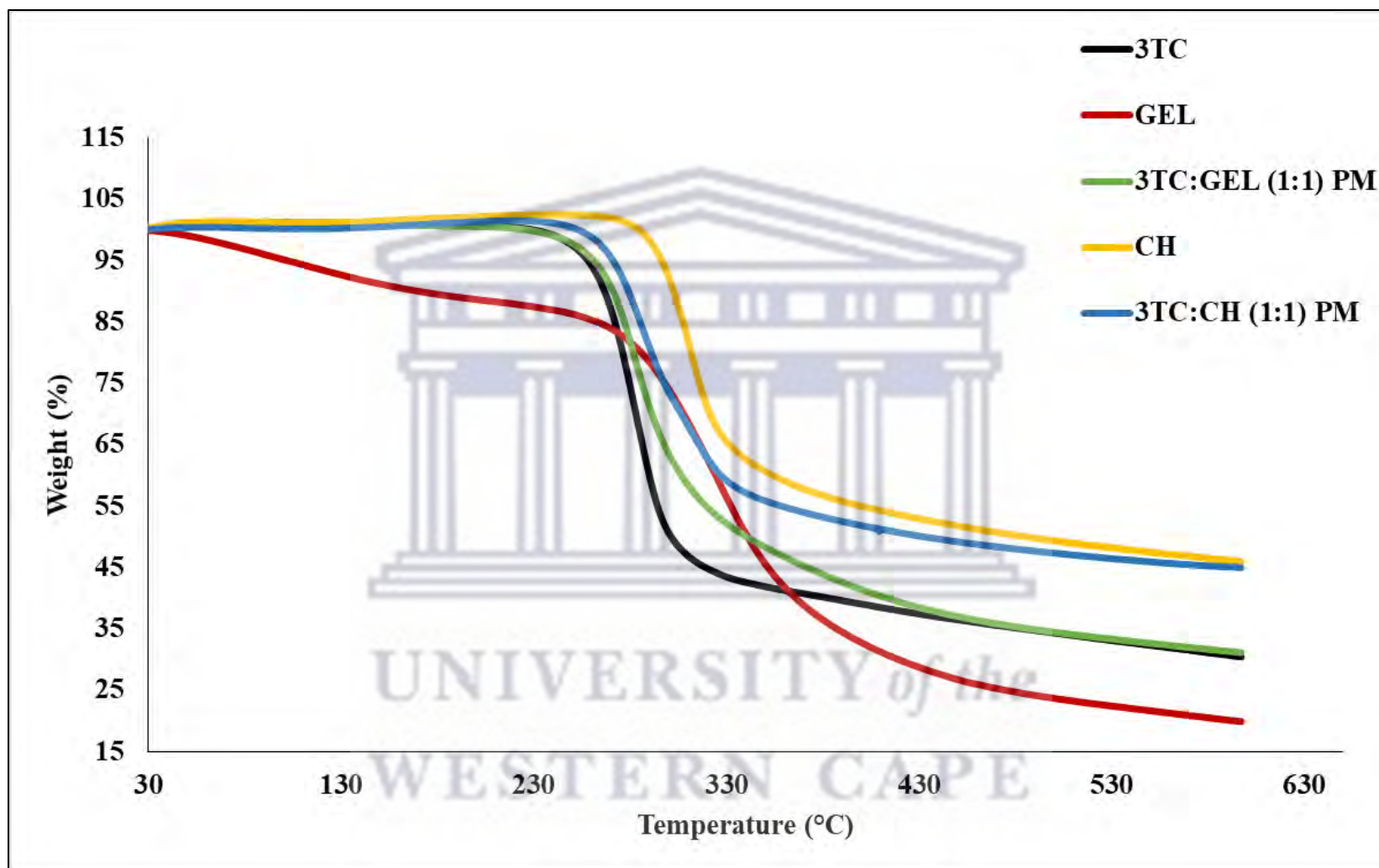


Figure A3: The overlay of TGA thermograms obtained for pure 3TC, GEL, 3TC-GEL(1:1) PM, CH, and 3TC-CH(1:1) PM during heating at a rate of 10°C/min from 30 to 600 °C.

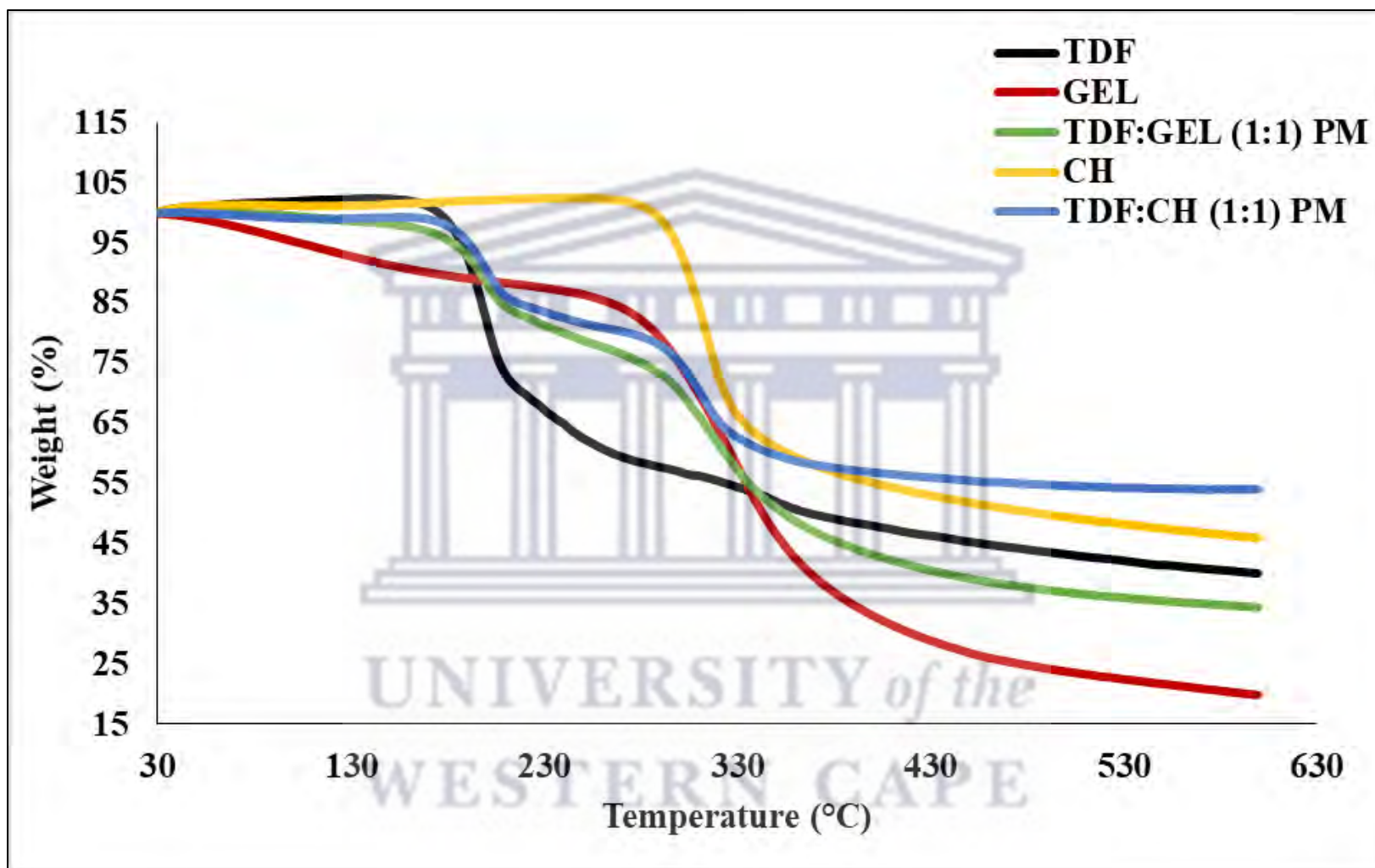


Figure A4: The overlay of TGA thermograms obtained for pure TDF, GEL, TDF-GEL(1:1) PM, CH, and TDF-CH(1:1) PM during heating at a rate of 10°C/min from 30 to 600 °C.

Table A3: The TGA summary table for pure 3TC, GEL, CHI, 3TC-GEL (1:1) PM, and 3TC-CH (1:1)PM; onset of degradation temperatures and percentage mass losses acquired between 30 to 600 °C at 10°C/min.

SAMPLE	Onset of Degradation Temperature (°C)	Percentage Weight Loss (%)
3TC	231.83	69.57
GEL	313.09	80.11
3TC-GEL (1:1)PM	246.18	68.88
CH	303.22	54.02
3TC-CH (1:1)PM	250.53	55.01

PM-physical mixture

The TGA curves of the PMs of 3TC-GEL (1:1)PM, 3TC-CH (1:1)PM, TDF-GEL (1:1)PM, and TDF-CH (1:1)PM showed onset of degradation temperatures close to their pure drugs (**Tables A3 and A4**). Whereas, 3TC-GEL (1:1)PM and TDF-GEL (1:1)PM revealed percentage mass loss close to pure drugs and 3TC-CH (1:1)PM and TDF-CH (1:1)PM close to CH (**Tables A3 and A4**). It were observed that all their physical mixtures had lower onset of degradation temperature than the polymer but higher than pure drugs. The TGA thermograms of these physical mixtures indicates the compatibility and stability of the pharmaceutical ingredients.

Table A4: The TGA summary table for pure TDF, GEL, CH, TDF-GEL (1:1) PM, and TDF-CH (1:1) PM; onset of degradation temperatures, second degradation temperatures and percentage cumulative mass losses acquired between 30 to 600 °C at 10°C/min.

SAMPLE	Onset of Degradation (°C)	Second Degradation Step (°C)	Percentage Cumulative Weight Loss (%)
TDF	172.67	342.09	59.90
GEL	313.01	-	80.11
TDF-GEL (1:1)PM	176.78	345.74	65.54
CH	303.22	-	54.02
TDF-CH (1:1)PM	180.98	334.63	45.91

PM-physical mixture

AI.2.3 Fourier-transform infrared (FTIR) spectroscopy

Fourier-transform infrared (FTIR) spectroscopy is used to identify functional groups in a sample and the presence of chemical bonds in a molecule. FTIR measures the intensity of a substance's functional group's peak absorbance using the light absorption phenomenon (Khan *et al.*, 2018).

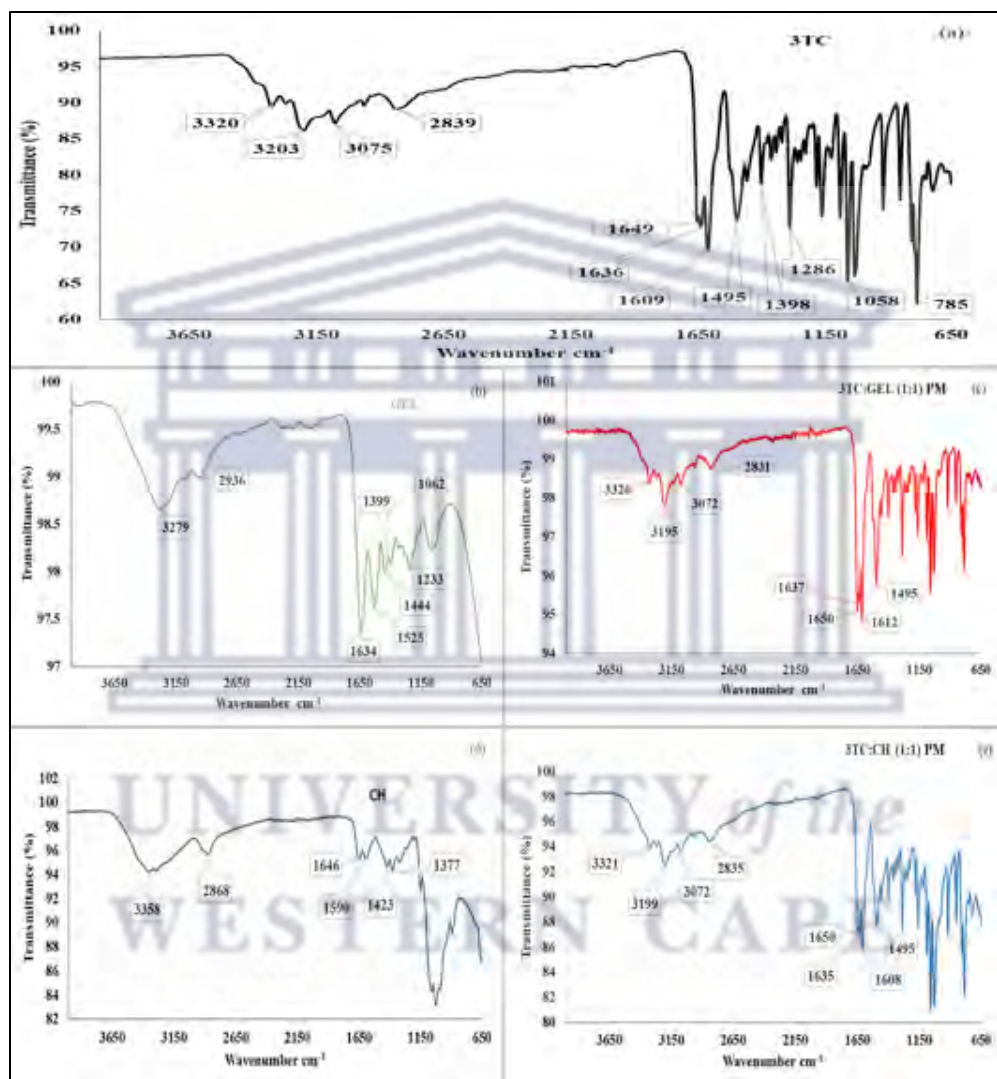


Figure A5: FTIR spectrum pure of (a) 3TC, (b) GEL, (c) 3TC-GEL (1:1) PM, (d) CH, and (e) 3TC-CH (1:1) PM obtained at ambient temperature within a scanning range of 650 - 4000 cm^{-1} .

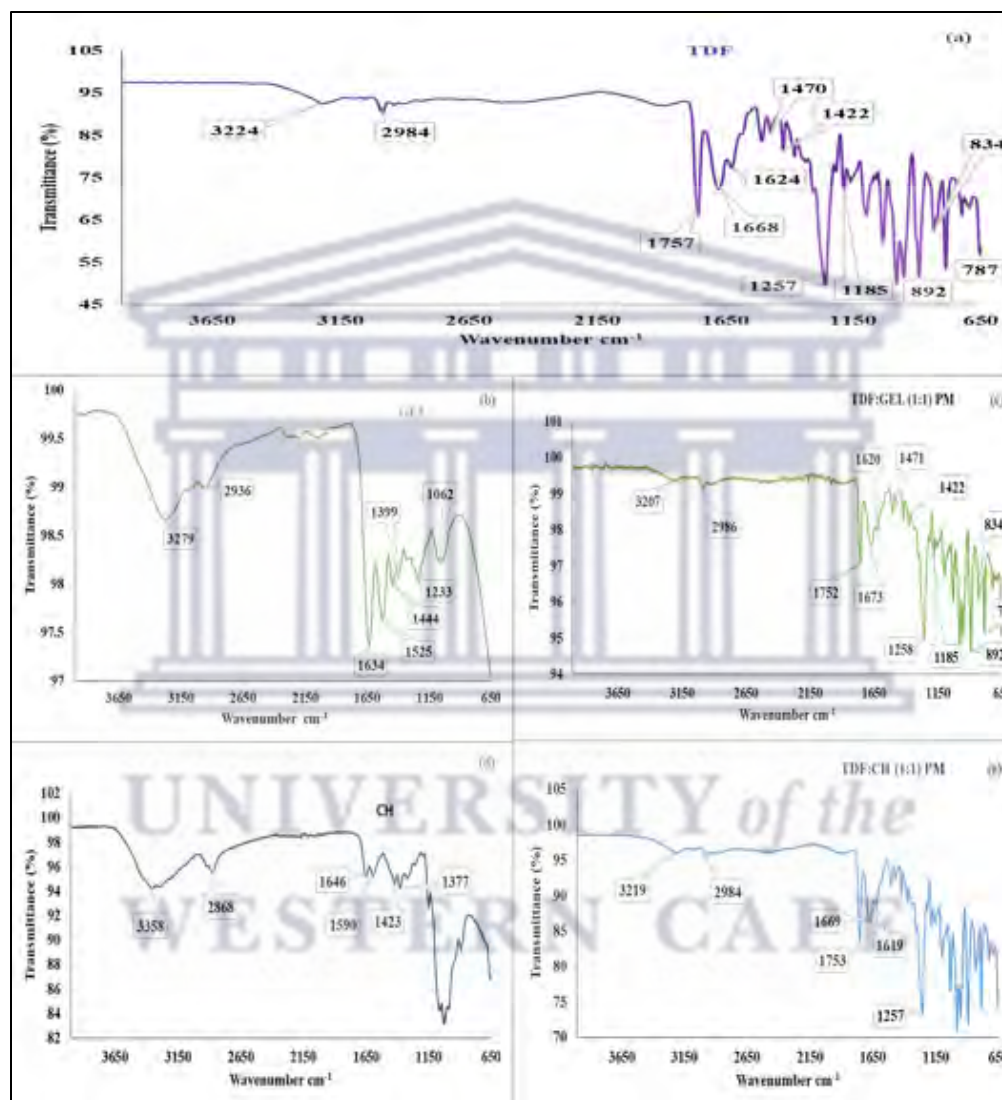


Figure A6: FTIR spectrum pure of (a) TDF, (b) GEL, (c) TDF-GEL (1:1) PM, (d) CH, and TDF-CH (1:1) PM obtained at ambient temperature within a scanning range of 650 - 4000 cm^{-1} .

The FTIR spectra for the pure samples 3TC, TDF, GEL, CH, and their physical mixtures 3TC-GEL (1:1), TDF-GEL (1:1), 3TC-CH (1:1), and TDF-CH (1:1) were displayed in **Figures A5** and **A6**. The IR absorption bands of these pure drugs (**Figures A5(a)**) and (**Figures A6(a)**) were already reported in chapter 4 paragraph 4.2.2. Also, GEL's IR spectrum (**Figures A5 (b)/ A6(b)**) was discussed in chapter 4 paragraph 4.4.4. CH's IR spectrum (**Figures A5(d)/ A6(d)**) revealed distinctive peaks at 3358 cm^{-1} and 2868 cm^{-1} , corresponding to hydroxyl group O-H and CH_2 stretching, respectively. The peaks at 1646 cm^{-1} and 1590 cm^{-1} were assigned to NH stretching of the primary amine groups. The C-N stretching vibrations caused the absorption bands at 1423 cm^{-1} , and 1377 cm^{-1} (Ogunjimi *et al.*, 2020; Prabhakar *et al.*, 2019; Song *et al.*, 2013).

The IR spectra of all the physical mixtures display all the prominent absorption bands of the pure 3TC and TDF with minor shifts in wavenumber and intensities of the peaks. However, these minor variations in the peaks are negligible. A significant peak shift may indicate the formation of hydrogen bonding or intermolecular interaction, whereas the presence of new peaks may indicate chemical interactions between drugs via covalent bonding (Rajeswari *et al.*, 2020). These results shows that there was no interaction between the 3TC-GEL (**Figure A5(c)**), 3TC-CH (**Figure A5(e)**), TDF-GEL (**Figure A6(c)**), and TDF-CH (**Figure A6(e)**) in their physical mixtures, therefore, these pharmaceutical ingredients are compatible.

UNIVERSITY of the
WESTERN CAPE

III.2.4 Powder X-ray diffraction (PXRD)

PXRD patterns and characteristic peaks of 3TC, TDF, GEL, CH, and their physical mixtures 3TC-GEL (1:1), TDF-GEL (1:1), 3TC-CH (1:1), and TDF-CH (1:1) recorded at room temperature (25 °C) over a scanning range of 4 - 40 °2 are shown in **Figures A7** and **A8**. The PXRD patterns and characteristic peaks of 3TC (**Figures A7(a)**) and TDF (**Figures A8(a)**) were already reported in chapter 4 paragraph 4.2.3. Also, GEL's PXRD pattern (**Figures A7(b)/ A8 (b)**) was discussed in chapter 4 paragraph 4.4.4. The PXRD pattern of CH (**Figures A7(d)/ A8(d)**) showed a diffraction profile with no sharp or narrow symmetric peaks, confirming its amorphous structure (Prabhakar *et al.*, 2019). The physical mixtures ((**Figures A7(c), A7(e), A8(c), and A8(e)**)) exhibited PXRD patterns similar to pure 3TC and TDF with sharp symmetric peaks. Notably, TDF-CH (1:1)PM ((**Figures A8(e)**)) demonstrated reduced sharp symmetric peaks of TDF, which might be due to the effect of high amorphousness of CH on the drug molecules or due to sample miscibility at mere physical combination or the variation in the mixture geometry and not due to incompatibility (Chadha & Bhandari, 2014; De Lima Gomes *et al.*, 2018; Singh & Nath, 2012).



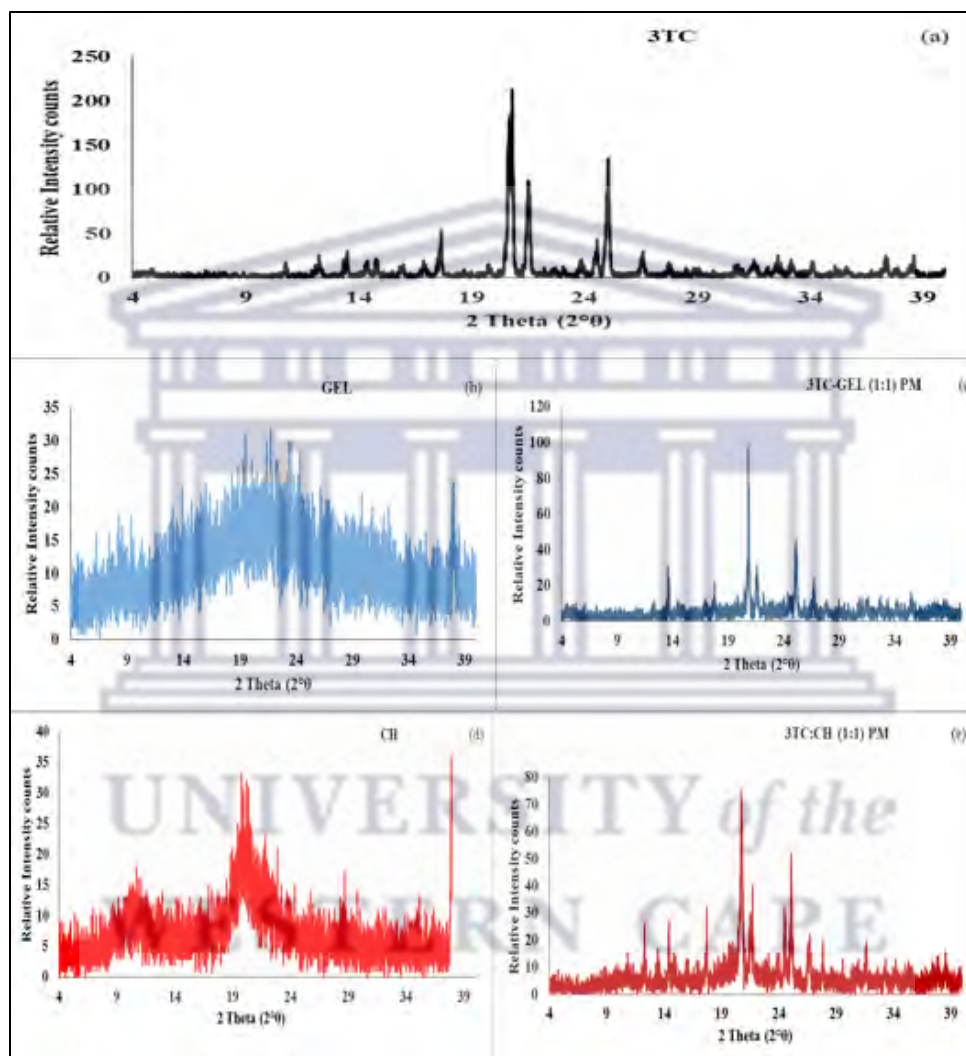


Figure A7: The PXRD patterns obtained for (a) 3TC, (b) GEL, (c) 3TC-GEL (1:1) PM, (d) CHI, and (e) 3TC-CHI (1:1) PM at room temperature within a scanning limit of 4 - 40° 2 θ .

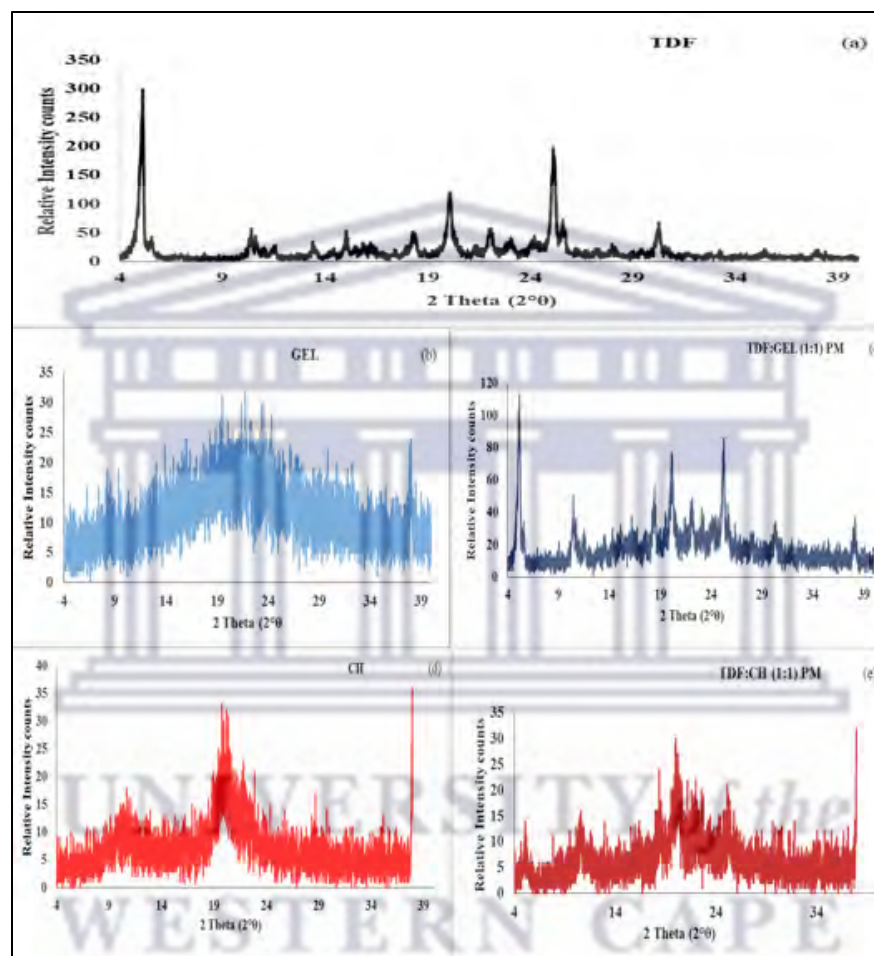


Figure A8: The PXRD patterns obtained for (a) TDF, (b) GEL, (c) TDF-GEL (1:1) PM, (d) CH, and (e) TDF-CH (1:1) PM at room temperature within a scanning limit of 4 - 40° 2θ.

In summary, the PXRD patterns of 3TC, TDF, and PMs showed high peak intensity due to the presence of molecules (atoms) with long lattice periodicity or ideal crystal alignment, which were absent in the polymers (Thakral *et al.*, 2016).

AII.3 Isothermal stress testing (IST)

IST is another method that is frequently used to determine drug-excipient compatibility. The process entails maintaining drug-excipient mixtures at high temperatures for an extended period, either with or without moisture. Subsequently, the drug-excipient mixture is inspected and analyzed regarding organoleptic properties, thermal behavior, and molecular vibrations (Gu *et al.*, 1990; Verma & Garg, 2005). After maintaining all samples (3TC, TDF, GEL, CH, and their PMs) at 60 ± 1 °C for 1 week, the raw materials and drug-excipient mixtures were physically examined for odour, discoloration, and melting. There was no discernible change in organoleptic properties of all the samples (Tables A5 and A6).

Table A5: Organoleptic properties of 3TC-GEL (1:1) PM and 3TC-CH (1:1) PM stored at 60 °C for 1 week (Isothermal stress testing).

ORGANOLEPTIC PROPERTIES	3TC-GEL (1:1)PM -IST	3TC-CH (1:1)PM -IST
Discoloration	No	No
Odor	Odourless	Odourless
Melting	No	No

Table A6: Organoleptic properties of TDF-GEL (1:1) PM and TDF-CH (1:1) PM stored at 60 °C for 1 week (Isothermal stress testing).

ORGANOLEPTIC PROPERTIES	TDF-GEL (1:1)PM -IST	TDF-CH (1:1)PM -IST
Discoloration	No	No
Odor	Odorless	Odorless
Melting	No	No

The thermal behaviours of samples (3TC, GEL, 3TC-GEL (1:1)PM, CH, 3TC-CH (1:1)PM, and TDF, TDF-GEL (1:1)PM, TDF-CH (1:1) PM) at room temperature (25 °C) determined over 24 hours compared to the samples (3TC, GEL, 3TC-GEL(1:1)PM, CH, 3TC-CH (1:1)PM, and TDF, TDF-GEL (1:1)PM, TDF-CH (1:1) PM) maintained at 60 ± 1 °C for 1 week were displayed in the DSC thermograms (**Figures A9, A10, and A11**) and TGA thermograms (**Figures A12, A13, A14, and Tables 7 and 8**), respectively, below.

The DSC thermograms of 3TC, GEL, CH, and their PMs (**Figures A9(b), A9(d), A9(f) and A10(d), A10(f)**) maintained at 60 ± 1 °C for 1 week demonstrated negligible difference with the prominent melting temperatures, compared to the corresponding endothermic and exothermic peaks in 3TC, GEL, CH, and their PMs (**Figures A9(a), A9(c), A9(e) and A10 (c), A10(e)**) stored at room temperature (25 °C) determined over 24 hours.

The DSC thermograms of TDF, TDF-GEL (1:1)PM, TDF-CH (1:1)PM (**Figures A11(b), A11(d), and A11(e)**) maintained at 60 ± 1 °C for 1 week showed the same two sharp thermal melting events observed in TDF, TDF-GEL (1:1)PM, TDF-CH (1:1)PM (**Figures A11(b), A11(d), and A11(e)**) stored at room temperature (25 °C) determined over 24 hours, with slight changes in the melting peaks intensities.



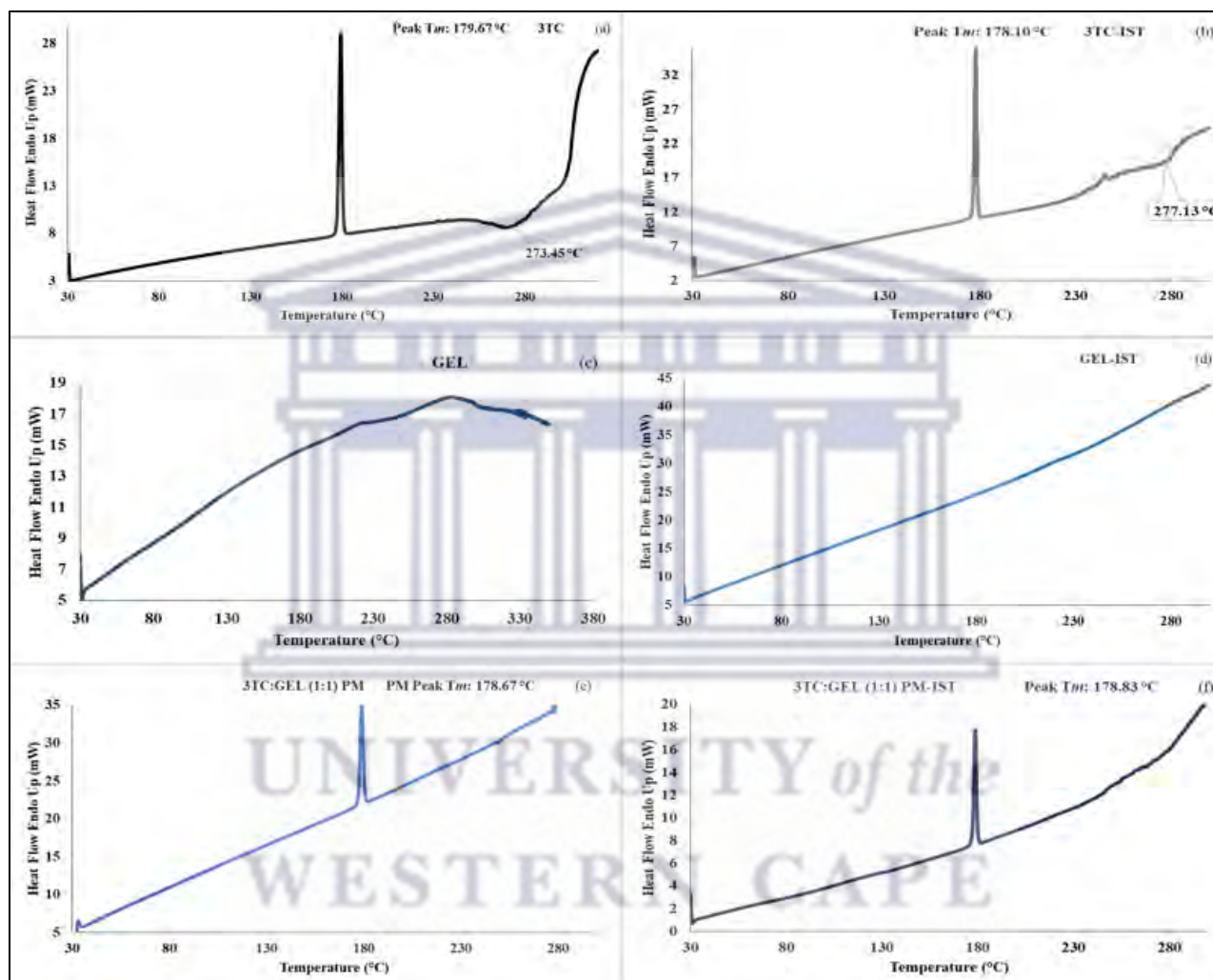


Figure A9: DSC thermograms obtained for pure (a) 3TC, (c) GEL, and (e) 3TC-GEL(1:1) PM stored at room temperature (25 °C) compared to (b) 3TC, (d) GEL, and (f) 3TC-GEL (1:1) PM maintained at 60 ± 1 °C for 1 week (Isothermal stress testing-IST) during heating ranges of 30 to 300 °C at a heating rate of 10 °C/min.

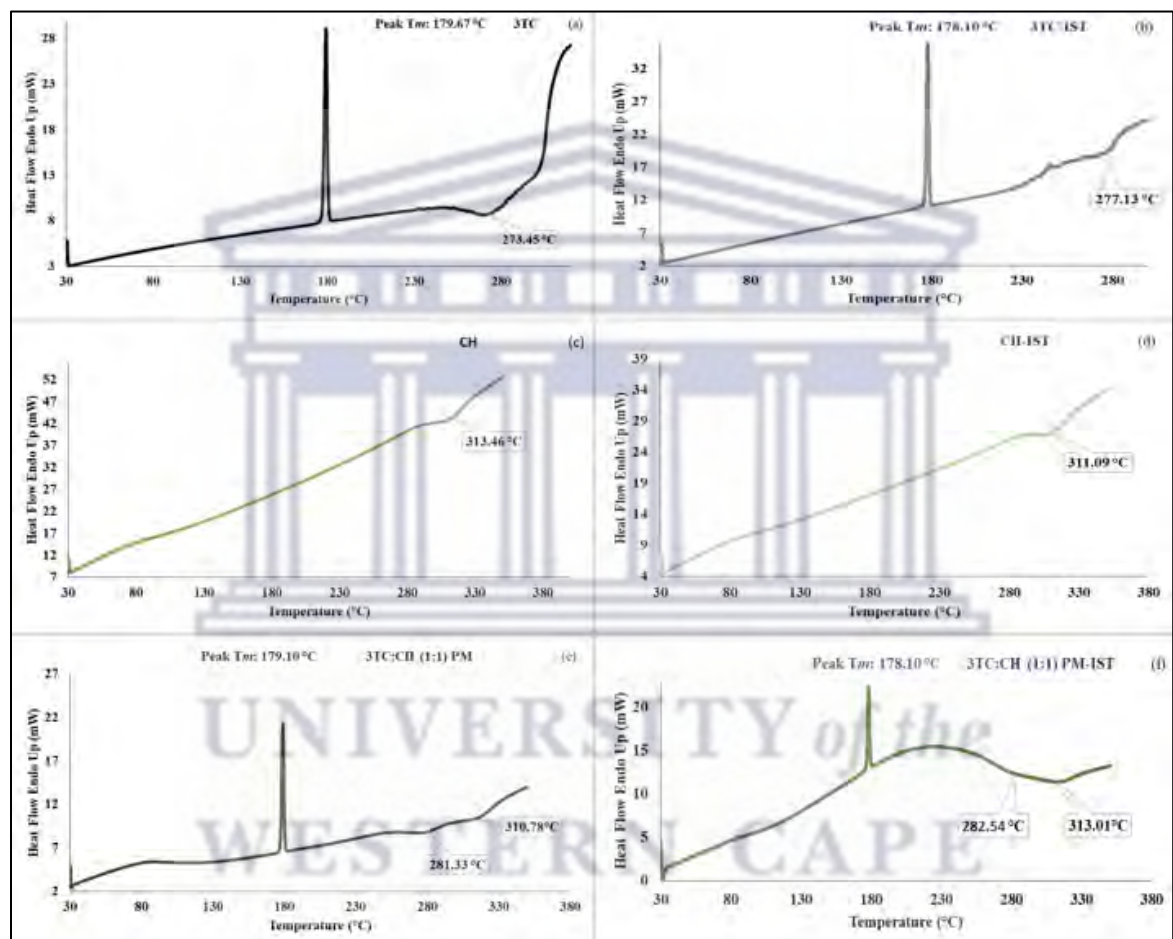


Figure A10: DSC thermograms obtained for pure (a) 3TC, (c) CH, and (d) 3TC-CH(1:1) PM stored at room temperature (25 °C) compared to (b) 3TC, (d) CH, and (e) 3TC-CH (1:1) PM maintained at 60 ± 1 °C for 1 week (Isothermal stress testing-IST) during heating ranges of 30 to 300 °C at a heating rate of 10 °C/min.

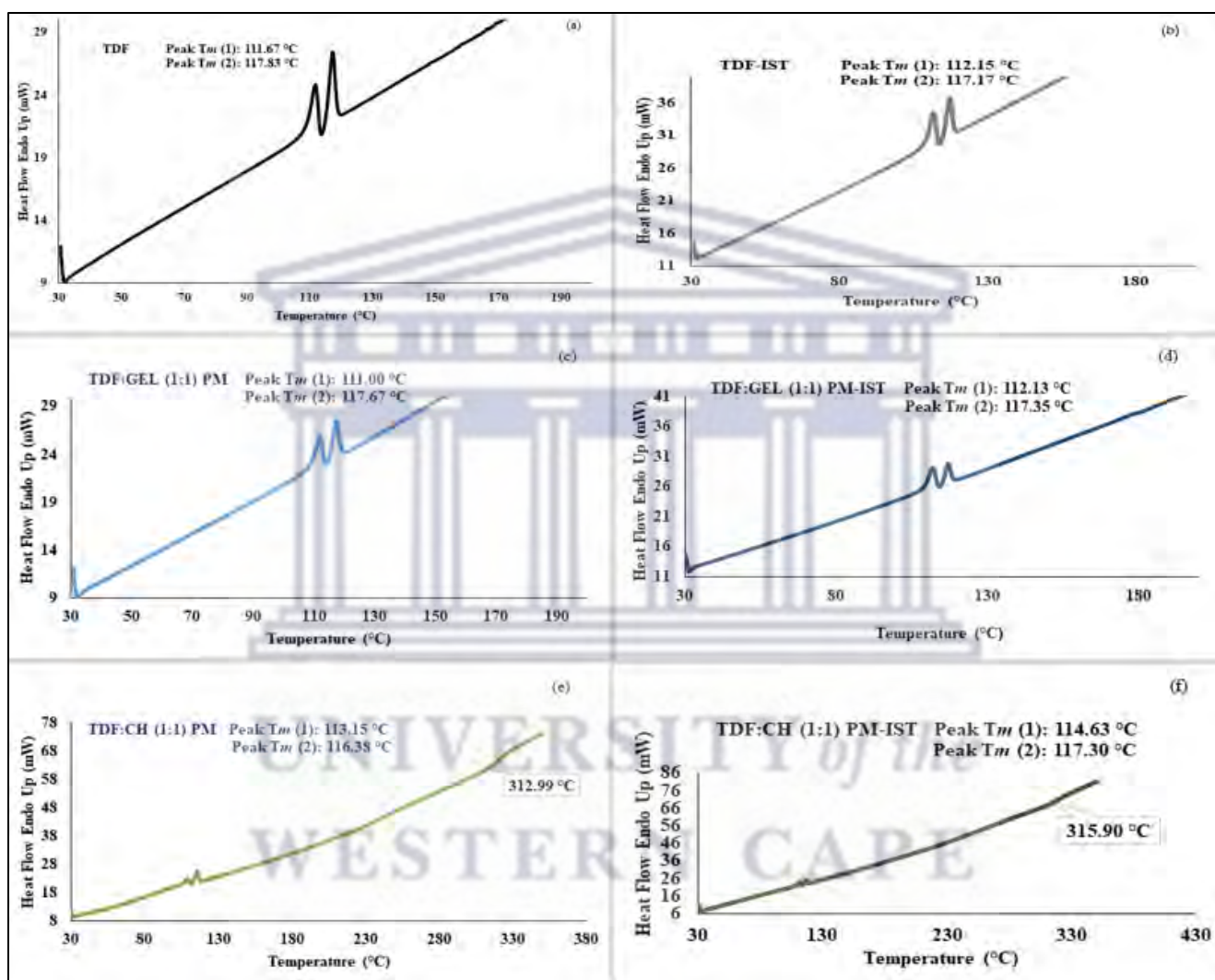


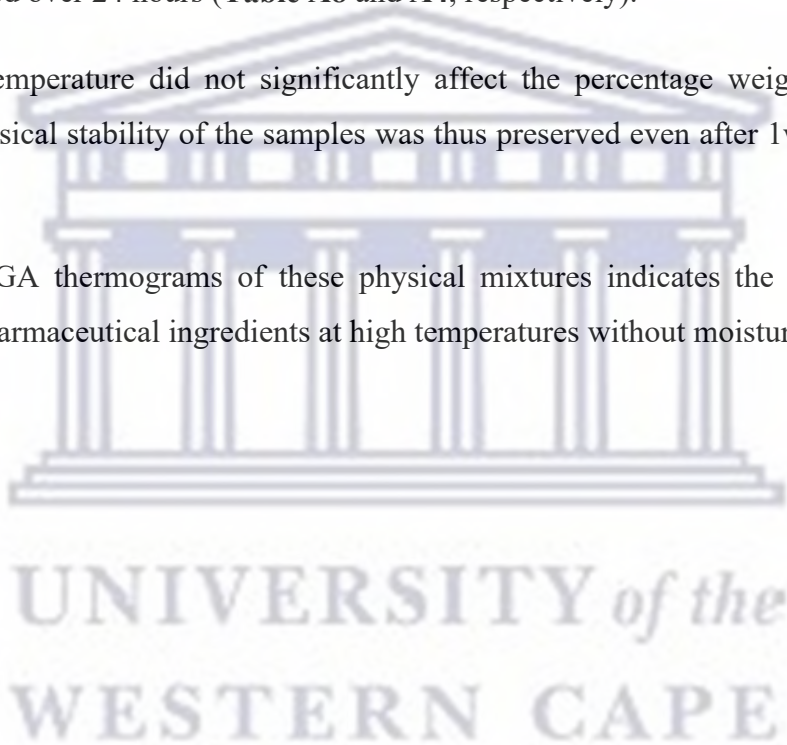
Figure A11: DSC thermograms obtained for pure (a) TDF, (c) TDF-GEL(1:1) PM, and (e) TDF-CH(1:1) PM stored at room temperature (25 °C) compared to (b) TDF, (d) TDF-GEL(1:1) PM, and (f) TDF-CH(1:1) PM maintained at 60 ± 1 °C for 1 week (Isothermal stress testing-IST) during heating ranges of 30 to 300 °C at a heating rate of 10 °C/min.

The TGA thermograms of 3TC, GEL, CH, and their PMs (**Figures A12 and A13**) maintained at 60 ± 1 °C for 1 week did not differ significantly in the onset degradation temperature and the percentage mass loss compared to 3TC, GEL, CH, and their PMs (**Figures A12 and A13**) stored at room temperature (25 °C) determined over 24 hours (**Table A7 and A3**, respectively).

The TGA thermograms of TDF, GEL, CH, and their PMs (**Figures A14**) maintained at 60 ± 1 °C for 1 week did not differ significantly in the onset degradation temperature and the percentage mass loss compared to TDF, GEL, CH, and their PMs (**Figures A14**) stored at room temperature (25 °C) determined over 24 hours (**Table A8 and A4**, respectively).

Higher storage temperature did not significantly affect the percentage weight loss of all the samples. The physical stability of the samples was thus preserved even after 1 week of storage at 60 ± 1 °C.

The DSC and TGA thermograms of these physical mixtures indicates the compatibility and stability of the pharmaceutical ingredients at high temperatures without moisture.



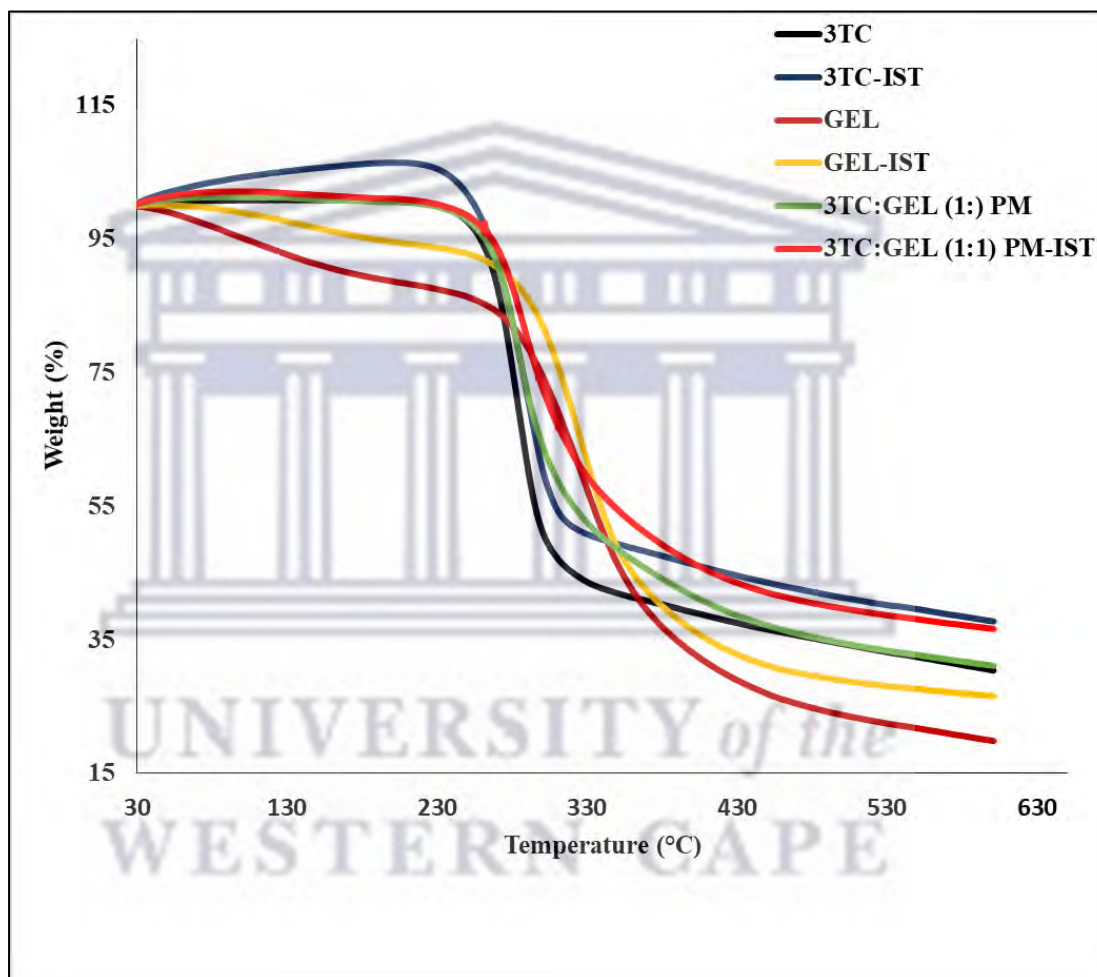


Figure A12: The overlay of TGA thermograms obtained for pure 3TC, GEL, and 3TC-GEL (1:1) PM stored at room temperature (25 °C) compared to 3TC, GEL, and 3TC-GEL (1:1) PM maintained at 60 ± 1 °C for 1 week (Isothermal stress testing-IST) during heating at a rate of 10 °C/min from 30 to 600 °C.

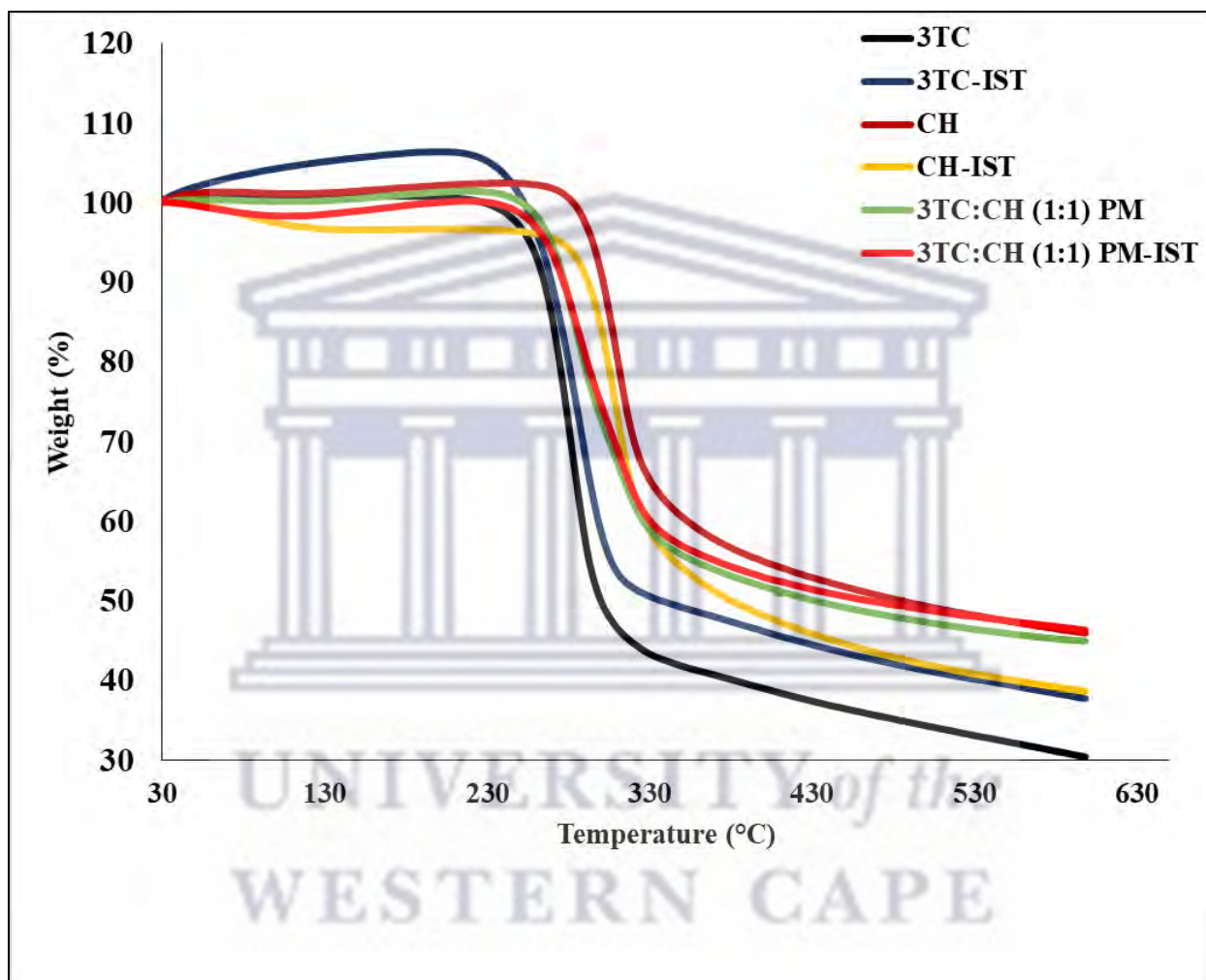


Figure A13: The overlay of TGA thermograms obtained for pure 3TC, CH, and 3TC-CH (1:1) PM stored at room temperature (25 °C) compared to 3TC, CH, and 3TC-CH (1:1) PM maintained at 60 ± 1 °C for 1 week (Isothermal stress testing-IST) during heating at a rate of 10 °C/min from 30 to 600 °C.

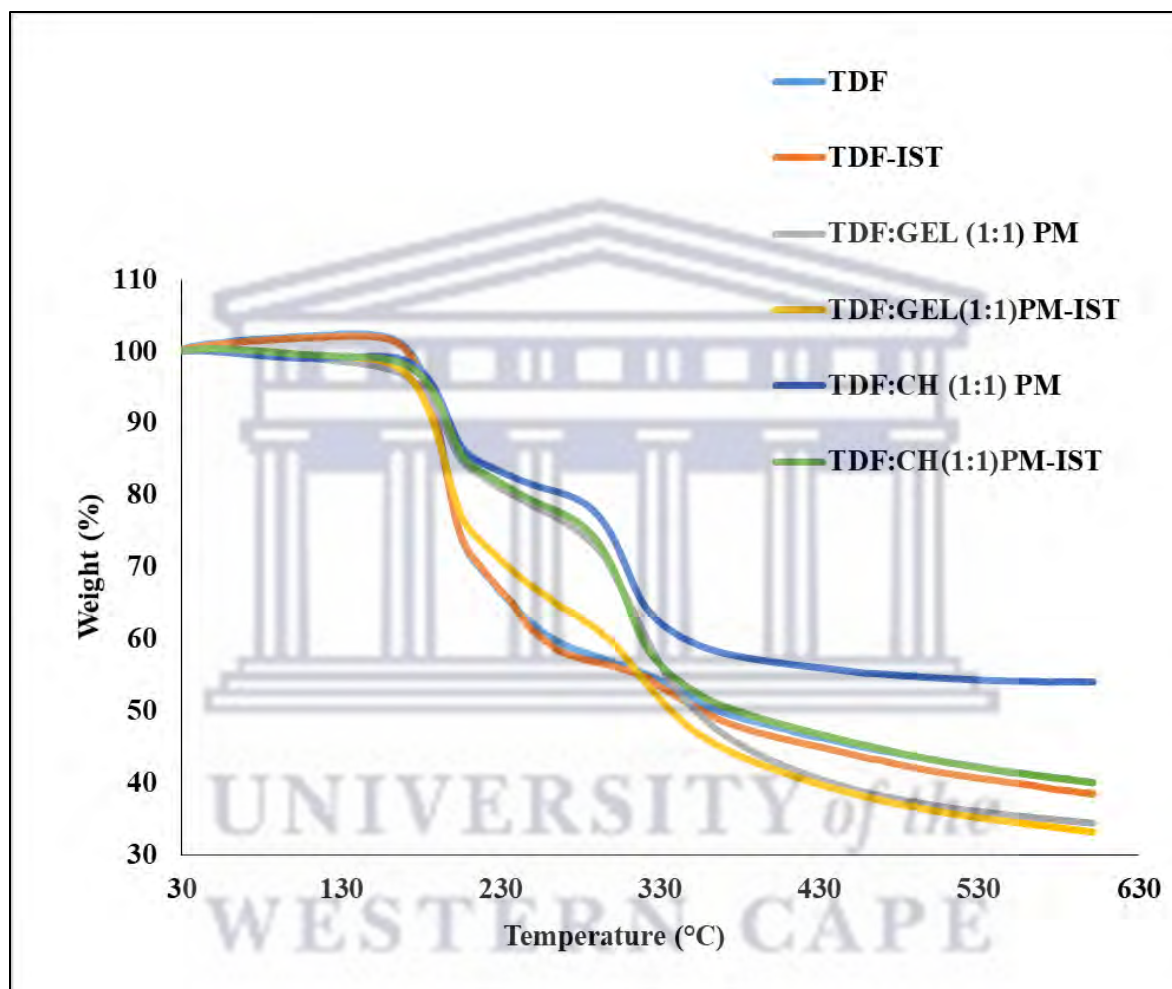


Figure A14: The overlay of TGA thermograms obtained for pure TDF, TDF-GEL (1:1) PM, and TDF-CH (1:1) PM stored at room temperature (25 °C) compared to TDF, TDF-GEL (1:1) PM, and TDF-CH (1:1) PM maintained at 60 ± 1 °C for 1 week (Isothermal stress testing-IST) during heating at a rate of 10 °C/min from 30 to 600 °C.

Table A7: The TGA summary table for pure 3TC, GEL, CH, 3TC-GEL (1:1)PM, and 3TC-CH (1:1)PM maintained at 60 ± 1 °C for 1 week (Isothermal stress testing); onset of degradation temperatures and percentage mass losses acquired between 30 to 600 °C at 10°C/min.

SAMPLE	Onset of Degradation Temperature (°C)	Percentage Weight Loss (%)
3TC-IST	232.34	62.23
GEL-IST	323.13	73.41
3TC-GEL (1:1)PM -IST	248.28	63.34
CH-IST	298.74	61.32
3TC-CH (1:1)PM -IST	251.37	53.66

IST- Isothermal stress testing, PM-physical mixture

Table A8: The summary table for TDF, GEL, CH, TDF-GEL (1:1)PM, and TDF-CH (1:1)PM maintained at 60 ± 1 °C for 1 week (Isothermal stress testing); onset of degradation temperatures, second degradation temperatures and percentage cumulative mass losses acquired between 30 to 600 °C at 10°C/min.

SAMPLE	Onset of Degradation (°C)	Second Degradation (°C)	Percentage Cumulative Weight Loss (%)
TDF-IST	172.88	340.79	61.46
TDF:GEL-IST	175.58	325.55	66.79
TDF:CHI-IST	180.72	313.88	59.93

IST- Isothermal stress testing, PM-physical mixture

The FTIR spectra of samples (3TC, GEL, 3TC-GEL (1:1)PM, CH, 3TC-CH (1:1)PM, and TDF, TDF-GEL (1:1)PM, TDF-CH (1:1) PM) stored at room temperature (25 °C) determined over 24 hours compared to the samples (3TC, GEL, 3TC-GEL (1:1)PM, CH, 3TC-CH (1:1)PM, and TDF, TDF:GEL (1:1)PM, TDF:CH (1:1)PM) maintained at 60 ± 1 °C for 1 week were demonstrated in the **Figures A15, A16, and A17**.

The FTIR spectra of 3TC, GEL, CH, and their PMs (**Figures A15(b), A15(d), A15 (f) and A16(b), A16(d), A16(f)**) maintained at 60 ± 1 °C for 1 week retained all the peaks from 3TC, GEL, CH, and their PMs (**Figures A15(a), A15(c), A15 (e) and A16(a), A16(c), A16(e)**) stored at room temperature (25 °C) determined over 24 hours with only slight changes in the peaks wavenumbers.

The FTIR spectra of TDF, GEL, CH, and their PMs (**Figures A17(b), A17(d), and A17(f)**) maintained at 60 ± 1 °C for 1 week retained all the peaks from TDF, GEL, CH, and their PMs (**Figures A17(a), A17(c), and A17(e)**) stored at room temperature (25 °C) determined over 24 hours with only slight changes in the peaks wavenumbers.

The presence or absence of new peaks could indicate chemical interactions between drug-excipients through covalent bonding (Rajeswari *et al.*, 2020). In this 1ST, no new peaks were formed during the exposure of all the raw materials and drug-polymer mixtures at 60 ± 1 °C for 1 week without the presence of moisture.



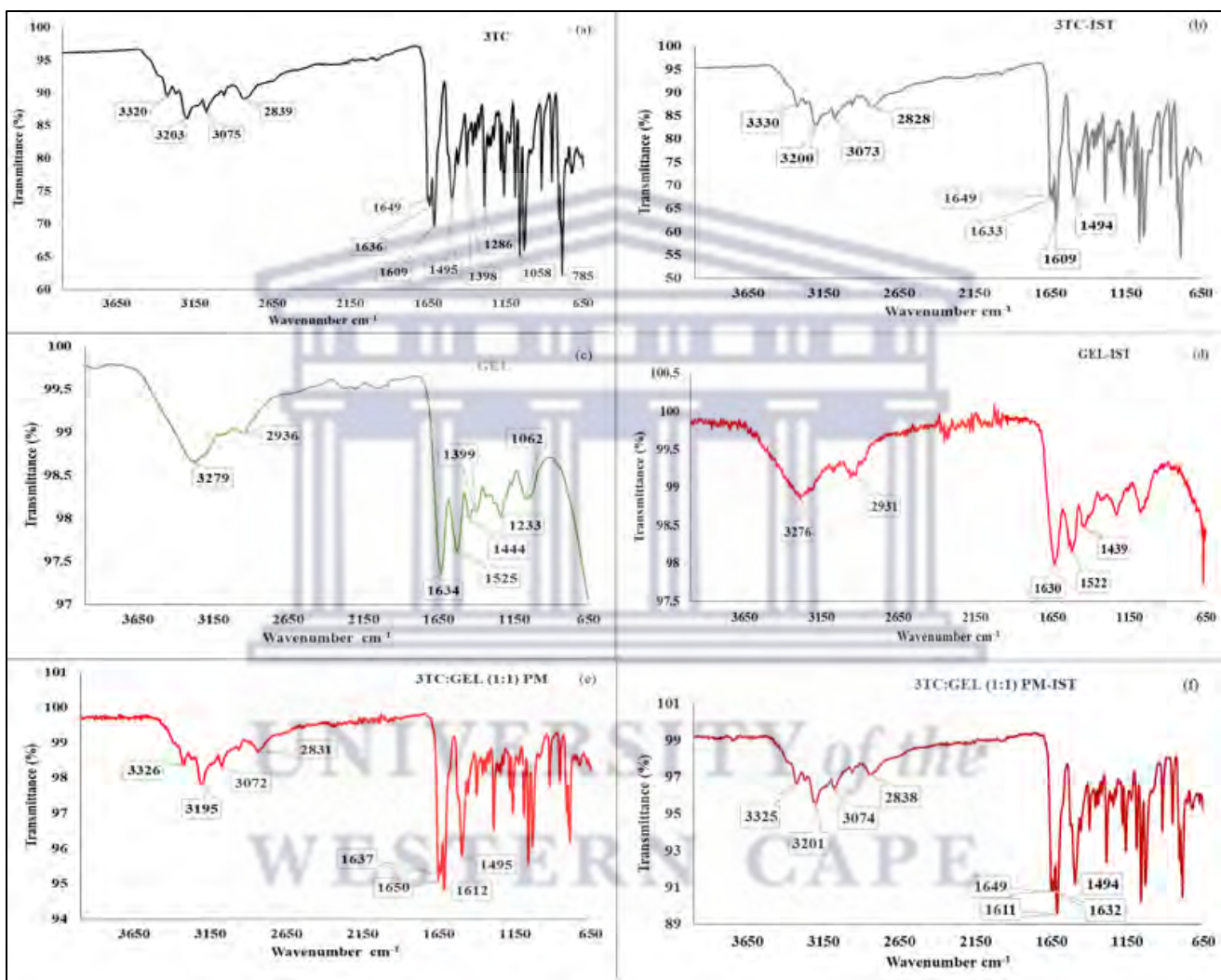


Figure A15: DSC thermograms pure pure (a) 3TC, (c) GEL, and (e) 3TC-GEL (1:1) PM stored at room temperature (25 °C) compared to (b) 3TC, (d) GEL, and (f) 3TC-GEL (1:1) PM maintained at 60 ± 1 °C for 1 week (Isothermal stress testing-IST) obtained at ambient temperature within a scanning range of 650 - 4000 cm^{-1} .

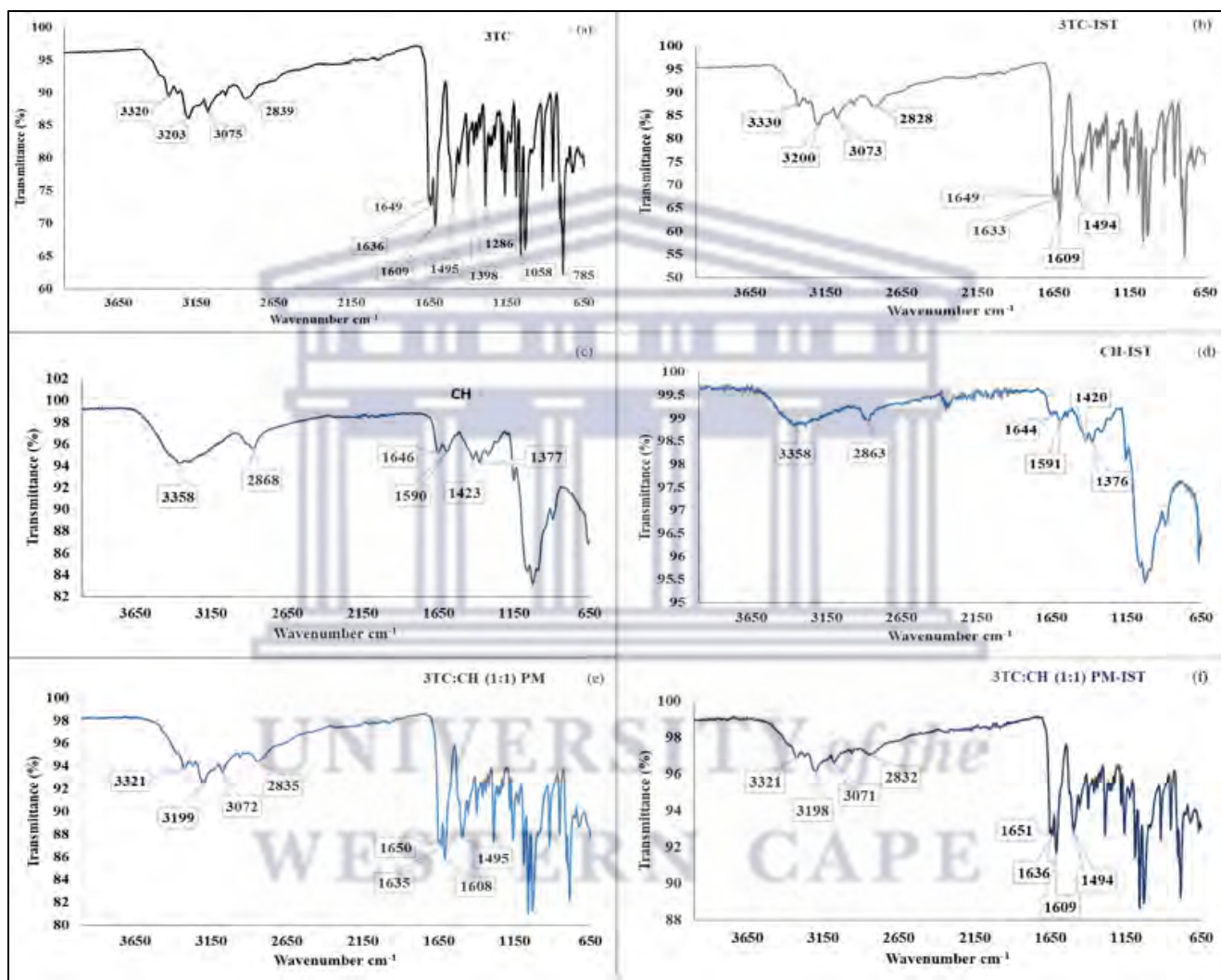


Figure A16: DSC thermograms pure pure (a) 3TC, (c) CH, and (e) 3TC-CH (1:1) PM stored at room temperature (25 °C) compared to (b) 3TC, (d) CH, and (f) 3TC-CH (1:1) PM maintained at 60 ± 1 °C for 1 week (Isothermal stress testing-IST) obtained at ambient temperature within a scanning range of 650 - 4000 cm⁻¹.

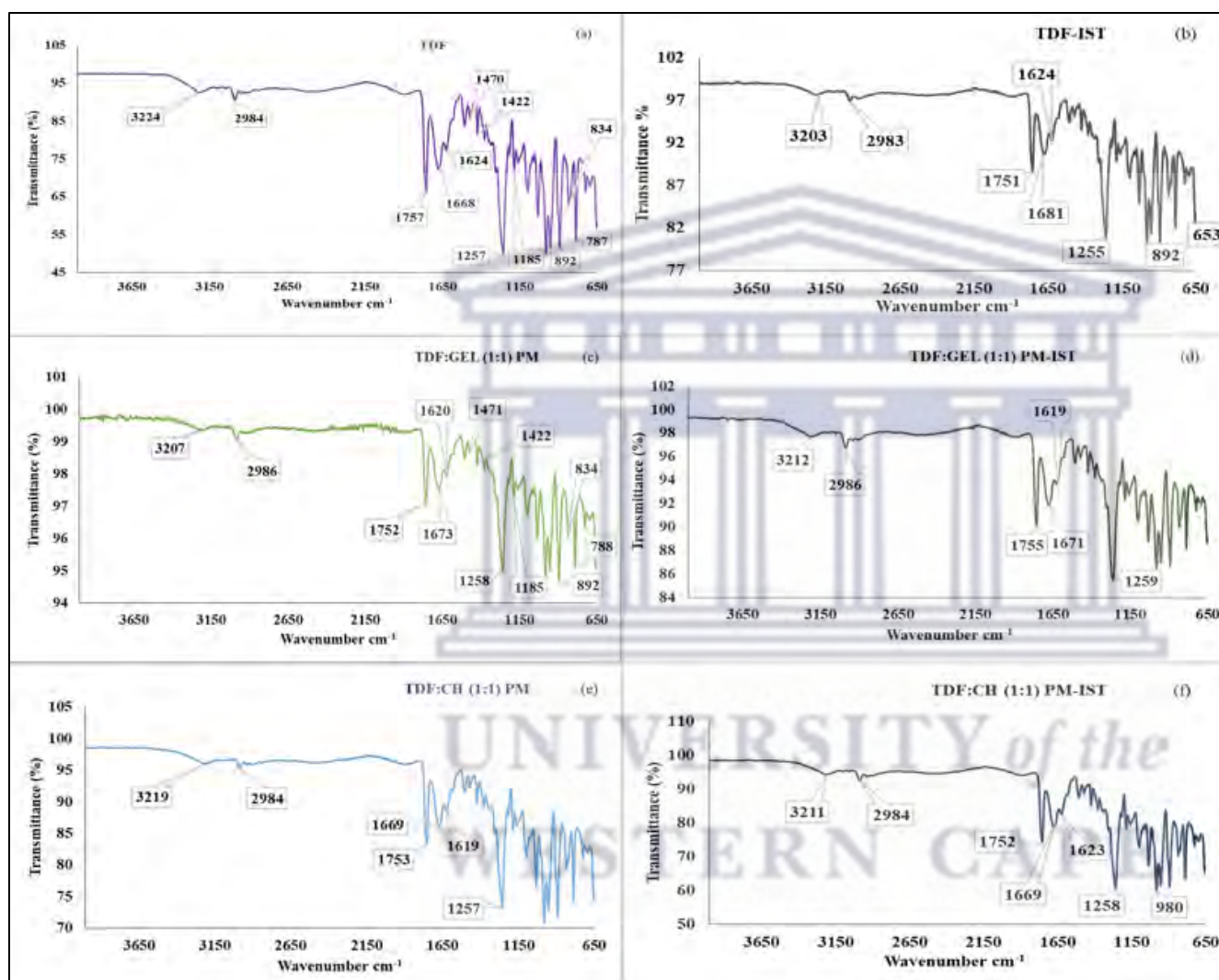


Figure A17: DSC thermograms pure (a) TDF, (c) TDF-GEL(1:1) PM and (e) TDF-CH (1:1) PM stored at room temperature (25 °C) compared to (b) TDF, (d) TDF-GEL (1:1) PM, and (e) 3TC-CH (1:1) PM maintained at 60 ± 1 °C for 1 week (Isothermal stress testing-IST) obtained at ambient temperature within a scanning range of 650 - 4000 cm⁻¹.

The PXRD patterns of samples (3TC, 3TC:GEL(1:1)PM, 3TC:CH (1:1)PM, and TDF, TDF:GEL (1:1)PM, TDF:CH (1:1)PM) stored at room temperature (25 °C) determined over 24 hours compared to the samples (3TC, 3TC:GEL(1:1)PM, 3TC:CH (1:1)PM, and TDF, TDF:GEL (1:1)PM, TDF:CH (1:1)PM) maintained at 60 ± 1 °C for 1 week were demonstrated in the **Figures A18** and **A19**.

The PXRD patterns of 3TC, 3TC:GEL(1:1)PM, and 3TC:CH (1:1)PM (**Figures A18(b)**, **A18(d)**, and **A18(e)**) maintained at 60 ± 1 °C for 1 week retained all sharp symmetric peaks from 3TC, 3TC:GEL(1:1)PM, and 3TC:CH (1:1)PM (**Figures A18(a)**, **A18(c)**, and **A18(f)**) stored at room temperature (25 °C) determined over 24 hours with only slight changes in the peaks intensities. Notably, 3TC-CH (1:1) PM (**Figures A18 (f)**) demonstrated absence of some sharp symmetric peaks of 3TC, which might be due to the effect of high amorphousness of CH at elevated temperature on the 3TC molecules and not due to incompatibility.

The PXRD patterns of TDF, TDF:GEL(1:1)PM, and TDF:CH (1:1)PM (**Figures A19(b)**, **A19(d)**, and **A19(e)**) maintained at 60 ± 1 °C for 1 week retained all sharp symmetric peaks from TDF, TDF:GEL(1:1)PM, and TDF:CH (1:1)PM (**Figures A19(a)**, **A19(c)**, and **A19(f)**) stored at room temperature (25 °C) determined over 24 hours with only slight changes in the peaks intensities.



UNIVERSITY of the
WESTERN CAPE

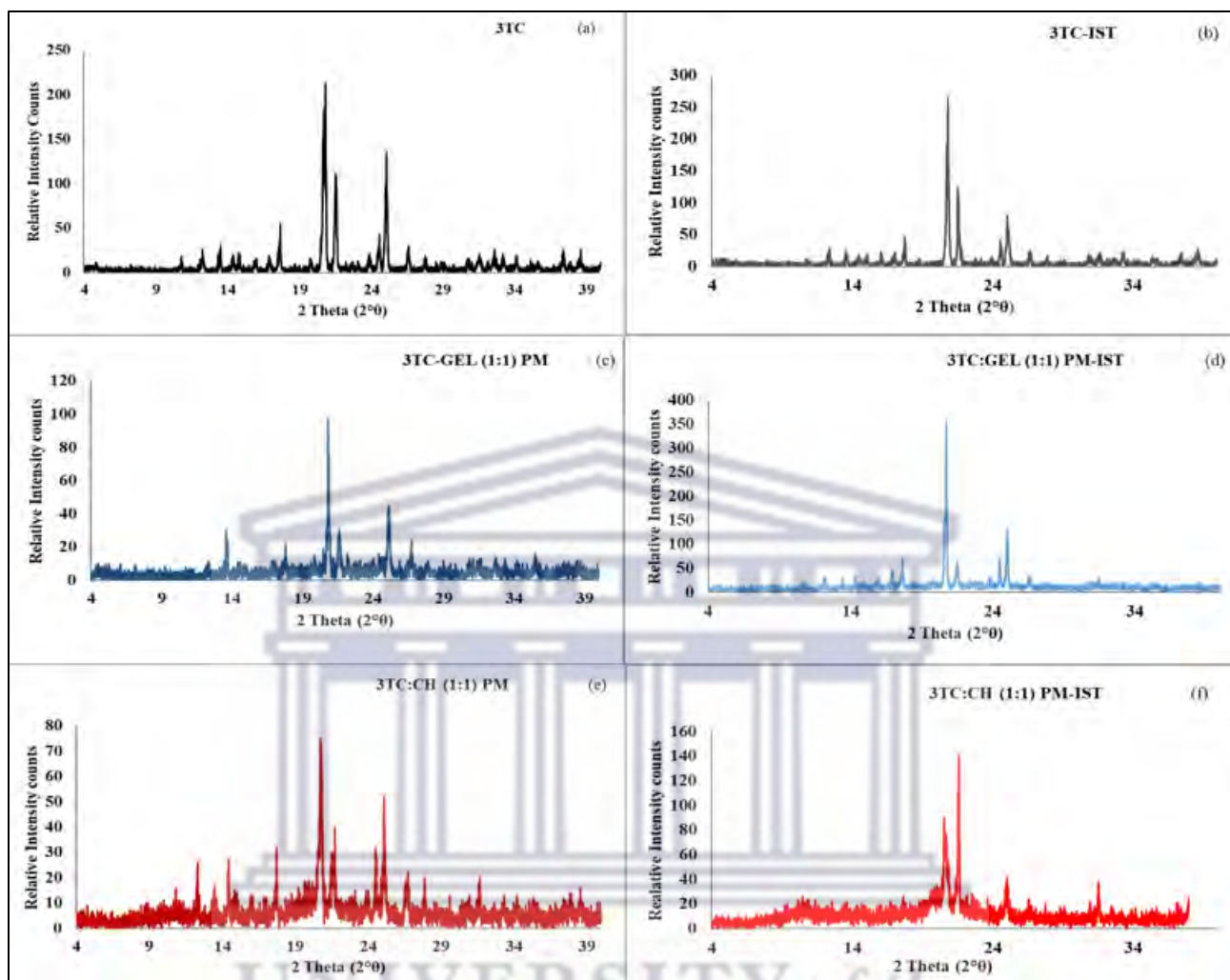


Figure A18: The PXRD patterns of (a) 3TC, (c) 3TC-GEL (1:1) PM, and (e) 3TC-CHI (1:1) PM stored at 25 °C compared to (b) 3TC, (d) 3TC-GEL (1:1) PM, and (f) 3TC-CH (1:1) PM maintained at 60 ± 1 °C for 1 week.

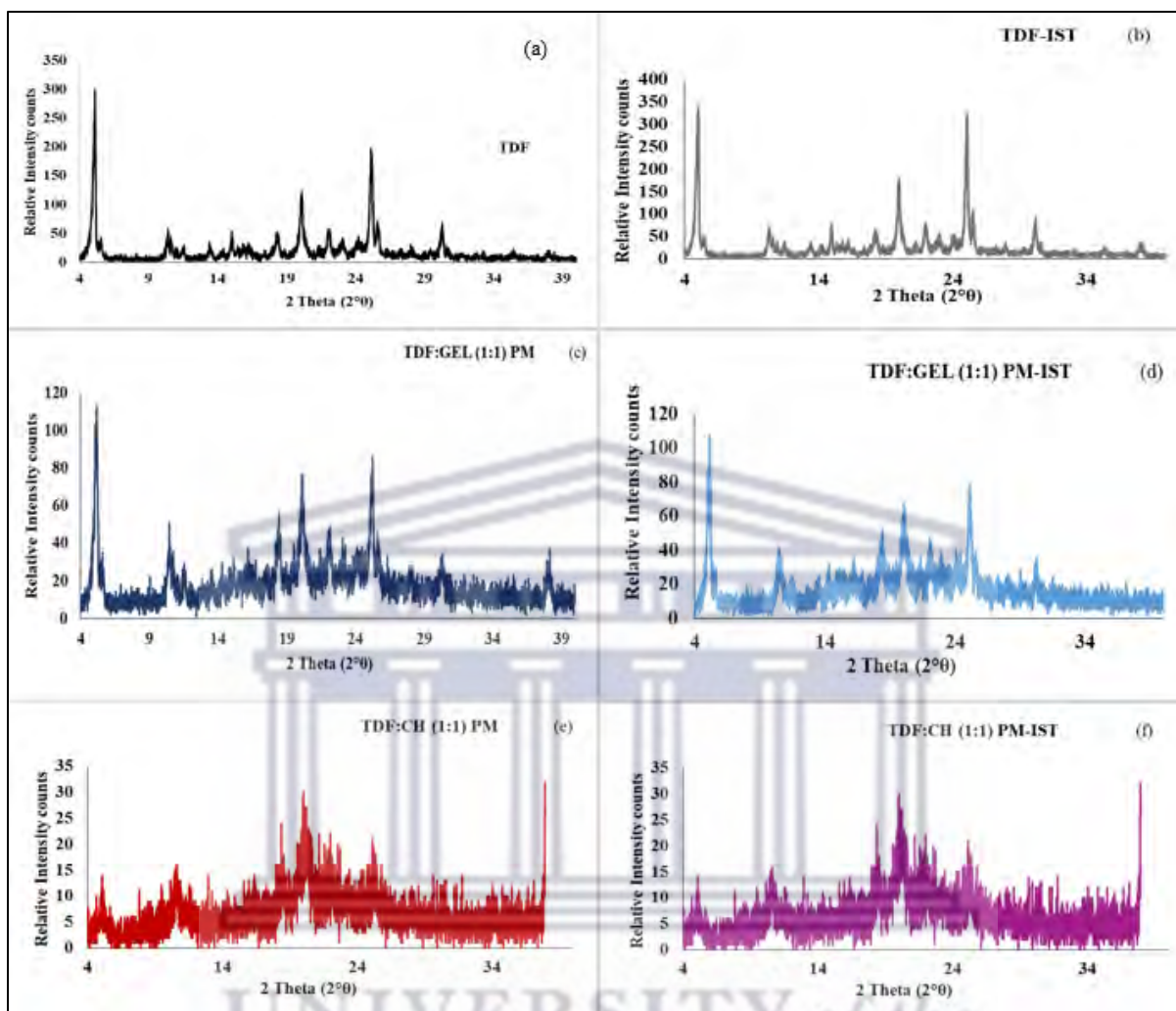


Figure A19: The PXRD patterns of (a) TDF, (c) TDF-GEL (1:1) PM, and (e) TDF-CHI (1:1) PM stored at room temperature (25 °C) compared to (b) TDF, (d) TDF-GEL (1:1) PM, and (f) TDF-CH (1:1) PM maintained at 60 ± 1 °C for 1 week (Isothermal stress testing-IST) obtained at room temperature within a scanning limit of 4 - 40° 2θ.

A114. Conclusion

One of the most pressing concerns in the development of drug dosage forms is drug-excipient incompatibility. Some stability issues encountered during drug development and post-commercialization can be attributed to insufficient constituent matching in the drug product. The identity, solid-state forms, purity, crystallinity, and stability of the two APIs and excipients and their physical mixture were established using thermal (DSC and TGA) and spectroscopy (FTIR and PXRD) data. This study concludes that the two ARVs drugs are compatible with GEL and

CH, as determined by DSC and confirmed by FTIR at room temperature. PXRD results, also revealed that there is no physicochemical interaction between 3TC, TDF, GEL, and CH when they are combined. Though, the results from TDF-CH (1:1) PM stored at room temperature (25 °C) was inconclusive. On DSC and FTIR, isothermal stress testing revealed no interaction when the drug(s) and excipient(s) were combined as physical blend. PXRD results, also revealed that there is no physicochemical interaction between 3TC, TDF, GEL, and CH when they are combined and maintained at 60 ± 1 °C for 1week, but the result for 3TC-CH (1:1) PM was inconclusive.



AII.5 Reference

Chadha, R. and Bhandari, S. (2014). Drug–excipient compatibility screening—role of thermoanalytical and spectroscopic techniques. *Journal of Pharmaceutical and Biomedical Analysis*, 87, pp.82-97. Doi: <https://doi.org/10.1016/j.jpba.2013.06.016>.

De Lima Gomes, E.C., Ercole de Carvalho, I., Fialho, S.L., Barbosa, J., Yoshida, M.I. and da Silva Cunha Júnior, A. (2018). Mixing method influence on compatibility and polymorphism studies by DSC and statistical analysis: Application to tenofovir disoproxil fumarate. *Journal of Thermal Analysis and Calorimetry*, 131, pp.2123-2128. Doi: <https://doi.org/10.1007/s10973-017-6827-x>.

Ebnesajjad, S. (2011). Surface and material characterization techniques. In *Handbook of Adhesives and Surface Preparation* (pp. 31-48). William Andrew Publishing. Doi: <https://doi.org/10.1016/B978-1-4377-4461-3.10004-5>.

Fortunato, A. (2013). DSC: history, instruments and devices. In *Drug-Biomembrane Interaction Studies* (pp. 169-212). Woodhead Publishing. Doi: <https://doi.org/10.1533/9781908818348.169>.

Gomes, E.C.D.L., Mussel, W.N., Resende, J.M., Fialho, S.L., Barbosa, J. and Yoshida, M.I. (2013). Chemical interactions study of antiretroviral drugs efavirenz and lamivudine concerning the development of stable fixed-dose combination formulations for AIDS treatment. *Journal of the Brazilian Chemical Society*, 24, pp.573-579. Doi: <https://doi.org/10.5935/0103-5053.20130071>

Gu, L., Strickley, R.G., Chi, L.H. and Chowhan, ZT (1990). Drug-excipient incompatibility studies of the dipeptide angiotensin-converting enzyme inhibitor, moexipril hydrochloride: dry powder vs wet granulation. *Pharmaceutical Research*, 7(4), pp.379-383. Doi: <https://doi.org/10.1023/A:1015871406549>.

Jeličić, M.L., Brusač, E., Amidžić Klarić, D., Nigović, B., Keser, S. and Mornar, A. (2020). Physicochemical compatibility investigation of Mesalazine and folic acid using chromatographic and thermoanalytical techniques. *Pharmaceuticals*, 13(8), p.187. Doi: <https://doi.org/10.3390/ph13080187>.

Khan, S.A., Khan, S.B., Khan, L.U., Farooq, A., Akhtar, K. and Asiri, A.M. (2018). Fourier transform infrared spectroscopy: fundamentals and application in functional groups and

nanomaterials characterization. In *Handbook of materials characterization* (pp. 317-344). Springer, Cham. Doi: https://doi.org/10.1007/978-3-319-92955-2_9.

Law, D. and Zhou, D. (2017). Solid-state characterization and techniques. In *Developing Solid Oral Dosage Forms* (pp. 59-84). Academic Press. Doi: <https://doi.org/10.1016/B978-0-12-802447-8.00003-0>.

Murthy, N.S. and Minor, H. (1990). General procedure for evaluating amorphous scattering and crystallinity from X-ray diffraction scans of semicrystalline polymers. *Polymer*, 31(6), pp.996-1002. Doi: [https://doi.org/10.1016/0032-3861\(90\)90243-R](https://doi.org/10.1016/0032-3861(90)90243-R).

Ogunjimi, A.T., Fiegel, J. and Brogden, N.K. (2020). Design and characterization of spray-dried chitosan-naltrexone microspheres for microneedle-assisted transdermal delivery. *Pharmaceutics*, 12(6), p.496. Doi: <https://doi.org/10.3390/pharmaceutics12060496>.

Prabhakar, M.N., Raghavendra, G.M., Vijaykumar, B.V.D., Patil, K., Seo, J. and Jung-il, S. (2019). Synthesis of a novel compound based on chitosan and ammonium polyphosphate for flame retardancy applications. *Cellulose*, 26, pp.8801-8812. Doi: <https://doi.org/10.1007/s10570-019-02671->

Rajeswari, A., Christy, E.J.S., Gopi, S., Jayaraj, K. and Pius, A. (2020). Characterization studies of polymer-based composites related to functionalized filler-matrix interface. *Interfaces in Particle and Fibre Reinforced Composites*, pp.219-250. Doi: <https://doi.org/10.1016/B978-0-08-102665-6.00009-1>.

Scrivens, G., Ticehurst, M. and Swanson, J.T. (2018). Strategies for improving the reliability of accelerated predictive stability (APS) studies. In *Accelerated Predictive Stability* (pp. 175-206). Academic Press. Doi: <https://doi.org/10.1016/B978-0-12-802786-8.00007-3>.

Singh, A.V. and Nath, L.K. (2012). Evaluation of compatibility of tablet excipients and novel synthesized polymer with lamivudine. *Journal of Thermal Analysis and Calorimetry*, 108(1), pp.263-267. Doi: <https://doi.org/10.1007/s10973-011-1650-2>.

Song, C., Yu, H., Zhang, M., Yang, Y. and Zhang, G. (2013). Physicochemical properties and antioxidant activity of chitosan from the blowfly *Chrysomya megacephala* larvae. *International*

journal of biological macromolecules, 60, pp.347-354. Doi: <https://doi.org/10.1016/j.ijbiomac.2013.05.039>.

Thakral, S., Terban, M.W., Thakral, N.K. and Suryanarayanan, R. (2016). Recent advances in the characterization of amorphous pharmaceuticals by X-ray diffractometry. *Advanced Drug Delivery Reviews*, 100, pp.183-193. Doi: <https://doi.org/10.1016/j.addr.2015.12.013>.

Verma, R.K. and Garg, S. (2005). Selection of excipients for extended release formulations of glipizide through drug–excipient compatibility testing. *Journal of Pharmaceutical and Biomedical Analysis*, 38(4), pp.633-644. Doi: <https://doi.org/10.1016/j.jpba.2005.02.026>.

Wang, W., Wang, Z., Liu, Y., Li, N., Wang, W. and Gao, J. (2012). Preparation of reduced graphene oxide/gelatin composite films with reinforced mechanical strength. *Materials Research Bulletin*, 47(9), pp.2245-2251. Doi: <https://doi.org/10.1016/j.materresbull.2012.05.060>.

Xiao, C., Liu, H., Lu, Y. and Zhang, L. (2001). Blend films from sodium alginate and gelatin solutions. Doi: <https://doi.org/10.1081/MA-100103352>.

Yousaf, A.M., Kim, D.W., Kim, J.K., Kim, J.O., Yong, C.S. and Choi, H.G. (2015). Novel fenofibrate-loaded gelatin microcapsules with enhanced solubility and excellent flowability: preparation and physicochemical characterization. *Powder Technology*, 275, pp.257-262. Doi: <https://doi.org/10.1016/j.powtec.2015.02.004>.

UNIVERSITY of the
WESTERN CAPE